DOCKET NO. 50-275

REGULATORY DOCKET FILE COPY trans w/1-16-67 ltr + suppl.

NUCLEAR PLANT
DIABLO CANYON SITE
PACIFIC GAS AND ELECTRIC COMPANY

PG and E

RECEIVED
JAN 18 1967
U.S. ATOMIC ENERGY COMMISSION
Regulatory
Mail Section

DOCKETED
USAEC
JAN 18 1967
REGULATORY
MAIL SECTION
DOCKET CLERK

PRELIMINARY
SAFETY ANALYSIS REPORT
VOLUME II

REGULATORY DOCKET FILE COPY

182

TABLE OF CONTENTS

Section	Title	Page
CHAPTER 1	SUMMARY DESCRIPTION - VOLUME 1	
1.1	Introduction	1-1
1.2	Design Highlights	1-2
1.3	Plant Site Summary	1-4
1.4	Summary Plant Description	1-6
1.5	Principal Architectural and Engineering Criteria for Design	1-21
1.6	Research and Development Requirements	1-52
1.7	Identification of Contractors	1-53
CHAPTER 2	SITE AND ENVIRONMENT - VOLUME 1	
2.1	Introduction	2-1
2.2	Site Description	2-2
2.3	Meteorology	2-9
2.4	Hydrology	2-16
2.5	Geology	2-17
2.6	Seismology	2-20
2.7	Seismic Design Criteria	2-23
2.8	Oceanography	2-31
2.9	Environmental Radioactivity Studies	2-35
CHAPTER 3	REACTOR - VOLUME 1	
3.1	Design Bases	3-1
3.2	Reactor Design	3-2

TABLE OF CONTENTS (Continued)

Section	Title	Page
CHAPTER 4	REACTOR COOLANT SYSTEM - VOLUME 1	
4.1	Design Bases	4-1
4.2	Reactor Coolant System Design and Fabrication Techniques	4-3
4.3	System Operation	4-9
4.4	Components	4-10
4.5	In-Service Inspection Capability	4-26
4.6	In-Service Reactor Coolant System Leakage Detection	4-28
CHAPTER 5	CONTAINMENT SYSTEM - VOLUME 1	
5.1	Containment System Structures	5-1
5.2	Containment Structure-Inspection and Testing	5-33
CHAPTER 6	ENGINEERED SAFEGUARDS - VOLUME 1	
6.1	Design Objectives	6-1
6.2	General Description	6-2
CHAPTER 7	PLANT INSTRUMENTATION AND CONTROL - VOLUME 1	
7.1	Protective Systems	7-1
7.2	Control and Regulating Systems	7-4
7.3	Nuclear Instrumentation Systems	7-9
7.4	Non-Nuclear Process Instrumentation	7-13
7.5	In-Core Instrumentation	7-14
7.6	Operating Control	7-17
7.7	Containment Instrumentation	7-18

TABLE OF CONTENTS (Continued)

Section	Title	Page
CHAPTER 8	ELECTRICAL SYSTEMS - VOLUME 2	
8.1	General Description	8-1
8.2	Design Bases	8-2
8.3	A-C System Design	8-2
8.4	D-C System Design	8-4
8.5	Control and Instrument Power Supply System	8-4
8.6	Inspection and Tests	8-5
CHAPTER 9	AUXILIARY AND EMERGENCY SYSTEMS - VOLUME 2	
9.1	Chemical and Volume Control System	9-1
9.2	Auxiliary Coolant System	9-14
9.3	Sampling System	9-21
9.4	Fuel Handling System	9-25
9.5	Facility Services	9-32
CHAPTER 10	STEAM AND POWER CONVERSION SYSTEM - VOLUME 2	
10.1	Design Basis	10-1
10.2	System Design and Operation	10-1
10.3	Turbine Controls	10-4
CHAPTER 11	RADIOACTIVE WASTES AND RADIATION PROTECTION - VOLUME 2	
11.1	Waste Disposal System	11-1
11.2	Radiation Protection	

TABLE OF CONTENTS (Continued)

Section	Title	Page
CHAPTER 12	SAFETY EVALUATION - VOLUME 2	
12.1	Core and Coolant Boundary Protection Analyses.....	12-1
12.2	Standby Safeguards Analysis.....	12-17
12.3	Major Rupture of a Reactor Coolant Pipe.....	12-27
12.4	Summary of Off-Site Exposures.....	12-71
CHAPTER 13	OPERATION - VOLUME 2	
13.1	Introduction.....	13-1
13.2	Organization and Responsibility.....	13-1
13.3	Personnel Training.....	13-2
13.4	Written Procedures.....	13-4
13.5	Records.....	13-4
13.6	Review and Operational Audit Procedure.....	13-5
13.7	Initial Tests and Operation.....	13-5

LIST OF APPENDICES

APPENDIX A MAPS - VOLUME 2

1. U.S. Geological Survey, San Luis Obispo
2. Geological Map of California, San Luis Obispo Sheet

APPENDIX B GEOLOGY - VOLUME 2

1. "Geology of the Diablo Canyon Power Plant Site, San Luis Obispo County, California," Richard H. Jahns
2. "Geology of the Diablo Canyon Power Plant Site, San Luis Obispo County, California (Supplementary Report)," Richard H. Jahns
3. "Nuclear Power Plant - Diablo Canyon Site," E. C. Marliave
4. "Diablo Canyon Nuclear Plant Site, Preliminary Geologic Investigation," M. Micheli

APPENDIX C SEISMOLOGY - VOLUME 2

1. "Seismic Evaluation of the Diablo Canyon Site," Hugo Benioff and S. W. Smith

APPENDIX D ASEISMIC DESIGN - VOLUME 2

1. "Earthquake Design Criteria for the Nuclear Power Plant - Diablo Canyon Site," John A. Blume & Associates, Engineers

APPENDIX E OCEANOGRAPHY - VOLUME 2

1. "An Evaluation of Tsunami Potential at the Diablo Canyon Site," Marine Advisors, Inc.

APPENDIX F METEOROLOGY - VOLUME 2

1. "Diablo Canyon Site, San Luis Obispo County, Report Prepared by the Meteorology Office, Pacific Gas and Electric Company"

LIST OF TABLES

Table	Title	Page
CHAPTER 1	SUMMARY DESCRIPTION - VOLUME 1	
1-1	Comparison of Design Parameters.....	1-12
CHAPTER 2	SITE AND ENVIRONMENT - VOLUME 1	
2-1	Population Trends of the State of California and the Counties Surrounding the Diablo Canyon Site.....	2-4
2-2	Growth of Communities over 1000 Population Within Sixty Miles of the Diablo Canyon Site.....	2-5
2-3	Population of Communities Within a Sixty-Mile Radius of Diablo Canyon Site (1960 Census).....	2-7
2-4	Site Dispersion Factors.....	2-15
CHAPTER 3	REACTOR - VOLUME 1	
3-1	Preliminary Nuclear Design Data.....	3-7
3-2	Results of Calculations as a Function of Laboratory Providing Experimental Data.....	3-21
3-3	Calculated and Measured Reactivity Effects of Void Tubes.....	3-24
3-4	Engineering Hot Channel Factors.....	3-51
3-5	Hydraulic and Thermal Design Parameters.....	3-54
3-6	Core Mechanical Design Parameters.....	3-62

Table	Title	Page
CHAPTER 4	REACTOR COOLANT SYSTEM - VOLUME 1	
4-1	Reactor Coolant System - Code Requirements....	4-2
4-2	Principal Design Parameters of the Reactor Coolant System.....	4-3
4-3	Reactor Coolant System Quality Assurance Program.....	4-7
4-4	Reactor Coolant Water Chemical Composition....	4-10
4-5	Principal Design Parameters of the Reactor Vessel.....	4-12
4-6	Principal Design Parameters of the Steam Generator.....	4-21
4-7	Principal Design Parameters of the Reactor Coolant Pumps.....	4-23
4-8	Principal Design Parameters for the Pressurizer and Pressurizer Relief Tank.....	4-25
CHAPTER 6	ENGINEERED SAFEGUARDS - VOLUME 1	
6-1	Accumulater Tanks Preliminary Design Parameters.....	6-12
6-2	Safety Injection Pump Design Parameters.....	6-13
6-3	Residual Heat Removal Pump Design Parameters.....	6-13
6-4	Connection to the Recirculation Loop.....	6-33
6-5	Recirculation Loop Leakage.....	6-37
6-6	Preliminary Containment Spray Pump Design Parameters.....	6-40
6-7	Containment Penetration List.....	6-52

LIST OF TABLES (Continued)

Table	Title	Page
CHAPTER 7	PLANT INSTRUMENTATION AND CONTROL - VOLUME 1	
7-1	Maximum Overpower Level.....	7-13
CHAPTER 9	AUXILIARY AND EMERGENCY SYSTEMS - VOLUME 2	
9-1	Auxiliary Coolant System Code Requirements....	9-14
CHAPTER 11	RADIOACTIVE WASTES AND RADIATION PROTECTION - VOLUME 2	
11-1	Principal Shielding of Plant.....	11-14
CHAPTER 12	SAFETY EVALUATION - VOLUME 2	
12-1	Natural Circulation Reactor Flow vs. Reactor Power.....	12-11
12-2	Summary of Maximum Estimated Off-Site Doses from Accidents.....	12-71

LIST OF FIGURES

Figure	Title
CHAPTER 1	SUMMARY DESCRIPTION - VOLUME 1
1-1	Plot Plan
1-2	Turbine Building - Plan at Elevation 10'-0"
1-3	Containment and Auxiliary Building - Plan at Elevation 59'-0"
1-4	Containment, Auxiliary and Turbine Building - Plan at Elevation 85'-0"
1-5	Containment and Auxiliary Building - Plan at Elevation 108'-0"
1-6	Auxiliary and Turbine Building - Vertical Section "A-A"
1-7	Containment and Turbine Building Vertical Section "B-B"
CHAPTER 2	SITE AND ENVIRONMENT
2-1	Map of California Showing Location of Plant Site
2-2	Site Location Map
2-3	Site Plan
2-4	Aerial Photograph - Site and Environs
2-5	Population Distribution - 0 to 10 Miles, 1960 Census
2-6	Population Distribution - 0 to 10 Miles, 1970 Projection
2-7	Population Distribution - 0 to 10 Miles, 1980 Projection
2-8	Population Distribution - 0 to 60 Miles, 1960 Census
2-9	Population Distribution - 0 to 60 Miles, 1970 Projection
2-10	Population Distribution - 0 to 60 Miles, 1980 Projection
2-11	Response Acceleration Spectra - Earthquake "D"
2-12	Response Acceleration Spectra - Earthquake "D"
2-13	Response Acceleration Spectra - Earthquake "B"
2-14	Response Acceleration Spectra - Earthquake "B"

LIST OF FIGURES (Continued)

Figure	Title
CHAPTER 3	REACTOR - VOLUME 1
3-1	Variation of Plutonium Mass with Depletion
3-2	Variation of Plutonium Fraction with Depletion
3-3	Variation of Plutonium Isotopes with Depletion
3-4	Plan of Critical Experiment (Unborated Case)
3-5	Plan of Critical Experiment (Borated Case)
3-6	With Boron Comparison of Experimental and Calculated Power Distribution
3-7	Case 2 (Unborated) Power Distribution Comparison
3-8	Case 1 (Unborated) Power Distribution Comparison
3-9	Power Scans Through Voided Region in an Unborated Core
3-10	Power Scans Through Voided Region in a Borated Core
3-11	Radial Fuel Rod Scan
3-12	Yankee Core 1 Power Distribution Comparison
3-13	Yankee Core 1 Burnup Distribution Comparison
3-14	Fast Absorption of Uniformly Distributed Absorbers
3-15	Fast Absorption of Clustered Absorbers
3-16	Selni Temperature Coefficients vs. Moderator Temperature
3-17	Selni Temperature Coefficients vs. Boron Concentration
3-18	Yankee Temperature Coefficients vs. Burnup
3-19	Comparison of Resonance Integral Correlations
3-20	Fuel Temperature Change vs. Power Density
3-21	Alpha vs. Heat Flux
3-22	Comparison of Effective Fuel Temperature with Changing Heat Flux
3-23	Comparison of W-3 Prediction in the Range of -0.15 to +0.15 Quality, Uniform Flux
3-24	W-3 Correlation Probability Distribution Curve
3-25	Stable Film Boiling Heat Transfer Data and Correlation

LIST OF FIGURES (Continued)

Figure	Title
3-26	Thermal Conductivity of Uranium Dioxide
3-27	Comparison of W-3 Prediction in the Range of -0.15 to +0.15 Quality, Non-Uniform Flux
3-28	Comparison of Predicted to Measured DNB Locations (Cosine)
3-29	Comparison of Predicted to Measured DNB Location (Peak Near Exit)
3-30	Comparison of Predicted to Measured DNB Location (Peak Near Inlet)
3-31	Core Cross Section
3-32	Core Loading Arrangement
3-33	Typical Control Cluster Assembly
3-34	Reactor Vessel and Internals
3-35	Lower Core Support Structure
3-36	Upper Core Support Structure
3-37	Control Cluster Guide Assembly
3-38	In-Core Flux Instrumentation
3-39	Fuel Assembly Outline
3-40	Fuel Assembly and Control Cluster Cross Section
3-41	Typical Spring Clip Grid Detail
3-42	Spring Clip Grid Assembly
3-43	Control Rod Cluster Outline
3-44	Control Rod Drive Mechanism Assembly
3-45	Control Rod Drive Mechanism Schematic
CHAPTER 4	REACTOR COOLANT SYSTEM - VOLUME 1
4-1	Radiation Effects on Pressure Vessel Steel
4-2	Reactor Coolant System
4-3	Reactor Vessel Outline
4-4	Steam Generator
4-5	Reactor Coolant Pump

LIST OF FIGURES (Continued)

Figure	Title
CHAPTER 5	CONTAINMENT SYSTEM - VOLUME 1
5-1	Containment Structure
5-2	Design Pressure Temperature Transient
5-3	1.25 Times Design Pressure - Temperature Transient
5-4	1.50 Times Design Pressure - Temperature Transient
5-5	Typical Electrical Penetrations
5-6	Typical Piping Penetrations
5-7	Fuel Transfer Tube
CHAPTER 6	ENGINEERED SAFEGUARDS - VOLUME 1
6-1	Safety Injection System
6-2	Containment Spray System
CHAPTER 7	PLANT INSTRUMENTATION AND CONTROL - VOLUME 1
7-1	Reactor Protection System
7-2	Simplified Block Diagram of Reactor Control System
7-3	Nuclear Instrumentation System
7-4	Sensitivity of the Reactor Neutron Detector
7-5	Arrangement of In-Core Flux Detector System
7-6	Schematic of In-Core Flux Detector Drive System
CHAPTER 8	ELECTRICAL SYSTEM - VOLUME 2
8-1	Plant Electrical Single-Line Diagram
8-2	Interconnections with P.G.and E. Transmission System

LIST OF FIGURES (Continued)

Figure	Title
CHAPTER 9	AUXILIARY AND EMERGENCY SYSTEMS - VOLUME 2
9-1	Chemical and Volume Control System - Sheet 1
9-2	Chemical and Volume Control System - Sheet 2
9-3	Chemical and Volume Control System - Sheet 3
9-4	Auxiliary Coolant System
9-5	Sampling System
9-6	Fuel Transfer System
9-7	Auxiliary Salt Water and Service Water System
CHAPTER 10	STEAM AND POWER CONVERSION SYSTEM - VOLUME 2
10-1	Steam and Feedwater System
CHAPTER 11	RADIOACTIVE WASTES AND RADIATION PROTECTION - VOLUME 2
11-1	Waste Disposal System, Sheet 1
11-2	Waste Disposal System, Sheet 2
CHAPTER 12	SAFETY EVALUATION - VOLUME 2
12-1	Steam System Diagram
12-2	Turbine Control and Protection System
12-3	Reactor Coolant System Element Designation for SATAN Code
12-4	Reactor Coolant System Element Designation for SATAN Code 2 Loop Analysis
12-5	Comparison of SATAN Code Results with LOFT Experiment (Reservoir Blowdown) Vessel Pressure

LIST OF FIGURES (Continued)

Figure	Title
12-6	A Comparison of SATAN Code Results with LOFT Experiment (Reservoir Blowdown) Discharge Pressure
12-7	A Comparison of SATAN Code Results with LOFT Experiment (Reservoir Blowdown) Vessel Temperature
12-8	A Comparison of SATAN Code Results with LOFT Experiment (Reservoir Blowdown) Discharge Temperature
12-9	Hot Leg - 0.0 Sec. Rupture Time, Core Pressure Transient, 0-4 Sec.
12-10	Hot Leg - 0.0 Sec. Rupture Time, Core Pressure Transient, 4-7 Sec.
12-11	Hot Leg - 0.0 Sec. Rupture Time, Core Barrel Pressure Transient, 0-4 Sec.
12-12	Containment Pressure Transient, Hypothetical Accident, 29-Inch I.D. Double Ended Break
12-13	Containment Pressure Transient, Various Break Sizes
12-14	Thyroid Inhalation Exposures
12-15	Whole Body Exposures
12-16	2 Hour Inhalation Dose at 1/2 Mile, Sensitivity Study
12-17	31 Day Inhalation Dose at 1/2 Mile, Sensitivity Study
CHAPTER 13	OPERATION - VOLUME 2
13-1	Ultimate Operating Organization

TABLE OF CONTENTS

Section	Title	Page
CHAPTER 8	ELECTRICAL SYSTEMS	
8.1	General Description	8-1
8.2	Design Bases	8-2
8.3	A-C System Design	8-2
8.3.1	Transmission System	8-2
8.3.2	Station Distribution System	8-3
8.4	D-C System Design	8-4
8.5	Control and Instrument Power Supply System	8-4
8.6	Inspection and Tests	8-5

CHAPTER 8 ELECTRICAL SYSTEMS

8.1 GENERAL DESCRIPTION

The electrical systems for the plant, shown in Figure 8-1, in general are similar to those used for conventional steam power plants of comparable size. Additional features, however, are designed into the systems to assure continuity of power supply to vital loads and instrument systems in the event of any credible accident.

Energy produced by the main generator at 25 kv will feed by means of the isolated phase bus to the main transformer and to the unit auxiliary transformers. The main transformer bank will step up the generator voltage to 500 kv and supply two 500 kv transmission lines. The unit auxiliary transformers will step down the generator voltage to 12,000 and 4160 volts and supply energy directly to the larger auxiliary loads. Additional transformers will reduce the voltage to 460 volts and 208/120 volts for the smaller loads and plant instrumentation.

A standby/startup transformer, supplied by two 230 kv lines from the Company's electric transmission system, wil step down the voltage to 12,000 volts. An additional standby/startup transformer will step down the 12,000 volts to 4160 volts. These two transformers feed the entire plant auxiliary system in a similar manner as the unit auxiliary transformers.

Additional power sources to the auxiliary system will consist of three diesel driven generators, any two of which will supply the vital load requirements of the plant in the event of loss of the normal power sources.

A station battery system will be provided to feed all d-c power, control and instrument loads, and a-c inverter loads.

8.2 DESIGN BASES

Continuity of supply to essential loads is assured by the following provisions:

1. Multiple power sources
   a. Main generator
   b. Two 230 kv transmission lines feeding the standby/startup transformers
   c. Diesel generator No. 1 (one-half size)
   d. Diesel generator No. 2 (one-half size)
   e. Diesel generator No. 3 (one-half size)
   f. Two 500 kv lines feeding the unit auxiliary transformers through the main transformer
   g. The battery d-c system in conjunction with the a-c inverter system

2. Electrical and physical segregation and isolation of power sources, feeders, buses, etc., so that trouble on any part of the power distribution system will not adversely affect the rest of the system.

8.3 A-C SYSTEM DESIGN

8.3.1 TRANSMISSION SYSTEM

The network interconnections between the plant at Diablo Canyon and the Company's transmission system are shown on Figure 8-2. Essentially, two 230 kv lines feeding the 230 kv to 12 kv standby/startup transformer and two 500 kv lines to the main and unit auxiliary transformers will be available to provide power to the plant auxiliary system. The 500 kv system and the 230 kv system are the mainstays of the Company's transmission system and will interconnect the plant with all other major sources of generation on the system. A complete outage of both of these systems is extremely unlikely. Protective relay systems will be designed to isolate any of the four lines connecting the plant to the system, in the event of a fault, without interruption to the remaining lines.

Environmental factors are generally favorable for transmission line operation in this part of California. These factors include moderate to low rain fall, absence of snow and icing conditions, and minimum lightning conditions. Based on long experience, special design considerations are given to line insulation in coastal regions, which guard against line failure due to salt contamination. In the few areas where trees exist, right-of-ways for lines are completely cleared of any trees which could cause line damage.

8.3.2 STATION DISTRIBUTION SYSTEM

As shown in Figure 8-1 the larger auxiliary loads are connected to two 12 kv and five 4160 volt buses. During normal plant operation, all these buses are fed from the generator through the unit auxiliary transformers. In the event of a turbine generator trip, auxiliary load is automatically transferred to the standby/startup transformers. Simultaneously, the diesel-generators will be started.

All vital a-c loads are connected directly to 4160 volt buses F, G, and H, or to transformers fed from these buses. Any unsuccessful transfer of these two buses to the standby/startup source will initiate a programed switching scheme, start the diesel-generators and connect them to their buses, and then switch on the essential loads in proper sequence.

The standby/startup transformers will also serve as a power source for plant startup. After synchronization of the main generator with the system, the 12,000 and 4160 volt buses are manually transferred, one at a time, to the unit auxiliary transformers.

Alternate feeders to essential buses and essential loads will be routed along separate paths throughout the plant. Separation will also be provided between essential control and instrument circuits, and power circuits. Care will be taken in routing all cable circuits to avoid, as much as possible such physical hazards as heat, moisture, steam etc. The three vital 4160 volt buses F, G, and H, and the lower voltage buses fed by them supplying essential load will have separation and effective fire barriers.

A motor operated link, operable from the main control room, will be provided in the isolated phase bus between the main generator and the main transformer bank. By opening this link when the main generator is out of service, the extremely reliable 500 kv transmission system can be used as a source of power for the plant auxiliaries.

8.4 D-C SYSTEM DESIGN

A 250/125 volt d-c station battery system shown in Figure 8-3 will be provided for emergency d-c loads, 12,000 volt, 4160 volt and 460 volt switchgear operation, vital bus inverters, emergency lighting, etc. The system is designed so that a separate 125 volt battery supplies switchgear control power to each of the three vital a-c buses.

The station battery system will be sized to supply the following loads:

Switchgear operation
Turbine generator emergency pumps
Emergency lighting
Control and indicating lights
Annunciators and all instruments and control, and d-c to a-c inverters.

8.5 CONTROL AND INSTRUMENT POWER SUPPLY SYSTEM

Nuclear instrumentation, pressurizer, Reactor Coolant System instrumentation, and various primary process instrumentation which require an uninterrupted supply and close voltage regulation draw their power from four instrument buses. These four instrument buses are isolated from the plant a-c auxiliary system. Two of these instrument buses are fed from an inverter which is supplied from the plant 125 volt d-c buses. This design maintains a transient-free 120 volt a-c, single phase, 60 cycle supply to these two instrument buses. The other two instrument buses are supplied from separate regulating transformers. A normally-open standby connection between the two inverter-fed instrument buses and the two transformer-fed instrument buses is available for use when the inverter(s) is out of service.

8.6 INSPECTION AND TESTS

Periodic inspection will be made of all electrical equipment, including circuit breakers, relays, motors, etc. Insulation tests will be made and records kept so that equipment can be removed from service before a fault occurs.

Periodic "on line" starting tests of the diesel generator sets and tests of the emergency power switching systems will be performed. The frequency and nature of these tests will be established after the detail system design has been completed.

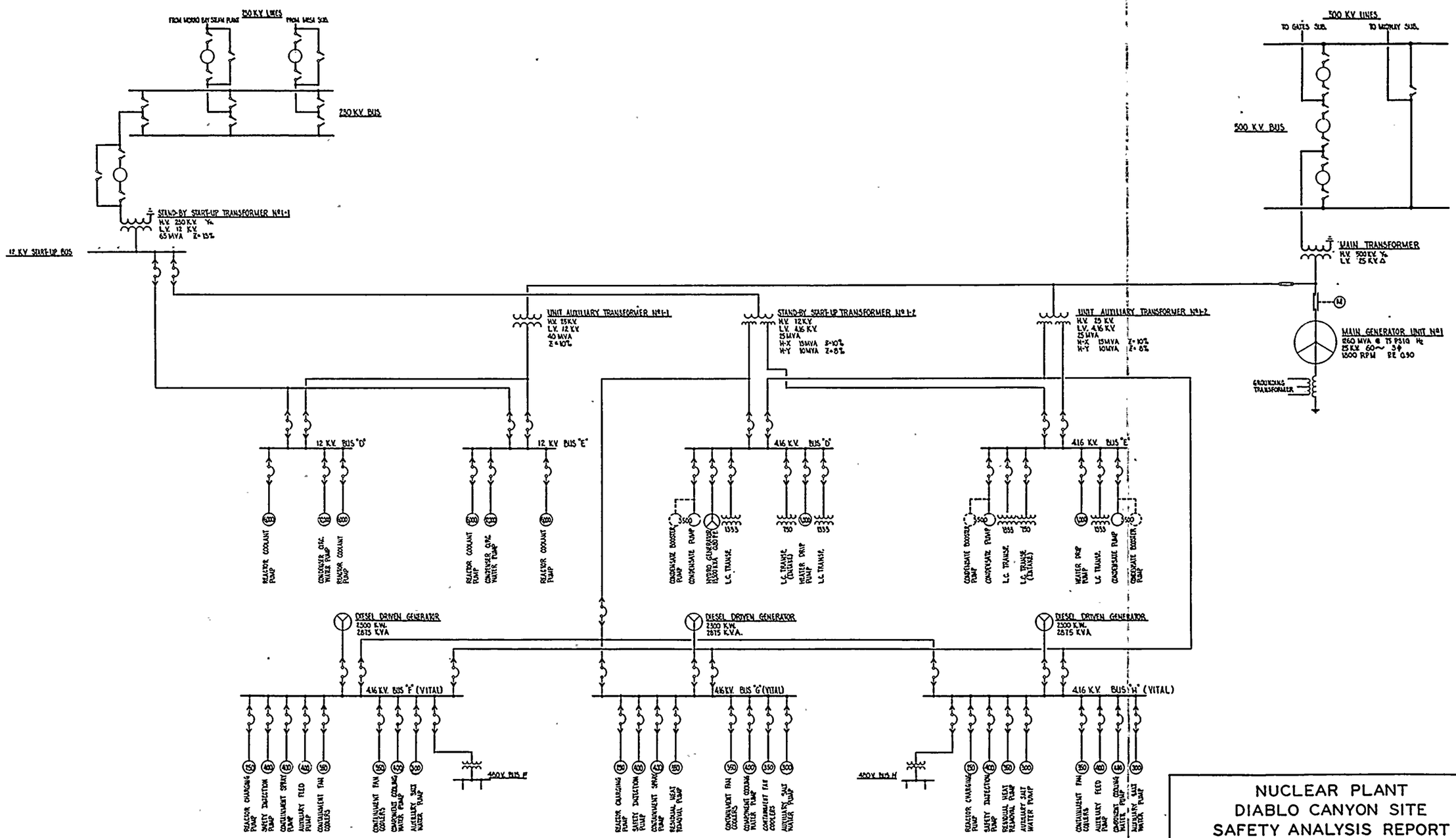

NUCLEAR PLANT
DIABLO CANYON SITE
SAFETY ANALYSIS REPORT

FIG. 8.1 PLANT ELECTRICAL SINGLE LINE DIAGRAM (Revised 7-24-67)

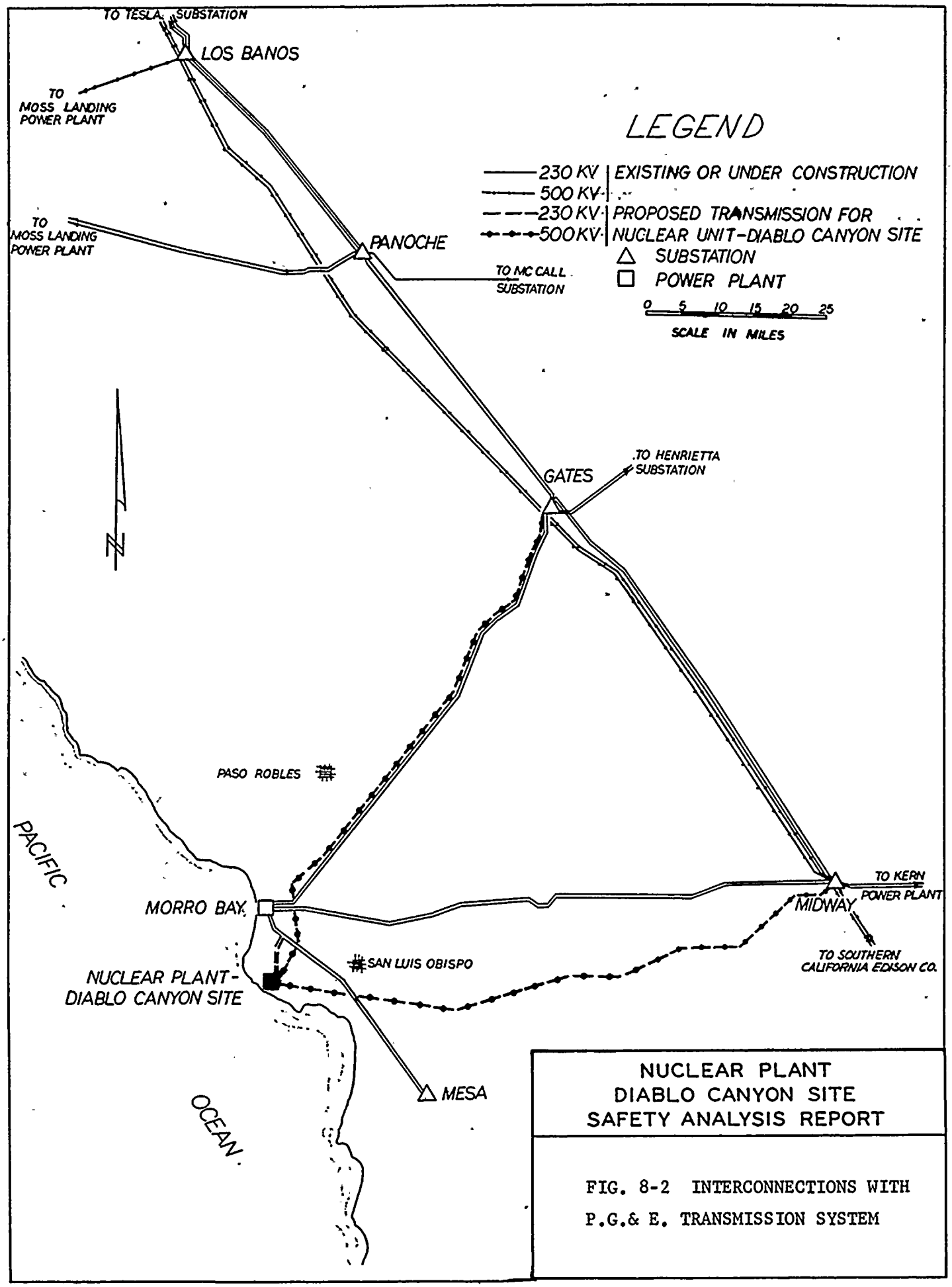

NUCLEAR PLANT
DIABLO CANYON SITE
SAFETY ANALYSIS REPORT

FIG. 8-2 INTERCONNECTIONS WITH P.G.& E. TRANSMISSION SYSTEM

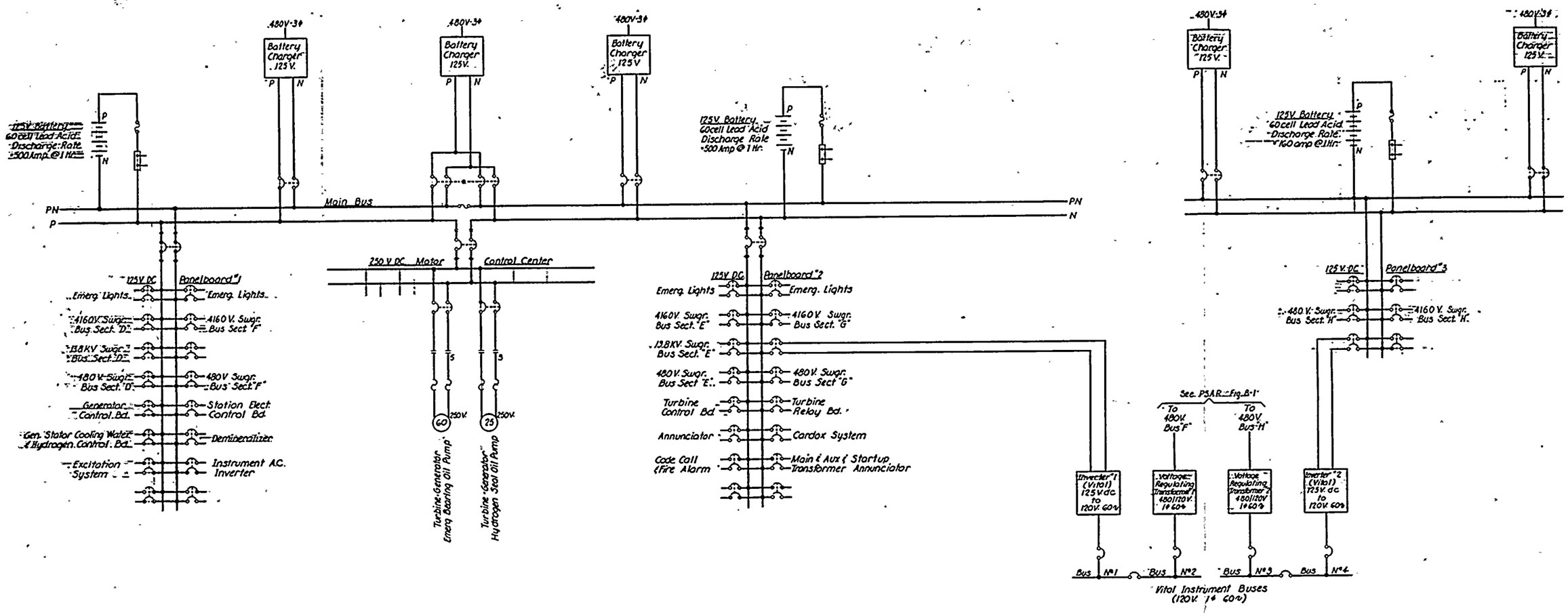

• - Key "Interlock" allows only one circuit breaker to be closed at a time.

NUCLEAR PLANT
DIABLO CANYON SITE
SAFETY ANALYSIS REPORT

FIG. 8-3 SINGLE LINE DIAGRAM 250/125 VOLT D-C SYSTEM

TABLE OF CONTENTS

Section	Title	Page
CHAPTER 9	AUXILIARY AND EMERGENCY SYSTEMS	
9.1	Chemical and Volume Control System	9-1
9.1.1	Design Bases	9-1
9.1.2	System Design and Operation	9-1
9.1.3	Components	9-4
9.2	Auxiliary Coolant System	9-14
9.2.1	Design Bases	9-14
9.2.2	System Design and Operation	9-15
9.3	Sampling System	9-21
9.3.1	Design Basis	9-21
9.3.2	System Design and Operation	9-22
9.3.3	Components	9-23
9.4	Fuel Handling System	9-25
9.4.1	Design Basis	9-25
9.4.2	System Design and Operation	9-25
9.4.3	Fuel Handling Structures	9-26
9.4.4	Fuel Handling Equipment	9-28
9.4.5	Refueling Operation	9-31
9.4.6	Handling of Failed Fuel Assemblies	9-32
9.5	Facility Services	9-32
9.5.1	Plant Fire Protection System	9-32
9.5.2	Service Water System	9-33
9.5.3	Auxiliary Salt Water System	9-35

CHAPTER 9. AUXILIARY AND EMERGENCY SYSTEMS

9.1 CHEMICAL AND VOLUME CONTROL SYSTEM

9.1.1 DESIGN BASES

The Chemical and Volume Control System maintains the proper water inventory in the Reactor Coolant System, provides the required seal water flow for the reactor coolant pump shaft seals, adjusts the concentration of chemical neutron absorber, reduces the quantity of fission product and corrosion product impurities, processes reactor coolant effluent for reuse of boric acid and demineralized water, and maintains the proper concentration of corrosion inhibiting chemicals in the reactor coolant. The system is also used to hydrostatically test the Reactor Coolant System.

System integrity is assured by conformance to applicable ASME B&PV Codes and USA. S. I. Pressure Piping Codes listed in Table 9-1 on the next page and by use of austenitic stainless steel or other corrosion resistant materials in contact with both reactor coolant and boric acid solutions.

9.1.2 SYSTEM DESIGN AND OPERATION

Flow diagrams of the Chemical and Volume Control System are shown in Figures 9-1, 9-2 and 9-3.

During plant operation, reactor coolant flows from a cold leg of the Reactor Coolant System and is returned to one cold and one hot leg via the charging line. Each of the connections to the Reactor Coolant System has an isolation valve located close to the loop piping. In addition, a check valve is located downstream of each charging line isolation valve. The reactor coolant entering the Chemical and Volume Control System is cooled in the shell side of the regenerative heat exchanger and its pressure is then reduced in passing through one of the letdown orifices. The cooled, low pressure water leaves the reactor containment and flows through the non-regenerative heat exchanger where the

TABLE 9-1

CHEMICAL AND VOLUME CONTROL SYSTEM CODE REQUIREMENTS

Regenerative heat exchanger	ASME III*, Class A
Mixed bed demineralizers	ASME III, Class C
Reactor coolant filter	ASME III, Class C
Volume control tank	ASME III, Class C
Seal water heat exchanger (tube side)	ASME III, Class C
Seal water filter	ASME III, Class C
Excess letdown heat exchanger (tube side)	ASME III, Class C
Boric acid filter	ASME III, Class C
Chemical addition tank	ASME VIII
Piping and valves	USA S.I. B31.1**, Section 1
Non-regenerative heat exchanger (tube side)	ASME III, Class C

* ASME III - American Society of Mechanical Engineers, Boiler and Pressure Vessel Code, Section III, Nuclear Vessels.

** USA S.I. B31.1 - Code for Pressure Piping, USA Standards Institute. and special nuclear cases, where applicable.

temperature is further reduced. On leaving the non-regenerative heat exchanger, the coolant undergoes a second pressure reduction and then passes through a mixed bed demineralizer where ionic impurities are removed. The coolant then passes through a filter and flows through a spray nozzle into the volume control tank. The atmosphere in this tank contains hydrogen which dissolves in the reactor coolant. Prior to a cold or refueling shutdown, fission gases are removed from the coolant and are vented from the volume control tank to the Waste Disposal System. Next, the coolant flows to the charging pumps which raise the pressure above that in the Reactor Coolant System. The coolant then enters the reactor containment, passes through the tube side of the regenerative heat exchanger, and returns to the Reactor Coolant System via a charging line.

A portion of the high pressure charging flow is injected into the reactor coolant pumps between the pump impeller and the shaft seal so that the seals are not exposed to high temperature reactor coolant. Part of the flow cools the lower radial bearing and enters the Reactor Coolant System through a labyrinth seal on the pump shaft. The remainder, which is the shaft seal leakage flow, is filtered, cooled in the seal water heat exchanger and returned to the volume control tank. Coolant injected through the reactor coolant pump labyrinth seals returns to the volume control tank by the normal letdown flow path through the regenerative heat exchanger. When the normal letdown route is not in service, labyrinth seal injection flow returns to the volume control tank through the excess letdown and seal water heat exchangers.

During plant startup, normal operation and shutdowns, liquid effluent from the Reactor Coolant System will be collected in the holdup tanks. Reactor coolant letdown flow is diverted to the holdup tanks by a high level signal from the volume control tank. The gas space in the holdup tanks is filled with nitrogen at a low pressure to prevent accumulation of a potentially explosive mixture of hydrogen and oxygen. As liquid enters the tanks, the cover gas is displaced to the gas decay tanks through the vent header. For convenience, a recirculation pump is provided to transfer liquid from one tank to another.

Liquid from a holdup tank is processed as a batch operation and is pumped initially through base and cation ion exchangers to remove radioactive contaminants and some fission products and then through the preheater and into the gas stripper where dissolved gases are stripped from the liquid. The effluent from the gas stripper is fed to the boric acid evaporator where the dilute boric acid solution is concentrated.

Vapor from the boric acid evaporator flows to a boric acid evaporator condenser. The condensate is then cooled to the operating temperature of the evaporator condensate demineralizer. After any evaporator carryover is removed by one of the two evaporator condensate demineralizers, condensate passes through a condensate filter and then accumulates in the monitor tanks.

Subsequent handling cf the condensate depends on the results of sample analysis. The condensate in the monitor tanks may be: (1) pumped to the primary water storage tank, (2) recycled through the demineralizers, (3) returned to the holdup tanks for reprocessing in the evaporator train, or (4) released to the Waste Disposal System for discharge to the environment via the condenser cooling water.

Boric acid evaporator bottoms may be discharged to the concentrates holding tank via a concentrates filter. Solution collected in the concentrates holding tank is sampled and then transferred to one of the boric acid tanks if analysis indicates that it meets specifications for use as boric acid makeup. Otherwise, concentrates are returned to the holdup tanks for reprocessing by the evaporator train.

The concentrated solution can also be drained from the boric acid evaporator to the Waste Disposal System for storage and ultimate shipment off-site for disposal.

Makeup to the Reactor Coolant System is provided by the Chemical and Volume Control System from the following sources:

a) The primary water storage tank, which provides demineralized water for dilution when the reactor coolant boron concentration is to be reduced.

b) The boric acid tanks, which supply concentrated boric acid solution when reactor coolant boron concentration is to be increased.

c) The refueling water storage tank which supplies borated water for emergency makeup.

d) The chemical addition tank, which is used to inject small quantities of solution when additions of hydrazine or pH control chemicals are necessary.

Makeup for normal plant leakage is provided by the reactor makeup control which is set by the operator to blend demineralized water and concentrated boric acid to match the reactor coolant boron concentration. Makeup is added automatically if the volume control tank level falls below a preset point.

9.1.3 COMPONENTS

9.1.3.1 Regenerative Heat Exchanger

The regenerative heat exchanger recovers heat from the reactor coolant letdown stream by heating the charging stream. The letdown coolant passes through the shell side while the charging stream flows through the tubes of the exchanger. The unit is austenitic stainless steel with the shell and heads of welded construction.

9.1.3.2 Letdown Orifices

Three letdown orifices control the rate of letdown flow from the Reactor Coolant System and reduce the coolant pressure. Each orifice is placed in and taken out of service by remote operation of an isolation valve. Normally, one orifice is operating while the others serve as standbys. The orifice bodies and trim are constructed of austenitic stainless steel or equivalent corrosion resistant material.

9.1.3.3 Non-Regenerative Heat Exchanger

The non-regenerative heat exchanger cools the letdown stream to the operating temperature of the mixed bed demineralizers. Letdown flows through the tube side of the exchanger while component cooling water flows through the shell. The unit is a single shell pass multiple tube pass heat exchanger. All surfaces in contact with the reactor coolant are austenitic stainless steel, and the shell is carbon steel.

9.1.3.4 Mixed Bed Demineralizers

Two flushable, mixed bed demineralizers maintain reactor coolant water purity. A strong base or ammonia form cation resin and a hydroxyl form anion resin are initially charged into the demineralizer. The anion resin is converted to the borate form by contact with the borated reactor coolant. One of the units is normally in service with the other providing full standby capacity. The demineralizer vessels are made of austenitic stainless steel.

9.1.3.5 Cation Bed Demineralizer

One flushable cation bed demineralizer is installed, capable of accepting a portion of the letdown flow. Hydrogen form ion exchange resin is employed to remove and control the cesium and lithium concentrations in the Reactor Coolant System.

9.1.3.6 Resin Fill Tank

A conically shaped, austenitic stainless steel resin fill tank is provided to prepare and sluice fresh resin slurry into the demineralizers.

9.1.3.7 Reactor Coolant and Condensate Filters

The filter collects resin fines and particulate matter larger than 25 microns. This filter uses replaceable cage assemblies which contain synthetic fiber cartridges. These cage assemblies may be replaced locally or remotely. Individual cartridges or a complete cage may be changed. The filter shells are of all welded austenitic stainless steel.

9.1.3.8 Volume Control Tank

The volume control tank collects excess water released from the Reactor Coolant System when the power level is increased from zero power to full power. Hydrogen pressure is maintained over the water in the volume control tank to control the hydrogen concentration in the reactor coolant water.

A spray nozzle located in the tank on the inlet line from the reactor coolant filter provides intimate contact between the gas and liquid phase. A remotely operated vent valve discharging to the Waste Disposal System permits removal of gaseous fission products which are stripped from the reactor coolant and collect in this tank. The volume control tank also acts as a head tank for the charging pumps. The tank is constructed of austenitic stainless steel.

9.1.3.9 Charging Pumps

Three charging pumps inject coolant into the Reactor Coolant System and reactor coolant pump shaft seals. Normally one pump is operating while the others serve as standby and provide additional capacity for certain plant operations. The pumps are the variable speed, positive displacement type with all parts in contact with the reactor coolant fabricated of austenitic stainless steel or equivalent corrosion resistant material. Stuffing box leakoffs are piped to the Waste Disposal System to prevent leakage of reactor coolant.

9.1.3.10 Seal Water Heat Exchanger

The seal water heat exchanger cools the reactor coolant pumps shaft seal leakoff flow and the discharge from the excess letdown heat exchanger. The unit is a shell and tube heat exchanger with seal leakage on the tube side and component cooling water on the shell side. The tubes and other surfaces in contact with reactor coolant are austenitic stainless steel, and the shell is carbon steel. Tubes are welded to the tube sheet.

9.1.3.11 Boric Acid Transfer Pumps

Two canned motor centrifugal pumps circulate boric acid solution through the boric acid tanks and boric acid filter, and inject boric acid into the charging pump suction header.

Either pump may function as standby for the other. All parts in contact with the solution are austenitic stainless steel or other material suitable for boric acid service.

9.1.3.12 Boric Acid Tanks

Boric acid solution recovered from the recycle processing train or mixed in the batching tank is stored in the boric acid tanks. One tank supplies boric acid for reactor coolant makeup while recycled solution from the concentrates holding tank is being accumulated in the second tank. The tanks are heated by electric immersion heaters. The concentration of boric acid.

solution used for makeup to the reactor coolant is maintained essentially constant by periodic manual sampling and corrective action. The concentration of recycle solution is determined by sampling the contents of the concentrates holding tank and corrected as required before storage in the boric acid tanks. The tanks are constructed of austenitic stainless steel.

9.1.3.13 Chemical Addition Tank

The chemical addition tank is used to inject chemical solution into the Reactor Coolant System. Its chief use is for the addition of caustic solutions for reactor coolant pH control and hydrazine for oxygen scavenging. The chemical addition tank is constructed of austenitic stainless steel.

9.1.3.14 Excess Letdown Heat Exchanger

The excess letdown heat exchanger provides a letdown flow path for coolant charged through the reactor coolant pump labyrinth seals if the normal letdown path through the regenerative heat exchanger is out of service. The high pressure letdown stream flows through the tubes while component cooling water flows through the shell. The tubes and tube sheet are austenitic stainless steel, and the shell is carbon steel. Tubes are welded to the tube sheet.

9.1.3.15 Batching Tank

The batching tank is used to mix boric acid solution for the boric acid tanks. The tank may also be used for solution storage. A local sampling point is provided for tank drainage and for checking the solution concentration prior to transferring to the boric acid tank. The batching tank is constructed of austenitic stainless steel with a carbon steel, steam jacketed lower head.

9.1.3.16 Electric Heaters

Two electric immersion heaters in each boric acid tank and the concentrates holding tank maintain the temperature of the acid at a level sufficient to assure solution. The heaters are sheathed in austenitic stainless steel.

9.1.3.17 Holdup Tanks

Three holdup tanks retain radioactive liquids. The contents of one tank are normally being processed by the gas stripper and boric acid evaporator while another tank is being filled. The third tank is normally kept empty to provide additional storage capacity if required. The tanks are stainless steel of welded construction.

9.1.3.18 Gas Stripper

The gas stripper removes dissolved gases from the borated water The stripper consists of a hot well to store stripped water, a stripping section packed with pall (or similar) rings, a spray type liquid inlet header, an overhead integral reflux condenser, and a discharge pump. The stripper is made of all welded austenitic stainless steel. Liquid fed to the gas stripper is automatically maintained at a constant rate by a flow controller. Liquid is pumped from the gas stripper to the boric acid evaporator.

9.1.3.19 Boric Acid Evaporator

The boric acid evaporator produces concentrated boric acid solution from the dilute boric acid feed on a semi-batch type basis. The boric acid evaporator package is a pre-assembled skid mounted unit. The evaporator package contains a feed tank, feed pumps, evaporator, condenser, distillate tank and pumps, piping and instrumentation.

The feed stream is concentrated using a low temperature, high vacuum evaporator process. Effluent from the feed tank is pumped into the evaporator where boiling takes place. The bottoms are continuously recycled back to the feed tank until the solution is concentrated to approximately 12% boric acid.

A series of demisters which remove aerosols from the steam are located above the U tube evaporator. Steam flows from the evaporator section to the condenser. Condensate from the condenser flows to the distillate tank. The entire evaporator package is austenitic stainless steel.

9.1.3.20 Deborating Demineralizers

Two anion demineralizers remove boric acid from the reactor coolant letdown flow through the Chemical and Volume Control System. They normally are used near the end of a core cycle, but can be used at any time. Hydroxyl form ion-exchange resin is used. Facilities are provided for regeneration of the resin whenever necessary. Resin which cannot be regenerated is flushed to the spent resin storage tank. The demineralizer vessels are made of all-welded austenitic stainless steel.

9.1.3.21 Boric Acid Evaporator Condensate demineralizer

Two anion demineralizers using hydroxyl form resin remove boric acid and negatively charged fission products contained in the boric acid evaporator condensate. Facilities are provided for regeneration of the resin whenever necessary. When spent resins cannot be regenerated, they are flushed to the spent resin storage tank. The demineralizer vessels are made of all-welded austenitic stainless steel.

9.1.3 22 Monitor Tanks

Two tanks collect boric acid evaporator condensate. Approximately once a day the contents are sampled and analyzed for radioactivity and purity. If the water is of sufficient purity and low in radioactivity, it may be transferred to the primary water storage tank for reuse by the primary plant or to the Waste Disposal System for discharge. When purity is low and radioactivity is high, the water is returned to the holdup tanks or evaporator condensate demineralizers for reprocessing. The monitor tanks are all-welded carbon steel lined with a suitable protective coating and have a flexible membrane to prevent aeration of the condensate.

9.1.3.23 Concentrates Holding Tank

The concentrates holding tank retains the evaporator concentrates for sampling and analysis. The concentrates are then pumped to the boric acid tanks or to the holdup tanks. The tank is constructed of austenitic stainless steel and is heated with electric immersion heaters.

9.1.3.24 Evaporator Feed Ion Exchangers

Three cation ion exchangers are installed for parallel or series operation to remove base ions and any cesium or molybdenum isotopes from the evaporator feed stream. Hydrogen form ion exchange resin is used. Spent resin is flushed to the spent resin storage tank. The ion exchange vessels are made of all-welded austenitic stainless steel.

9.1.3.25 Concentrates Filter

A filter with a bypass is provided to remove particulate matter from the evaporator concentrates. The filter has multiple disposal cartridges constructed of viscose or similar material. The filter shell is constructed of austenitic stainless steel.

9.1.3.26 Pumps

Pumps used throughout the recycle processing train are as follows:

a) Two gas stripper feed pumps
b) Two boric acid evaporator condensate pumps
c) Two monitor tank pumps
d) One holdup tanks recirculation pump
e) Two concentrates holding tank transfer pumps
f) Two boric acid evaporator concentrates transfer pumps
g) Two gas stripper bottoms pumps

The wetted surfaces of all pumps are stainless steel or other materials of equivalent corrosion resistance.

9.1.3.27 Valves

Valves that perform a modulating function are equipped with two sets of packing and an intermediate leakoff connection that discharges to the Waste Disposal System. All other valves have stem leakage control. Globe valves are installed with flow over the seats when such an arrangement reduces the possibility of leakage.

Stop valves are provided to isolate all connections to the Reactor Coolant System. Lines entering the reactor containment also have check valves to prevent reverse flow from the containment.

Relief valves are provided for lines and components that might be pressurized above design pressure by improper operation or component malfunction. Pressure relief for the tube side of the regenerative heat exchanger is provided by the auxiliary spray line isolation valve which is designed to open when pressure under the seat exceeds reactor coolant pressure by 250 psi.

9.1.3.28 Piping

All Chemical and Volume Control System piping is austenitic stainless steel except for the steam supply lines. All piping joints and connections are welded, except where flanged connections are required to facilitate equipment removal for maintenance and hydrostatic testing. Piping, valves, equipment and line-mounted instrumentation, which normally contain concentrated boric acid solution, are heated by electrical tracing to ensure solubility of the boric acid.

9.2 AUXILIARY COOLANT SYSTEM

9.2.1 DESIGN BASES

The Auxiliary Coolant System removes residual and sensible heat from the Reactor Coolant System during plant shutdown, cools the containment fan coolers, cools the spent fuel pit water, removes heat from the Waste Disposal System, cools the letdown flow in the Chemical and Volume Control System during power operation and provides cooling to dissipate waste heat from various primary plant components.

All piping and components of the Auxiliary Coolant System are designed to the applicable codes and standards listed in Table 9-2. The component cooling loop water contains a corrosion inhibitor to protect the carbon steel piping. Austenitic stainless steel piping is used in the residual heat removal loop, which contains reactor coolant, and in the spent fuel pit cooling loop, which contains water without inhibitor.

TABLE 9-2
AUXILIARY COOLANT SYSTEM CODE REQUIREMENTS

Component Cooling Heat Exchangers	ASME III*, Class C
Component Cooling Surge Tank	ASME III, Class C
Component Cooling Loop Piping and Valves	USA S.I. B31.1, Section 1
Residual Heat Exchangers	ASME III, Class C
Residual Heat Removal Piping and Valves	USA S.I. B31.1, Section 1
Spent Fuel Pit Heat Exchanger	ASME III, Class C
Spent Fuel Pit Filter	ASME III, Class C
Spent Fuel Pit Loop Piping and Valves	USA S.I. B31.1, Section 1

*ASME Boiler and Pressure Vessel Code, Section III, Nuclear Vessels

The Auxiliary Coolant System provides cooling for the following components and systems:

a) The seal water heat exchanger
b) The excess letdown heat exchanger
c) The sample heat exchangers
d) The residual heat exchangers
e) The non-regenerative heat exchanger
f) The spent fuel pit heat exchanger
g) The reactor coolant pumps
h) The Waste Disposal System
i) The residual heat removal pumps
j) Gas stripper package and the boric acid evaporator package (CVCS)
k) The containment fan coolers

The Auxiliary Coolant System consists of three loops: the Component Cooling Loop, the Residual Heat Removal Loop and the Spent Fuel Pit Cooling Loop as shown on Figure 9-4.

9.2.2 SYSTEM DESIGN AND OPERATION

9.2.2.1 Component Cooling Loop

The Component Cooling Loop removes heat from the residual, spent fuel pit, seal water, non-regenerative, excess letdown and sample heat exchangers, the containment fan coolers, the residual and reactor coolant pumps and Waste Disposal System. Component cooling water flows through these units in parallel flow circuits, picks up heat from the various components, and flows to the component cooling heat exchangers which are cooled by the Auxiliary Salt Water System. The Component Cooling Loop thus serves as an intermediate system between the reactor coolant and the Auxiliary Salt Water System. This double barrier arrangement reduces the probability of leakage of high pressure, potentially radioactive coolant to the Auxiliary Salt Water System.

During normal full power operation, two component cooling pumps and one component cooling heat exchanger accommodate the heat removal loads. A third standby pump provides 50% backup and a second heat exchanger provides 100 per cent backup during normal operation. Three pumps and two heat exchangers are used to remove the residual and sensible heat during plant shutdown. If one of the pumps or one of the heat exchangers is not operative, orderly shutdown is not affected; only the time for cooldown is extended.

Component cooling water circulated through the reactor coolant pumps removes heat from the bearing oil and the thermal barrier. The surge tank accommodates expansion, contraction and in-leakage of water and assures a continuous component cooling water supply until a leaking cooling line can be isolated. Because the tank is normally vented to the atmosphere, a radiation monitor in the component cooling pump inlet header annunciates in the control room and closes a valve in the vent line in the unlikely event that the radiation level reaches a preset level above the normal background.

9.2.2.2 Residual Heat Removal Loop

During the first phase of shutdown, the temperature of the Reactor Coolant System is reduced by transferring heat from the Reactor Coolant System to the steam generators. The Residual Heat Removal Loop removes residual heat from the core and reduces the temperature of the Reactor Coolant System during the second phase of plant cooldown. The Residual Heat Removal Loop is also used for Safety Injection and core cooling and its function in that capacity is described in Chapter 6.

The Residual Heat Removal loop consists of heat exchangers, pumps, piping and the necessary valves and instrumentation. During plant shutdown, coolant flows from the Reactor Coolant System to the residual heat removal pumps, through the tube side of the residual heat exchangers and back to the Reactor Coolant System. The inlet line to the Residual Heat Removal Loop starts at the hot leg of one reactor coolant loop and the return line connects to

the safety injection manifold which returns the fluid to the cold legs of all four loops. The residual heat exchangers are also used to cool the water circulated during the latter phase of Safety Injection System operation. The heat loads are transferred by the residual heat exchangers to the component cooling water.

During shutdown, the cooldown rate of the Reactor Coolant System is controlled by regulating the flow through the tube side of the residual heat exchangers. Two sets of parallel remotely-operated control valves downstream of the residual heat exchangers are used to control flow.

Double, remotely-operated valving is provided to isolate the Residual Heat Removal Loop from the Reactor Coolant System. When Reactor Coolant System pressure exceeds the design pressure of the Residual Heat Removal Loop, an interlock between the Reactor Coolant System wide range pressure channel and the first isolation valve prevents the valve from opening. A sealed control is provided for the second isolation valve. Two remotely-operated valves in parallel, and two check valves isolate each line to the Reactor Coolant System cold legs from the Residual Heat Removal Loop.

9.2.2.3 Spent Fuel Pit Cooling Loop

The Spent Fuel Pit Cooling Loop removes residual heat from fuel stored in the spent fuel pit. The loop is normally required to handle the heat load from 1/3 of the core freshly discharged from the reactor but it can safely accommodate the heat load from 1-1/3 cores for which there is available storage space. The spent fuel is placed in the pit during refueling and is stored until it is shipped to a reprocessing facility.

The Spent Fuel Pit Cooling Loop consists of a pump, heat exchanger, filter, demineralizer, piping and associated valves and instrumentation. The pump draws water from the pit, circulates it through the heat exchanger and returns it to the pit. A second pump is used to circulate refueling water during purification. Component cooling water cools the heat exchanger. Redundancy of this equipment is not required because of the large heat capacity

of the pit and the slow heat up rate. However, in the event of failure of the spent fuel pump alternate cooling connections are provided for connecting a temporary pump to the Spent Fuel Pit Cooling Loop.

The clarity and purity of the spent fuel pit water is maintained by passing approximately 10 per cent of the loop flow through a filter and demineralizer. The spent fuel pit pump suction line which is used to drain the pit penetrates the spent fuel pit wall above the fuel assemblies stored in the pit to prevent loss of water as a result of a suction line rupture.

9.2.2.4 Component Cooling Loop Components

a) Component Cooling Heat Exchangers

The component cooling heat exchangers are of the shell and straight tube type. The Auxiliary Salt Water System circulates water through the tubes while component cooling water circulates through the shell side. The shell is carbon steel and the tubes are of aluminum brass.

b) Component Cooling Pumps

The component cooling pumps which circulate component cooling water through the Component Cooling Loop are horizontal, centrifugal units of standard commercial construction.

c) Component Cooling Surge Tank

The component cooling surge tank which accommodates changes in component cooling water volume is constructed of carbon steel. In addition to piping connections, the tank has a flanged opening at the top for the addition of the chemical corrosion inhibitor to the Component Cooling Loop.

d) Valves

The valves used in the Component Cooling Loop are standard commercial valves constructed of carbon steel with bronze or stainless steel trim. Since the component cooling water is not normally radioactive, special features to prevent leakage to the atmosphere are not provided. Self-actuated, spring loaded relief valves are provided for lines and components that could be pressurized to their design pressure by improper operation or malfunction.

e) Piping

All Component Cooling Loop piping is carbon steel with welded joints and connections except at components which might need to be removed for maintenance.

9.2.2.5 Residual Heat Removal Loop Components

a) Residual Heat Exchangers

The residual heat exchangers are of the shell and U-tube type with the tubes welded to the sheet. Reactor coolant circulates through the tubes, while component cooling water circulates through the shell side. The tube and other surfaces in contact with reactor coolant are austenitic stainless steel and the shell is carbon steel.

b) Residual Heat Removal Pumps

The residual heat removal pumps are horizontal, centrifugal units with special seals to prevent reactor coolant leakage to the atmosphere.

All pump parts in contact with reactor coolant are austenitic stainless steel or equivalent corrosion resistant material.

c) Residual Heat Removal Loop Valves

The valves used in the Residual Heat Removal Loop are constructed of austenitic stainless steel or equivalent corrosion resistant material.

Manual stop valves are provided to isolate equipment for maintenance. Throttle valves are provided for remote and manual control of residual heat exchanger tube side flow. The Residual Heat Removal Loop is isolated from the cold legs of the Reactor Coolant System by stop valves and check valves.

Remotely operated stop valves, one with a pressure interlock the other with a sealed control, isolate the Residual Heat Removal Loop from the hot leg connection to the Reactor Coolant System.

Overpressure in the Residual Heat Removal Loop is relieved through a check valve to the low pressure letdown stream in the Chemical and Volume Control System.

Valves that perform a modulating function are equipped with two sets of packing and an intermediate leakoff connection that discharges to the Waste Disposal System. All other valves have stem leakage control features such as backseats. Leakoff connections are provided where required by valve size and fluid conditions.

d) Residual Heat Removal Piping

All Residual Heat Removal Loop piping is austenitic stainless steel. The piping is welded with flanged connections at the pumps.

9.2.2.6 Spent Fuel Pit Loop Components

a) Spent Fuel Pit Heat Exchanger

The spent fuel pit heat exchanger is of the shell and U-tube type with the tubes welded to the tube sheets. Component cooling water circulates through the shell, and spent fuel pit water circulates through the tubes. The tubes and other surfaces in contact with the spent fuel pit water are austenitic stainless steel and the shell is carbon steel.

b) Spent Fuel Pit Pump

The spent fuel pit pump circulates water in the spent fuel pit cooling loop. All wetted surfaces of the pump are austenitic stainless steel, or equivalent corrosion resistant material. The pump is operated manually from a local station.

c) Spent Fuel Pit Filter

The spent fuel pit filter removes particulate matter larger than 5 microns from the spent fuel pit water. The filter cartridge is a synthetic fiber and the vessel shell is austenitic stainless steel.

d) Spent Fuel Pit Cooling Loop Valves

Manual stop valves are used to isolate equipment and lines and manual throttle valves provide flow control. Valves in contact with spent fuel pit water are austenitic stainless steel or equivalent corrosion resistant material.

e) Spent Fuel Pit Cooling Loop Piping

All piping in contact with spent fuel pit water is austenitic stainless steel. The piping is welded except where flanged connections are used at the pump, heat exchanger, and filter to facilitate maintenance.

f) Spent Fuel Pit Demineralizer

A flushable, mixed bed demineralizer utilizing a hydrogen form cation resin and hydroxyl form anion resin maintains spent fuel pit water purity.

9.2.2.7 CONTAINMENT FAN COOLERS

The containment fan coolers are supplied from the component cooling water loop by dual supply and return headers which provide redundant flow paths to this equipment. The inlet line to each cooler unit can be connected to either supply header by normal shutoff valves and drain valves. Similarly, each discharge line from the coolers can be connected to either return header by manual shutoff valves and drain valves. This arrangement allows each cooler to be isolated individually for leak testing or to be drained and maintained open to the atmosphere during the integrated leakage tests.

--+

Since the coiling coils and component cooling water lines are completely closed inside containment, no leakage is expected from these units. The component cooling water system pressure at the inlet to the fan coolers is expected to be about 65 to 100 psig.

9.3 SAMPLING SYSTEM

9.3.1 DESIGN BASIS

The Sampling System provides a means to obtain fluid samples for laboratory analysis of reactor coolant chemistry and radiochemistry.

9.3.2 SYSTEM DESIGN AND OPERATION

The Sampling System, shown in Figure 9-5, is designed to provide representative samples for laboratory analysis used to guide the operation of the Reactor Coolant System, Auxiliary Coolant System and the Chemical and Volume Control System. These samples are used to determine both chemical and radiochemical conditions. Typical of the analyses performed on such samples are reactor coolant boron concentrations, fission product radioactivity level, dissolved gas content, and corrosion product concentration.

Analytical results are used in regulating boron concentration adjustment, evaluating fuel element integrity, evaluating mixed bed demineralizer performance, and in regulating additions of corrosion controlling chemicals to the systems. The Sampling System is designed to be operated manually, on an intermittent basis for conditions ranging from full power operation to cold shutdown.

Reactor coolant liquid and steam sample lines which are normally inaccessible or which require frequent sampling are sampled by means of permanently installed tubing leading to a central sampling room. Each of these sample lines inside the reactor containment has a remotely operated isolation valve close to the source of the sample. A delay coil is provided for decay of short-lived radioactive isotopes present in the reactor coolant system liquid sample. The samples are cooled as they flow through the sample heat exchangers and the pressure is reduced by pressure reducing valves. The reactor coolant then flows to the volume control tank or the Waste Disposal System through a purge line until sufficient purge volume has passed to permit collection of a representative sample in the sample vessels, or at the sample sink.

Liquid samples originating upstream and downstream of the Chemical and Volume Control System mixed bed demineralizer pass through the low pressure sample header to the sample sink.

A sample line from the accumulator tanks of the Safety Injection System permits the collection of a sample at the sample sink in order to check the boron concentration in the accumulator tank water.

Gaseous samples from the pressurizer relief tank of the Reactor Coolant System and the volume control tank of the Chemical and Volume Control System are collected in a sample vessel. The vessel is purged to the vent header of the Waste Disposal System. Local samples are collected in a sample vessel or other suitable container for transfer to the laboratory.

Because the pressurizer steam phase sample, the reactor coolant dissolved gas sample and volume control tank gas phase sample may contain accumulated radioactive gases, the respective sample vessel stations are located in small, well ventilated and shielded cubicles within the sampling room.

If remote handling of the sample vessels becomes necessary, extension handles can be used to operate the isolation valves and the quick-disconnect couplings.

The sample sink, which is contained in the laboratory bench as a part of the sampling hood, contains a drain line to the Waste Disposal System and is provided with a supply of demineralized water for flushing and cleanup purposes.

9.3.3 COMPONENTS

a) Sample Heat Exchangers

The sample heat exchangers reduce the sample temperature before it reaches the sample vessels. These units consist of coiled sections of tubing inside jackets. The sample stream flows through the coils and component cooling water from the Auxiliary Coolant System circulates through the jackets. All parts of the heat exchangers contacting the reactor coolant are austenitic stainless steel. The inlet and outlet ends have socket-weld joints for connection to the high pressure sample lines. Three heat exchangers are provided, one for pressurizer steam samples, one for pressurizer liquid samples, and the other for Reactor Coolant System or Residual Heat Removal Loop Samples.

b) Delay Coil

The high pressure reactor coolant sample line contains a delay coil consisting of tubing which has sufficient length to provide the required sample transit time to allow for decay of short lived isotopes.

c) High Pressure Sample Vessels

Each high pressure sample train contains a sample pressure vessel which is used to obtain dissolved gas samples. Integral isolation valves are furnished with the vessel and quick-disconnect coupling valves (containing poppet-type check valves) are connected to nipples extending from the valves on each end. The vessel, valves and couplings are austenitic stainless steel.

d) Sample Sink

The sample sink is located in a hooded enclosure which is equipped with an exhaust ventilator. The work area around the sink and the enclosure is large enough to provide space for radiation monitoring equipment in addition to the space needed for sample collection and storage. The sink perimeter has a raised edge to contain any spilled liquid.

In addition to the incoming sample lines, which may include lines from the secondary system, the enclosure is penetrated by a demineralized water line, which discharges into the sink. The sink and work area are stainless steel.

e) Volume Control Tank Sample Vessel

The volume control tank sample vessel is used to collect gas samples from the volume control tank in the Chemical and Volume Control System or from the pressurizer relief tank to determine the composition of the gases (primarily hydrogen and any fission gases) in the tanks.

f) Piping and Fittings

All liquid and gas sample lines are austenitic stainless steel tubing and are designed for high pressure service. With the exception of the sample vessel quick-disconnect couplings, socket welded joints are used throughout the Sampling System. Lines are located so as to be protected from accident damage during routine operation and maintenance.

g) Valves

Remotely operated stop valves are used to isolate all sample points and to route sample fluid flow inside the reactor containment. Manual stop valves are provided for component isolation and flow path control at all normally accessible Sampling System locations. Manual throttle valves are provided to adjust the sample flow rate. A check valve prevents excessive reverse flow of gas from the volume control tank into the sample sink. All valves in the system are constructed of austenitic stainless steel or equivalent corrosion resistant material.

9.4 FUEL HANDLING SYSTEM

9.4.1 DESIGN BASIS

The Fuel Handling System is designed to provide a safe, effective means of transporting and handling fuel from the time it reaches the plant in an unirradiated condition until it leaves the plant after post-irradiation cooling. The system is designed to minimize the possibility of mishandling or maloperations that would cause fuel damage and potential fission product release.

9.4.2 SYSTEM DESIGN AND OPERATION

The reactor is refueled with equipment designed to handle the spent fuel under water from the time it leaves the reactor vessel until it is placed in a cask for shipment from the site. Underwater transfer of spent fuel provides an effective, economic and transparent radiation shield, as well as a reliable cooling medium for removal of decay heat. Boric acid is added to the water to assure subcritical conditions during refueling.

The Fuel Handling System may be generally divided into two areas: the reactor cavity which is flooded only during plant shutdown for refueling and the spent fuel pit which is kept full of water and is always accessible to operating personnel. These two areas are connected by the Fuel Transfer System consisting of an underwater conveyor that carries the fuel through an opening in the reactor containment.

In the reactor cavity fuel is removed from the reactor vessel, transferred through the water and placed in the fuel transfer system by a manipulator crane. In the spent fuel pit the fuel is removed from the transfer system and placed in storage racks with long manual tools suspended from an overhead crane. After a sufficient decay period, the fuel is removed from storage and loaded into a shipping cask for removal from the site.

New fuel assemblies are stored in racks in the new fuel storage area. New fuel is transferred to the reactor by lowering it into the spent fuel pit and taking it through the transfer system. Alternately, the new fuel may be taken through the reactor containment equipment hatch and lowered directly into the reactor cavity. The new fuel storage area is sized for storage of the fuel assemblies and control rods normally associated with the replacement of one-third of a core. The fuel for the initial core loading will be temporarily stored in the spent fuel storage pit. The pit will be kept dry during this period.

9.4.3 FUEL HANDLING STRUCTURES

9.4.3.1 Reactor Cavity

The reactor cavity is a reinforced concrete structure that forms a pool above the reactor when it is filled with borated water for refueling. The cavity is filled to a depth that limits the radiation at the surface of the water to 50 milliroentgens per hour during those brief periods when a fuel assembly is transferred over the reactor vessel flange and is at the closest approach to the surface of the water.

The reactor vessel flange is sealed to the bottom of the reactor cavity by a bolted, gasketed seal ring which prevents leakage of refueling water from the cavity. This seal is fastened and closed after reactor cooldown but prior to flooding the cavity for refueling operations.

The cavity is large enough to provide storage space for the reactor upper internals, the control cluster drive shafts, and miscellaneous refueling tools. Space is also allowed for the storage of the lower internals if required.

The floor and sides of the reactor cavity are lined with stainless steel.

9.4.3.2 Fuel Transfer Canal

The fuel transfer canal is a passageway extending from the reactor cavity to the inside surface of the reactor containment. The canal is formed by two concrete shielding walls, which extend upward to the same elevation as the reactor cavity. The floor of the canal is at a lower elevation than the reactor cavity to provide the greater depth required for the Fuel Transfer System tipping device and the control cluster changing fixture located in the canal. The transfer tube enters the reactor containment and protrudes through the end of the canal. Canal wall and floor linings are stainless steel similar to the reactor cavity.

9.4.3.3 Spent Fuel Storage Pit

The spent fuel storage pit is designed for the underwater storage of spent fuel assemblies and control rods after their removal from the reactor. It is designed to accommodate a total of one and one-third cores. Space is provided in the pit for approximately 257 fuel assemblies and a shipping cask.

Spent fuel assemblies are handled by a long handled tool suspended from an overhead monorail electric hoist and manipulated by an operator standing on a movable bridge over the pit. The spent fuel storage pit is constructed of reinforced concrete. The entire interior basin face and transfer canal are lined with stainless steel plate.

A storage rack erected on the pit floor is provided to hold spent fuel assemblies. Fuel assemblies will be placed in vertical cells, continuously grouped in parallel rows approximately 21 inches on centers in both directions. The racks are designed so that it is impossible to insert fuel assemblies in other than the prescribed locations, thereby assuring the necessary spacing between assemblies to prevent criticality even if the pit were inadvertantly filled with unborated water. Control rod clusters are stored in the fuel assemblies.

9.4.3.4 New Fuel Storage and Decontamination Facilities

New fuel assemblies and control rods are stored in a separate area where they are unloaded from trucks. This separate storage vault is designed to hold 64 new fuel assemblies in specially constructed racks and is used primarily for the storage of the one-third replacement core. The assemblies which make up the remaining two-thirds of a first core will be stored in the spent fuel pit. The new fuel assemblies are stored in racks in parallel rows having a center-to-center distance of approximately 21 inches.

Decontamination facilities, consisting of an equipment and cask pit, are located adjacent to the spent fuel storage pit. Cask handling and other tools can be cleaned and decontaminated in the cask decontamination pit. The outside surfaces of the casks are decontaminated, if required, by using steam, water, detergent solutions, and manual scrubbing to the extent required.

9.4.4 FUEL HANDLING EQUIPMENT

9.4.4.1 Reactor Vessel Stud Tensioner

Stud tensioners are used to make up the head closure joint and during this process all studs are stretch tested to more than nominal working loads at every refueling.

The stud tensioner is a hydraulically operated (oil as the working fluid) device provided to permit preloading and unloading of the reactor vessel closure studs at cold shutdown conditions. Stud tensioners were chosen in order to minimize the time required for the tensioning or unloading operations. Three tensioners are provided and they are applied simultaneously to three studs 120° apart. One hydraulic pumping unit operates the tensioners which are hydraulically connected in series. The studs are tensioned to their operational load in two steps to prevent high stresses in the flange region and unequal loadings in the studs. Relief valves are provided on each tensioner to prevent overtensioning of the studs due to excessive pressure.

Charts indicating the stud elongation and load for a given oil pressure are included in the tensioner operating instructions. In addition, micrometers are provided to measure the elongation of the studs after tensioning.

9.4.4.2 Reactor Vessel Head Lifting Device

The reactor vessel head lifting device consists of a welded and bolted structural steel frame with suitable rigging to enable the crane operator to lift the head and store it during refueling operations. The lifting device is permanently attached to the reactor vessel head and includes means for directing cooling air to the control cluster drive mechanisms.

9.4.4.3 Reactor Internals Lifting Device

The reactor internals lifting device is a structural frame suspended from the overhead crane on a long sling. The frame is lowered onto the guide tube support plate of the internals and air operated latching pins are remotely actuated to engage lifting lugs on the support plate. Bushings on the frame engage guide studs in the vessel flange to provide close guidance during removal and replacement of the internals package.

9.4.4.4 Manipulator Crane

The manipulator crane is a motor driven rectilinear bridge and trolley crane with a vertical mast tube extending down into the refueling water. The bridge spans the reactor and refueling cavity and runs on rails set into the floor along the edge of the cavity. The bridge and trolley motions are used to position the vertical mast over a fuel assembly in the core. A long tube with a pneumatic gripper on the end is lowered down out of the mast tube to grip the fuel assembly. The gripper tube is long enough so the upper end is still contained in the mast tube when the gripper end contacts the fuel. A winch mounted on the trolley raises the gripper tube and fuel assembly up into the mast tube. The fuel is transported while inside the mast tube to its new position.

9.4.4.5 Spent Fuel Pit Bridge

The spent fuel pit bridge is a wheel-mounted motor driven walkway spanning the spent fuel pit. An overhead beam over one side of the walkway supports a monorail electric hoist for use with long handled tools. The hoist travel, tool, and sling length are designed to limit the maximum lift of a fuel assembly to a safe shielding depth.

9.4.4.6 Fuel Transfer System

The Fuel Transfer System, shown in Figure 9-6, is an underwater cable, motor driven conveyor car that runs on tracks extending from the refueling canal through the transfer tube and into the spent fuel pit. The conveyor car receives a fuel assembly in the vertical position from the manipulator crane. The fuel assembly is lowered to a horizontal position for passage through the tube, and then it is raised to a vertical position in the spent fuel pit.

During plant operation, the conveyor car is stored in the refueling canal. A gate valve in the transfer tube is closed to permit placement of the seal flange at the reactor end of the refueling canal tube.

9.4.4.7 Rod Cluster Control Changing Fixture

A fixture is mounted on the reactor cavity wall for removing rod cluster control (RCC) elements from spent fuel assemblies and inserting them into new fuel assemblies. The fixture consists of two main components; a guide tube mounted to the wall for containing and guiding the RCC element, and a wheel-mounted carriage for holding the fuel assemblies and positioning fuel assemblies under the guide tube. The guide tube also contains a pneumatic gripper on a winch that grips the RCC element and lifts it out of the fuel assembly. By repositioning the carriage, a new fuel assembly is brought under the guide tube and the gripper lowers the RCC element and releases it. The manipulator crane loads and removes the fuel assemblies into and out of the carriage.

9.4.5 REFUELING OPERATION

The refueling operation will follow a detailed procedure which will be established to provide a safe, efficient refueling operation. The following significant points will be assured by the refueling procedure:

1) The refueling water and the reactor coolant will contain approximately 2,100 ppm boron. The concentration together with the control rods is sufficient to keep the core approximately 10% $\delta k/k$ subcritical during the refueling operations. It is also sufficient to maintain the core shutdown if all of the RCC assemblies were removed from the core.

2) The water level in the refueling canal will be high enough to keep the radiation levels within acceptable limits when the fuel assemblies are being removed from the core. This water also provides adequate cooling for the fuel assemblies during transfer operations.

3) Fuel handling operations and equipment will be designed so that the possibility of fuel mishandling or damage is minimized.

9.4.6 HANDLING OF FAILED FUEL ASSEMBLIES

Equipment will be provided to permit detection of fuel assemblies which contain cladding defects. The presently contemplated method would be used during core refueling and would consist of placing suspected fuel assemblies in an isolated chamber and testing for the presence of fission products. Appropriate safeguards to prevent fuel damage during leak testing will be included in the design of this equipment.

Defective fuel assemblies will be suitably contained during movement from the reactor cavity (where leak testing will be performed) to the spent fuel storage pit. Containers for the off-site shipment of spent fuel will be designed to comply with the requirements of 10 CFR 71.

9.5 FACILITY SERVICES

9.5.1 PLANT FIRE PROTECTION SYSTEM

9.5.1.1 Protective Equipment

Normal fire protection will be provided by sprinkler systems, fixed water deluge systems, a fixed CO_2 system, hose lines, and portable extinguishers.

9.5.1.2 Coverage

Wet pipe sprinkler systems will provide protection for the warehouse and miscellaneous combustible storage areas. Fixed remote manual actuated deluge systems will provide protection for the turbine lube oil system and for oil storage and handling areas which are not protected by fixed CO_2 systems. Readily accessible 1-1/2 inch rubber lined hose lines and continuous flow type hose reels will be distributed throughout the plant so that all hazards in the plant are within reach of at least two nozzels when attached to not more than 100 foot lengths of hose.

A fixed CO_2 system will supply automatic temperature operated discharge to lube oil reservoirs, closed oil storage rooms, diesel generator sets, and main turbine generator journal bearings. This system is also used for manual purging of the generator casing and to supply manually operated hose reels located near other potential fire hazards.

The plant will be provided with portable chemical fire extinguishers.

9.5.1.3 Water Supply

The plant will be looped with a fire water line of sufficient size to deliver an adequate quantity of water throughout the plant at sufficient pressure to service all outlets. The plant fire water loop will have two separate sources of supply and will be sized for 1500 GPM with 100 psig available at the highest plant operating level. The normal source will be from the plant raw water system with provisions for a minimum fire system reserve storage of 300,000 gallons. The emergency source will be from two 1500 GPM wet pit, vertical, centrifugal sea water fire pumps located at the plant intake structure. One pump is electric motor driven and one is diesel engine driven. Both emergency pumps are automatically started by low fire system pressure or high fire system demand.

9.5.1.4 Alarm System

A fire warning system will be provided as an integral part of the automatic CO_2 system, the sprinkler systems, and the water deluge systems to indicate automatic operation or alarm in the control room in case of fire.

9.5.2 SERVICE WATER SYSTEM

The service water system is a closed cooling water system which supplies buffered cooling water for plant equipment in the turbine building. The water in the service water system is cooled in the service water heat exchangers by the condenser circulating water system. During demusseling, cooling water is provided by the Auxiliary Salt Water System. Figure 9-7 shows a flow diagram of the service water system.

9.5.3 AUXILIARY SALT WATER SYSTEM

The Auxiliary Salt Water System supplies cooling water to the component cooling heat exchangers and to the emergency diesel-generator sets.

Four half-size electric-motor-driven centrifugal auxiliary salt water pumps are provided. Figure 9-8 shows a flow diagram of the system. Two auxiliary salt water pumps are sufficient to supply cooling water requirements for these exchangers during a normal shutdown or loss-of-coolant accident.

All valves in the Auxiliary Salt Water System are manually operated. The auxiliary salt water pumps are powered from separate electrical buses which can be fed from the emergency diesel-generators in the event of loss of normal auxiliary power.

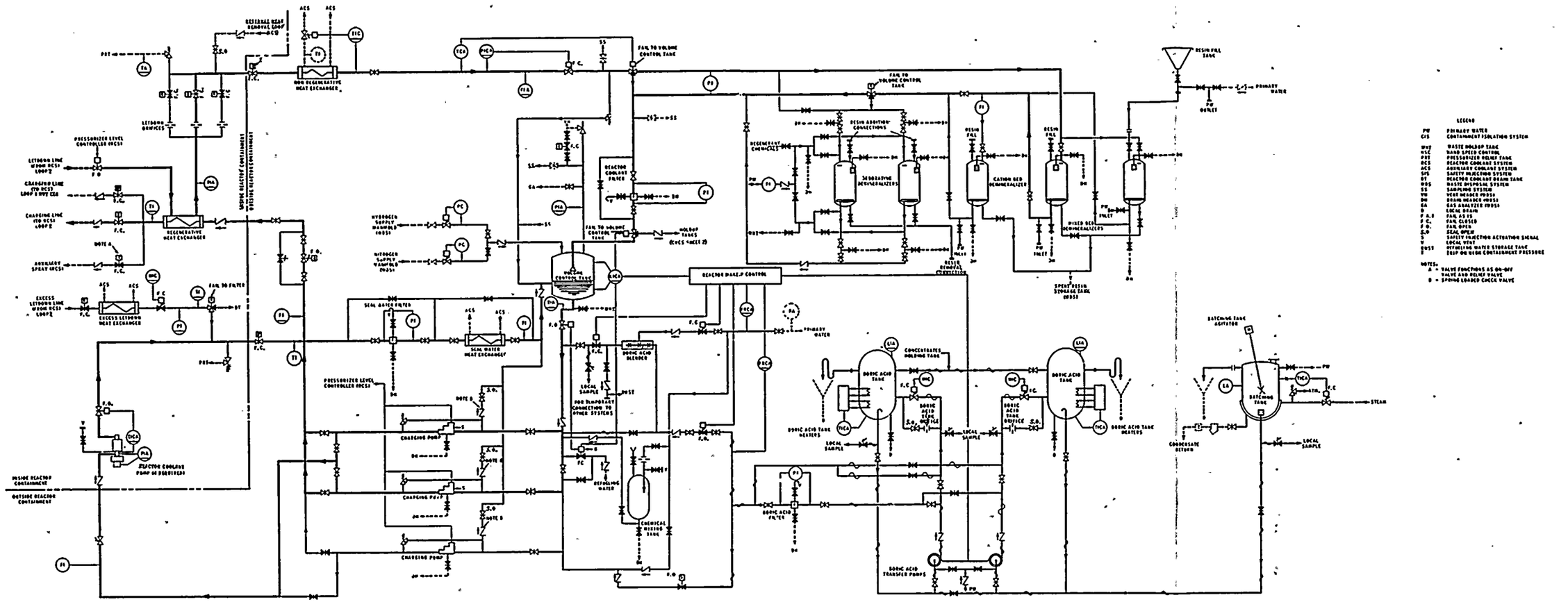

LEGEND

PW	PRIMARY WATER
CIS	CONTAINMENT ISOLATION SYSTEM
WHT	WASTE HOLDUP TANK
HSC	HAND SPEED CONTROL
PRT	PRESSURIZER RELIEF TANK
RCS	REACTOR COOLANT SYSTEM
ACS	AUXILIARY COOLANT SYSTEM
SFS	SAFETY INJECTION SYSTEM
RT	REACTOR COOLANT DRAIN TANK
WDS	WASTE DISPOSAL SYSTEM
SS	SAMPLING SYSTEM
VN	VENT HEADER (WDS)
DH	DRAIN HEADER (WDS)
GA	GAS ANALYZER (WDS)
D	LOCAL DRAIN
F.A.O	FAIL AS IS
F.C.	FAIL CLOSED
F.O.	FAIL OPEN
S.O	SEAL OPEN
S	SAFETY INJECTION ACTUATION SIGNAL
V	LOCAL VENT
DOSS	DEFUELING WATER STORAGE TANK
	TRIP ON HIGH CONTAINMENT PRESSURE

NOTES:
A - VALVE FUNCTIONS AS ON-OFF VALVE AND RELIEF VALVE
B - SPRING LOADED CHECK VALVE

CHEMICAL AND VOLUME CONTROL SYSTEM (Sht. 1)
(Revised 7-24-67) FIG. 9-1

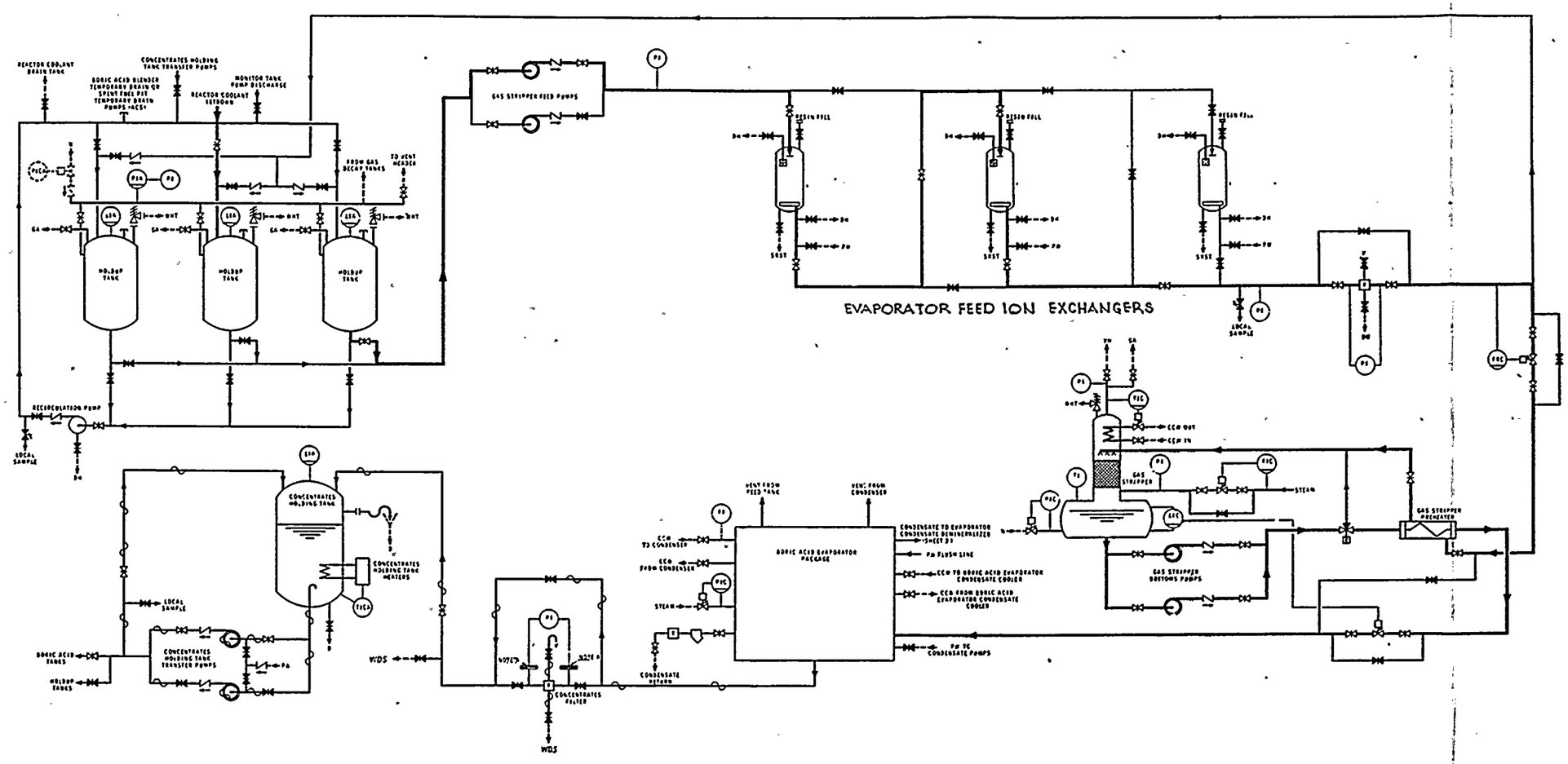

LEGEND

PW - PRIMARY WATER
CCW - COMPONENT COOLING WATER
WDS - WASTE DISPOSAL SYSTEM
VS - VENTILATION SYSTEM
DH - DRAIN HEADER
VH - VENT HEADER
GA - AUTOMATIC GAS ANALYZER (WDS)
N - NITROGEN SUPPLY MANIFOLD (WDS)
V - LOCAL VENT
D - LOCAL DRAIN
HEAT TRACING
SRST - SPENT RESIN STORAGE TANK
WHT - WASTE HOLDUP TANK

NOTE
A. DIAPHRAM SEAL

CHEMICAL AND VOLUME CONTROL SYSTEM (Sht. 2)
(Revised 7-24-67) FIG. 9-2

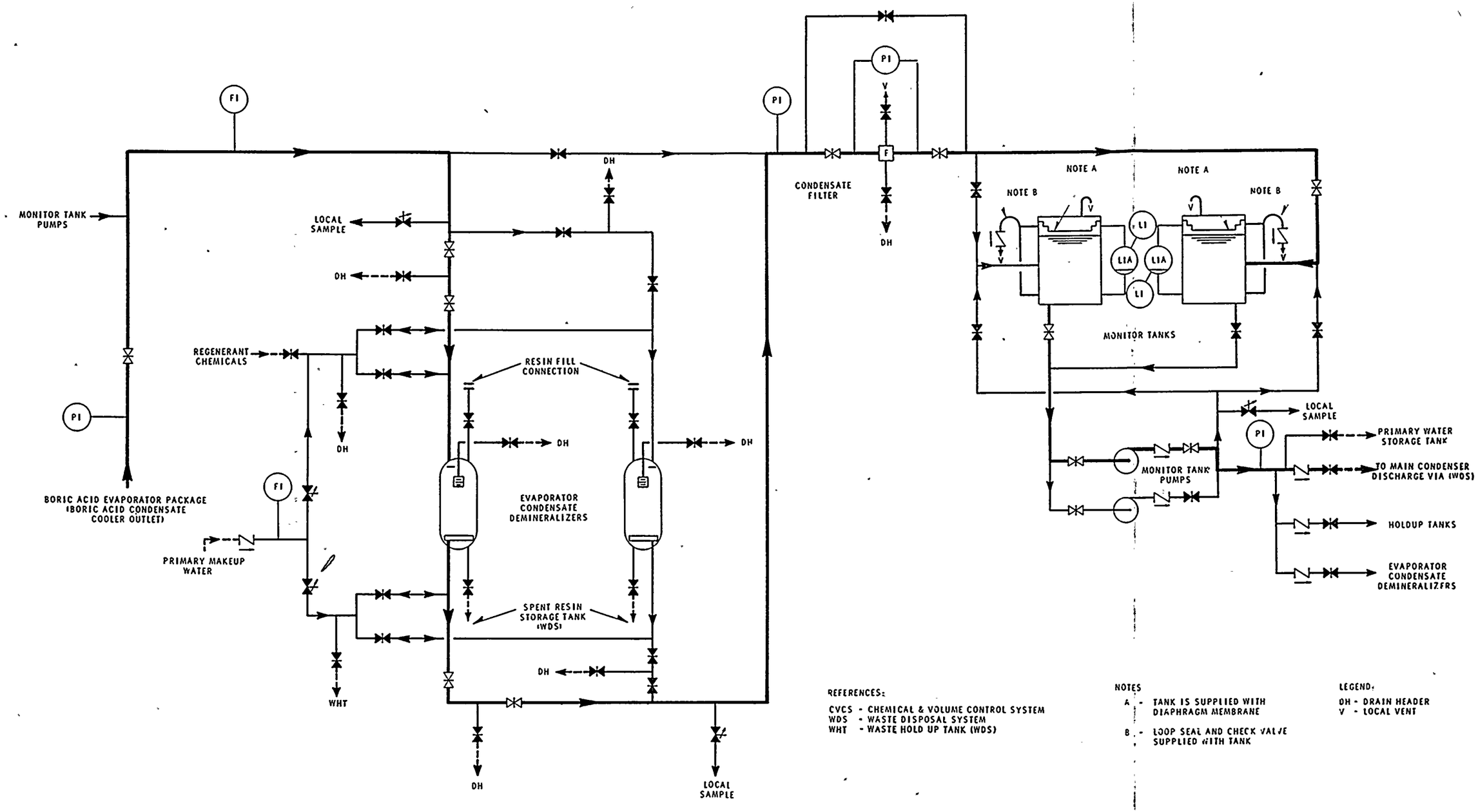

REFERENCES:

CVCS - CHEMICAL & VOLUME CONTROL SYSTEM
WDS - WASTE DISPOSAL SYSTEM
WHT - WASTE HOLD UP TANK (WDS)

NOTES

A - TANK IS SUPPLIED WITH DIAPHRAGM MEMBRANE

B - LOOP SEAL AND CHECK VALVE SUPPLIED WITH TANK

LEGEND:

DH - DRAIN HEADER
V - LOCAL VENT

CHEMICAL AND VOLUME CONTROL SYSTEM (Sht. 3)
(Revised 7-24-67) FIG. 9-3

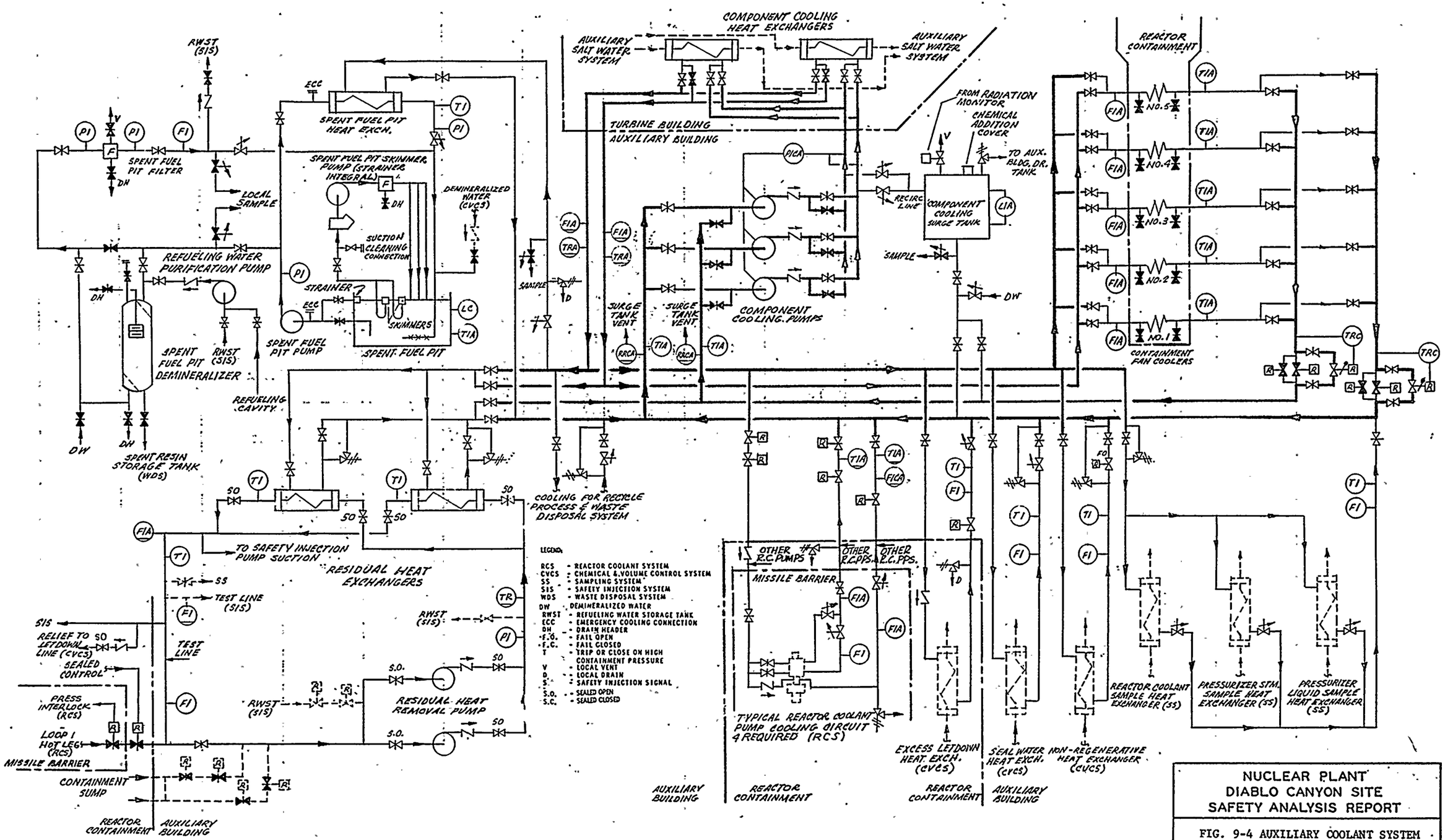

NUCLEAR PLANT
DIABLO CANYON SITE
SAFETY ANALYSIS REPORT

FIG. 9-4 AUXILIARY COOLANT SYSTEM
(Revised 7-31-67)

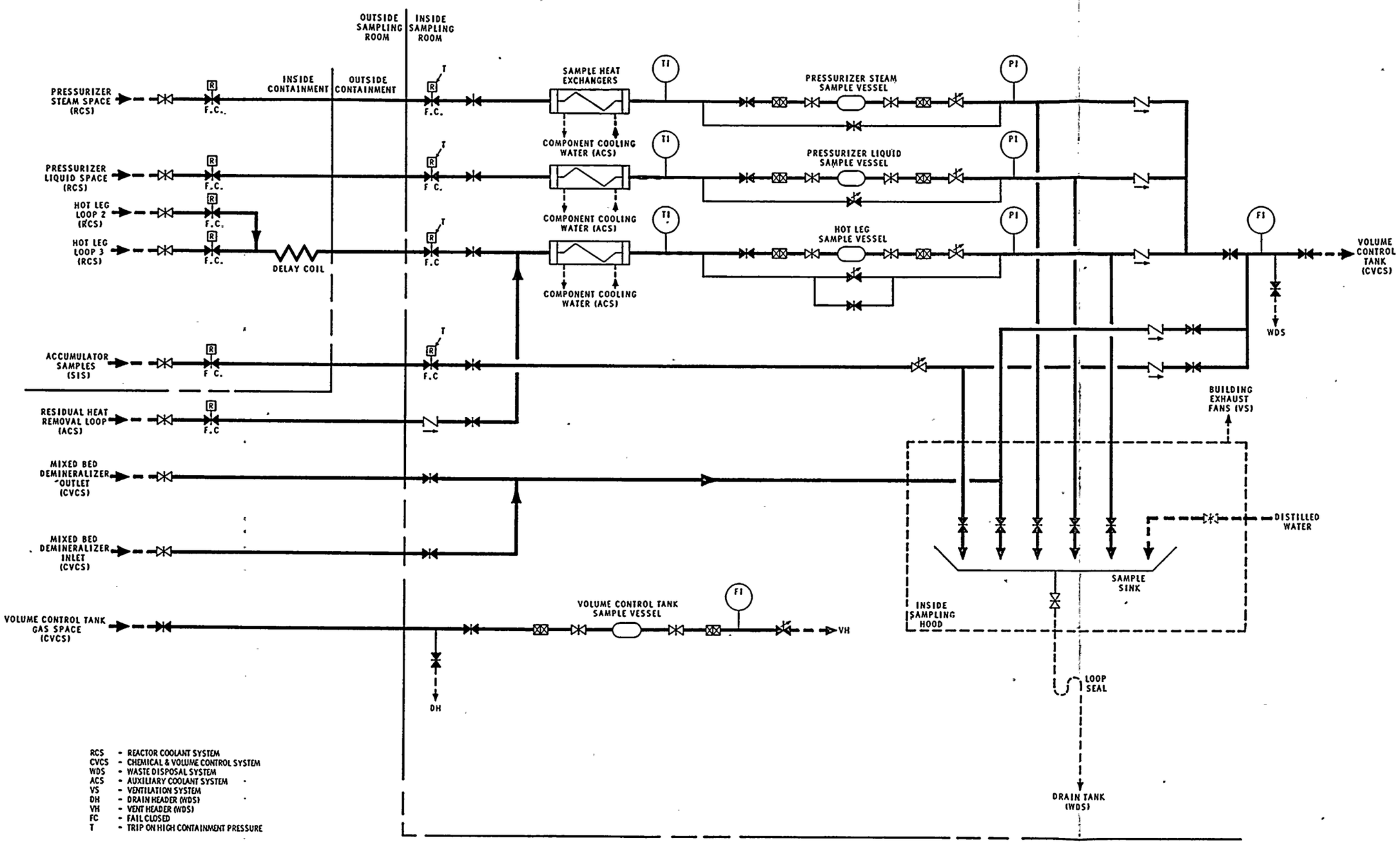

SAMPLING SYSTEM
(Revised 7-24-67) FIG. 9-5

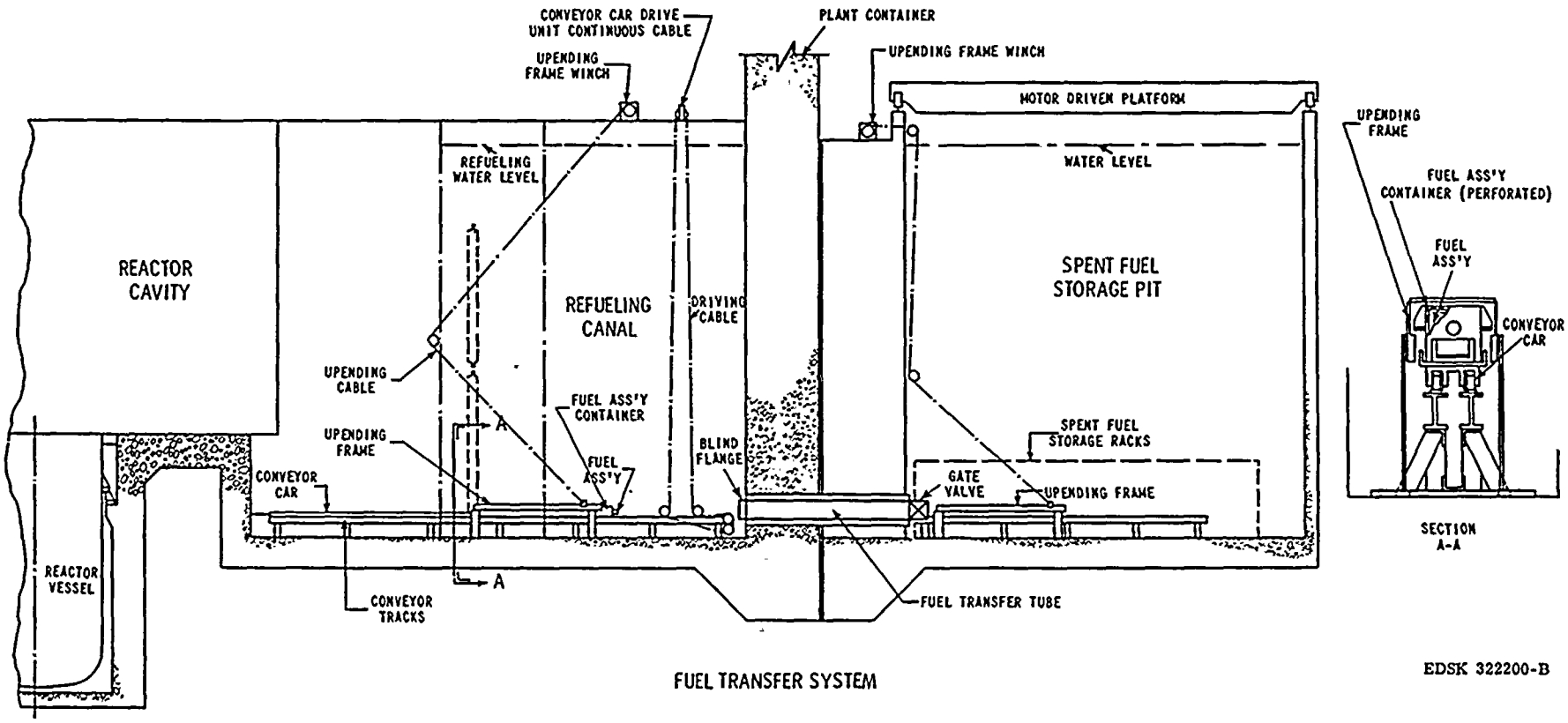

FUEL TRANSFER SYSTEM

EDSK 322200-B

FUEL TRANSFER SYSTEM
FIG. 9-6

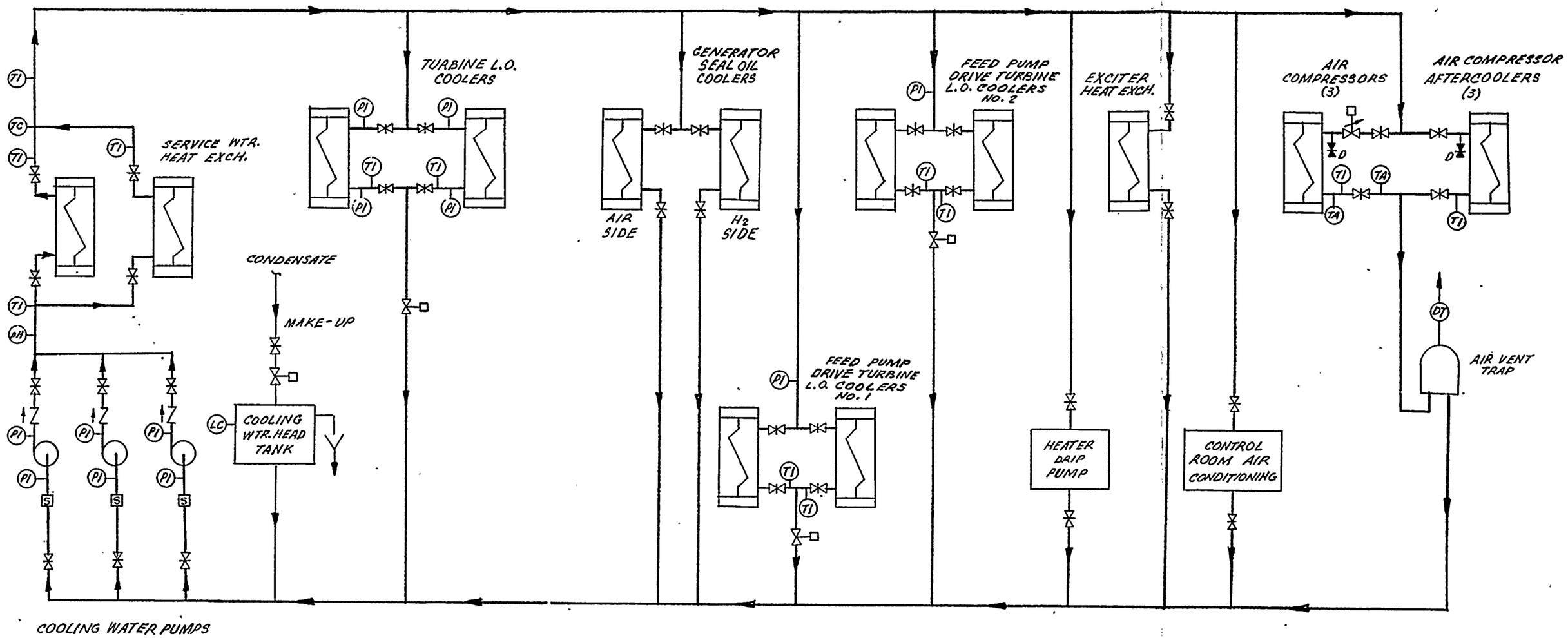

NUCLEAR PLANT
DIABLO CANYON SITE
SAFETY ANALYSIS REPORT

FIG. 9-7 SERVICE WATER SYSTEM
(Revised 7-24-67)

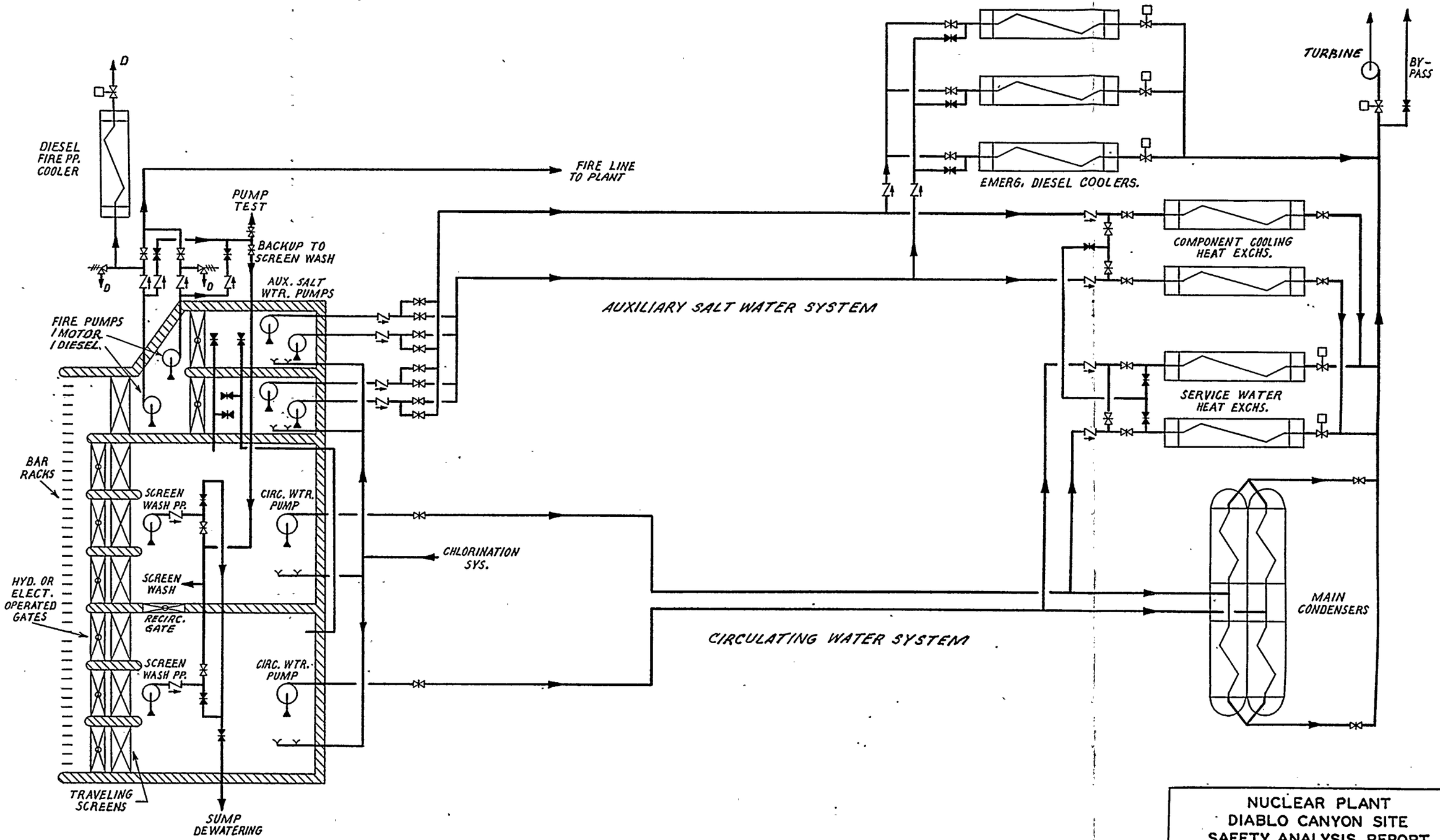

NUCLEAR PLANT
DIABLO CANYON SITE
SAFETY ANALYSIS REPORT

FIG. 9-8. SALT WATER SYSTEMS
(Revised 7-24-67)

TABLE OF CONTENTS

Section	Title	Page
CHAPTER 10	STEAM AND POWER CONVERSION SYSTEM	
10.1	Design Basis	10-1
10.2	System Design and Operation	10-1
10.2.1	Turbine Generator	10-1
10.2.2	Steam System	10-1
10.2.3	Condensate and Feedwater	10-2
10.2.4	Circulating Water	10-4
10.3	Turbine Controls	10-4
10.3.1	Electro-Hydraulic Control System	10-4
10.3.2	Steam Flow Control	10-4
10.3.3	Protective Devices	10-5

CHAPTER 10 STEAM AND POWER CONVERSION SYSTEM

10.1 DESIGN BASIS

The steam and power conversion system is designed to convert the reactor heat into useful electric energy. Four steam generators transfer the heat from the reactor coolant to the main steam system. Sufficient steam is produced to drive a turbine generator unit rated at 1090 MWe gross. The turbine by-pass system is designed to pass sufficient steam to prevent a reactor trip following a loss of system load.

10.2 SYSTEM DESIGN AND OPERATION

10.2.1 TURBINE GENERATOR

The turbine is a four casing, tandem-compound, six flow exhaust, 1800 rpm unit with 44-inch last row blades. The turbine consists of one double-flow high-pressure element in tandem with three double-flow low-pressure elements. Combination moisture-separator steam reheater assemblies are provided. The turbine generator has a maximum guaranteed rating of 1090 MWe gross with inlet steam conditions of 710 psia, 504.7^{o}F, exhausting at 1.5 inches of mercury absolute, with zero percent makeup and six stages of feedwater heating.

The hydrogen inner-cooled generator with a water cooled stator is rated at 1,260 mva at 75 psig gas pressure. Field excitation is provided by a coupled brushless exciter.

10.2.2 STEAM SYSTEM

The preliminary arrangement of the equipment associated with the steam and power conversion system is shown in Figure 10-1. Steam from the four steam generators supplies the turbine generator unit. After expanding through

the high-pressure turbine element, steam flows through reheaters to the three low-pressure turbine elements. Six stages of extraction for feedwater heating are provided, two from the high-pressure element and four from the low-pressure elements.

There are six combined moisture separator-steam reheater assemblies between the high-pressure and low-pressure elements. Wet steam from the exhaust of the high-pressure turbine element enters an assembly and is distributed by internal manifolds in the lower section. The steam then rises through a wire mesh moisture separator where the moisture is removed and drained to a drain tank. The steam leaving the wire mesh separator is reheated by flowing over a tube bundle before going to the low-pressure turbine elements and to the boiler feed pump drive turbines. The tube bundle is heated with steam from ahead of the turbine throttle. This steam condenses in the tubes and leaves as condensate which flows to the high-pressure heater drain tank.

The main condenser consists of four single-pass tube banks contained in two welded steel shells. The condenser tubes are arranged parallel to the turbine shaft. The hotwells are the deaerating type with sufficient storage for five minutes operation at maximum plant load. Sufficient surface is provided to condense turbine by-pass steam following a full load rejection, or under controlled startup conditions, or from residual and decay heat at shutdown.

Air will be removed from the condenser by steam jet air ejectors or wet-type, rotary vacuum pumps.

10.2.3 CONDENSATE AND FEEDWATER

The feedwater heating system is the closed type with deaeration accomplished in the condenser hotwells. Condensate is pumped through generator hydrogen coolers and stator coolers, the air ejector condensers, and the gland steam condenser to the suction of the condensate booster pumps which pump the con-

densate through five stages of low pressure feedwater heaters to the feedwater pumps. The water discharged from the feedwater pumps flows through the high pressure heaters into the steam generators. All feedwater heaters are horizontal, one-third size units (three strings).

There are three multi-stage one-half capacity, vertical, can-type, centrifugual condensate pumps with vertical motor drives and common suction and common discharge manifolds. Three condensate booster pumps are provided. These are one-half capacity horizontal, split case, centrifugal, motor-driven pumps with common suction and discharge manifolds. Two one-half capacity, high-speed, turbine driven feedwater pumps are provided with common suction and discharge manifolds. Each pump is equipped with minimum flow protective devices.

Feedwater will flow to the steam generators through four lines penetrating the containment, one line for each steam generator. A flow regulator, motor operated stop valve and a check valve will be installed in each line outside the containment.

Three emergency feedwater pumps are provided. One 800 gpm, full-size pump is steam-turbine driven, using steam from the steam generators produced from decay heat removal, and is suitable to assure adequate feed flow to the steam generators for decay heat removal during a complete loss of auxiliary power. The two other pumps are each half-size, motor-driven units and are fed from the vital 4.16 kv buses.

Drains from the high pressure heaters drain to a high pressure heater drain tank with the flashed steam vented to the preceding low-pressure heater. The heater drip pumps take suction from the heater drain tank and discharge to the feedwater pump suction manifold. Drains from the four lower pressure heaters cascade to the condenser.

10.2.4 CIRCULATING WATER

Condenser circulating water will be sea water from the Pacific Ocean. The ocean water level will normally vary between 0.0 and (+)7.0 feet mean lower low datum.

A pump-turbine head recovery circulating water system will be used to recover a major portion of the energy available in the water falling from the condenser elevation to sea level. The pump-turbine system will consist of two circulating water pumps with motors at the intake structure and one hydraulic turbine-generator unit at the circulating water discharge outfall. The hydraulic generator will feed electrically into the station auxiliary bus. The plant will be able to operate at full load with the hydraulic turbine-generator out of operation and by-passed.

The sea water flowing into the intake structure will flow under a curtain wall, through bar racks and automatic starting traveling water screens with 3/8" square openings to prevent debris from entering the intake structure

Provisions will be made in the circulating water system to demussel the tunnels and piping by thermal shock. The water temperature in the system may be raised to about 110°F by recirculation.

10.3 TURBINE CONTROLS

10.3.1 ELECTRO-HYDRAULIC CONTROL SYSTEM

The turbine is equipped with an electro-hydraulic control system which uses a solid state electronic controller and a high-pressure fire resistant fluid supply system to control valve movement. The high-pressure hydraulic fluid system is independent of the lubricating oil system.

The electro-hydraulic control system includes the following features:

1. Control of the turbine from a central control room

2. Solid state electronic controller including:
   a. Load limit control
   b. Auxiliary governor control
   c. Speed control
   d. Load control
3. High-pressure, hydraulic fluid pumping unit

10.3.2 STEAM FLOW CONTROL

The flow control of the main inlet steam is accomplished by the use of four stop valves and four control valves. One stop and one control valve form a single assembly which is anchored to the foundation.

An electro-hydraulic, servo-actuator controls each stop valve so that it is either in the wide-open or fully closed position. The major function of these stop valves is to shut off the flow of steam to the turbine.

whenever the unit is tripped for any reason. Trip closing of the stop valves is accomplished by actuation of the emergency trip device, (see Section 10.3.3) which is independent of the electronic controller.

The turbine control valves are positioned by an electro-hydraulic servo-actuator in response to a signal from the electronic controller. The controller signal will position the control valves for wide range speed control during startup and for load control after the unit is synchronized. The auxiliary governor section of the electronic controller will respond to a preset acceleration rate (caused by a loss of electrical load) causing the control valves to close rapidly.

Main steam passes through the stop and control valves, through the main steam inlet leads into the blade path of the high-pressure turbine. The high-pressure turbine exhausts into the moisture-separators and reheaters. Located between each reheater and a low-pressure turbine inlet are two valves; a reheat stop valve and a reheat intercept valve. Their purpose is to control the steam flow to the low-pressure turbines in the event of turbine overspeed or turbine trip. The reheat stop valves and the reheat intercept valves are open-closed type valves. Both are closed immediately upon operation of the emergency trip device (see Section 10.3.3). The reheat intercept valves are actuated by the auxiliary governor in response to a high acceleration rate following a loss of electrical load.

10.3.3 PROTECTIVE DEVICES

The following protective devices are independent of the electronic controller and when initiated will cause tripping of all turbine valves through the emergency trip valve:

1. Mechanical hydraulic overspeed trip
2. Low bearing oil pressure trip
3. Low vacuum trip
4. Thrust bearing trip
5. Electrical solenoid trip

The mechanical overspeed trip mechanism consists of an eccentric weight mounted in the end of the turbine shaft, which is balanced in position by a spring until the speed reaches approximately 110 percent of rated speed. Centrifugal force then overcomes the spring and the weight flies out striking a trigger which trips the overspeed trip valve and releases the protection system fluid (auto stop circuit) to drain. The resulting decrease in auto stop pressure causes the governing emergency trip valve to dump the hydraulic fluid pressure to drain thereby closing the main stop and control valves and the reheat stop and intercept valves.

The auto stop valve is also tripped when any one of the protective trip devices is actuated. The protective devices are all included in a separate assembly, but connect hydraulically to the overspeed trip valve through the trip relay.

Additional protective features include:

1. Automatic load runback initiated by a dropped rod signal
2. Turbine trip following a reactor trip
3. Stop-check valve in each steam generator steam line
4. Safety valves in each steam generator outlet main steam line
5. Safety valves in the moisture separator - reheater inlet piping
6. Extraction line non-return valves.

Automatic turbine load runback is initiated by a signal from a dropped rod control cluster assembly as indicated by either a rapid decrease in nuclear flux or by the rod bottom on-off controllers.

An air pilot valve, used to control extraction non-return valves, is also actuated from the auto stop pressure.

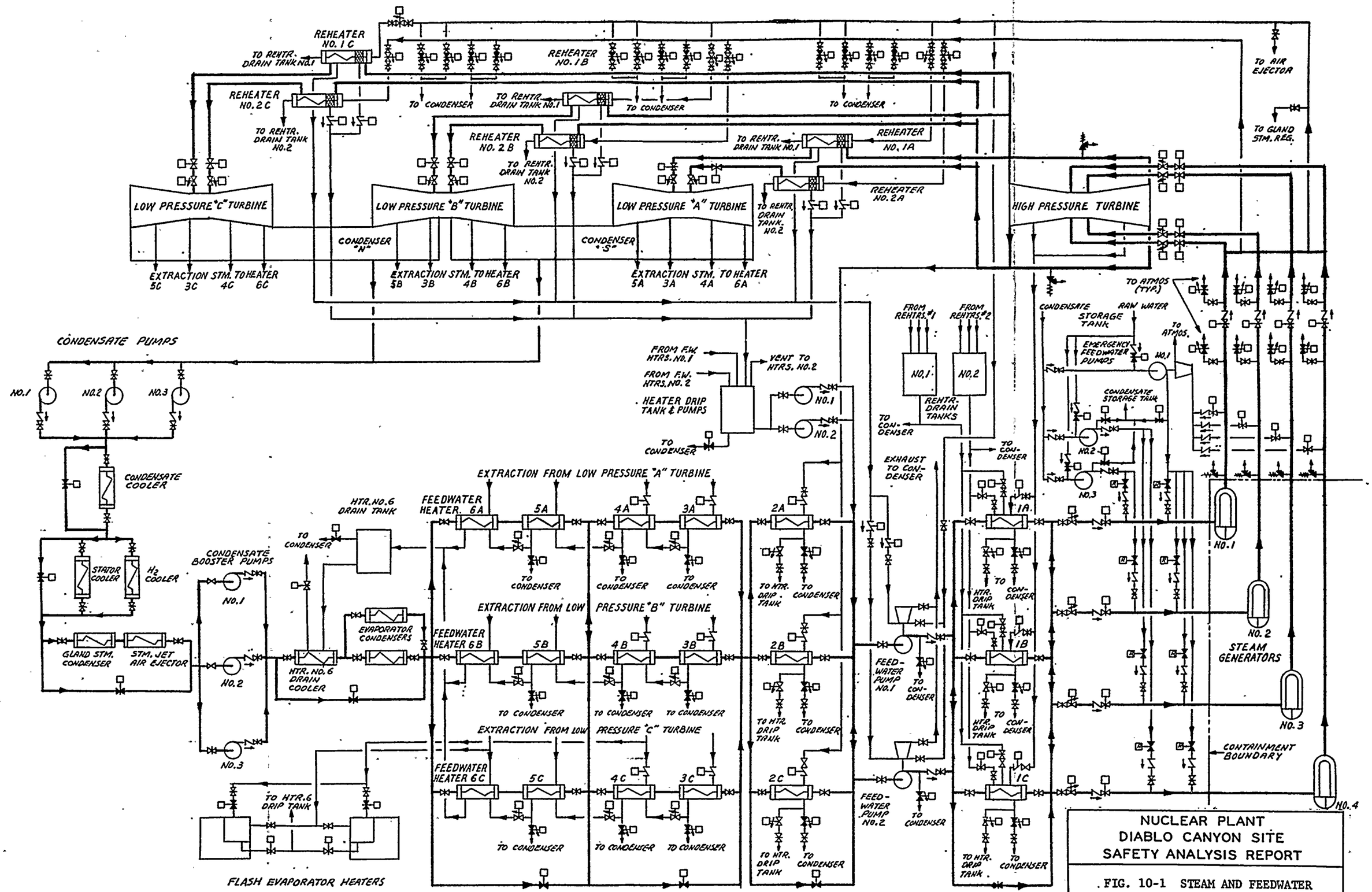

NUCLEAR PLANT
DIABLO CANYON SITE
SAFETY ANALYSIS REPORT

FIG. 10-1 STEAM AND FEEDWATER SYSTEM (Revised 7-24-67)

TABLE OF CONTENTS

Section	Title	Page
CHAPTER 11	RADIOACTIVE WASTES AND RADIATION PROTECTION	
11.1	Waste Disposal System.....	11-1
11.1.1	Design Bases.....	11-1
11.1.2	Systems Design.....	11-2
11.1.3	Waste Disposal System Components.....	11-5
11.2	Radiation Protection.....	11-11
11.2.1	Shielding.....	11-11
11.2.2	Radiation Monitoring.....	11-14
11.2.3	Radiation Control Procedures.....	11-21

CHAPTER 11 RADIOACTIVE WASTES AND RADIATION PROTECTION

11.1 WASTE DISPOSAL SYSTEM

11.1.1 DESIGN BASIS

The Waste Disposal System collects, monitors and processes for safe disposal all liquid, solid and gaseous wastes. The system is designed to process fluid wastes for discharge to the environment within the radioactive level tolerances established by applicable governmental regulations. Suitable facilities are provided for handling and on-site storage of solid wastes prior to disposal. The system is controlled from a local control board in the auxiliary building. All system equipment is located in or near the auxiliary building, except for the reactor coolant drain tank and pumps which are located in the reactor containment. Secondary containment is provided for radioactive waste piping and equipment by locating pipes and equipment inside of buildings. Any liquid spill will be picked up and returned to tanks within the building. Monitoring instruments are provided to detect leakage within the buildings. The activity concentration of liquid and gaseous wastes will be determined prior to discharge to assure that releases are within the limits of 10 CFR 20. Radioactive fluids will be continuously monitored during discharge. At least two valves must be deliberately opened to permit discharge from the Waste Disposal System. One valve is automatically closed upon receipt of a high activity signal from the discharge stream monitor.

System design is based on one percent of the fuel rods releasing fission products by diffusion out of the pellet through defects in the cladding into the coolant. It is assumed that these defects exist at the beginning of the initial core cycle and each following cycle. Experience from operating nuclear plants of this type has shown that the expected amount of defective fuel rods is much less than one percent.

11.1.2 SYSTEMS DESIGN

The preliminary Waste Disposal System process flow diagrams are shown on Figures 11-1 and 11-2.

11.1.2.1 Solid Waste Processing

The rate of accumulation of solid waste will vary widely. The maximum rate occurs during refueling periods and the minimum rate during normal operation. The average rate of collection assumed for system design is a few hundred pounds per week which is equivalent to one 55-gallon drum filled per week at the maximum density produced by the baler. Solid wastes such as sampling paper, cardboard, wood, paper, broken or contaminated glassware, filter cartridges, etc., will be collected in containers and placed in the storage area. When a sufficient amount of wastes has been accumulated, a baler will compress the wastes into suitable containers. These will be placed in the storage area prior to shipment. The storage area includes space for items that cannot be baled, and also for contaminated but potentially reuseable tools and equipment.

Spent ion-exchanger resin will be stored in the spent resin storage tank until a sufficient quantity has accumulated for packaging. Normally a minimum of six months will be allowed for decay. The total resin and shielding weight, limited to the amount which can be hauled by one truck, is equivalent to approximately 130 cubic feet of resin. The spent resin storage tank contains additional space for a liquid level above the resin to prevent resin degradation due to heat generation by decaying fission products, and for a gas blanket above the liquid.

11.1.2.2 Liquid Waste Processing

The Waste Disposal System collects, treats, stores, and disposes of radioactive liquid wastes originating anywhere in the plant. Such wastes are collected in sumps and drain tanks and pumped to the Waste Disposal System in the auxiliary building. In the Waste Disposal System, wastes are handled on a batch basis with each batch analyzed and handled appropriately in accordance with the analysis.

Treatment consists first of filtration, then evaporation as necessary. Certain waste may be sent to the Chemical and Volume Control System for treatment and re-use.

Disposal consists of removal to a licensed storage facility, or discharge to the circulating water discharge tunnel. Such discharges will be in accordance with the limits set by 10 CFR 20.

Figure 11-1 is a flow diagram of the liquid waste portion of the Waste Disposal System and shows the principle sources of liquid wastes.

All waste discharges will be continuously monitored. Two valves must be opened to provide a discharge path; one of these valves will close automatically on a high radiation signal from the monitor. Additionally, a continuous sample will be taken from the circulating water discharge tunnel downstream from the waste discharge point. This sample will be accumulated and analyzed at regular intervals.

The major soluble and insoluble radionuclides anticipated in liquid wastes assuming 1% fuel failure are:

Cs-137	Co-58
Cs-134	Mn-54
I-131	Mo-99
Y-91	Co-60
Cs-136	

It is expected that these isotopes would comprise about 99.9% of total activity discharged.

11.1.2.3 Gaseous Waste Processing

During plant operations, gaseous wastes will originate from:

a) Degassing reactor coolant discharge to the Chemical and Volume Control System

b) Degassing reactor coolant and purging the volume control tank prior to a cold or refueling shutdown

c) Displacement of cover gases as liquids accumulate in various tanks

d) Miscellaneous equipment vents and relief valves

e) Sampling operations and automatic gas analysis for hydrogen and oxygen in cover gases.

Most of the gaseous waste is nitrogen cover gas. A small fraction (approximately 3%) is hydrogen removed from the reactor coolant.

One of two gas compressors is always in operation to maintain an operating pressure of one-half psi to one psi in components vented to the vent header. The standby unit is available to handle peak waste gas conditions. The compressors discharge waste gases through a manifold to storage tanks where gases are held for a suitable decay period. When the tank reaches a predetermined pressure and activity level, it is isolated and a second tank is placed in service. After the gas has undergone sufficient radioactive decay, the tank contents are released to the environment through the station vent at a predetermined controlled rate to maintain the radiation levels on the site and environs within limits established by 10 CFR 20. Four tanks are used for normal operation.

To release effluent from the waste gas tanks to the environment, two valves must be opened deliberately. As the gases leave the Waste Disposal System, they are monitored continuously at the plant vent and if an unexpected increase in radioactivity is sensed, one of the discharge valves will be closed automatically on signal from the monitor.

The discharged gaseous effluent will be diluted in the atmosphere due to the turbulence in the wake of the containment building in addition to the effects of normal dispersion. The plant will be operated in accordance with the permissible emission rate to be established. This rate will take into account building wake, the topography of the site and environs, and meteorological conditions at the site.

11.1.3 WASTE DISPOSAL SYSTEM COMPONENTS

11.1.3.1 Chemical Drain Tank

This tank receives the wastes from the regeneration of the demineralizers and drainage from the hot section of the chemical laboratory. Chemicals, as necessary, will be added to produce a sufficiently neutral solution for further treatment. The tank is provided with a pump or mixer to recirculate the contents for mixing and sampling. The tank is made of stainless steel.

After sampling, the wastes may be discharged to the circulating water tunnel after filtration, or sent to a waste holdup tank for further treatment.

11.1.3.2 Reactor Coolant Drain Tank

The reactor coolant drain tank is a right circular cylinder with spherically dished heads. The tank is made of all-welded stainless steel or lined carbon steel and has a manhole mounted on the top portion of the tank. This tank serves as a drain collecting point for the Reactor Coolant System and other equipment located inside the reactor containment.

11.1.3.3 Containment Sump

The containment sump is installed in the floor at the low point of the containment and collects floor drains, drips from the ventilating system coolers, and any overflow from the reactor coolant drain tank.

11.1.3.4 Auxiliary Building Drain Tank

This tank, similar in design to the reactor coolant drain tank, receives low solid wastes, principally from the Chemical and Volume Control Systems and the Component Cooling System.

11.1.3.5 Auxiliary Building Sump

The sump is located at the lowest point in the auxiliary building and serves as a collecting point for floor drains. All floor drains entering this tank contain loop seals to prevent gas from leaving the pressure vent system.

11.1.3.6 Spent Resin Storage Tank

The spent resin storage tank retains spent resin normally discharged from the mixed bed, spent fuel pit and base removal and cation demineralizers. The de-borating demineralizers and evaporator condensate demineralizers are regenerated and therefore will be discharged infrequently. Normally, the tank is filled over a long period of time, the contents are allowed to decay and then emptied prior to receiving any additional resin. However, the contests can be removed at any time, if sufficient shielding is provided for the spent resin shipping vessel. A layer of water is maintained over the resin surface to prevent resin degradation due to heat generation from decaying fission products. Resin is removed from the tank by first back flushing with nitrogen to loosen the resin and then flushing the resin out with nitrogen entering the top of the tank. The tank is made of all-welded stainless steel or lined carbon steel.

11.1.3.7 Waste Holdup Tanks

These two tanks normally collect liquid waste from the containment sump, auxiliary building sump, and auxiliary building drain tank. Wastes from the reactor equipment drain tank, waste neutralizer tank, and laundry and hot showers can also be collected in these tanks. The tanks are made of lined carbon steel.

11.1.3.8 Liquid Waste Filters

All wastes will be filtered before discharge from the Waste Disposal System. Filter units with replaceable cartridges are provided. These filters will remove 98% of all suspended particles down to 25 microns. Spent cartridges will be placed in containers for storage and off-site disposal.

11.1.3.9 Waste Evaporator

The waste evaporator concentrates dissolved solids in the waste liquid. The concentrating solution is collected below and in the lower portion of the vessel and periodically discharged to the concentrated waste storage. A vapor dome allows water droplets to return to the boiling liquid. Steam leaves the vapor dome and enters the demister. The demister contains a section packed with very fine stainless steel wool designed to remove aerosols from the steam. The aerosols coalesce into water droplets and are returned to the boiling liquid. The flow of steam from the evaporator to the waste evaporator condenser is automatically controlled by a level controller which controls the supply of auxiliary steam to the waste evaporator. The waste evaporator is stainless steel welded construction.

The evaporator condenser is a vertical shell and tube exchanger with steam condensing on the shell side. The tube bundle is removable and the tubes are welded to the tube sheet. Component cooling water circulates through the tubes. The condenser is stainless steel.

11.1.3.10 Waste Condensate Tanks

Two tanks collect waste evaporator condensate and filtered waste from the holdup tanks. Before discharge, the contents are sampled and analyzed for radioactivity and purity. If the water is sufficiently low in radioactivity, it may be discharged with the condenser cooling water. When radioactivity is high, the water is returned to the waste holdup tank for reprocessing.

11.1.3.11 Concentrate Waste Storage Tanks

These two tanks receive the concentrated residue from the waste evaporator for storage prior to off-site disposal.

11.1.3.12 Gas Decay Tanks

Welded carbon steel tanks are provided to contain compressed waste gases (hydrogen, nitrogen, oxygen and fission gases). Four tanks contain waste gases received during normal operation, and collect gases discharged when the reactor coolant is degassed prior to a cold shutdown. After a period for radioactive decay, these gases may be released at a controlled rate to the atmosphere through the plant vent.

11.1.3.13 Compressors

Two compressors are provided to maintain the vent header pressure at 1/2 psi to one psi. These compressors are of the centrifugal displacement type, consisting of a round, multi-blade rotor revolving freely in an elliptical casing partially filled with water. The water provides a seal between the rotor blade tips and the casing and a heat sink for the heat of compression. A chevron type moisture separator and interconnecting piping are attached to the compressor. The compressors are cast iron. Water from the moisture separator is cooled and returned to the compressor. The heat exchangers and piping are ferrous or non-ferrous materials as required. The operation of the compressors is automatically controlled by the gas manifold pressure.

11.1.3.14 Baler

A hydraulically operated baler equipped with a dust shroud is used to compress soild wastes into containers. The baler is operated manually from a local station.

11.1.3.15 Nitrogen Manifold

Nitrogen, used as purge gas for the vapor space of various components or as cover gas for tanks in which the liquid level may vary, is supplied from a dual manifold. The manifolds are made of all-brazed brass.

1.1.3.16 Hydrogen Manifold

Hydrogen is supplied to the volume control tank to maintain the specified hydrogen concentration in the reactor coolant. The hydrogen is supplied from a dual manifold. The manifolds are made of all-brazed brass.

11.1.3.17 Gas Analyzer

An automatic gas analyzer is provided to eliminate the possibility that an explosive mixture of hydrogen and oxygen might accumulate in any of the auxiliary system equipment. Upon indication that a gas is approaching a hazardous condition, provisions are made to purge the equipment to the gaseous waste system with an inert gas, or to isolate the component to prevent a hazardous condition from being reached.

11.1.3.18 Pumps

Pumps used throughout the system for draining tanks and transferring liquids are as follows:

a) Two reactor coolant drain tank pumps
b) Two containment sump pumps
c) One auxiliary building drain tank pump
d) Two auxiliary building sump pumps
e) One laundry and hot shower drain tank pump
f) One chemical drain tank pump
g) Two waste transfer pumps
h) Two waste discharge pumps
i) One waste evaporator feed pump

11.1.3.19 Laundry and Hot Shower Tanks

Two laundry and hot shower tanks retain liquid wastes containing detergents originating from the laundry and/or the hot shower. Each tank is carbon steel. When a tank has been filled, its contents are analyzed. Depending on the activity level, the tank contents are drained to the waste holdup tanks or discharged to the condenser cooling water.

11.1.3.20 Piping

Piping carrying wastes is predominately carbon steel. Stainless steel piping will be used where required. Piping connections are welded except where flanged connections are necessary to facilitate equipment maintenance.

11.1.3.21 Valves

Valves are normally carbon steel; stainless steel will be used where required. Globe valves are installed with flow over the seats when such an arrangement reduces the possibility of leakage.

Stop valves are provided to isolate equipment for maintenance, to direct the flow of fluids through the system, or to isolate storage tanks for radioactive decay.

Relief valves are provided for tanks containing radioactive wastes if the tanks might otherwise be overpressurized by improper operation or component malfunction. Tanks containing wastes which are normally of low radioactivity are vented locally. Tanks containing higher activity levels and/or hydrogen gas are vented to and dilute in the auxiliary building ventilation system and ultimately to the monitored plant discharge vent.

11.2 RADIATION PROTECTION

11.2.1 SHIELDING

Shielding is provided for biological protection against radiation from all sources contained in the reactor plant and those associated with refueling and maintenance. Maximum radiation doses for plant personnel are limited to those specified in AEC regulations. The reactor is capable of continued safe operation with greater than 1% fuel rod defects. The radiation shielding is further designed to permit uninterrupted operation of future units on this site in the unlikely event that this unit experiences the hypothetical loss of coolant accident. These radiation sources are located in the reactor vessel, the Reactor Coolant System, and the reactor auxiliary systems. The shielding for these sources is divided into four categories according to function: primary shield, secondary shield, fuel handling shield, and auxiliary shields.

11.2.1.1 Primary Shield

The primary shield is a reinforced concrete structure immediately surrounding the reactor vessel. It attentuates the nuclear radiation from the reactor to a level comparable to the gamma radiation emanating from the reactor coolant loops, prevents neutron activation of equipment near the reactor and reduces the dose rate from the core to a safe level so that maintenance may be performed on Reactor Coolant System components after shutdown.

The lower portion of the primary shield is seven feet thick and is an integral part of the main structural concrete support for the reactor vessel. It extends upward to join the concrete cavity over the reactor. The reactor cavity, which is approximately rectangular in shape, extends upward to the operating floor with vertical walls four feet thick, except in the area adjacent to fuel handling, where the thickness is increased to six feet. A steel plate is provided at each point where the eight reactor coolant pipes penetrate the primary shield. Shield cooling is provided to prevent damage to concrete from overheating.

11.2.1.2 Secondary Shield

The secondary shield, a part of which also serves as the reactor containment, consists of a reinforced concrete cylinder and dome and a steel inner liner. The secondary shield surrounds the reactor and Reactor Coolant System to reduce the radiation from the reactor plant to acceptable levels. In the event of loss of reactor coolant biological shielding is provided by the concrete structure. This shielding will reduce the radiation intensity at the outside surface of the reactor containment to a negligible level during normal plant operation and to an acceptable level during maximum hypothetical accident conditions at the plant exclusion boundary.

11.2.1.3 Fuel Handling Shield

The fuel handling shield facilitates the removal and transfer of spent fuel assemblies and control rod clusters from the reactor vessel to the refueling canal. It is designed to attentuate radiation from spent fuel, control clusters, and reactor vessel internals to tolerable levels.

The reactor cavity, flooded during refueling operations, provides a temporary water shield above the components being withdrawn from the reactor vessel. The water height during refueling is approximately 24 ft. above the reactor vessel flange. This height assures that a minimum of 10 ft. of water will be above a withdrawn fuel assembly. The refueling canal is a passageway connected to the reactor cavity and extending to the inside surface of the reactor containment. The canal is formed by two concrete walls each approximately 6 feet thick, which extends upward to the same height as the reactor cavity. During refueling the canal is flooded with borated water to the same height as the reactor cavity.

The spent fuel assemblies and control rod clusters are remotely removed from the reactor containment through the horizontal spent fuel transfer tube and placed in the spent fuel pit. Concrete, approximately 6 ft. thick, shields the spent fuel transfer tube. This shielding is designed to protect personnel from radiation during the time a spent fuel assembly is passing through the main concrete support of the reactor containment and the transfer tube.

The concrete walls of the reactor cavity and the refueling canal are designed to shield personnel from radiation emanating radially from the spent fuel assemblies and control rod clusters during refueling. The sections of the wall are 4 and 6 ft. thick. Water in the spent fuel pit protects personnel who are above the fuel assemblies and control rod clusters during handling operations. The water level above the pit floor, assures sufficient shielding above the fuel assemblies and control rods at all times during storage and handling.

11.2.1.4 Auxiliary Shielding

Auxiliary shielding is designed to protect personnel in the sampling room in the vicinity of the Waste Disposal, Chemical and Volume Control, and Auxiliary Coolant Systems. The demineralizers are located in the auxiliary building and are provided with 4 ft. of concrete shielding. Filters are also located in this building and provided with shielding.

Other auxiliaries housed in the reactor auxiliary building are shielded to protect operating and maintenance personnel. The concrete walls and floors in this building vary in thickness, depending upon the radiation from equipment and piping. In some cases, the concrete block walls are removable to allow personnel access to equipment during maintenance periods. The shielding design is based on the radiation levels outside of the shielded areas not exceeding 0.75 millirem per hour in normally occupied areas, and at or below 2.0 millirem per hour in intermittently occupied areas.

In summary, the principal auxiliary equipment shielding provided is as given in Table 11-1.

TABLE 11-1

PRINCIPAL SHIELDING OF PLANT

Equipment	Estimated Shielding, Ft-In. (Ordinary Concrete)
Demineralizers	4-0
Charging Pumps	2-6
Volume Control Tank	3-6
Liquid Waste Storage Tanks	2-6
Gaseous Waste Storage Tanks	3-6

11.2.2 RADIATION MONITORING

The Radiation Monitoring System detects, computes, indicates, annunciates, and records the radiation at selected locations inside and outside the reactor plant and is divided into the following subsystems:

a) The Operational Radiation Monitoring System consists of channels which primarily give early warning of a plant malfunction and secondarily warn personnel of increasing radiation which might result in a radiation health hazard.

b) The Area Radiation Monitoring System consists of channels which primarily warn personnel of increasing radiation that might result in a radiation health hazard.

The Radiation Monitoring System continuously monitors plant effluents and various in-plant points selected to provide indication and warning in areas where radioactive sources exist and operating personnel are required to be present. A single multi-point recorder automatically sequences to provide a record of the radioactivity at the various in-plant points. Laboratory

analysis equipment provides analytical information on the chemical and radiochemical contents from the many samples taken throughout and adjacent to the plant. Personnel monitors are provided to record integrated exposure for all site personnel. The above provides adequate information and warning for the continued safe operation of the plant.

11.2.2.1 Operational Radiation Monitoring System

This system consists of several channels with detectors located throughout the plant. The computing and readout equipment is located in cabinets in the control room.

a) Containment Air Particulate Monitors

Continuous air samples are taken from the containment atmosphere, drawn outside the containment in closed, sealed systems and monitored by a scintillation counter filter paper detector assembly. The filter paper collects all particulate matter greater than 1 micron in size on its constantly moving surface, which is viewed by a photomultiplier-scintillation crystal combination. The air samples are returned to the containment after passing through the gas monitor.

The preamplified detector output is transmitted to a rate meter in the Radiation Monitoring System cabinets in the control room. The activity is indicated on a meter and recorded by a multipoint recorder. High-activity alarm indication is displayed on the control board annunciator in addition to the radiation monitoring cabinets. Local alarms provide operational status of supporting equipment such as the pumps, motors, and flow and pressure controllers.

This monitor will principally detect the particulate daughters of the noble gases and has a sensitivity range of 10^{-9} to 10^{-6} microcuries per cubic centimeter.

b) Containment Gas Effluent-Radio Gas Monitors

Continuous air samples are taken from the containment atmosphere after they pass through the air particulate monitor through a closed, sealed system to the gas monitor assembly. The samples flow continuously to the fixed shielded volume, where they are viewed by a Geiger-Mueller tube. The samples are then returned to the containment.

The detector output is transmitted to the Radiation Monitoring System cabinets in the control room. The activity is indicated by meters and recorded by a multipoint recorder. High-activity alarm indications are displayed on the control board annunciator in addition to the radiation monitoring cabinets. Local alarms annunciate the supporting equipment's operational status.

This monitor will principally detect I_{131}, Xe_{133} and Xe_{135} and has a sensitivity range of 10^{-6} to 10^{-3} microcuries per cubic centimeter.

c) Plant Vent Gas Detector

The plant vent gas detector consists of four, thin-walled, self-quenching type Geiger-Mueller tubes (high sensitivity beta-gamma detector) operated in parallel together with an impedance matching network.

The detector output is transmitted to the Radiation Monitoring System cabinets in the control room. The activity is indicated by a meter and recorded by a multipoint recorder. High activity alarm indications are displayed on the control board annunciator in addition to the radiation monitoring cabinets.

This monitor will principally detect Kr_{85} and Xe_{135} and has a maximum sensitivity of 5×10^{-7} microcuries per cubic centimeter.

d) Condenser Air Ejector Gas Monitor

This channel receives a continuous air sample from the air ejector exhaust header and monitors it for gaseous activity which is indicative of an unlikely primary to secondary system leak. The sample gas is returned to the plant gas effluent.

The Geiger-Mueller detector output is transmitted to the Radiation Monitoring System cabinets in the control room. The activity is indicated by a meter and recorded by a multipoint recorder. High-activity alarm indications are displayed on the control board annunciator in addition to the radiation monitoring cabinets. Local alarms annunciate the supporting equipment's operational status.

This monitor has a maximum sensitivity of 10^{-6} microcuries per cubic centimeter for Kr_{85}, I_{131} and Xe_{135}.

e) Steam Generator Liquid Sample Monitor

This channel monitors the liquid phase of the secondary side of the steam generator for activity, which would indicate a primary to secondary system leak, providing backup information to that of the air ejector gas monitor. Samples from each of the four steam generator bottoms are mixed in a common header and the common sample is continuously monitored by a scintillation counter and holdup tank assembly. Upon indication of a high-activity, each steam generator is individually sampled in order to determine which unit is leaking. This sampling sequence is achieved by manually selecting the desired unit to be monitored and allotting sufficient time for sample equilibrium to be established. This channel controls valves to shut off the blowdown flow in case of excessive radioactivity.

The detector output is preamplified and transmitted to the Radiation Monitoring System cabinets in the control room.

High activity alarm indications are displayed on the control board annunciator, the Radiation Monitoring System cabinets, and in the sampling room. The activity of the sample being monitored is indicated and recorded by a multi-point recorder.

The sensitivity range of this monitor is 10^{-5} to 10^{-2} microcuries per cubic centimeter for Co_{60}.

f) Component Cooling Loop Liquid Monitor

This channel continuously monitors the component coolant loop of the Auxiliary Coolant System for activity indicative of a leak of reactor coolant from the Reactor Coolant System, Chemical and Volume Control System, Sampling System, and/or the residual heat removal loop of the Auxiliary Coolant System. A scintillation counter is inserted in an in-line well. The detector assembly output is preamplified and transmitted to the Radiation Monitoring System cabinets in the control room. The activity is indicated on a meter and recorded by a multipoint recorder. High-activity alarm indications are displayed on the control board annunciator in addition to the radiation monitoring cabinets. The alarm signal also closes the valve in the component cooling surge tank vent line to prevent gaseous activity release.

The sensitivity range of this monitor is 10^{-5} to 10^{-2} microcuries per cubic centimeter for Co_{60}.

g) Waste Disposal System Liquid Effluent Monitor

This channel continuously monitors all Waste Disposal System liquid releases from the plant. Automatic valve closure action is initiated

by this monitor to prevent further release after a high activity is indicated and alarmed. A scintillation counter and hold-up tank assembly monitors all effluent discharges. The detector assembly output is preamplified and transmitted to the Radiation Monitoring System cabinets in the control room. The activity is indicated on a meter and recorded by a multipoint recorder. High-activity alarm indications are displayed on the control board annunciator in addition to the radiation monitoring cabinets.

The sensitivity range of this monitor is 10^{-5} to 10^{-2} microcuries per cubic centimeter for Co_{60}.

--+

11.2.2.2 Area Radiation Monitoring System

This system consists of several channels which primarily monitor and indicate radiation levels in various areas of the plant.

Several channels continuously monitor areas such as the control room, containment, radiochemistry laboratory, and auxiliary building for gamma radiation with a fixed position G-M tube detector. The detector output is amplified and the log count-rate is determined by the integral amplifier at the detector. The radiation activity is shown at the detector and is transmitted to the Radiation Monitoring System cabinets in the control room where it is indicated on a meter and recorded on a multi-point recorder. High-activity alarms are displayed on the control board annunciator, the radiation monitoring cabinets and at the detector location.

The range of the area monitors is 0.1 milliroentgen per hour to 10 roentgen per hour.

The control board annunciator provides a single window which alarms for any channel being alarmed. Verification of which channel has alarmed is done at the Radiation Monitoring System cabinets.

11.2.3 RADIATION CONTROL PROCEDURES

11.2.3.1 Radiation Protection Program

The radiation protection program for the plant will be carried out in accordance with the Company's Radiation Control Standards for nuclear power plants. The Radiation Control Standards are statements of policy covering each aspect of the radiation protection program and are based on appropriate AEC and State regulations. The Radiation Control Standards are implemented by a Radiation Control Procedures Manual for each nuclear plant. All personnel whose work involves the potential for exposure to radiation or radioactive materials will receive a training program on radiation safety based on these two documents.

The subject index of the Radiation Control Standards and the Radiation Control Procedures Manual is as follows:

1. Personnel External Exposure - This section covers external exposure limits, the personnel dosimeter program, and off-site industrial and medical exposure. Film badge service is supplied by a outside contractor. Badges will be routinely changed monthly. Continuous exposure estimates are provided by use of dosimeter pencils and dose estimates based on monitoring results.

2. Personnel Internal Exposure - This section covers internal exposure control measures including the use of respiratory protection equipment. A request for authorization to use respiratory protection equipment in accordance with the provisions of 10 CFR 20.103(c)(3), similar to the one which was recently authorized for the Humboldt Bay Nuclear Unit, will be made. This section also covers the Company's bioassay program for nuclear plant personnel which currently consists of routine semi-annual whole body counting by an outside contractor.

3. Personnel Contamination - This section covers methods of control of personnel contamination (personnel contamination surveys, use of radiological protective clothing and handling of personnel injuries in radioactive material areas) as well as personnel decontamination procedures.

4. Control of Access to Radiation Areas - This section defines plant controlled areas, discusses posting of such areas and describes the Special Work Permit (SWP) and Radiation Work Procedure (RWP) which will be used in performing all controlled area work. Access to "high radiation areas" and other potentially hazardous areas will be controlled by locked doors and gates or by doors which, when opened, initiate an audible alarm locally and in the control room. Procedural control of the use of the key for locked doors and gates (supervisory control of a single "in use" key and entry into those areas under specified conditions of either an SWP or RWP) will be similar to that which has been in effect since initial operation for the Humboldt Bay Nuclear Unit. There may be situations where the doors are used for emergency egress that will require special consideration.

5. Medical - This section covers the Company's medical examination program for radiation workers. The program provides for routine radiological physical examination for each employee prior to his being accepted for radiation work and an examination for employees terminating radiation work. Routine examinations at two year intervals are given to personnel holding AEC Operator Licenses in accordance with the provisions of 10 CFR 55. The results of all examinations are reviewed by the Company's medical consultant who is an expert in the field of nuclear medicine.

6. Releases of Material from the Controlled Area - This section covers procedures for the release of liquid and gaseous radioactive wastes, the procedure for off-site shipment of radioactive material including solid waste and the unconditional release of materials from radiation zone status.

7. Storage and Transfer of Radioactive Material - This section covers procedures for on-site storage and transfer of radioactive materials.

8. Control of Radiation - This section establishes policy on the training of employees in radiation safety. The procedure for the review of all new facilities and all changes and modification from the standpoint of radiation safety is also covered.

9. Radiation Monitoring - This section covers the plant routine monitoring programs and describes the use of radiation survey and monitoring equipment.

10. Reports and Records - This section covers requirements for internal Company reports and records and reports to regulatory agencies on the radiation protection program.

11.2.3.2 Radiation Protection Equipment

Radiation protection equipment will be similar to that in use at the Humboldt Bay Power Plant and will include:

1. Normal and emergency range dosimeter pencils for use in estimating personnel exposure.

2. Portable radiation survey instruments for alpha, beta and gamma radiation detection and dose rate instruments for measuring beta, gamma and neutron dose rate.

3. Air samplers and at least one semi-portable continuous air monitor.

4. Protective clothing and suitable respiratory protection equipment including various types of filter masks and self-contained breathing apparatus.

5. Personnel decontamination kits. (One of these kits will be located in the plant access control area and a second will be a part of each of the plant emergency kits discussed below.)

6. Emergency kits containing portable survey and dose rate instruments (including high range instruments), protective equipment, decontamination equipment, drawing and photographs of interior area within the plant. (One of these kits will be maintained at the plant and a second at off-site location designated as an evacuation center).

11.2.3.3 Radiation Protection Facilities

The principal radiation protection facilities for the plant will be as follows:

1. An access control area at the entrance to the controlled area of the plant. This area will be used for changing into protective clothing before entering the controlled area, the survey of personnel and equipment leaving the controlled area and personnel decontamination. A beta-gamma hand and foot counter will be located near the exit from the access control area as a final check to assure that radioactive contamination is not brought beyond this point.

2. A radiation instrument calibration facility. Suitable beta, gamma and neutron sources and calibration fixtures will be provided to permit on-site calibration of radiation dose rate instruments and dosimeter devices.

3. A radiochemical laboratory and counting room. These facilities will be used in the plant chemistry program as well as for radiation protection work. Equipment will include alpha, beta and gamma counting equipment for the quantitative measurement of radioactivity. A multichannel gamma scintillation spectrometer will be provided for isotopic analysis. The numbers and types of counting equipment will be similar to those provided for the Humboldt Bay Nuclear Unit (two gas flow internal proportional counters, a single channel gamma scintillation system and a 256 channel analyzer).

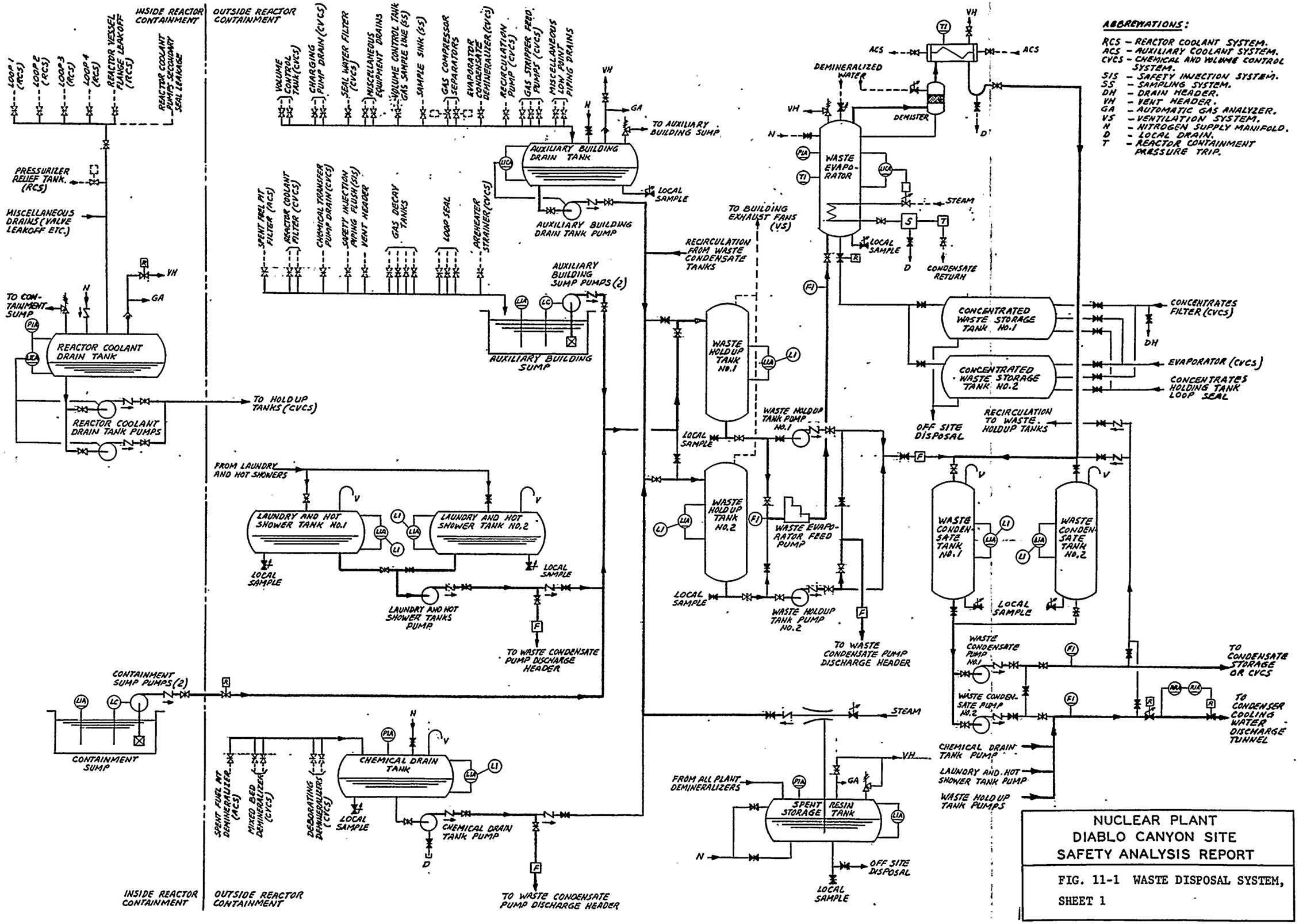

NUCLEAR PLANT
DIABLO CANYON SITE
SAFETY ANALYSIS REPORT

FIG. 11-1 WASTE DISPOSAL SYSTEM, SHEET 1

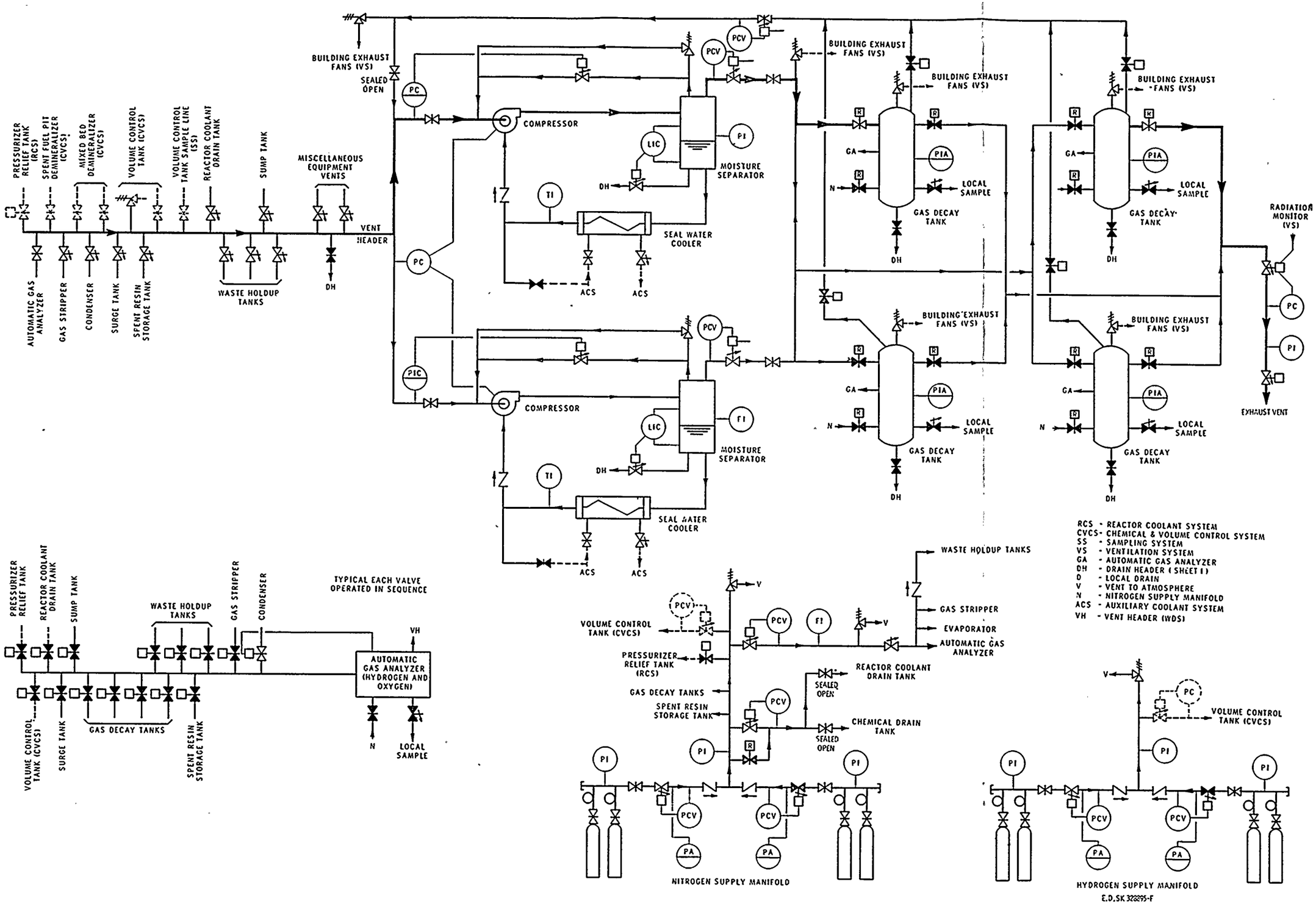

WASTE DISPOSAL SYSTEM
SHEET 2 FIG. 11-2

TABLE OF CONTENTS

Section	Title	Page
CHAPTER 12	SAFETY EVALUATION	
12.1	Core and Coolant Boundary Protection Analysis	12-1
12.1.1	Plant Abnormalities and Transients Considered	12-1
12.1.2	Rod Cluster Control Assembly (RCCA) Withdrawal	12-2
12.1.3	Rod Cluster Control Assembly (RCCA) Drop	12-4
12.1.4	Chemical and Volume Control System Malfunction	12-5
12.1.5	Loss of Reactor Coolant Flow	12-6
12.1.6	Startup of an Inactive Reactor Coolant Loop	12-6
12.1.7	Loss of External Electrical Load	12-6
12.1.8	Turbine Trips due to Steam and Power System Malfunctions	12-7
12.1.9	Loss of all A-C Power to the Plant Auxiliaries	12-9
12.1.10	Likelihood and Consequences of Turbine-Generator Unit Overspeed	12-11
12.2	Standby Safeguards Analysis	12-17
12.2.1	Situations Analyzed	12-17
12.2.2	Fuel Handling Accidents	12-17
12.2.3	Accidental Release of Waste Liquids	12-21
12.2.4	Accidental Release of Waste Gases	12-21
12.2.5	Rupture of a Steam Generator Tube	12-23
12.2.6	Rupture of a Steam Pipe	12-24
12.2.7	Rupture of a Control Rod Drive Mechanism Housing - Rod Cluster Control Assembly (RCCA) Ejection	12-25
12.3	Major Rupture of a Reactor Coolant Pipe	12-27
12.3.1	General	12-27
12.3.2	Loss of Coolant Accident Evaluations	12-30
12.3.3	Evaluation of Radiation Protection	12-51
12.4	Summary of Off-Site Exposures	12-71

CHAPTER 12 SAFETY EVALUATION

12.1 CORE AND COOLANT BOUNDARY PROTECTION ANALYSIS

12.1.1 PLANT ABNORMALITIES AND TRANSIENTS CONSIDERED

For the following plant abnormalities and transients, the reactor control and protection system is relied upon to protect the core and reactor coolant boundary from damage:

a) Rod Cluster Control Assembly (RCCA) Withdrawal,
b) Rod Cluster Control Assembly (RCCA) Drop,
c) Chemical and Volume Control System (CVCS) Malfunction,
d) Loss of Reactor Coolant Flow,
e) Startup of an Inactive Reactor Coolant Loop,
f) Loss of External Electrical Load,
g) Turbine Trips Due to Steam and Power System Malfunctions,
h) Loss of All A-C Power to the Station Auxiliaries, and
i) Turbine Overspeed.

During the detailed design of the plant, analyses will be performed to verify that the safeguards and safety margins embodied in the design are adequate to protect the core and reactor coolant boundary and to prevent hazardous conditions from arising as a consequence of any of these abnormalities and transients. These analyses require the use of data which are developed only after engineering of the reactor core and related systems has progressed to an advanced stage. Experience with designs of this type, however, provides a general knowledge of the course of events to be expected and gives assurance that the reactor control and protection system will be able to satisfy the criteria for protection of the core and reactor coolant boundary.

All reactor protection criteria are met presupposing the most reactive RCC assembly in its fully withdrawn position. Therefore, trip is defined for analytical purposes as the insertion of all RCC assemblies except the most

reactive assembly, which is assumed to remain in the fully withdrawn position. This is to provide margin in shutdown capability against the remote possibility of a stuck RCC assembly condition existing at a time when emergency shutdown is required.

--+ Means will be provided for monitoring all individual RCC assemblies together
--+ with their respective group position. This is in the form of a continuous
--+ digital display of all RCC assemblies (both shutdown and control groups). The operator would thus become readily aware of any malfunction. The reactor would then be shut down in an orderly manner and the condition corrected. Such occurrences are expected to be extremely rare based on operation and test experience to date

In summary, reactor protection is designed on a fail-safe basis to prevent cladding failure in all transients and abnormalities listed above. The most probable modes of failure in each protection channel result in a signal calling
--+ for the protective trip. Coincidence of two-out-of-three (or two-out-of-four)
--+ signals is required in the power range of operation where single channel malfunc-
--+ tions could cause spurious trips. (In the startup range of operation, one-out-
--+ of-two coincidence is used). A single component or channel failure in the
--+ protection system itself coincident with one stuck RCCA is allowed for as contingent failures and will not cause violation of the protection criteria. The reactor control and protection system will be designed using the proposed IEEE "Standard for Nuclear Plant Protection Systems" as a guide.

12.1.2 ROD CLUSTER CONTROL ASSEMBLY (RCCA) WITHDRAWAL

12.1.2.1 General

An RCCA withdrawal incident is defined as an uncontrolled addition of reactivity to the reactor core by withdrawal of rod cluster control assemblies resulting in a power excursion. While the probability of a transient of this type is extremely low, such a transient could be caused by a malfunction of the reactor control or control rod drive systems. This could occur with the reactor either subcritical or at power.

12.1.2.2 Uncontrolled RCCA Withdrawal from a Subcritical Condition

Reactivity is added at a prescribed and controlled rate in bringing the reactor from a shutdown condition to a low power level during startup by RCCA withdrawal. Although the initial startup procedure uses the method of boron dilution, the normal startup is with RCCA withdrawal. RCCA motion can cause much faster changes in reactivity than that which could be provided by changes in boron concentration.

--+ Should the rate of reactivity addition be excessive, an abnormally high
--+ neutron flux level would initiate an alarm in the control room.
If corrective action is not taken by the operator to reduce the startup rate, an automatic "RCC-stop" signal deactivates the cycling mechanism on the cluster drive control, causing cluster withdrawal to cease. In addition, trip relays
--+ would open automatically on high nuclear flux in the source range and intermediate range nuclear instrumentation channels. Trip relays would open also when the nuclear power level detected by any two of four power range channels exceeds a preset fractional power limit established for startup. With only the power range trip occurring (the last trip in the sequence of trips), the startup accident is terminated with a DNB ratio of 1.30 or greater.

The maximum possible number of RCC assemblies which can be moved and their maximum withdrawal speed are established by detailed plant design. This information and the maximum incremental RCCA reactivity worth, will be used to verify that the protection afforded by the startup rate and the fractional power trip settings is adequate to terminate the transient safely. Protection in this case is adequate if DNB is not reached, thus assuring that no fuel damage or fission product release will result. A practical combination of limiting RCCA speed and trip set point will be selected.

12.1.2.3 Uncontrolled RCCA Withdrawal at Power

If RCC assemblies are improperly withdrawn when the reactor is operating in the power range, an approach to an unsafe operating condition might result. Protection is first provided by automatic RCC-stops from the power range channels when indicated nuclear power exceeds a preset limit. Should this device fail to limit the transient, a nuclear overpower signal from any two of four power range channels will cause automatic trip. Additional protection is provided by the overpower-overtemperature trip. The set point for this trip is continually calculated from Reactor Coolant System temperatures and pressure and prevents an unacceptable combination of power, temperature and pressure.

These trips will terminate the transient in time to prevent DNB. This conclusion will be verified for a range of reactivity insertion rates, including the maximum rate, by computer simulation methods. The required trip time will be determined and demonstrated to be within the capability of the protection system.

12.1.3 ROD CLUSTER CONTROL ASSEMBLY (RCCA) DROP

The four power range nuclear channels and the rod bottom detection from the rod position indication system serve as a means of sensing a dropped rod cluster. A dropped RCCA will rapidly depress the neutron flux in one region of the core. A sudden reduction in flux at any one of the four power range detectors will actuate the RCCA drop protection. Either protection system (ion chambers or rod position) will initiate protective action in the form of a turbine load cutback and blocking of automatic rod withdrawal. This action compensates for possible adverse core power distributions and permits an orderly retrieval of the dropped RCCA.

Criteria for design of these countermeasures will be based on preserving a safe margin against DNB; hence, no fuel damage or fission product release to the coolant system will result from a dropped RCCA.

12.1.4 CHEMICAL AND VOLUME CONTROL SYSTEM MALFUNCTION

Changes of the reactor coolant boron concentration and reactor coolant makeup are accomplished by means of the Chemical and Volume Control System.

Reduction of boric acid concentration by any process is a means of reactivity insertion. When this occurs by operation of the reactor makeup control while the reactor is critical, the protection described in the preceding cases for RCCA withdrawal is applicable. The maximum reactivity insertion rates attainable by the charging and letdown operation are much less than by RCCA motion, hence the protection is adequate.

When reactivity is added by reducing boric acid concentration while the reactor is shut down, the margin of shutdown is reduced. Since the rate of change of k_{eff} attainable under these circumstances is quite slow, there is time for corrective action to be taken before criticality can be achieved.

Under certain abnormal conditions, the charging pumps could introduce cold water into the reactor. However the rate at which reactivity changes can occur during operation of the charging pumps is far less than that possible with control rod cluster motion. Therefore, the reactor protection system is capable of providing adequate protection.

If either the boric acid flow or the demineralized water flow deviates from the control set point during reactor coolant boration, dilution or normal leakage makeup, alarms will warn the operator to deactivate the makeup system manually.

Should a condition ever arise when reactor coolant boron is changing without the operator's knowledge, RCC group position indication is a positive means of detecting any significant change when the reactor is critical.

Subcritical count rate from the source range nuclear detectors would warn of an undetected malfunction in the subcritical condition. Section 7.3 has a more detailed description of the nuclear instrumentation.

12.1.5 LOSS OF REACTOR COOLANT FLOW

The reactor is tripped if flow is below a preset limit in one loop or when power is lost to one reactor coolant pump when operating above a preset power level.

Simultaneous loss of electrical power to all reactor coolant pumps at full power is the most severe loss-of-coolant flow condition. In these cases, however, reactor trip together with flow sustained by the inertia of the coolant and rotating pump parts will be sufficient to prevent fuel failure and Reactor Coolant System overpressure. Detailed analysis of this type of accident will be performed during the design phase to verify system performance and cladding conditions for various loss-of-flow accidents.

12.1.6 STARTUP OF AN INACTIVE REACTOR COOLANT LOOP

Because there are no isolation or check valves in the reactor coolant loops, there will be reverse flow through an inactive reactor coolant loop. This back flow inherently prevents excessive mismatch in the coolant temperature and boron concentration between the inactive loop and the operating loops. In addition, a temperature interlock is provided to prevent starting a reactor coolant loop if the reverse ΔT is greater than a preset amount. The change in reactivity in the core associated with the starting of an inactive loop is therefore well within the capability of the control and protection system.

12.1.7 LOSS OF EXTERNAL ELECTRICAL LOAD

The plant will be designed to accept a loss of all external electrical load without a reactor or turbine trip. No unique or unproven features are required

in the reactor control system to accomplish this. The automatic system which dumps steam to the condenser and atmosphere is designed for use in this situation as a short term supplemental load to provide time for the reactor control system to reduce the thermal output of the reactor without exceeding acceptable core and coolant conditions. The amount of steam dump is reduced as the control is effective in reducing the reactor thermal output to the desired steady state turbine load. The condenser hotwell provides an adequate supply of water which is delivered to the steam generators by the normal feedwater system.

12.1.8 TURBINE TRIPS DUE TO STEAM AND POWER SYSTEM MALFUNCTIONS

There are various steam and power system malfunctions which could cause a turbine trip. These include such things as improper response of the turbine control valves to a loss in external load, loss of condenser vacuum, and loss of feedwater flow. A turbine trip is accompanied by a direct reactor trip and a controlled short term release of steam to the condenser and atmosphere which removes sensible heat from the Reactor Coolant System while avoiding steam generator safety valve actuation. In the unlikely event that the automatic dump system failed, and no reactor trip occurred, the steam generator safety valves would open for overpressure protection, and the reactor would attempt to meet the apparent load demand. In order to prevent DNB in the core in this case, a reactor trip from two of three high pressurizer pressure signals is provided. The pressurizer safety valves are sized to protect the Reactor Coolant System against overpressure in this accident.

Vacuum loss in the main condensers may be precipitated by loss of circulating water flow or by mechanical failures which may permit air to enter the condensate system. Should the vacuum loss be small, a reduction in turbine load may be necessary, with a corresponding decrease in reactor loading, until corrective action is taken to minimize the vacuum loss. A large vacuum loss below a preset limit will cause the turbine to trip automatically. The resulting effect of turbine trip on plant operation has been described previously. For this condition, the automatic steam dump to the condenser is blocked and the atmospheric safety valves would provide the necessary heat release.

A complete loss of normal feedwater flow to all steam generators is unlikely and could occur only if steam is lost to the feedwater pump or power is lost to the condensate pumps or if rupture of non-duplicated lines occurs. Assuming no protective action is taken and full power generation in the reactor continues, the secondary side of the steam generators would be emptied in a very short period of time. Protection is provided by a low feedwater level reactor trip actuated by a difference in steam and feedwater flow from any steam generator in coincidence with a low water level in the same steam generator. Additional protection against core damage is given by the overpower-overtemperature reactor trip which would initiate a trip because of increasing coolant temperatures as heat transfer to the secondary system is reduced.

In the event of a loss of normal feedwater flow, a protective circuit is also actuated to provide emergency feed flow from the condensate storage using either a steam driven or two motor driven emergency feedwater pumps and a duplicate feedwater line. These pumps will prevent excessive temperatures in the Reactor Coolant System resulting from continued addition of core residual heat and will prevent the steam generator tube sheets from being uncovered. The core residual heat will provide enough heat to the steam generators to supply steam for the emergency steam driven pump and the emergency generators will be sized to power the motor driven emergency feedwater pumps.

Protective circuits to prevent Reactor Coolant System overpressurization consist of:

a) Loss of feedwater supply trip
b) Fixed pressurizer high pressure trip
c) Overpower-overtemperature trip
d) Actuation of emergency feedwater system

Feedwater flow sufficient to handle residual heat generation (3 to 5% of full load flow) will be restored before the Reactor Coolant System pressure increases to the relief valve set point which would cause loss of coolant through the valves.

12.1.9 LOSS OF ALL A-C POWER TO THE PLANT AUXILIARIES

In the unlikely event of a complete loss of all auxiliary a-c power while the reactor plant is at power, the reactor and the turbine will be tripped in accordance with the following sequence:

a) The turbine trip and reactor coolant average temperature program deviation signals will cause the automatic initiation of steam dump to the main condenser.

b) Because of the loss of all outside a-c and turbine trip, there is simultaneous loss of the condenser circulating water pumps and the condenser dump will be blocked.

c) As the steam system pressure subsequently increases, the atmospheric steam dump valves will be automatically tripped open.

d) As the steam flow rate through the atmospheric dump valves is not sufficient, the steam generator safety valves will temporarily lift to augment the steam flow until the rate of heat dissipation through the atmospheric dump valves is sufficient to carry away the stored heat of the fuel and coolant above no-load temperature plus the residual heat of the reactor.

e) As the no-load temperature is reached, the atmospheric steam dump valves will be used to dissipate the residual heat and to maintain the plant at the hot shutdown condition.

The loss of normal feedwater supply will signal for the start of the
--+ emergency feedwater pumps. The emergency turbine utilizes steam flow from the secondary system, in parallel with the atmospheric dump valves, to provide makeup water for the steam generators. The turbine driver
--+ exhausts the secondary steam to the atmosphere. The two motor driven feedwater pumps are supplied by the emergency generators. The emergency feedwater pumps take suction directly from the condensate storage tank for delivery to the steam generators.

If at the time of complete loss of normal auxiliary power and turbine trip, the plant is operating at full load, there will be a rapid reduction of steam generator water level. This is due partly because of the reduction of steam bubble void fraction on the secondary side of the steam generator and partly because steam flow continues after normal feedwater stops. During the first two minutes, the level will drop to about 35% of normal. By the end of this time flow will be established from the emergency feedwater pumps and further reduction of water level will be slow. The capacity of the emergency feedwater pumps is selected so that either the steam driven or the two motor driven pumps will prevent the water level in the steam generators from receding below the lowest level within the indicator range during the transient. This will prevent the tube sheet from becoming uncovered at any time during the transient. The reactor operator in the control room will monitor the steam generator level and will control the feedwater addition with remote operated emergency feedwater control valves. The condensate storage tank capacity is sufficient to dissipate residual heat and maintain the plant at hot shutdown for in excess of eight hours.

The steam driven feedwater pump can be tested at any time by admitting steam to the turbine driver. The electrically driven emergency feedwater pumps can be tested at any time, also. The emergency feedwater pumps will circulate water from the condensate storage tank through a test line connection to the main condenser. The emergency feedwater control valves and atmospheric dump valves can be operationally tested whenever the plant is at hot shutdown and the remaining valves in the system will be operationally tested whenever the plant is at hot shutdown and the remaining valves in the system will be operationally tested when the turbine driver and pump are tested.

Upon the loss of power to the reactor coolant circulating pumps, coolant flow necessary for core cooling and the removal of residual heat is maintained by natural circulation in the reactor coolant loops. The natural circulation capability for the Plant has been calculated for the conditions of equilibrium flow and maximum loop flow impedance. The natural circulation flow ratio as a function of reactor power is given in Table 12-1. The computer code model used to calculate the natural circulation flow has given results within 15% of the measured flow values obtained during natural circulation tests conducted at the Yankee-Rowe plant.

TABLE 12-1

NATURAL CIRCULATION REACTOR COOLANT FLOW
VS REACTOR POWER

REACTOR POWER % Full Power	REACTOR COOLANT FLOW % Nominal Flow
0.5	2.3
1.0	3.0
2.0	3.9
5.0	5.4
7.0	6.2

12.1.10 LIKELIHOOD AND CONSEQUENCES OF TURBINE-GENERATOR UNIT OVERSPEED

The likelihood of a turbine-generator unit overspeeding is extremely remote because of the reliability and redundancy of the turbine. Due to conservative design, very careful rotor forging procurement and rigid inspection, Westinghouse turbogenerators have never experienced such a massive failure.

A survey of the available literature on turbogenerator failure shows that the last massive failure of a turbogenerator occurred about eight years ago. The causes of failure were identified at that time, and provisions were adopted to prevent the recurrence of massive failures. The record since that time demonstrates the soundness of these provisions and correct design.

The no-failure record of Westinghouse turbogenerators, plus the experience gained from the documented incidents, together with the improvement in the design and inspection techniques in the past eight years indicates that the likelihood of massive turbogenerator failure is extremely remote.

With regard to design and inspection techniques, it is worthwhile to mention that a technical committee of forging suppliers and equipment manufacturers was formed about ten years ago under ASTM to study turbine and generator rotor failures. This group developed the high-toughness NiCrMoV material now used in all turbine rotors and disks. This Task Force has been very active in making additional improvements in quality and soundness of large forgings and is still in existance.

The survey of the literature on massive turbine failures in the last 20 years indicates that all of them occurred between 1953 and 1958. This survey has pointed out that the rare events of catastrophic failure of turbines fell into one of two categories:

1) Failure by overstressing arising from accidental and excessive overspeed; and
2) Failure, due to defects in the material, occurring at about normal speed.

The causes of the failures that fall in the second category, i.e., failures due to defects to the material occurring about normal speed, were completely identified and, if the ultrasonic test were used as one of the bases for rejection or acceptance of forging, many of them would not have occurred. Further, the stress concentration points that initiated failure in some units are strictly correlated to the peculiar design characteristics of those units. These discontinuities are not present in Westinghouse units.

Westinghouse specifies the quality and method of manufacturing of the purchased forgings. Written specifications cover the manufacture process, the chemical and mechanical properties, the tests to be performed, etc. Specifically, the tests performed are of a destructive and non-destructive nature. The destructive tests include tension tests, impact tests, and transition temperature measurement tests. The tension test specimens are taken in a radial and/or longitudinal direction. The tensile properties are determined in accordance with ASTM A-370 on a Standard Round 1/2 inch Diameter 2 Inch Gage Length Test specimen. The yield strength is taken as the load per unit of original cross section at which the material exhibits an offset of 0.2 per cent of the original length. The Charpy impact specimens are taken in a radial direction, and the minimum impact strength at room temperature measured. The transition temperature is determined from 6 specimens tested at different temperatures in accordance with ASTM A-443. The specimens are taken in a radial direction and machined in such a manner that the V-notch is parallel to the forging axis. Two specimens are machined from each test bar. All specimens are taken following all heat treatment. Curves of impact strength and per cent brittle failure versus test temperature are drawn.

The nondestructive tests include bore inspection, sulfur printing, magnetic particle test, thermal stability test, and ultrasonic test. The bores are visually inspected and the walls of finished bores shall be free from cracks, pipe, shrinkage, gas cavities, non-metallic inclusions, injurious scratches, tool marks, and similar defects. A magnetic particle test is made on each forging to demonstrate the freedom from surface discontinuities. The end faces of the main body and down over and beyond the fillets joining the main body to the shaft portions are magnetic particle tested. The bore is also magnetic particle tested at a high sensitivity level in accordance with ASTM A-275. These inspections are done by Westinghouse inspectors prior to Westinghouse accepting these forgings. After final machining by Westinghouse, rotors are again magnetic particle inspected on the external surfaces.

The face of the test prolongations at each end of the rotor body or an area on the end faces of the rotor body equivalent to the test prolongations is sulfur printed to determine the freedom from undue ingot corner segregation and excessive sulfide inclusions. A thermal stability test is performed on the forging at the place of manufacture after all heat treatment has been completed. The forgings are ultrasonically inspected at the place of manufacture by Westinghouse inspectors.

No failure falling in the first category given on Page 12-12 has occurred in the USA. The only two documented examples occurred in the United Kingdom. Both accidents were caused by the main steam admission valves sticking in the open position after full load rejection, because of impurities in the turbine control and lubrication oil. The probability of this occurrence in the plant is very remote as the following description of the turbine control and protection system indicates.

The reliability of the the plant turbine control and protection system, the close control of the oil purity, the periodic check of the main steam admission valve spindle freedom, and the high value of the bursting overspeed reduce the likelihood of rotating parts overstressing, due to excessive overspeeding, to practically zero.

Figure 12.1 illustrates the steam path between the steam generators and the turbine. The main steam is supplied to the high-pressure turbine by means of four headers. One stop valve and one governing control valve are installed on each header. All these valves are of the fail-safe design, i.e., they close on loss of oil pressure.

Each stop valve is either in the wide-open or closed position. The major function of these stop valves is to shut off the flow of steam to the turbine in the event the unit overspeeds beyond the setting of the mechanical overspeed trip. These valves are also tripped when other protective devices function. These protective devices include the low vacuum tripping device, the low bearing oil pressure trip, the thrust bearing trip, and the remote operated manual trip. These devices operate in parallel.

The control valves are positioned to regulate the steam flow to the turbine. These valves close on coincidence of high turbine speed and high rate of speed change as measured by a magnetic pickup device. The overspeed sensors that actuate the stop valves and the governing-control valves are completely independent. The steam passing through the stop and governing-control valves, passes through the high pressure turbine, the moisture seperator-reheaters, the reheat-stop valves, the interceptor valves and the two low-pressure turbines.

The reheat-stop valves are controlled just like the stop valves, and the interceptor valves are controlled just like the governing-control valves.

As Figure 12-1 shows, any steam path has two valves in series. Figure 12-2, which illustrates the control of the steam admission valves, shows that the two valves in series are controlled by completely independent systems. Furthermore, the high pressure oil system that actuates the steam valves is completely independent of the low pressure lubrication oil. The

control and protection system is fail-safe: any loss of oil pressure or voltage causes closure of the steam valves.

As the unit speed deviates from the nominal value (1800 rpm), the main governor gradually closes or opens the control valves to bring the unit speed back to the nominal value. As long as the electrical generator breakers are closed, these are the only expected speed deviations and can be handled by the main governor alone. Should the electrical generator breakers open, a sudden speed change and at a high rate takes place. Upon coincidence of high speed level (∿ 102% of nominal) and high speed increase rate (∿ 90 rpm/sec), the auxiliary governor system is actuated. An electrical signal is sent to the solenoids of the emergency trip valves No. 3 and No. 4 to open them and drain the 1800 psi oil. As a consequence, the control valves close and limit the unit overspeeding within the design limit (15% of nominal).

Should the control valves not close for unknown reasons or should they not be able to keep the overspeed below the setpoint (+ 8% of nominal) of the mechanical overspeed protection, an eccentric is triggered, the 300 psi lubrication oil pressure drops, the emergency trip valve No. 1 opens, the 1800 psi system pressure drops and the stop valves are closed.

To increase the reliability of this system, a pressure switch is installed on the 300 lb. system. Should the pressure of this system drop and opening of the emergency trip valve No.1 fail, this pressure switch will open the emergency trip valve No. 2 and allow the 1800-psi system to drain.

As either the emergency trip valve No. 1 or the emergency trip valve No. 2 opens and drains the 300 psi oil pressure, a check valve opens and causes drainage of the 1800 psi pressure that was keeping the control valves open. Therefore the emergency mechanical overspeed trip closes all the main steam admission valves.

Actuation of the mechanical overspeed trip, independently of the auxiliary governor trip, limits the unit overspeed within the design valve.

Besides these provisions in the design, the stop valves, that are fully open during plant operation, will be exercised on a periodic basis to further preclude the possibility of a valve stem sticking. All the unit tripping devices are periodically checked.

Should all the main steam admission valves and the reheat stop and interceptor valves fail to close on a full load rejection, a unit runaway would take place, causing some damage of the rotating parts. However, no missiles are anticipated to leave the unit, for analysis of the potential mode of failure shows that all parts would be contained within the unit casings.

Assuming, for purpose of analysis, that all the above mentioned valves fail to close, and a turbine runaway occurs, the first disk (turbine wheel) to fail would be one of the low-pressure turbine disks closest to the steam admission point. As this disk bursts the unit would be decelerated because of the loss of the driving force from the blades of this disk and the drop in unit efficiency. An analysis of the energy required to violate the integrity of the low pressure turbine casings shows that there is a large margin between the kinetic energy of the broken parts of the burst disks at their bursting speed and the energy required to penetrate the low pressure turbine cylinders.

A stress analysis of the remaining disks shows that their bursting speed is no more than 15% higher than the bursting speed of the first disks. The assumption is made that even these disks might fail at the bursting speed of the first disks. A plastic analysis of the energy required to penetrate the low pressure turbine casings shows that even the broken parts of these disks will not have enough energy to be ejected outside the casing.

A stress analysis of the high pressure turbine spindle shows that its bursting speed is of the order of 300% of nominal. The large margin between this bursting speed and the maximum speed at which the unit can be driven keeps the proability of a high pressure turbine spindle bursting to practically zero.

Based on conservative design, reliable turbine control system, careful rotor forging procurement and rigorous inspection, the probability of a combination of excessive overspeed, new-born large forging defects, and operating temperature below the transition temperature is considered practically zero, as confirmed by years of major-failure-free operation of the many Westinghouse units.

12.2 STANDBY SAFEGUARDS ANALYSIS

12.2.1 SITUATIONS ANALYZED

Adequate provisions have been included in the design of the plant and its standby engineered safeguards to limit potential exposure of the public to well below the limits of 10 CFR 100 for situations which could conceivably involve uncontrolled releases of radioactive materials to the environment. The situations which have been considered are:

a) Fuel Handling Accidents
b) Accidental Release of Waste Liquid
c) Accidental Release of Waste Gases
d) Rupture of a Steam Generator Tube
e) Rupture of a Steam Pipe
f) Rupture of a Control Rod Drive Mechanism Housing - Rod Cluster Control Assembly (RCCA) Ejection

12.2.2 FUEL HANDLING ACCIDENTS

12.2.2.1 Fuel Handling and Storage Facilities

a) Fuel Transfer System

This system provides for underwater transfer of the fuel assemblies and control rod clusters from the reactor by means of a manipulator crane, fuel transfer carriage, and spent fuel hoist to the spent

storage pit. In the spent fuel storage pit, a second fuel handling device removes the individual spent fuel assemblies from the transfer carriage and places them in the spent fuel storage racks. They remain in the storage racks for a sufficient time to allow decay to a level which permits shipment to a reprocessing plant. Before fuel assemblies containing reuseable control rod clusters leave the reactor cavity, they are placed in the control rod cluster changing fixture where the control rod clusters are removed for insertion into fresh assemblies. Spent control rod clusters are transferred within a spent fuel assembly where they remain when the assemblies are placed in the storage racks.

The following handling accidents will be evaluated during the course of design to assure that no hazards are created:

1) A fuel assembly becomes stuck inside reactor vessel.

2) A fuel assembly or control rod cluster is dropped onto the floor of the reactor cavity or spent fuel pit.

3) A fuel assembly becomes stuck in the penetration valve.

4) A fuel assembly becomes stuck in the transfer carriage or the carriage becomes stuck.

5) A fuel assembly is dropped onto the bottom of the transfer tank under the carriage.

Since all of the operations are under water and since there is always ample cooling for the fuel assembly, regardless of the accident postulated, there is no danger of overheating of the fuel. Further, since such circulation is available naturally, it is possible to prevent excessive local accumulations of activity in the water resulting from defective fuel. Necessary shielding during all fuel handling operations is assured by designing the fuel transfer equipment and facilities such that a fuel assembly is always immersed in water to a depth sufficient to protect personnel.

If the spent fuel assembly or RCC assembly were to come loose from the manipulator crane or spent fuel hoist, it would be easy to see the item through the water and retrieve it remotely.

The simplicity of the system and the ability to establish the water level in the spent fuel storage pit outside the containment at the same level as inside tends to prevent accidents due to misoperation or human error.

During refueling, reactivity accidents are prevented by control of boric acid concentration in the refueling water. The reactor coolant and refueling water are borated sufficiently to yield k_{eff} of approximately 0.90 for cold conditions with all rods in. This concentration is also sufficient to prevent criticality even with all control rods removed. The boron concentration in the refueling water is periodically sampled and continuous mixing is maintained through the reactor vessel by utilizing a residual heat removal pump. During this period, the relative reactivity status (neutron source multiplication) is continuously monitored and indicated by BF_3 counters and count rate indicators. Any appreciable increase in the neutron source multiplication including that caused by the maximum physical boron dilution rate (approximately 600 ppm per hour) is slow enough to give ample time to start corrective action (boron dilution stop and/or emergency boron injection) to prevent the core from becoming critical. The maximum dilution rate is based on the abnormal condition of both charging pumps operating at full speed delivering unborated water to the Reactor Coolant System at a particular time during refueling when the boron concentration is at the maximum value and the water volume in the system is at a minimum.

b) Spent Fuel Storage

The spent fuel storage area is sized for the normal storage of one and one-third complete core and associated control rod clusters. The fuel is spaced to prevent criticality even with unborated water. If an accident were to damage the cooling system, the heat capacity of the water affords ample time for countermeasures. Even if an entire day were to elapse, no serious condition would arise.

Radioactivity and clarity of the water are controlled by means of an ion exchanger and filter built into the spent fuel pit water recirculating system. Any radioactivity which escapes into the atmosphere above the pit is carried off by the ventilating system.

12.2.2.2 Fuel Handling Accident Analysis

Potential off-site consequences of a fuel handling accident have been examined. The only credible cause of cladding failure during handling would be severe mechanical loading of the fuel rods. The chance of such damage is minimized by the design of the spring clip fuel assembly. Since the remote possibility exists of damage occurring during handling of an assembly, this has been selected as the maximum credible fuel handling accident.

The upper limit of this accident is judged to be the sudden release of the gaseous fission products held in the voids between the pellets and the cladding of one row of 15 rods in the fuel assembly. The low temperature of the fuel during handling precludes a further significant evolution of gases from the pellets themselves after the cladding is breached. Halogen release is also greatly minimized due to their relatively low volatility at these temperatures. The tendency for iodine in vapor and particulate form to be scrubbed out of the bubbles of gas during their ascent to the surface of the water also minimizes the inhalation hazard.

The most significant aspect of the incident is the release of the noble gases Xe-133 and Kr-85 which leave the surface of the pit water and are discharged through the ventilation system to the plant vent.

The maximum exposure to a person off-site was estimated, based on approximately 100 hours cooling prior to rupture. The noble gas release from one row of
--+ 15 fuel rods in the assembly is calculated to be equivalent to 1.03×10^3
--+ curies of Xe-133. This release was calculated by dividing the fuel pellets
--+ into five concentric rings with the release rate from each ring assumed to
--+ be dependent on the mean fuel temperature within that ring. A diffusion
--+ coefficient of 1×10^{-11} sec^{-1} for noble gases at 1400°C was used as the

basis for determining diffusion coefficients at different temperatures. This value was determined from data at burnups greater than 10^{19} fissions/cc to account for release by mechanisms such as pellet cracking during irradiation.

Discharge of the equivalent quantity of Xe-133 indicated in the preceding paragraph from the plant vent under conditions represented by the 2 hour dispersion column of Table 2-4 would result in an integrated whole body dose of less than 0.018 rem which is much less than 25 rem set forth in the 10 CFR 100 for accidental exposure.

12.2.3 ACCIDENTAL RELEASE OF WASTE LIQUIDS

Accidents in the Waste Disposal or Chemical and Volume Control Systems which would result in the release of liquid wastes are those which may involve the rupture or leaking of system pipe lines, the waste storage tanks, the volume control tank and pumps. Spillage or leakage of any liquids will be retained within the auxiliary building housing the Waste Disposal and Chemical and Volume Control Systems. Accumulation of any released liquids is accomplished through the building floor drains which flow by gravity into a drain tank. The ventilation system will collect any gaseous radioactivity and discharge it via the plant vent.

All liquid waste processing components are located within the building and any leakage from tanks or piping will be collected in sumps to be pumped back into the liquid waste system.

Piping external to the containment running between the containment and the auxiliary building and the holdup tank area will be run below grade in concrete trenches. Where necessary, because of radiation level, manual valves in radioactive lines will be operated by extension stems run through shield walls.

12.2.4 ACCIDENTAL RELEASE OF WASTE GASES

12.2.4.1 Situations Considered

Gaseous activity which could be released in the unlikely event of a tank rupture will not result in an off-site whole body or inhalation dose in excess of 10 CFR 100 limits. The main sources of gaseous radioactivity are in the volume control tank, waste holdup tank and gas decay tanks.

12.2.4.2 Volume Control Tank Rupture Analysis

In the event that a rupture should occur in the volume control tank, caused by undetermined means, the integrated whole body dose at the site boundary --+ during passage of the cloud of escaped gases would be less than 0.35 rem.

This is based on a release from the plant vent under conditions represented by the 2 hour dispersion column of Table 2-4. The calculations also assume the TID 14844 energy sources for the noble gas isotopes Xe-133, Xe-135, Kr-85, Kr-85m, Kr-87 and Kr-88 and no allowance is made for decay during the entire period of gaseous release. The fission product inventory in the tank is based upon operation with defects in 1% of the fuel rods and the liquid level in the tank at its maximum.

The inhalation hazard at the site boundary from this accident is negligible due to low concentrations and low volatility of the halogens and other non-gaseous isotopes at the temperature and pH of the fluid in the volume control tank. The normal temperature is about 130°F.

The calculations show that the general public will not be exposed to any radiation hazard from this accident as the exposure is sufficiently below the dose limits of 10 CFR 100 for accidental exposure.

12.2.4.3 Gas Decay Tank Rupture Analysis

A sudden failure of a gas decay storage tank or release of its contents by an unspecified mechanism would yield a maximum integrated whole body --+ dose at the site boundary (1/2 mile) of less than 0.85 rem as compared to the 25 rem set forth in 10 CFR 100 for accidental exposure. This is based on a release from the plant under conditions represented by the 2 hour dispersion column of Table 2- 4. It is also assumed that the accident occurs at the end of a 500-day operating period, with a coolant activity equivalent to 1% defective fuel resulting in maximum Kr-85 and Xe-133 in the gas decay tank. This is equivalent to 35,700 curies of Xe-133. The maximum activity level occurs shortly after a cold startup at low boron concentrations with maximum Xe in the reactor coolant.

Safety considerations based on an assumed release of the gaseous activity of the coolant, therefore, would not preclude operation with as many as 1% defective fuel elements. The expected incidence of fuel defects, based on experience to date, is lower than this value by a factor of at least 10.

12.2.5 RUPTURE OF A STEAM GENERATOR TUBE

A preliminary analysis has been performed for the case of double-ended steam generator tube rupture, occurring while the coolant contains fission products equivalent to continuous operation with 1% defective fuel rods. As stated above, it is expected that the activities actually encountered in operation will be less than one tenth of these values.

A conservative evaluation was made by assuming that in the course of cooling down and depressurizing the Reactor Coolant System, requiring about five hours following detection of a tube failure, the steam generator containing the faulty tube is not isolated. A volume equal to slightly less than 1/2 of the Reactor Coolant System is blown down to the secondary system prior to cooldown. If the noble gases are then discharged by the air removal system, the maximum integrated
--+ whole body dose at the site boundary would be less than 0.95 rem. The assumptions used in this analysis are the same as those for the gas decay tank rupture in Paragraph 12.2.4.3. The contribution of iodine activity, which may be transported to the condenser and escape in part by way of the air removal system, was also assessed. Because of the tendency to approach equilibrium partition of I_2 between the condensate and steam phases, only a small fraction of the I_2 activity in the main condenser would be vented to the atmosphere. Assuming a partition factor of 10^{-4} in the main condenser and neglecting further separation in the steam generator, the calculated release is approximately 0.04 curie as equivalent I-131. The maximum off-site thyroid dose which could result from this release
--+ is less than 0.0075 rem.

It should be noted also that the planned procedure for recovery from a tube rupture incident would call for isolation of the steam line leading from the affected steam generator after the primary pressure is reduced below the secondary safety valve setting (about 1100 psia). This action could be completed about ten minutes after rupture, even in the event the incident remains undetected until reactor trip occurs due to a safety injection signal. The discharge of radioactive vapors would be greatly reduced in this case.

since contamination of the secondary system would then be terminated in ten minutes instead of five hours as assumed in the analysis. As the radioactivity in the steam is principally volatile, it does not present a contamination problem in the steam systems. Also, the accumulated radioactivity in the condenser hot well for the period of the accident does not interfere with maintenance.

12.2.6 RUPTURE OF A STEAM PIPE

A break in the steam piping between the steam generator and the turbine will not constitute an environmental hazard because the steam is not radioactive.

Regardless of the location of the steam line break, i.e., between a steam generator and its associated stop valve or beyond the stop valve in the steam line common to the steam generators, alternate paths and adequate feedwater capacity are available by use of the main or emergency feedwater pumps to remove heat from the steam generators.

Core protection is provided in the same manner as for reactivity insertion accidents by the combination of overpower and overtemperature trips. The criteria for the hypothetical steam break accident are as follows:

--+ 1. With a stuck rod, no off site power and minimum engineered safeguards
--+ there will be no consequential damage to the primary system and the
--+ core will remain in place and intact.

--+ 2. With no stuck rod, with off site power and all equipment operating at
--+ design capacity, there will be insignificant cladding rupture.

The accident requires protective action, however, because the reactor control system, sensing the loss of steam pressure as an increase in load, will tend to increase reactor power. If the increase is not excessive, an appropriate manual shutdown procedure can be executed. If reactor power exceeds the overpower setpoint, automatic trip will occur.

--+ The steam line break constitutes an uncontrolled heat removal from the
--+ Reactor Coolant System which is limited by the steam line non-return and
--+ trip isolation valves. These valves cannot preclude the blowdown of one
--+ steam generator, for example, a break upstream of the isolation valve.
--+ In this case there would be a rapid cooldown of the Reactor Coolant System
--+ which, particularly at the end of core life, results in a reduction in
--+ shutdown reactivity margin after trip. The resultant coolant contraction
--+ has the characteristics of the beginning of loss of coolant and results
--+ in the initiation of engineered safeguard systems as the pressurizer
--+ empties. These systems compensate for the temperature effect on reactivity
--+ in all anticipated cases by boron addition. If the flux distribution re-
--+ sulting from a single stuck RCCA is sufficiently distorted, DNB may occur
--+ at relatively low power, causing cladding deformation and possible clad-
--+ ding rupture in a limited core region. Only in the extreme case, where
--+ the combined effects of a stuck RCC assembly, largest steam line rupture
--+ and the most adverse reactivity coefficients are imposed, would the possi-
--+ bility exist for sufficient power generation to cause cladding damage. The
--+ extent of possible damage, if any, will be determined during detailed design.
--+ The duration and magnitude of the peak power generation is limited such that
--+ conditions are significantly below those which could lead to fuel cladding
--+ melting and there is no possible mechanism for primary system pressure
--+ pulses. Public and plant personnel safety is assured by the fact that
--+ the transient is self-limiting because rising coolant temperatures, blow-
--+ off of available coolant in the secondary system and continued boron ad-
--+ dition act to terminate the transient, and by the fact that any fission
--+ products released from the fuel would be contained in the Reactor Coolant
--+ System.

--+
--+
--+
--+
--+
--+
--+
--+

The steam piping is adequately anchored at the containment wall and is routed so that any whipping of the ruptured pipe will not result in compounding of the break. The rupture of secondary piping has been assumed to impose a maximum pressure differential of 2485 psi across the tubes and tube sheet from the primary side to the secondary side. The design of the steam generators is such that under these conditions there shall be no rupture of the primary to secondary boundary, thus preventing any violation of the Reactor Coolant System integrity.

12.2.7 RUPTURE OF A CONTROL ROD DRIVE MECHANISM HOUSING - ROD CLUSTER CONTROL ASSEMBLY (RCCA) EJECTION

The reactor protection system provided for the pressurized water reactor is capable of terminating any credible reactivity excursion without DNB. Thus, even if a group of RCC assemblies having maximum reactivity worth are withdrawn from the core at the maximum drive speed, there would be no significant temperature rise in the cladding and no zirconium water reaction. The only conceivable way of exceeding the maximum reactivity insertion rate for which the protection system prevents DNB is for a rupture of a control rod mechanism housing to occur. Such a rupture is not considered credible for the following reasons:

a) The housings are of conservative design and initially hydrostatically tested to approximately 4100 psi prior to operation.

b) Stress levels in the housing are not affected by system transients at power or by thermal movements of the coolant loops.

c) The housing is constructed of Type 304 stainless steel which shows excellent notch toughness at all temperatures that will be encountered during the operation of the plant. A significant margin of strength in the inelastic range is thus provided and gives additional assurance that gross failure of the housing will not occur.

If a rupture of a control rod mechanism housing were assumed to occur, the resulting loss of coolant would be small compared with the hypothetical accident for which the containment is designed. The significance of this accident derives from the possibility that the RCCA could be ejected from the core in a very short time by full system pressure differential acting on the drive shaft. The resultant power excursion is limited by the Doppler reactivity effect of the increased fuel temperature and terminated by reactor trip actuated by high nuclear power signals. Due to the extremely low probability of the incident, fuel damage is considered acceptable. However, the plant is designed such that there is no possibility of a consequential pressure surge causing further rupture of the Reactor Coolant System.

The amount of fuel damage that could result from such an accident is governed mainly by the peak power attained in the transient which in turn depends on the worth of the ejected rod and the power distribution attained with the remaining control rod pattern.

An analysis will be performed in the course of detailed design to determine the spatial distribution of excess energy in the fuel, the resulting fuel temperature and the heat transfer to the coolant as a function of reactivity insertion in this transient. If there is any likelihood of this dispersal due to fragmentation of the fuel pellet-clad system, a detailed analysis will be made to demonstrate the rapid dissipation of this energy into the water does not create a significant pressure surge to jeopardize either the integrity of the vessel or that of the Reactor Coolant System.

The core design for the plant does not represent a significant departure from previous plants for which detailed rod ejection analyses have been made. By using the flexibility in the selection of control rod groupings, radial locations and position as a function of load, the final design will limit the maximum fuel temperature for the highest worth ejected rod to a value which will preclude any further rupture of the primary system.

The results of the sensitivity analysis performed for the Indian Point Unit No. 2 and reported in the "Second Supplement to Preliminary Safety Analysis Report" Docket No. 50-247 are applicable to the this plant. The expected maximum ejected rod worth for the zero power case is 0.6% as for Indian Point Unit No. 2 and using a conservative analysis there would be no fuel melting and no potential rupture of the Reactor Coolant System for this case. The expected maximum ejected worth at full power is considerably less than 0.5% $\Delta k/k$ and as reported for Indian Point Unit No. 2, even this case resulted in no fuel dispersal and hence no potential rupture. The increased thermal rating for this plant above Indian Point Unit No. 2 is accompanied by lower hot channel factors resulting in a lower specific power. The initial conditions for the hot spot are therefore no worse for this plant than for Indian Point Unit No. 2 with respect to the rod ejection analysis. The upper limit for potential insertion from the positive moderator coefficient is also comparable to Indian Point Unit No. 2 e.g., approximately 1.5% $\Delta k/k$.

12.3 MAJOR RUPTURE OF A REACTOR COOLANT PIPE

12.3.1 GENERAL

A loss-of-coolant accident may result from a rupture of the Reactor Coolant System or of any line connected to that system up to the first closed valve. Ruptures of very small cross section will cause expulsion of coolant at a rate which can be accommodated by the charging pumps. Should such a small rupture occur, these pumps would maintain an operational level of water in the pressurizer, permitting the operator to execute an orderly shutdown. A moderate quantity of coolant containing such radioactive impurities as would normally be present in the coolant, would be released to the containment.

Should a larger break occur, resultant loss of system pressure and pressurizer liquid level will cause reactor trip and initiation of safety injection. These countermeasures will limit the consequences of the accident in two ways:

a) Reactor trip and borated water injection will supplement void formation in causing rapid reduction of the nuclear power to a residual level corresponding to delayed fissions and fission product decay.

b) Injection of borated water ensures sufficient flooding of the core to prevent excessive temperatures.

Operation of all components of the Safety Injection System prevents any melting of fuel cladding and limits metal-water reaction to a negligible amount for reactor coolant piping ruptures up to and including the diameter of the largest pipe connected to the reactor coolant loops (the pressurizer surge line or residual heat removal lines). Consequences of these ruptures are well within those described later in this section for the hypothetical accident and are therefore well within the limits of 10 CFR 100.

Supports for the reactor vessel and the other main reactor coolant piping will be sufficient to prevent rupture or failure of any safety injection line which is not connected to the pipe assumed to rupture. All piping which is connected to the Reactor Coolant System and which penetrates the containment will be provided with sufficient anchorage and load limit controls to prevent violation of the containment at the containment penetration as a result of a reactor coolant pipe break or a seismic disturbance. The design of the steam generator is such that the maximum differential pressure of 1100 psi acting on the tubes and tube sheet after reactor coolant blowdown will not cause failure of the primary/secondary boundary.

The steam generators will be supported in a manner which will prevent rupture of the secondary side of a steam generator and/or main steam and feedwater piping as a result of the forces created by the rupture of a reactor coolant pipe or by a seismic disturbance. In general, the forces due to pipe rupture are considerably larger than seismic forces. As necessary, each steam generator will be provided with additional supports which will supplement the gravity supports and will limit the motion of the steam generators under the reaction forces due to the reactor coolant pipe break to a distance that is compatible with the flexibility of the main steam and feedwater piping. The support system design will be sufficient to resist the forces from an assumed break at any point in the Reactor Coolant System.

Whenever possible, piping and valves, except root valves and their connections to the coolant piping, will be run in the annular space between the primary shielding and the containment wall. Thus, these components will be completely outside the area occupied by the primary equipment and the reactor coolant loops and will be protected from possible effects of a loss-of-coolant accident.

Special precautions will be taken with the pressurizer relief valves (which must be located above the operating floor) to protect these valves from mechanical damage which could lead to a loss-of-coolant accident.

Valves necessary for operation under accident conditions will be specified and selected so that they will not be rendered inoperative by the temperature and pressure conditions existing at the time of an accident. Organic material used for electrical insulation and other uses, such as valve stem packing, will be selected so that prolonged exposure to high temperatures will not cause excessive deterioration.

The design criteria for the Safety Injection System are presented in Chapter 6 along with a description of the system.

The zirconium-water reaction following a loss of coolant accident is considered in the analyses and is based on the zirconium water reaction characteristics given by Baker[2], Epstein[3], and Lustman[4].

12.3.2 LOSS OF COOLANT ACCIDENT EVALUATIONS

To determine the requirements of the containment structural design and to evaluate the engineered safeguards systems, analyses were performed to describe the transient condition inside the containment following a postulated loss of coolant accident. The analysis is based on mathematical models which reflect the phenomena occurring within the Reactor Coolant System, the reactor core, and the containment during and after a loss of coolant accident. Conservative approaches and parameter values have been assumed for these mathematical models.

Previous analyses have shown that the double-ended rupture of the 29-inch I.D. piping near the reactor vessel outlet nozzle causes the largest initial containment pressure rise due to lack of time to transfer heat to the containment structural heat sinks and active cooling systems. For smaller breaks, the initial discharge carries additional residual heat and stored heat into the containment due to longer blowdown times, but considerably more heat is absorbed by the containment cooling systems and containment structure.

The reactor coolant pipe rupture was first analyzed on the basis that electrical power from external sources was available and all components of the Safety Injection System, containment spray and containment ventilation fan coolers operate. Normal delays associated with instrument and relay time lags, the time required to open flow paths, and to bring pumps to operating speed are considered in the analysis.

To demonstrate the adequacy of the engineered safeguards and containment even in the event that all the external sources of power to the station fail, an analysis was made for the more severe condition that only those --+ safeguards function which can be powered by two of the three emergency generators.

12.3.2.1 Coolant Blowdown Transient

The analyses of the transient flows, coolant inventory, temperature and pressure of the Reactor Coolant System following various assumed large-area ruptures were performed using the digital computer code FLASH.[5] This code calculates rate of coolant blowdown and rate of influx from the Safety Injection System, pressure drop and flow through the core and intact loops, and accounts for energy entering and leaving the system, by way of the core and steam generators. Reactor power is forced by moderator reactivity entered as a function of time, and a reactor trip model which represents insertion of the RCC's. The moderator density reactivity contribution is pre-calculated using a more detailed core model than is now available in FLASH, with predicted pressure and flow transients which are checked with FLASH results for consistency and conservatism.

For smaller breaks up to the surge line break, the digital computer code, LOCO, is employed to calculate the transient depressurization of the Reactor Coolant System as well as the mass and enthalpy flux through the break at any time. The conservation equations of continuity and energy are written for the Reactor Coolant System, together with critical flow momentum relationships for the discharge flow rate, appropriate equations of state, and initial and boundary conditions. There are two distinct phases in the discharge process.

Phase I: Discharge of subcooled water through the break results in a rapid system depressurization to saturation pressure. During the period of subcooled blowdown, the reactor trip is initiated by low pressurizer pressure. Prior to the trip, full reactor power is added to the coolant but this heat is removed by forced convection heat transfer in the steam generator tubes. After the reactor trip is completed with an allowance for trip delay, core residual heat (delayed neutron residual fission plus fission and capture product decay) and sensible heat are transferred to the coolant. Sensible heat includes the heat stored in both the core and core structures, and a portion of the thick metal in the reactor vessel.

Phase II: Continued discharge of the coolant water through the rupture results in a change to flashing two-phase flow after a very short time, and discharge of coolant into the containment is restricted by choking flow. Energy is added to the coolant by the core and by cooling of metal parts which are above saturation temperature, and is removed by loss of coolant and by heat transfer to the steam generator secondary water. When the reactor coolant water level falls below the steam generator tube inlet level, all heat removed from the coolant is by way of the break into the containment.

Discharge of the homogeneous steam-water mixture continues to add mass and energy to the containment until almost no water remains in the system. Because of the high blowdown rate for a complete severance of a large reactor coolant pipe, the rapid steam evolution results in transport of large quantities of entrained liquid. A distinct interface may not exist as the core becomes uncovered. When the calculated liquid entrainment is less than 1 w/o, steam flow is assumed to exist. The computer calculation shows that very little water will remain in the bottom of the reactor vessel because of the rapid blowdown.

During the coolant blowdown, the pressurizer low pressure signals cause reactor trip and in conjunction with low pressurizer water level signals, actuate safety injection. The accumulators automatically discharge their contents into the Reactor Coolant System when the system pressure falls below 600 psi.

Residual heat generation and any zirconium-water reaction heat increase the stored energy in the core and reactor vessel for the short period of time until borated safety injection water reaches the vessel through connections in the cold leg piping. A portion of the initial safety injection flow is flashed to steam as it comes in contact with the hot core, vessel, and internals structure. This steam flows into the ccontainment through the break.

After the core has been covered and the vessel filled with safety injection water, the residual heat generation rate and stored energy release rate are not sufficient to cause further boiling. The safety injection water continues to absorb the residual heat and stored heat, but remains a liquid as it spills out of the break into the containment.

Once the core is covered by the injected water and the Reactor Coolant System is depressurized, long-term cooling of the core is accomplished by switching to the recirculation mode of operation after the injection phase is completed due to the emptying of the refueling water storage tank. Spilled borated water is drawn from the containment sump, passed through the residual heat exchangers, and returned into the reactor vessel by the residual heat removal pumps.

An additional energy source is stored heat in hot components which are not touched by the safety injection flow because they are located above the break location. Examples include the vessel head, pressurizer, and steam generators. Treatment of these energy sources is covered in Section 12.3.2.3.

12.3.2.2 Core Thermal Transient Analysis

The LOCTA-R2 transient digital computer program was developed for evaluating fuel pellet and cladding temperatures during a loss of coolant accident. It determines the extent of the Zircaloy-steam reaction and the magnitude of the resulting energy release in Zircaloy clad cores.

The transient heat conduction equation is solved by means of finite differences, considering only heat flow in the radial direction. A lumped parameter method is used - the fuel containing three nodes and the cladding, one node.

Internal heat generation can be specified as a function of time, or the decay heat from any initial power level can be calculated by the code. The decay heat is based on the heat generated from:

a) Fission Products,
b) Capture Products, and
c) Delayed Neutrons

It is assumed that the core has been irradiated for an infinite period of time.

In addition to decay heat, the code calculates the heat generated due to the Zircaloy-steam reaction. The Zr-H_2O reaction is governed by the parabolic rate law unless there is an insufficient supply of steam available, then a "steam limited" evaluation is made. The buildup of the Zircaloy-oxide film is calculated as a function of time, and its effect on heat transfer is considered. An isothermal cladding melt is considered based on the heat
--+ of fusion of Zircaloy. Once the Zircaloy metal melts, it is retained by the
--+ Zirc-oxide, and slumps against the fuel. The Zircaloy-steam reaction may
--+ continue until the oxide melts. If the oxide melts, the remaining Zircaloy
--+ is assumed to fall, and 10% of this metal is assumed to react with additional
--+ water which is available in the vessel.

--+ The computer program stacks axial sections and thereby describes the behavior
--+ of a full length region as a function of time. A mass and energy balance is
--+ used in evaluating the temperature rise in the steam as it flows through
--+ the core.

--+ The initial conditions of the fuel rod are specified as a function of power.
--+ The following core conditions are also introduced as a function of time as
--+ determined by the Flash Code:

--+ a) Mass flow rate through the core
--+ b) Coolant quality
--+ c) Pressure

--+ Heat transfer coefficients during the various phases of the accident are
--+ evaluated in the following manner:

--+ a) Nucleate boiling film coefficients on the order of 20,000 Btu/hr ft^2 ^{o}F are used until DNB occurs.

--+ b) When DNB occurs, it is assumed that the fuel rods can immediately
--+ develop a condition of stable film boiling. No credit is taken for
--+ higher transition boiling coefficients that exist prior to the
--+ establishing of a stable film on the fuel rods. The correlation used
--+ during this period is

--+ $$h = .023 \frac{k_v}{D_e} \left[\frac{\rho_v D_e}{\mu_v} \left(\frac{Q_1 + Q_v}{A_c} \right) \right]^{0.8} \left(\frac{c_p \mu}{k} \right)_v^{0.4}$$

--+ c) During the time the core is uncovered (period of steam flow through
--+ the core), laminar or turbulent forced convective coefficients and
--+ radiative coefficients are evaluated.

For laminar forced convection to steam:

$$\left(\frac{hD}{k} \right)_{iso} = 3.66$$

$$h/h_{iso} = (T_b/Tw)^{.25}$$

For turbulent forced convection to steam:

--+ $$\frac{hD}{k} = .020 \, (Re_b)^{.8} (Pr_b)^{0.4} \left(\frac{Tw}{T_b} \right)^{0.5}$$

--+ d) Conservative heat transfer coefficients of the order of 25 Btu/hr ft^2 ^{o}F are all that is needed to turn back the rising clad temperature when the core is recovered.

Information generated by LOCTA-R2 as a function of time includes:

a) Fuel Temperature,
b) Cladding Temperature,
c) Steam Temperature,
d) Amount of metal-water reaction,
e) Volume of core melt, and
f) Total heat released to coolant.

--+ Symbols for Equations

--+ h - Heat transfer coefficient on outer surface of fuel rod (Btu/hr-ft^2-^{o}F)
--+ D_e - Equivalent diameter of flow channel - (ft)
--+ ρ - Density (lbs/ft^3)
--+ μ - Viscosity (lbs/ft-hr)
--+ Q - Volumetric flow rate (ft^3/hr)
--+ A_c - Area of flow channel (ft^2)
--+ c_p - Specific heat (Btu/lb-^{o}F)
--+ k - Thermal conductivity (Btu/hr-ft-^{o}F)
--+ T - Temperature ^{o}F

--+ Subscripts

--+ v - Evaluation of the property at the saturated vapor condition
--+ l - Evaluation of the property at the saturated liquid condition
--+ b - Evaluation of the property at the saturated bulk fluid condition
--+ w - Evaluation of the property at the cladding surface temperature

--+ 12.3.2.2.1 Blowdown and Recovery Transient - Large Breaks

--+ The operation of the Safety Injection System with accumulators was analyzed
--+ for a range of reactor coolant pipe breaks up to the double ended severence
--+ for a typical four loop PWR (2758 MWt) in Supplement 6 for Indian Point
--+ Unit No. 2, Docket No. 50-247. The performance of the core cooling system

--+ will be re-evaluated on the basis of the maximum expected rating of the
--+ Diablo Canyon Unit, 3391 MWt, to verify that the criteria of Section 12.3.2.3
--+ are met. The effect of the higher power level on the analyses presented is
--+ not expected to be significant. The blowdown and recovery transient will
--+ be essentially unchanged. The margin to hot spot recovery may be reduced
--+ slightly as a result of the increase in heat generation rate.

--+ 12.3.2.3. Core and Internals Integrity Analyses

a) Integrity Requirements

The basic requirement of any loss of coolant accident, including the maximum hypothetical accident, is that sufficient integrity exist to permit the safe and orderly shutdown of the reactor. To assure that the basic requirement is met the following three sub-requirements must be met:

1) The basic configuration must be maintained. This implies that gross fracture and/or deformation of core and internals must not occur.

2) The ability to move control rods must be maintained so that they can be used to provide shut down even though insertion is not necessarily required following an accident.

3) Internals deformation must be sufficiently small so that primary loop flow, and particularly, adequate safety injection flow, is not impeded.

b) Analysis of Forces and Pressures on Internals and Core

The forces exerted on reactor internals and core, following a loss of coolant accident, are computed by employing the SATAN digital computer program developed for the space-time-dependent analysis of multi-loop PWR plants.

This computer program generally provides a means for the study of the nuclear plant dynamic behavior for a variety of conceivable plant transient operations and accidents. In particular, it can be used to determine the Reactor Coolant System dynamic characteristics after the occurrence of a rupture in the main coolant piping. SATAN is generally similar to, yet more elaborate than, the FLASH code. It can be employed to determine the shock-wave effects in the Reactor Coolant System over short time periods in great detail. It can also handle a larger number of elements along the reactor coolant loops.

The SATAN mathematical formulation employs a three-dimensional approach (length along the flow path, radius and time) in the reactor core; a two-dimensional approach (length along the flow path and time) in the reactor coolant loops; and a lumped-parameter representation for the secondary system. The Reactor Coolant System is assumed to consist of one or two parallel loops. The reactor core and the primary loops

are sectionalized into elements with variable spatial mesh size. The present memory capacity of the IBM-7094 allows a maximum of 70 spatial elements for the system, which may be distributed between the core and the reactor coolant loops in any desirable fashion. Two typical schemes for the simulation of the Reactor Coolant System are shown on Figures 12-3 and 12-4. Figure 12-3 portrays a one-loop representation which can accommodate leaks over an appropriate size range in the hot leg (element 7) or in the cold leg (element 11). Figure 12-4 is a two-loop representation. In this arrangement three parallel loops are lumped as one-loop and double-ended complete severance ruptures can be accommodated on the fourth loop either in the hot leg (between elements 6 and 7) or in the cold leg (between elements 13 and 14).

The thermodynamic state of the coolant in any element is defined by:

a) a set of main dependent variables and
b) a set of auxiliary dependent variables.

The main dependent variables are those variables computed by the integration of a differential equation. The main dependent variables are: coolant pressure, enthalpy, element liquid mass, element vapor mass, axial mass flow rate and radial (or branch) mass flow rate. The auxiliary dependent variables are: coolant steam quality, density and temperature. To compute the main and auxiliary dependent variables, the following fundamental equations are first expressed for each element:

a) The continuity equation,
b) The energy equation,
c) The momentum equation, and
d) The state equation.

These equations are then rearranged so that the time derivative of the main dependent variables and the values of the auxiliary dependent variables are explicitly defined in terms of the present system variables. These explicit equations form a system of simultaneous differential equations which is integrated numerically on the computer to obtain the time-variation of all dependent variables.

The SATAN program has several distinctive features summarized as follows. The code can accommodate:

a) A leak or a complete-severance double-ended rupture of a desired size with zero or a given rupture time for any element in the hot or the cold leg.
b) Flow reversal for any element.
c) Subcooled, two-phase, or superheat flow in any element.
d) Critical choking flow at the rupture point.
e) Heat transfer in the core and the steam generator.

To verify the correctness of the mathematical formulation and the various numerical techniques employed, the code was checked against LOFT experimental results presently available. The LOFT reservoir blowdown tests consists of a 12 inch dia. 10 ft. long cylindrical reservoir connected to a 4 inch dia. pipe plugged at the end by rupture discs. The reservoir is filled with high enthalpy, high pressure water. The rupture discs are then broken. The pressure and temperature time-variation in the reservoir and the discharge pipe are then recorded.

The SATAN program was used to simulate the LOFT reservoir blowdown test numbers 530 and 522. Figures 12-5 through 12-8 show that the pressure and temperature time history obtained from SATAN are in good agreement with LOFT experimental data from test 530. The discrepancies observed at the onset of two-phase blowdown is due to metastability phenomenon when the fluid undergoes a non-equilibrium flow and predicts higher pressures with subsequently larger and more conservative blowdown discharge and reduced blowdown time.

Having gained confidence in the validity of the SATAN program results, the code was applied to the blowdown analysis for this plant. The plant was first brought to steady-state from initially uniform pressure and enthalpy distributions throughout the system. The computed steady-state variables were then checked against the available plant thermal and hydraulic characteristics and found to be in a very good agreement. This steady-state verification provided a further proof for the validity of the digital program. Starting from these steady-state values, the following blowdown analyses were performed:

1) One-loop system with large leak (area equal to double-ended rupture from one actual loop) on hot leg with zero rupture time;

2) One-loop system with large leak (area equal to double-ended rupture from one actual loop) on cold leg with zero rupture time;

3) Two-loop system with double-ended rupture (complete severance) on the hot leg of one actual loop with zero rupture time; and

4) Two-loop system with double-ended rupture (complete severance) on the cold leg of one actual loop with zero rupture time.

From the pressure time history of core inlet and outlet plenums and the vessel inlet and outlet plenums the pressure difference across the core and the upper plenum was respectively computed and used to determine forces on the reactor internals. Figures 12-9, 12-10, and 12-11 show typical pressure-time histories.

Sensitivity studies were performed to evaluate the effect of rupture time on pressure gradients. It was found that rupture times of the order of 0.3 sec. considerably reduces the values of pressure gradients on reactor internals by at least a factor of two as compared with the pressure gradients obtained with zero rupture time used in the present analysis.

12.3.2.4 Containment Pressure and Temperature Transient Analysis

Calculation of containment pressure and temperature transients is accomplished by use of the digital computer code, COCO. The analytical model is restricted to the containment volume and structure. Transient phenomena within the Reactor Coolant System affect containment conditions by means of convective mass and energy transport through the pipe break.

For analytical rigor and convenience, the containment air-steam-water mixture is separated into two systems. The first system consists of the air-steam phase, while the second is the water phase. Sufficient relationships to describe the transient are provided by the equations of conservation of mass and energy as applied to each system, together with appropriate boundary conditions. As thermodynamic equations of state and conditions may vary during the transient, the equations have been derived for all possible cases of superheated or saturated steam, and subcooled or saturated water. Switching between states is handled automatically by the code. The following are the major assumptions made in the analysis:

i) Discharge mass and energy flow rates through the Reactor Coolant System break are established from the coolant blowdown and core thermal transient analysis (described in the preceding paragraphs).

ii) At the break point, the discharge flow separates into steam and water phases. The saturated water phase is at the total containment pressure, while the steam phase is at the partial pressure of the steam in the containment.

iii) Homogeneous mixing is assumed. The steam-air mixture and the water phase have uniform properties. More specifically, thermal equilibrium between the air and steam is assumed. This does not imply thermal equilibrium between the steam-air mixture and the water phase.

iv) Air is taken as an ideal gas, while compressed water and steam tables are employed for water and steam thermodynamic properties.

During the transient, there is energy transfer from the steam-air and water systems to the internal structures and equipment within the shell.

Provision is made in the containment pressure transient analysis for heat transfer through, and heat storage in, both interior and exterior walls. Every wall is divided into a large number of nodes. For each node, a conservation of energy equation expressed in finite difference form accounts for transient conduction into and out of the node as well as temperature rise of the node. The film heat transfer coefficients between the containment contents and a wall surface may be specified either as a function of time or temperature difference. For this study, test values obtained by Kolflat[6] were used to set inner surface film coefficients for condensing steam. Initial values of 620 and 240 BTU/hr-ft^2-°F were assumed for condensation on steel and concrete, respectively, as recommended in the proposed USA S.I. Section N-6.7, Proposed Design And Pressure Decay Requirements. The coefficients were then linearly decreased with time to a value of 40 BTU/hr-ft^2-°F at the end of the blowdown.

The latter value is typical of steady state heat transfer coefficients for steam condensing through a stagnant surface air layer where the ratio of air to steam is high. The former values are reasonable since the initial blowdown will produce large amounts of steam in the containment together with high turbulence. Thus the ratio of air to steam will be low and a turbulent boundary layer will exist leading to a high film coefficient of heat transfer. The assumed reduction in film coefficient is conservative since, as predicted by Jakob and demonstrated by Uchida[7] the film coefficient will be a function of the ratio of air to steam in the containment which will not be reduced significantly until pressure reduction due to steam condensation occurs.

Provision is made in the computer analysis for the effects of several engineered safeguards, including internal spray, fan coolers, and recirculation of sump water. The heat removal from containment steam-air phase by internal spray is determined by allowing the spray water temperature to rise to the steam-air temperature. This procedure has been experimentally verified[8].

Finally, hot metal surfaces not cooled by safety injection water are simulated as hot walls in contact with the containment steam-air mixture. A small film heat transfer coefficient is employed to reflect actual condition since these surfaces are covered by stagnant steam inside the Reactor Coolant System.

During the brief period between completion of the initial blowdown and addition of safety injection water, the transfer of heat into the containment vessel by convection from the Reactor Coolant System insulation and by the small residual steam flow is relatively ineffective. Consequently, most of the residual heat generation serves to raise the temperature of the core, internals structure, and the reactor vessel. As the Zircaloy cladding temperature in any portion of the core rises above the threshold at which a significant rate of reaction occurs (1800°F), additional energy is produced and stored inside the reactor vessel. Unless the steam evolution rate exceeds the maximum possible zirconium consumption rate established by the parabolic rate law, all steam evolved is considered to contribute to the core stored heat by reacting with zirconium, and the energy addition to the containment during this portion of the transient is a result of the burning of the hydrogen generated by the zirconium-water reaction.

The analysis is performed on the basis that the hydrogen generated within the Reactor Coolant System as a result of a metal-water reaction following a loss of coolant accident will burn as it discharges from the break into the containment atmosphere. The reaction does not start until the cladding temperature exceeds the threshold of 1800°F for zirconium, and the hydrogen will be formed at temperatures between 1800°F and 4800°F.

Studies conducted by the U. S. Bureau of Mines[9] indicate that hydrogen can ignite without an external energy source when its temperature is above well defined limits. This spontaneous ignition temperature (SIT) of hydrogen varies with the break flow velocity and the steam content. For low velocities and high vapor content the SIT is conservatively taken as 1250°F. Thus, in order to prevent spontaneous ignition, the hydrogen must be cooled from its formation temperature by at least 550°F (1800°F minus 1250) and by an even more substantial amount considering the higher formation temperatures associated with any significant evolution of hydrogen. The hydrogen exit temperature has been evaluated for two possible cooling mechanisms for a formation temperature of 1800°F.

i) The first mechanism evaluated is the heat transferred to the reactor coolant system piping. The temperature of hydrogen as it enters the containment atmosphere is computed assuming the following:

1. The rate of hydrogen evolution is based upon the steam limited reaction which is consistent with the assumption of no core quenching and produces the maximum reaction with the cladding and the maximum quantity of evolved hydrogen.

2. The amount of hydrogen produced is determined by assuming that all the steam formed by boiling of the water remaining in the reactor vessel below the core reacts with the cladding. Hence, no mixing of hydrogen with water vapor has been assumed to occur. This mechanism produces the maximum quantity of hydrogen.

3. Hydrogen flows directly from the core, through a 50-foot length of reactor coolant hot-leg pipe before reaching the atmosphere.

4. A conservatively low value of 300°F is assumed for the pipe wall temperature.

5. The physical properties of hydrogen are evaluated at 1800°F.

6. The heat transfer coefficient in the coolant pipes is calculated using the Dittus-Boelter relationship.

Applying these conservative assumptions the hydrogen is found to be cooled to 1335°F before discharge. This temperature is 80°F above the most conservative value of the SIT and 365°F above the expected SIT. Higher formation temperatures produced as the reaction proceeds without core quenching would result in even higher exit temperatures and spontaneous combustion.

ii) The second cooling mechanism investigated is the effect of mixing with a flow of cooler steam which might by-pass the metal-water reaction. In this case less hydrogen would be produced. Assuming again that the hydrogen is formed at 1800°F and that steam is present at 300°F saturation conditions, it is found that a steam bypass flow of 36% will only reduce the hydrogen temperature to 1200°F (a value comparable to the conservative value of the SIT). Volume fractions of steam higher than 36% bypassing the point of reaction would limit the reaction rate due to dilution and cooling.

The hydrogen-oxygen reaction is the only significant source of energy reaching the containment from the zirconium-water reaction between the time that blowdown is complete and safety injection starts. If any zirconium-water reaction occurs before cooling by safety injection becomes effective, only a fraction of the total zirconium available for reaction will be consumed, because the Safety Injection System is actuated in a very short time and the core temperature rise does not progress to a great extent. The energy released from this reaction does not enter the containment concurrently with the blowdown energy, since cladding temperature does not increase during blowdown. An influx of safety injection water is necessary to liberate the stored heat and safety injection cooling does not begin until after blowdown is complete.

12.3.2.5 Force and Pressure Transient Results on Core and Internals

a) Core

During a hot leg break, the difference in pressure across the core is oscillatory for approximately 2 seconds (Figures 12-9 to 12-11)

and later on is approximately constant. The largest longitudinal force on the fuel assembly will occur during the initial transient and will reach a value of 6,700 pounds per fuel assembly in compression.

During a cold leg break the longitudinal compressive force on the fuel assembly has a peak value of approximately 9,900 pounds.

The force to buckle a fuel assembly is of the order of 85,000 pounds. The Inconel grids connecting the fuel rods are able to maintain the rods in position during the transient.

b) Core Support Structure

As a consequence of the dynamic effect during the initial transient following a hot leg break, the upper core support structure has a maximum deflection upward of 0.120 inches and the maximum total stresses (approximately 12,000 psi) occur at the grid and upper support plate ligaments.

After the first 2 seconds, the force on the upper core support structure becomes approximately constant; each fuel assembly exerts a force of approximately 2920 pounds. The upper core support structure deforms 0.057 inches under this load. Maximum total stresses are at the grid and upper support plate (approximately 12,700 psi).

Following a cold leg break, there will be no significant effects on the upper core support structure because the external forces on the core are predominantly downward.

c) Lower Core Support Structure

Following a hot leg break the maximum total stress occurs at the lower girth weld during the initial transient and is approximately 15,000 psi.

Following a cold leg break, the maximum total girth weld stress is approximately 11,000 psi.

d) Thermal Shield

The thermal shield is rigidly connected to the core barrel and will not be adversely affected by pressure and flow transients following either a hot or cold leg break.

e) Upper Core Barrel

The pressure across the upper core barrel becomes oscillatory during an accident and, to establish its behaviour, buckling and radial natural frequency as a short cylinder were computed. The results are:

Buckling Pressure	- 850 psi < p_{cr} < 2400 psi
Extensional Natural Frequency	- f > 1180 cps
Bending Natural Frequency	- f = 60 cps - 100 cps

During the first 0.5 seconds following a hot leg break, the difference in pressure across the core oscillates between +400 and -400 psi at a frequency of 15 cps which is small compared with the natural frequencies listed above. The corresponding stress level is $\sigma = \pm 13{,}500$ psi. After this initial transient, this difference in pressure remains approximately constant and much smaller ($\sim$ 75 psi inward).

The maximum pressure oscillation following a cold leg break is $\Delta p = \pm 600$ psi at a frequency of f = 17 cps producing a stress level of $\pm 20{,}300$ psi assuming completely elastic behaviour.

f) RCC Guide System

The RCC guide system will not be adversely affected following either a hot or cold leg break. Compressive stresses (approximately 16,800 psi), which are below the yield strength of the material will be present in the fuel assembly thimbles without affecting the integrity and/or the stability of the system.

During a hot leg break, cross flow in region above the core will stress the guide column near the outlet nozzle leading to the break producing a maximum bending stress of 6,000 psi for the initial flow peak immediately after the break. Then the flow reduces to a value below the normal steady-state flow.

During a cold leg break the effect of transverse flow across the guide columns is much smaller than for the hot leg break.

In each of the cases described above, the stresses and deformations which would result following either a hot or cold leg break are less than those which would adversely affect the integrity of the structures. Also, the natural and applied frequencies are such that resonance problems would not occur. Therefore, it is concluded that:

a) The forces imposed, due to either a hot or cold leg break, can be sustained by the internals system,

b) The integrity of the internals system is maintained, and,

c) The basic requirements described in Section 12.3.2.3 are met.

12.3.2.6 <u>Containment Pressure Transient Results</u>

a) Containment Pressure Transient for a Reactor Coolant Break Assuming Partial Safeguards

Figure 12-12 shows the containment pressure transient resulting when only partial engineered safeguards are operating on emergency power. In addition to the three of four accumulators delivering to the core, the engineered safeguards started automatically are:

--+ 1) Two high head safety injection pump
2) One residual heat removal pump
--+ 3) Three air recirculation fan cooler units
4) One containment spray pump
--+ 5) Two component cooling water pumps.
6) Two auxiliary salt water pumps

--+ One residual heat exchanger, and one auxiliary building ventilation fan are placed into service manually during the recirculation phase.

A 20 second delay in initiation of safety injection water flow via pumps and a 50 second delay in the start of containment spray flow is assumed. The residual heat exchangers are used for long-term recirculation cooling, and are not operated until 75% of the water in the refueling water storage tank is used.

The Reactor Coolant System blowdown is essentially completed at 10 seconds, at which time the containment pressure has reached an initial peak of 42 psig. Continued heat absorption by the steel and concrete in the containment and internal structure leads to a slight decrease from the peak pressure. For the reactor coolant pipe break, the assumption is also made that the injection lines feeding into the affected loop spill one third of the total injection water flow through the pipe break. As cool water from the accumulators fills the vessel, a portion of the injection water boils (due to core stored heat, residual heat generation, and stored heat in the core structure and vessel), and flows into the containment. The heat sinks more than compensate for the heat addition, and containment pressure remains below the blowdown pressure peak. The prompt injection and core cooldown limit the amount of zirconium-water to an insignificant amount.

After 106 seconds, the rate of residual heat generation plus stored heat release is not sufficient to raise the safety injection water temperature to the saturation point. Hence, the flow to the containment remains subcooled and has little influence on containment pressure. The containment pressure then decreases as steam is condensed by the action of the fan coolers and containment spray, as well as by continued energy absorption of the concrete and internal structure.

When the refueling water storage tank is depleted, containment spray and safety injection using refueling water is stopped. Hot water is then drawn from the bottom of the containment, and pumped back into the vessel through the residual heat exchangers by means of the residual heat removal pumps. The flow spilling out the break continues to remain subcooled, and containment pressure decreases further.

The design philosophy requires that the cooling capacity with one spray pump operating be equal to that of 2-1/2 air recirculation coolers. Therefore virtually the same pressure transient shown by Figure 12-12 would be obtained for the following combinations of containment engineered safeguards.

1) Two containment spray pumps only, or
2) Three air recirculation coolers and one spray pump.

b) Containment Pressure Transients for Smaller Pipe Breaks

--+ The double-ended rupture of the 29-inch I.D. piping near the reactor
--+ vessel outlet nozzle causes the most rapid blowdown and the highest initial
--+ containment pressurization rate. The initial discharge in slightly
--+ smaller breaks carries more residual heat and stored heat into the
--+ containment due to longer blowdown times. The analysis of a range
--+ of break sizes shows the greatest initial pressure peak occurs
--+ with a 3 square foot break.

Figure 12-13 compares the maximum hypothetical accident curve with partial operation of the engineered safeguards on emergency power to curves for three representative breaks.

a) A break area of 3 square feet (smaller than the double-ended 29-inch break but larger than the severance of the largest connecting line).

b) A break equivalent to the surge line (a 14" pipe).

c) A break equivalent to a 4-inch connecting line.

These results show that the containment pressure remains well below safe limits for any break. All of these cases were studied for the same conditions, which are:

--+ 1) Partial engineered safeguards operating from the emergency diesel power supply.

2) Three accumulators delivering to the core.

3) One low-head, residual heat removal pump effective after a delay when reactor coolant pressure falls below the pump shutoff head but no less than 20 seconds (the estimated starting time delay with only emergency power).

--+ 4) Two high-head safety injection pump effective after 20 seconds delay (the estimated starting time delay with only emergency power).

5) Three of the five ventilation fan cooler units after 50 seconds delay.

6) One containment spray pump effective after 50 seconds delay (the estimated starting time delay with only diesel power).

--+ 7) Two component cooling water pumps for the fan coolers and residual heat exchangers.

8) Two auxiliary salt water pumps to cool the component cooling water heat exchangers.

For an assumed rupture opening of three square feet, the pressure transient resulting from these conditions is depicted on Curve A of Figure 12-13. A longer time is required to reach the first pressure peak because of the increased blowdown time, and the peak is slightly higher than that obtained for a reactor coolant pipe break.

Although there is more heat absorption by the containment structure, this is offset by the additional residual and stored heat transported into the containment during the lengthened blowdown.

For each of the smaller sized breaks, the analysis is the same. Each case shows a correspondingly lower initial peak.

In all cases, the engineered safeguards operating on emergency power and only partially effective are adequate to prevent overpressuring the containment and to significantly reduce the pressure within half an hour.

12.3.3 EVALUATION OF RADIATION PROTECTION

Chapters 5 and 6 describe the protective systems and features of the unit which are specifically designed to limit the consequences of the major loss of coolant accident. The capacity of these safeguards is evaluated in terms of the off-site radiation exposure which is calculated relative to the exposure which are given as guides in 10 CFR 100. In the following discussion, the performance obtained with each safeguard feature is derived on the basis of both complete and minimum availability. The off site exposures thus obtained are then checked for conformance to 10 CFR 100 requirements.

The features of the safeguards evaluated are the:

Safety Injection System
and Containment Spray System

12.3.3.1 Expected Performance of Safeguards

In the event of a major loss of coolant accident resulting in rapid depressurization of the reactor and exposure of the core to a steam atmosphere, the combined effects of the safeguards features of this plant would limit the radiation dose to persons exposed for two hours outside the site boundary to a maximum dose of approximately 3.1 rem to the thyroid and 0.20 rem to the whole body compared to the 10 CFR 100 limits of 300 rem and 25 rem, respectively. This conclusion is derived from the following physical and mathematical bases:

a) A loss of coolant results from the complete, double-ended severance of the reactor coolant loop at that point resulting in the earliest uncovering of the fuel. Although a break of this description is of little more than a theoretical possibility, it is used as a physical model to define the upper limit of pipe rupture consequences. The analysis of the coolant pressure-volume transient follows the method described in Section 12.3.2.

b) The fuel temperature increase and rapid system depressurization may result in cladding failure in the hotter regions of the core. Release of the inventory of volatile fission products in the pellet-cladding gaps of all fuel rods is conservatively assumed to occur during the interval of core uncovering and prior to core flooding by the accumulator tanks and Safety Injection System. The dose-equivalent quantity of radio iodine thus released is calculated to be less than 3% of the equilibrium core inventory. It is conservatively assumed that all of this iodine escapes from the reactor coolant system. The noble gas in the gap represents about 2.5% of the core inventory.

c) As fuel cladding temperatures rise above the threshold of zirconium-water reaction, the additional heat input from the reaction is included in the transient calculation; the analysis follows the method described in Section 12.3.2. The remainder of the iodine contained in the UO_2 is assumed to be liberated as the local UO_2 temperature reaches 2500°F. The tendency of the liberated iodine to form compounds of limited volatility (iodides of Fe, U, Cs, etc.), and to condense and deposit in the cooler regions of the reactor system is represented by a 50% retention factor, consistent with the TID-14844 model. The iodine not retained is assumed to be dispersed to the containment atmosphere as liberated.

d) The Safety Injection System, whose active components are actuated by the coincidence of pressurizer low pressure and low water level conditions delivers borated water to the reactor by means of the accumulators, three high-head and two residual heat removal pumps powered by the external electrical system. The integrated release of iodine from ruptured cladding and from those fuel regions above 2500°F up to the time of reflooding is estimated to be less than 10% of the core inventory. The corresponding quantity escaping deposition in the Reactor Coolant System is 5%.

e) The fission products other than iodine released during this period and escaping retention in the reactor systems are calculated on the basis of 100% noble gas, 50% other volatiles, and 1% other elements. The source of this release is also considered to be the fuel regions exceeding 2500°F in the transient.

f) The whole body dose resulting from dispersion of the combined fission product sources in the shielded containment was calculated to be less
--+ than 0.45 mrem in two hours and about 2.7 mrem over one month at the site boundary. This calculation allows for the shielding effect of
--+ the 3.5 foot concrete vertical wall and the 2.5 foot concrete dome.

g) The containment leak rate, through unblocked paths, of 0.1% of the contained volume per day is assumed to persist during the first day following the accident. During the next 30 days the leakage rate is assumed to be 0.045% per day based on a reduction of containment to pressure to approximately 3 psig and assuming the leakage is proportional to the square root of the pressure ratio when the pressure is below about 15 psig.

h) The inhalation dose incurred by a person in two hours at the site boundary of one half mile is determined using the site meteorological dispersion model given in Chapter 2. Exposure to the plume during the two hour period results in a maximum thyroid dose to an adult of about 3.1 rem, which is less than 0.011 times the 10 CFR 100 limits for thyroid dose.

i) Subsequent to the emptying of the refueling water storage tank during the initial phase of safety injection and containment spray, water from the containment sump is recirculated by the residual heat removal pump and cooled via the residual heat exchangers and then returned to the containment. Because the hypothetical loss-of-coolant accident may cause the sump water to contain significant amounts of radioactivity, the potential off-site exposures due to the operation of the recirculation loop have been evaluated.

As shown in Section 6.2, the maximum estimated leakage to the auxiliary building from the components and joints of the Safety Injection System components during recirculation is approximately 1380 cubic centimeters per hour.

During the recirculation phase of post-accident cooling, the sump water temperature is calculated to be about 200°F at the initiation of recirculation so that essentially no leakage will flash to vapor. For con-

servatism in the analysis, it is assumed that approximately 10 per cent of the leakage or 138 cc/hr will flash to vapor and carry the entrained iodine to the atmosphere of the auxiliary building for a period of 1 hour following initiation of recirculation. The auxiliary building ventilation system is designed as an engineered safeguard system and will maintain the building at a slight negative pressure with only one fan running and will discharge the vapor through absolute filters and out the plant vent.

Leakage from the mechanical seals of the safety injection and residual heat removal pumps and the valve stem leakoffs is piped to the drain tank in the auxiliary building. For the calculated leakage of 38 cc/hr, an additional 4 cc/hr will be vented from the drain tank through the ventilation filters to the plant vent.

It was also assumed that 5 per cent of the core iodine inventory is in the water in the sump which has a total volume of about 1.3×10^9 cc including reactor coolant and injection water. The combined leakage from the recirculation subsystem results in a dose of about 0.14 rem to the thyroid in the one hour at the site boundary. The actual dose would be negligible as the temperature of the recirculated water will be substantially reduced so that little or no flashing should occur. Also, the iodine in the sump will be combined with the thiosulfate from the containment spray and will remain trapped in any leakage.

12.3.3.2 Effect of Loss of External Power on the Capability of Safeguards

In the following section, the situation is analyzed in which safeguards performance is less than that which would be expected in the event of an accident, due to the simultaneous loss of external power. The evaluation shows that reliance is not placed on the continuity of outside power sources.

It is shown that the limits of 10 CFR 100 are met in the case of a complete core meltdown per TID-14844 with partial or delayed operation of the post-accident sprays. Thus the sprays serve as an adequate backup for the containment with testable double penetrations and weld channels and isolation valves, and for safety injection in meeting the regulatory site limits.

In the event that power is not available from the external electrical system immediately following the loss of coolant accident, the on-site emergency power
--+ would automatically start, permitting operation of at least the minimum safety
--+ components (i.e. two high head safety injection pump, one residual heat
--+ removal pump, one spray pump, three fan coolers, two component cooling water pumps, and two auxiliary salt water pumps). The effect of loss of outside power on the performance of the safeguards functions is not severe.

As described in Chapter 6, minimum containment heat removal requirements are sat-
--+ isfied by the operation of air coolers and spray pumps driven by the available emergency power. The associated reduction in leakage source concentration which is obtained with the sprays is only slightly limited by the use of
--+ emergency power as three fan units and one of the two spray pumps can be operated simultaneously. Operation of the accumulators and one high-head safety injection and residual heat removal pump on the emergency power supply will restrict the amount of fuel melting so that the equivalent fission product release is not significantly different than that calculated for operation of the safeguards on outside power. As previously stated, the whole body dose due to direct radiation from the containment at the site
--+ boundary is 0.45 rem in two hours and 2.7 mrem in one month. The inhalation
--+ doses are 3.1 rem in 2 hours and 4.6 rem in one month.

12.3.3.3 Failure to Limit Core Meltdown

Should an accident be postulated in which the Safety Injection System fails to limit the extent of fuel melting, the ultimate release of fission products

to the containment would exceed that presented in the preceeding paragraphs. For this hypothetical accident, the following models and assumptions have been used.

a) Method of Analysis

The evaluation under hypothetical accident conditions was performed using a reactor power level of 3391 MWt. Immediately following the loss of coolant, the leak rate of the containment is assumed to rise to a value of 0.1 per cent of the containment volume per day which corresponds to the maximum expected leak rate at the containment design pressure. In spite of the fact that containment pressure will fall, the leak rate is assumed to be constant at this value for the first 24 hours of the accident. For the next 30 days after this period the assumed containment leak rate is reduced to 0.045 per cent of the containment volume per day. This reduced leak rate corresponds to a containment pressure of 3 psig. At the end of this 30 day period, leakage is assumed to stop.

The radiation sources for the dose calculations are based on the TID-14844 (10) recommendations. For the core meltdown, the core inventory release fractions to the containment are 100% for noble gases, 50% for halogens and 1% for particulate fission products. These are sources used in the calculation of the direct whole body dose. These sources are assumed to be available in the containment atmosphere immediately after the accident.

To limit the consequences of such an event, the containment spray is available to trap the more significant air-transmissable isotopes and thus reduce the consequences of potential leakage. Containment spray is automatically initiated at the time of the loss-of-coolant accident by coincidence of the safety injection signal and the high containment pressure signal.

Calculations are based on 0.2% of the core iodine issuing in the organic form, and subsequent buildup at the rate of 0.05% per hour by deposition of elemental iodine, conversion to methyl iodide and desorption of the methyl iodide.

The conservatism of the assumptions underlying these performance factors is supported by the following bases:

i) Iodine issuing from the cooling system rupture is expected to be predominantly in the form of iodides owing to the strong reducing influence of molten cladding and hydrogen liberated from the reaction of cladding with steam. Stable iodides will tend to agglomerate as particles, absorb on other particles, condense on cool surface, or dissolve in condensing water vapor. A deposition factor of 0.50 is assumed in the TID-14844 model to account for the early removal of iodine by condensation and deposition effects. This factor has not been used in this analysis.

ii) Of the airborne iodine, it is assumed that elemental iodine (I_2) formed by air-oxidation of iodides, and methyl iodide (CH_3I) formed by reaction with trace organics will determine the efficiency of the removal process. Solid particulates and vapors such as HI are more readily trapped than I_2 or CH_3I.

iii) Two sources of CH_3I are considered: first, formation within the fuel during operation followed by direct release during the accident; and second, surface-activated reaction of sorbed iodine with trace organic materials on containment surfaces followed by desorption of the CH_3I produced.

The assumption of 0.2% direct release of CH_3I is believed to be pessimistic because of the tendency of the molecules to decompose under the influence of heat and radiation in the fuel. If 0.2% of the iodine were to exist, the fuel as CH_3I, the first-order rate constant for decomposition of CH_3I molecules would have to be less than 500 times the radioactive decay constant for the isotope in question (that is, less than 5×10^{-4} sec^{-1} for the biologically more significant isotope I-131). The thermal decomposition rate of CH_3I in the high beta and gamma fluxes attained in the fuel would be expected to add substantially to the total decomposition rate. This assumption of 0.2% as the relative inventory of I-131 as CH_3I is therefore conservative.

The rate of formation of CH_3I by desorption from surfaces was estimated from experiments simulating the conditions for such a process. These experiments, performed at Zenith[11], at Hanford[12], and at Oak Ridge[13] measured CH^3I formation in enclosures following release and deposition of I_2 in a moist air environment. The Zenith and Hanford data were attained in painted enclosures, while the ORNL data were obtained in stainless steel systems. The yields, when corrected for the surface to volume ratios of the respective surface materials in the containment were in every case less than 0.005% of the iodine inventory converted to CH_3I per hour of exposure. For the present analysis, the assumed formation rate of 0.05% per hour is therefore conservative.

b) Spray Removal Capability

The basis used for predicting iodine removal by the sodium thiosulfate spray follows the method described by Griffiths[14]. The fundamental assumption is that elemental iodine (I_2) absorbed by the liquid drop is rapidly reduced to the highly soluble iodide by the reagent sodium thiosulfate, with the result that the partial pressure of I_2 at the

drop surface is very small compared with that in the atmosphere. The experimental work of Taylor[15], performed in a column of controlled geometry, confirms this assumption for the aqueous thiosulfate absorption process. These tests show the overall mass transfer rate of I_2 to be independent of liquid flow rate, a parameter which would be expected to alter liquid film resistance. By contrast the transfer rate was found to be gas-velocity dependent, indicative of the fact that gas film is controlling. The HI present in the atmosphere is readily absorbed by the aqueous spray without chemical reaction; hence consideration is directed in this discussion to the behavior of elemental iodine (I_2).

In a gas film controlled process, the dependence of the mass transfer rate on film conditions is expressed by

$$V_g = \frac{D_v}{d} (2 + 0.6\ Re^{1/2}\ Sc^{1/3}) \qquad (1)$$

Where

V_g = transfer coefficient expressed moles transferred per unit time, area, and concentration differential, cm/sec.

D_v = Diffusion coefficient for iodine in air, cm^2/sec.

d = drop diameter, cm.

Re = Reynolds number, $\frac{d\ v\ \rho}{\mu}$ where ρ and v and μ are the density, velocity, and viscosity of the vapor, respectively (consistent units).

Sc = Schmidt number, $\frac{\mu}{\rho\ D_v}$ (consistent units).

Equation (1) is well substantiated by experiments in a variety of systems in which the gas film resistance is controlling, as reported by Ranz and Marshall[16].

The removal capability for the spray is calculated on the basis of an exponential removal of the inorganic vapor form iodine as the spray passes through the containment atmosphere.

The removal of iodine is then calculated by the equation:

$$A_t = A_o e^{-\lambda_s t} \qquad (2)$$

Where

A_t = The amount of elemental iodine in the containment atmosphere at time t - curies

A_o = The amount of elemental iodine initially in the containment atmosphere - curies

λ_s = Elemental iodine removal coefficient as defined by equation (3) - sec^{-1}

The removal coefficient, λ_s, is calculated by the following relationship:

$$\lambda_s = V_g \frac{S_d}{V_c} \quad sec^{-1} \qquad (3)$$

Where

V_g = Previously defined - cm/sec

S_d = Total surface area of drops in the containment volume - cm^2

V_c = Containment volume being covered by the spray - cm^3

The total surface area of the spray drops in the containment atmosphere is calculated on the following basis:

$$S_d = \frac{A_d \; F \; \bar{t}}{V_d} \qquad cm^2 \qquad (4)$$

Where

A_d = Surface area per drop - cm^2

V_d = Volume per drop - cm^3

F = Spray flow rate - cm^3/sec

$\bar{t}$ = Average residence time of the drop in the atmosphere - sec

For spherical drops, the ratio A_d/V_d is equal to 6/d where d is the drop diameter so that equation (4) now becomes

$$S_d = \frac{6 \; F \; \bar{t}}{d} \qquad cm^2 \qquad (5)$$

and the removal factor λ_s is now

$$\lambda_s = \frac{6 \; V_g \; F \; t}{V_c \; d} \qquad sec^{-1} \qquad (6)$$

For the plant, the removal coefficient can be evaluated using the following parameters

$V_c = 2.6 \times 10^6$ ft^3 - Free Volume of the containment.

t = 2.0 sec - Average fall time for the drops assuming a maximum fall velocity of 70 feet/sec and average fall distance of 140 feet. The fall velocity considers the exit velocity from the spray nozzles and gravity effects. The fall distance is assumed to be the distance available from the spray headers to the operating deck.

F = 2600 gpm - Design flow rate for one spray pump. (5.8 ft^3/sec)

V_g = 14 cm/sec - Based upon the data of Griffiths which gives a V_g/d ratio of 200 for a drop diameter of 700 microns.

The resulting removal coefficient is

$$\lambda_s = \frac{6 \times 5.8 \times 14 \times 2.0}{0.07 \times 2.6 \times 10^6} \quad \text{sec}^{-1}$$

$$\lambda_s = 5.35 \times 10^{-3} \quad \text{sec}^{-1} \text{ or}$$

$$\lambda_s = 19.3 \text{ hr}^{-1}$$

c) Off-site Inhalation Dose Evaluation

The following paragraphs present the calculations of off-site doses.

The initial halogen source available in the core was determined using the following parameters:

Isotope	Saturation Inventory
I-131	2.47×10^4 C/MWt
I-132	3.74×10^4 C/MWt
I-133	5.63×10^4 C/MWt
I-134	6.47×10^4 C/MWt
I-135	5.03×10^4 C/MWt

A dose-equivalent inventory of I-131 was calculated using the above inventories and the following TID 14844 dose-per-curies factors for the individual isotopes of iodine:

Isotope	Dose per Curie Inhaled
I-131	1.48×10^6 rem
I-132	5.35×10^4 rem
I-133	4.00×10^5 rem
I-134	2.50×10^4 rem
I-135	1.24×10^5 rem

A dose equivalent inventory of iodine 131 as a function of time was obtained by multiplying the initial iodine 131 inventory by the following factors, that take into consideration the radioactive decay of all the iodine isotopes and the contribution of the tellurium isotopes.

Time	Equivalence Factor
0	1.880
Aver. first 2 hrs	1.837
Aver. next 22 hrs.	1.472
Aver. next 30 days	.3423

Using the above figures, an initial dose equivalent inventory of iodine
--+ 131 of 1.57×10^8 curies is in the core at a power of 3391 MWt.

The meteorological model developed in Chapter 2 is used in calculating the resulting dispersion of the leakage from the containment.

Adult breathing rates have been assumed in the dose calculatioss and are 1.25 m^3/hour for the first 2 hours, 0.795 m^3/hour for the next 22 hours and 20 m^3/day for the next 30 days. Using the models and assumptions outlined above, the off-site doses were calculated using the following equations:

2 Hour Period:

$$D_2 = 2 \times B_2 \times L_2 \times \bar{A}_2 \times (\chi/Q)_2 \times DCF_{131} \left(\bar{\alpha}_2 + \frac{\beta_2}{\beta^{DRF_2}}\right) \qquad (7)$$

B_2 = Breathing rate for the 2 hour period

L_2 = Leak rate for the 2 hour period

$\bar{A}_2$ = Average dose equivalent total inventory of I^{131} over the 2 hour period

$(\chi/Q)_2$= Dispersion parameter for the 2 hour period from Table 2-4

DCF_{131} = Dose conversion factor for inhaled curies of I^{131}

$\bar{\alpha}_2$ = Average fraction of core inventory as methyl iodide that is available for leakage over the 2 hour period

β_2 = Fraction of core inventory as elemental iodine that is available for leakage at the beginning of the 2 hour period

βDRF_2 = Dose reduction factor for iodine forms due to functioning of air clean up system during the two hour period.

22 Hour Period:

$$D_{22} = 22 \times B_{22} \times L_{22} \times \bar{A}_{22} \times (\chi/Q)_{22} \times DCF_{131} \left(\bar{\alpha}_{22} + \frac{\beta_{22}}{\beta^{DRF_{22}}}\right) \qquad (8)$$

30 Day Period:

$$D_{30} = 30 \times B_{30} \times L_{30} \times \bar{A}_{30} \times (\chi/Q)_{30} \times DCF_{131} \left(\bar{\alpha}_{30} + \frac{\beta_{30}}{\beta^{DRF_{30}}}\right) \qquad (9)$$

The terms for these last two periods are similar to those defined for the 2 hour period. The calculated doses as a function of distance are shown on Figure 12-5.

Because the process of iodine removal by sprays and the formation of methyl iodide are both dynamic processes, the instantaneous plateout model of TID-14844 is not representative of either process. The model used assumed that the 50% of the core inventory reaching the atmosphere is all airborne initially and the time dependent leakage source is then calculated considering the combined dynamic processes of spray cleanup, plateout, conversion to methyl iodide and desorption of methyl iodide.

The amount of methyl iodide in the containment atmosphere at any time can be calculated as follows:

$$\alpha_t = \frac{R\,\beta_o}{\lambda_s + R}\,[1-e^{-(\lambda_s + R)t}] + \alpha_o \qquad (10)$$

Where

α_t = Fraction of the core inventory as methyl iodide in the atmosphere at time t

β_o = Fraction of the core inventory as elemental iodine which forms the source for the methyl iodide by plateout, conversion to methyl iodide and desorption

R = Formation rate of methyl iodide (This is an overall constant to represent the total process of plateout, conversion and desorption) - hr^{-1}

α_o = Fraction of the core inventory as methyl iodide in the containment atmosphere due to release from the core

λ_s = Spray removal constant for the airborne elemental iodine - hr^{-1}

If the process rate constant (R) of 0.05% per hour, an initial release fraction of 0.2%, a value of λ_s of 19.3 hr and a value of β_o of 0.50 are used equation (10) becomes:

$$\alpha_t = 1.29 \times 10^{-5} \left[1 - e^{-19.3t}\right] + 0.002$$

The average value of α for any time period may be found by integrating equation (10) and averaging over the time period t_1 to t_2

$$\bar{\alpha}_{\Delta t} = \alpha_o + \frac{R\,\beta_o}{\lambda_s + R}\left[1 + \frac{\left(e^{-(\lambda_s + R)t_2} - e^{-(\lambda_s + R)t_1}\right)}{(\lambda_s + R)(t_2 - t_1)}\right] \qquad (11)$$

For the 2 hour period calculation, the following constants were used.

$B_2 = 1.25\ m^3/hr$ $\qquad$ $L_2 = 1.16 \times 10^{-8}\ sec^{-1}$

--+ $\bar{A}_2 = 1.57 \times 10^{8}$ curies $\qquad$ $DCF_{131} = 1.48 \times 10^{6}$ rem/curies

--+ $\beta_2 = 0.50 = \beta_o$ $\qquad$ $\bar{\alpha}_2 = 0.002013$ (based on equation (11))

$$\beta^{DRF_2} = \frac{2\lambda_s}{1-e^{-2\lambda_s}} = 38.6$$ Based on 1 spray pump operating

--+ So that $D_2 = 9.10 \times 10^{4}\ (\chi/Q)_2$

For the next 22 hour period, the constants used were:

$B_{22} = 0.795\ m^3/hr$ $\qquad$ $L_{22} = 1.16 \times 10^{-8}\ sec^{-1}$

--+ $\bar{A}_{22} = 12.1 \times 10^{7}$ curies $\qquad$ $DCF_{131} = 1.48 \times 10^{6}$ rem/curies

$\beta_{22} = 0.50\ e^{-38.6}$ $\bar{\alpha}_{22} = 0.002013$

$\beta DRF_{22} = 425$

--+ So that $D_{22} = 7.4 \times 10^4\ (\chi/Q)_{22}$

For the thirty day period, the constants used were

$B_{30} = 20\ m^3/day$ $L_{30} = 5.22 \times 10^{-9}\ sec^{-1}$

--+ $\bar{A}_{30} = 2.84 \times 10^7$ curies $DCF_{131} = 1.48 \times 10^6$ rem/curie

$\beta_{30} = \sim 0$ $\bar{\alpha}_{30} = 0.002013$

--+ So that $D_{30} = 2.67 \times 10^5\ (\chi/Q)_{30}$

The off-site exposures also assume that

$$D_{24} = D_2 + D_{22}$$

$$D_\infty = D_2 + D_{22} + D_{30}$$

d) Off-site Doses Assuming Complete Melt-down

(1) Inhalation Doses

As described in Chapter 2, the closest approach to the plant site boundary is about 800 meters (1/2 mile) from the reactor. From Figure 12-14, the two hour thyroid dose at this exclusion distance
--+ is about 31 rem, which is well below the 10 CFR 100 limit of 300
--+ rem. The D_∞ at the boundary is about 46 rem, which is well below the 10 CFR 100 guide lines of 300 rem.

(2) Whole Body Exposures

In addition to the thyroid inhalation exposure, the whole body exposures were also evaluated, both due to direct radiation from the containment and from exposure due to immersion in a leakage plume.

(a) Radiation from the Containment

The direct whole body dose under the hypothetical loss-of-coolant accident conditions is calculated assuming that a complete core meltdown occurs resulting in the release of the following sources to the reactor containment: (From TID-14844).

a) 100% of the noble gases
b) 50% of the halogens
c) 1% of the remaining fission product inventory.

The above sources are assumed to be homogeneously distributed within the free volume of the reactor containment. The source intensity as a function of time after the accident is determined by considering natural decay only, with no credit taken for filtration or washdown.

The direct dose rate due to this activity dispersed within the containment is calculated by a digital computer program which is based on a point kernel attenuation model. The source region is divided into a number of incremental source volumes and the associated attenuation, gamma ray buildup, and distance through regions between each source point and the control room are computed. The summation of all point source contributions gives the total direct dose rate at the control room.

In addition to the direct dose, the contribution of scattered radiation was also estimated. These estimates indicate that scattered radiation levels will contribute less than 10% of the direct dose. Scattered radiation levels include both scattering from air (sky-shine) and scattering from large surfaces in the vicinity of the container. The integrated

direct dose exposures are shown on Figure 12-15. The two hour exposure of the site boundary is approximately 0.45 mrem; the exposure for the duration of the accident is less than 2.7 mrem; both doses are well below the 10 CFR 100 limit of 25 rem.

(b) Immersion in the Leakage Plume

The whole body exposure due to immersion in the leakage plume has also been investigated for a leak rate of 0.1 per cent per day and considering the noble gases and halogens (subject to removal as a leakage source by the sprays) available for leakage (100 per cent of the noble gases); the two hour exposure at the site boundary is calculated to be about 2.0 rem. The integrated exposure at the 1/2 mile distance for the duration of the accident is also calculated to be less than 11 rem so that the total whole body exposures are still well below 10 CFR 100 limits.

e) Sensitivity of Inhalation Doses

In order to demonstrate that more than adequate margins exist in the inhalation dose evaluations previously presented, a sensitivity study was made to determine the change in calculated off-site doses using various combinations of assumptions for the spray system and organic iodine behavior. The range of parameters from equations (7), (8), (9) and (11) evaluated are:

$$\lambda_s = 20\ hr^{-1} \text{ to } 2\ hr^{-1}$$
$$\alpha_o = 0.002 \text{ to } 0.015$$
$$R = 5 \times 10^{-4}\ hr^{-1} \text{ to } 5 \times 10^{-2}\ hr^{-1}$$

The results of these studies are presented in Figures 12-16 and 12-17 which show the 2 hour dose and the 31 day dose at the site boundary (1/2 mile or 800 meters) as functions of the above parameters.

12.4 SUMMARY OF OFF-SITE EXPOSURES

Table 12-2 presents a summary of the resulting potential off-site doses for
--+ the various accidents described in this chapter based on operation at 3391 MWt.

TABLE 12-2

SUMMARY OF MAXIMUM ESTIMATED OFF-SITE DOSES FROM ACCIDENTS

	Accident	Reference	2 Hour Exposure at 1/2 Mile in Rem		31 Day Exposure at 1/2 Mile in Rem	
			Thyroid	Whole Body	Thyroid	Whole Body
--+	1. Fuel handling (mechanical damage to one row of rods in one assembly	12.2.2.2	-	<0.018	-	<0.018
--+	2. Volume control tank rupture with defects in 1% of the fuel rods	12.2.4.2	-	<0.35	-	<0.35
--+	3. Gas decay tank rupture with defects in 1% of the fuel rods	12.2.4.3	-	<0.85	-	<0.85
--+	4. Rupture of steam generator tube with defects in 1% of the fuel rods	12.2.5	<0.0035	<0.45	<0.0075	<0.95
	Loss-of-Coolant Accident:					
--+	5. All safeguards function	12.3.3.1	3.1	0.20	-	-
--+	containment shine		-	0.00045	-	0.0027
--+						
--+	6. With loss of outside power	12.3.3.2	3.1	0.20	4.6	-
--+	7. With failure to limit core meltdown	12.3.3.3	31	2.0	46	<11
	8. 10 CFR 100 guide lines		300	25	300	25

REFERENCES - CHAPTER 12

1. Curran, R. M., "History of the Special ASTM Task Force on Large Turbine and Generator Rotors" ASTM Meeting, Purdue University, 1965

2. Baker, L., "Studies of Metal-Water Reactions at High Temperatures, III Experimental and Theoretical Studies of the Zirconium-Water Reaction," ANL-6548

3. Epstein, L. F., "Metal-Water Reactions, VIII," GEAP-3279

4. Lustman, B., "Zirconium-Water Reactions," WAPD-137

5. Margolis, S. G. and Redfield, S. A., "FLASH: A Program for Digital Solution of the Loss of Coolant Accident," WAPD-TM-534, May, 1966

6. A. Kolflat and W. A. Chittenden, "A New Approach to the Design of Containment Shells for Atomic Power Plants," Proceedings of American Power Conference, Pg. 651, Volume XIX, 1957

7. Uchida, "Evaluation of Post-Incident Cooling Systems of Light Water Power Reactors," 3rd U. S. Int'l Conference on Peaceful Uses of Atomic Energy, Vienna, May, 1964

8. D. Hasson, D. Luss, U. Navon, "An Experimental Study of Steam Condensation on a Laminar Water Sheet," Int. J. Heat Mass Transfer 7, 983-1001 (1964)

9. M. B. Zabetakis, "Research on the Combustion and Explosion Hazards of Hydrogen-Water Vapor-Air Mixture," AECU-3327, Sept. 1965

10. TID-14844 "Calculation of Distance Factors for Power and Test Reactor Sites," J. J. DiNunno, et. al. USAEC, March, 1962

11. J. F. Croft, et. al. "Experiments on the Deposition of Airborne Iodine of High Concentration," AEEW-R265, June, 1963

12. J. D. McCormack and R. K. Hilliard, "Natural Removal of Fission Products Released from UO_2 Fuel in Condensing Steam Environments," International Symposium on Fission Product and Transport Under Accident Conditions, CONF-650407, April, 1965

13. G. W. Parker, et. al. "Behavior of Fission Products Released from Simulated Fuels in the Containment Mockup Facility," p. 83, Nuclear Safety Program Semiannual Progress Report for Period Ending June 30, 1965, ORNL-3843

14. V. Griffiths, "The Removal of Iodine from the Atmosphere by Sprays, AHSB (S) R 45

15. R. F. Taylor, "Absorption of Iodine Vapor by Aqueous Solutions," Chemical Engineering Science, 1959, Vol. 10, pp. 68-79

16 W. E. Ranz and W. R. Marshall, Jr., "Evaporation from Drops," Chemical Engineering Progress, Vol. 48, No. 3, p. 141 and No. 4, p. 173

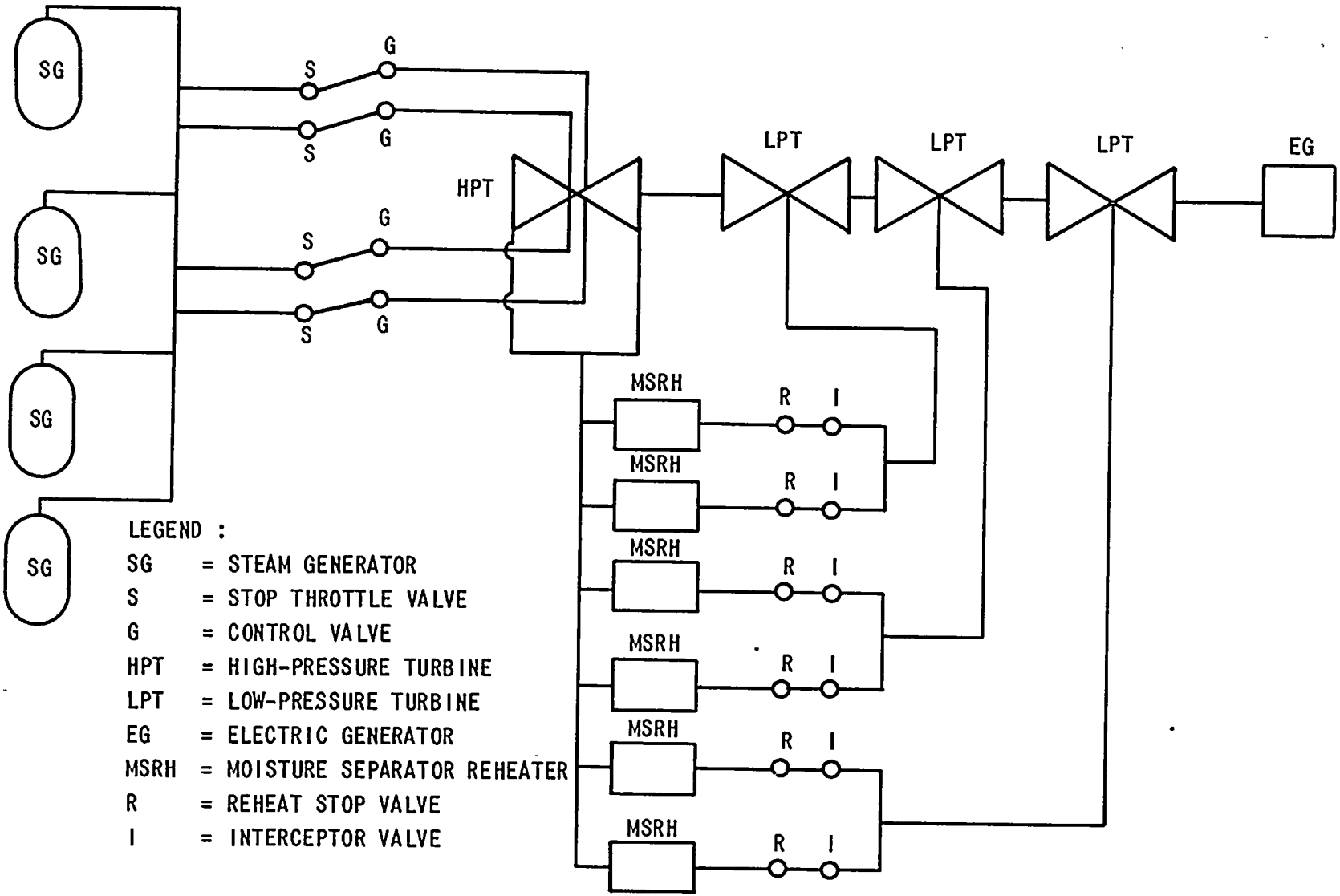

STEAM SYSTEM DIAGRAM

FIG. 12-1

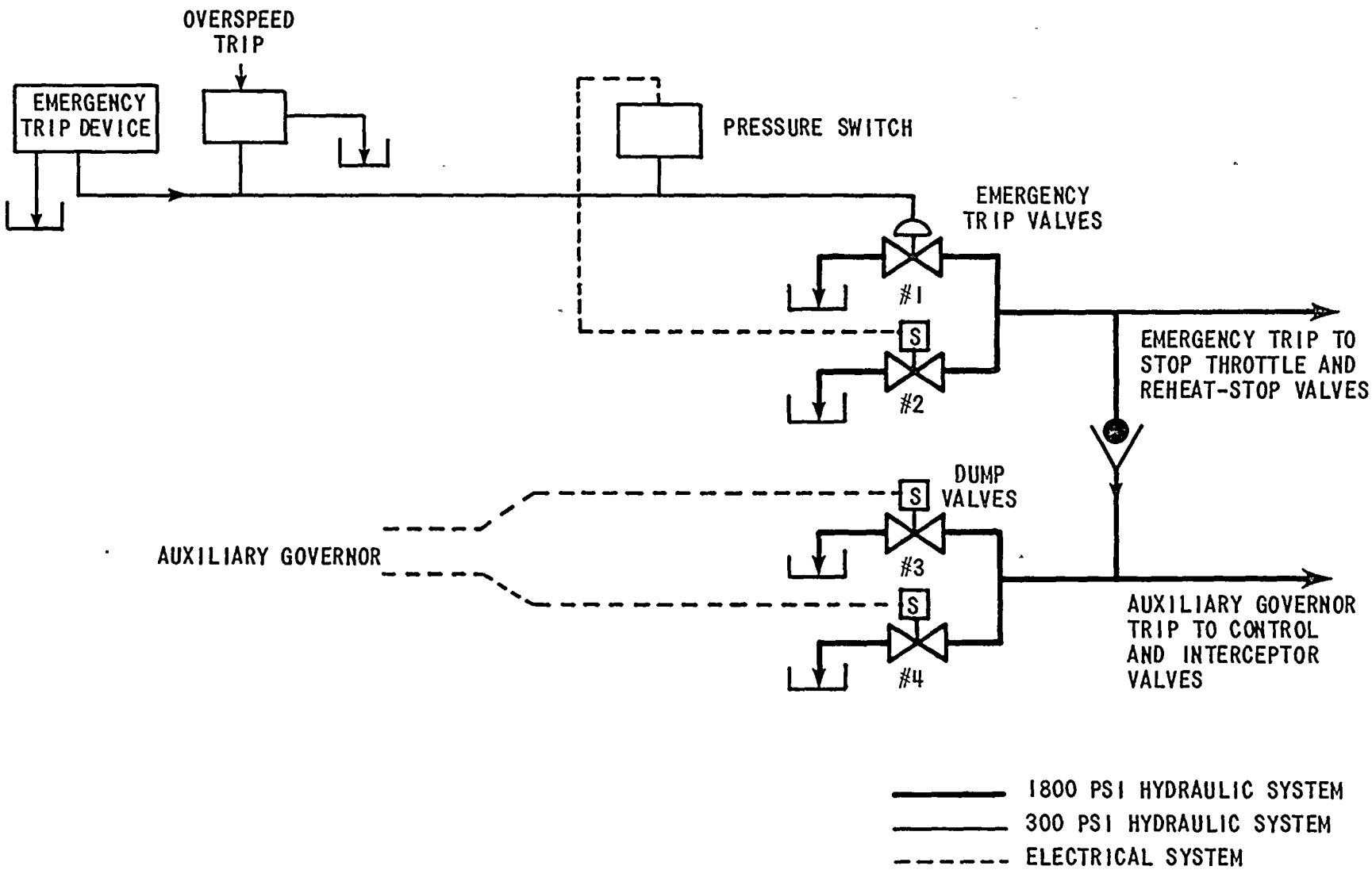

TURBINE CONTROL AND PROTECTION SYSTEM

FIG. 12-2

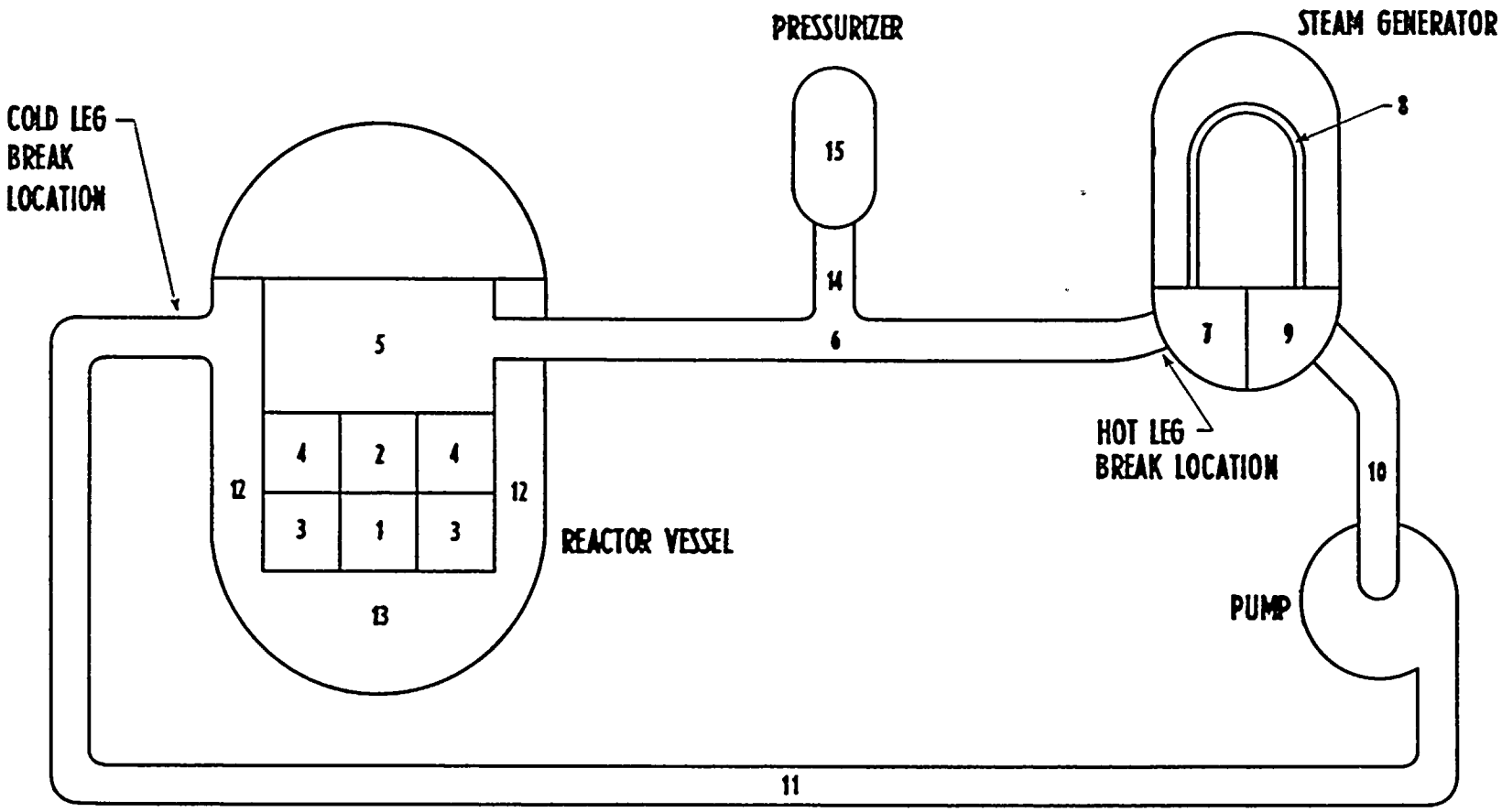

REACTOR COOLANT SYSTEM ELEMENT DESIGNATION FOR SATAN CODE

FIG. 12-3

REACTOR COOLANT SYSTEM ELEMENT DESIGNATION FOR SATAN CODE 2 LOOP ANALYSIS

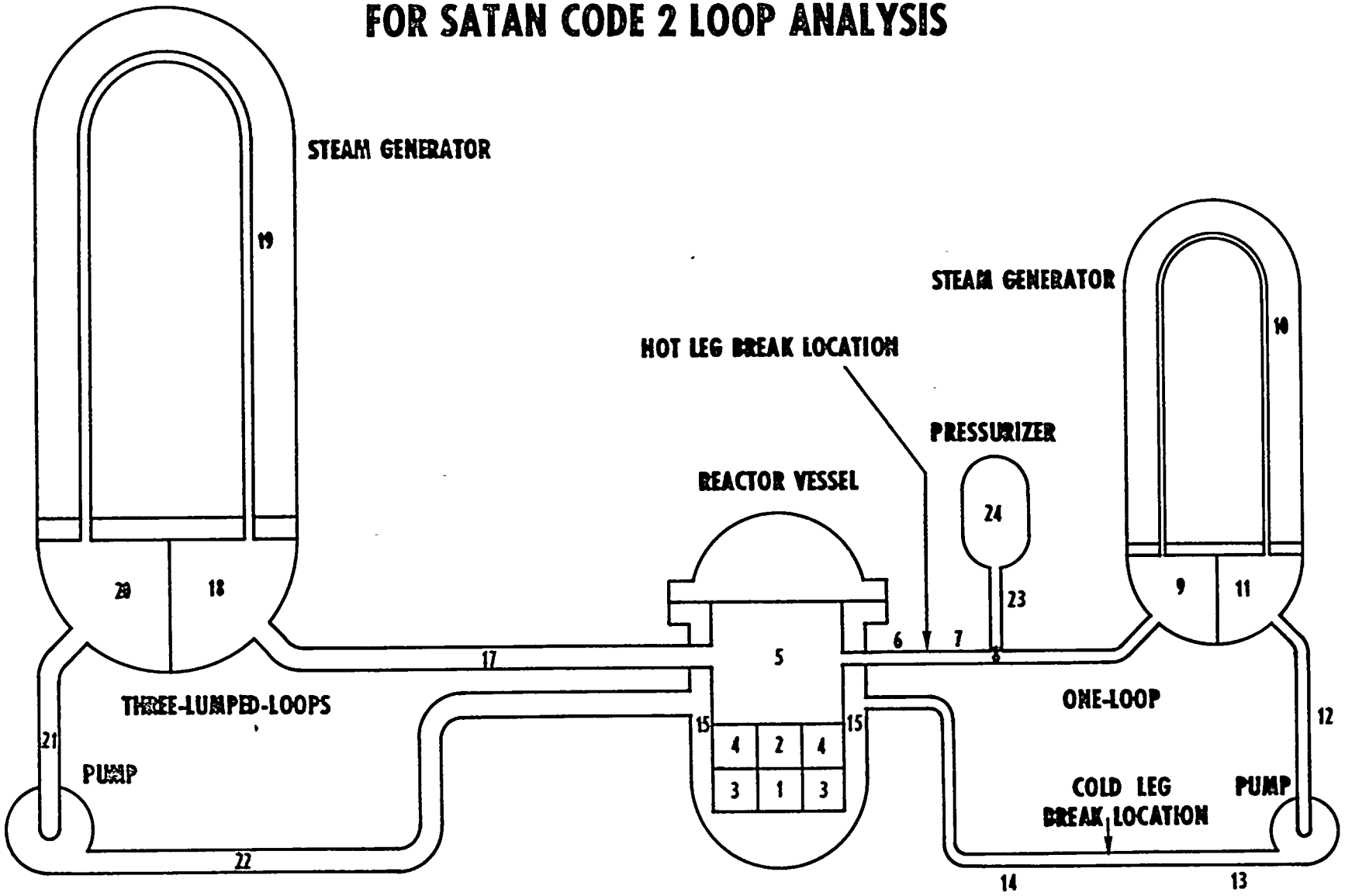

FIG. 12-4

COMPARISON OF SATAN CODE RESULTS WITH LOFT EXPERIMENT
(RESERVOIR BLOWDOWN)
VESSEL PRESSURE

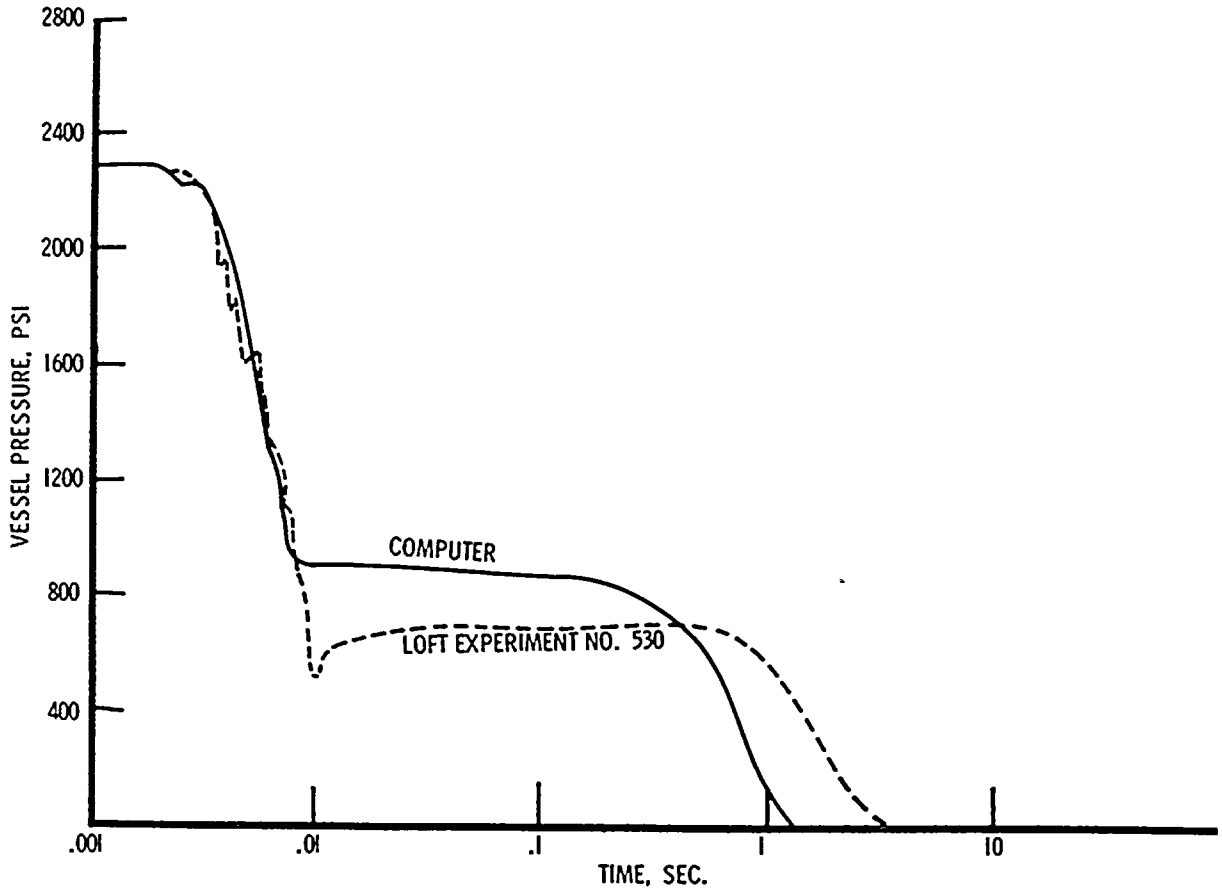

FIG. 12-5

A COMPARISON OF SATAN CODE RESULTS WITH LOFT EXPERIMENT
(RESERVOIR BLOWDOWN)
DISCHARGE PRESSURE

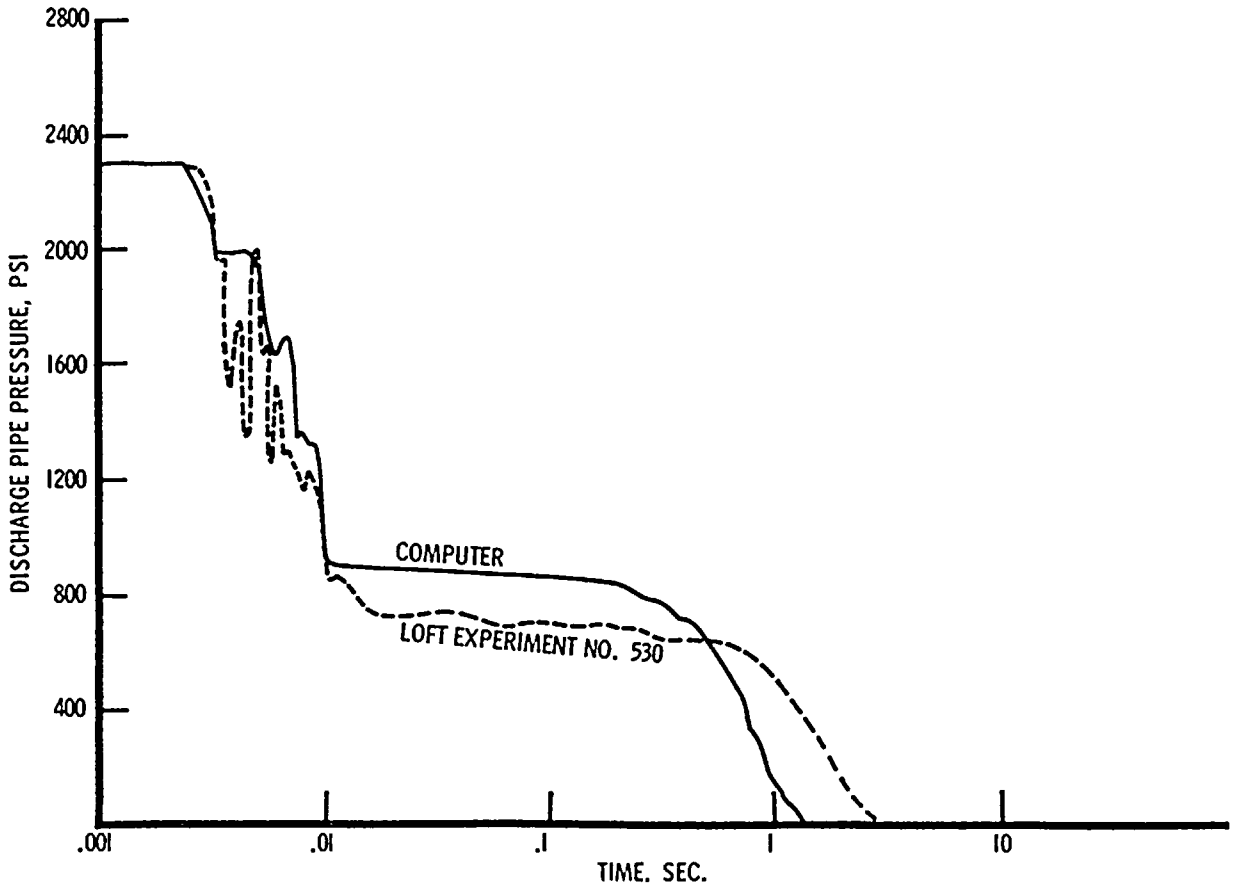

FIG. 12-6

A COMPARISON OF SATAN CODE RESULTS WITH LOFT EXPERIMENT
(RESERVOIR BLOWDOWN)
VESSEL TEMPERATURE

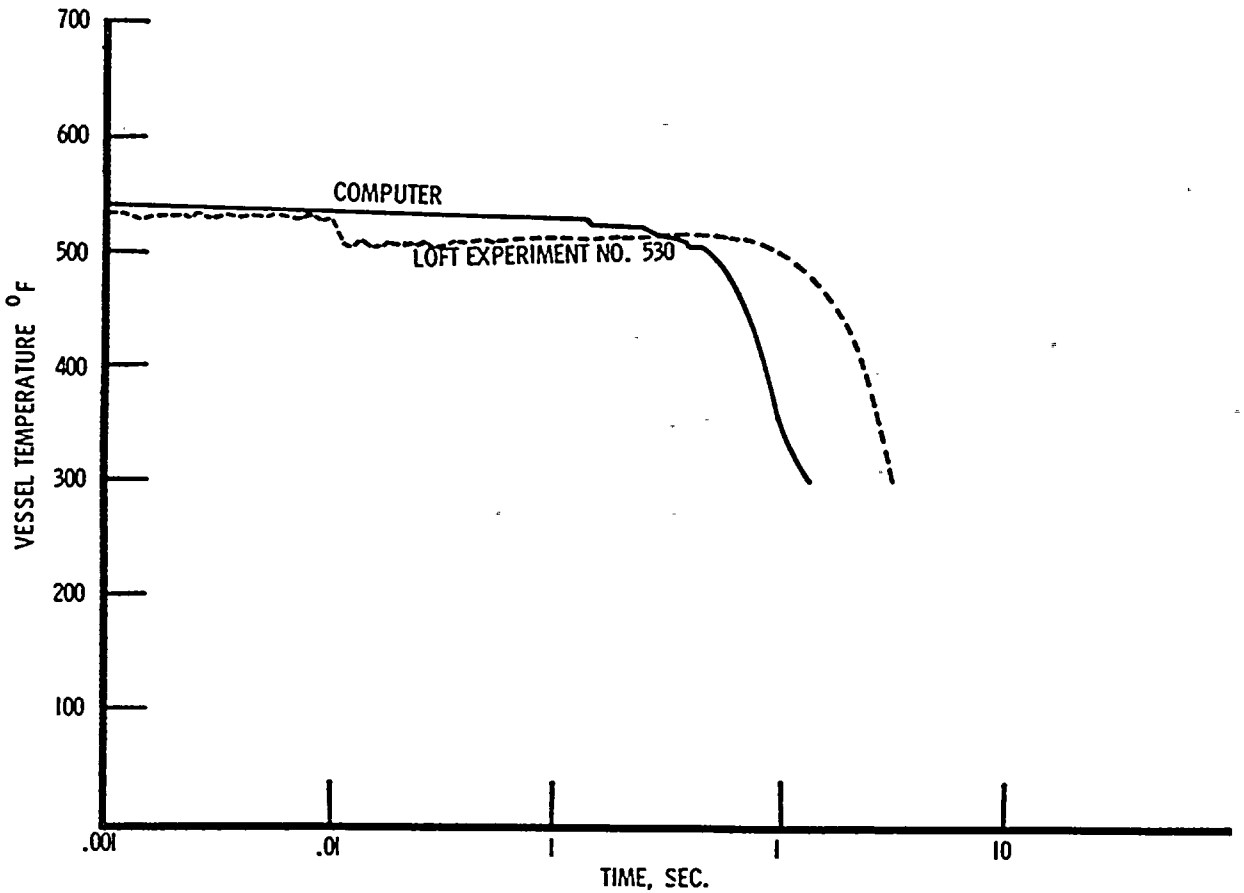

FIG. 12-7

A COMPARISON OF SATAN CODE RESULTS WITH LOFT EXPERIMENT
(RESERVOIR BLOWDOWN)
DISCHARGE PIPE TEMPERATURE

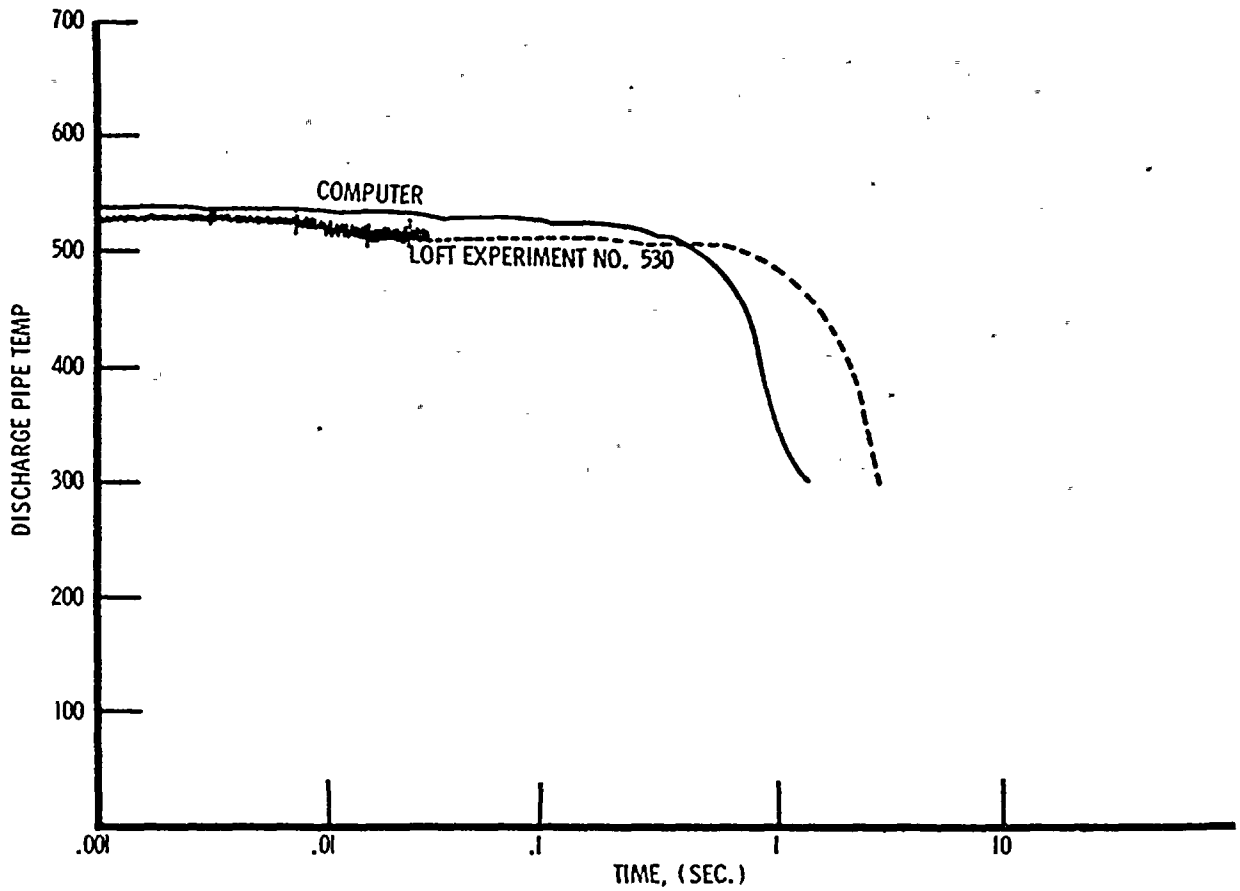

FIG. 12-8

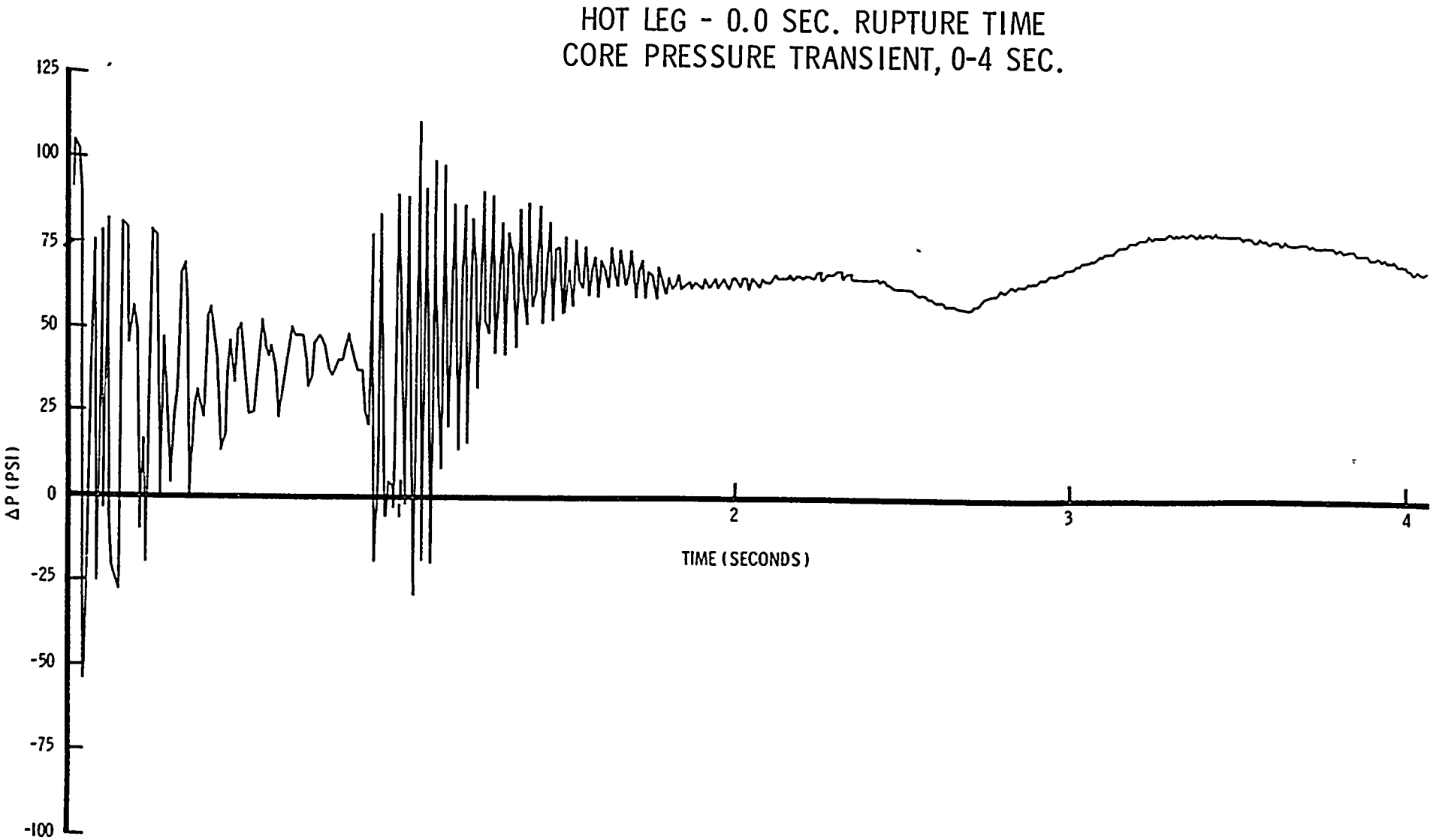
HOT LEG - 0.0 SEC. RUPTURE TIME
CORE PRESSURE TRANSIENT, 0-4 SEC.
125
100
75
50
25
0
-25
-50
-75
-100
ΔP (PSI)
2
3
4
TIME (SECONDS)

FIG. 12-9

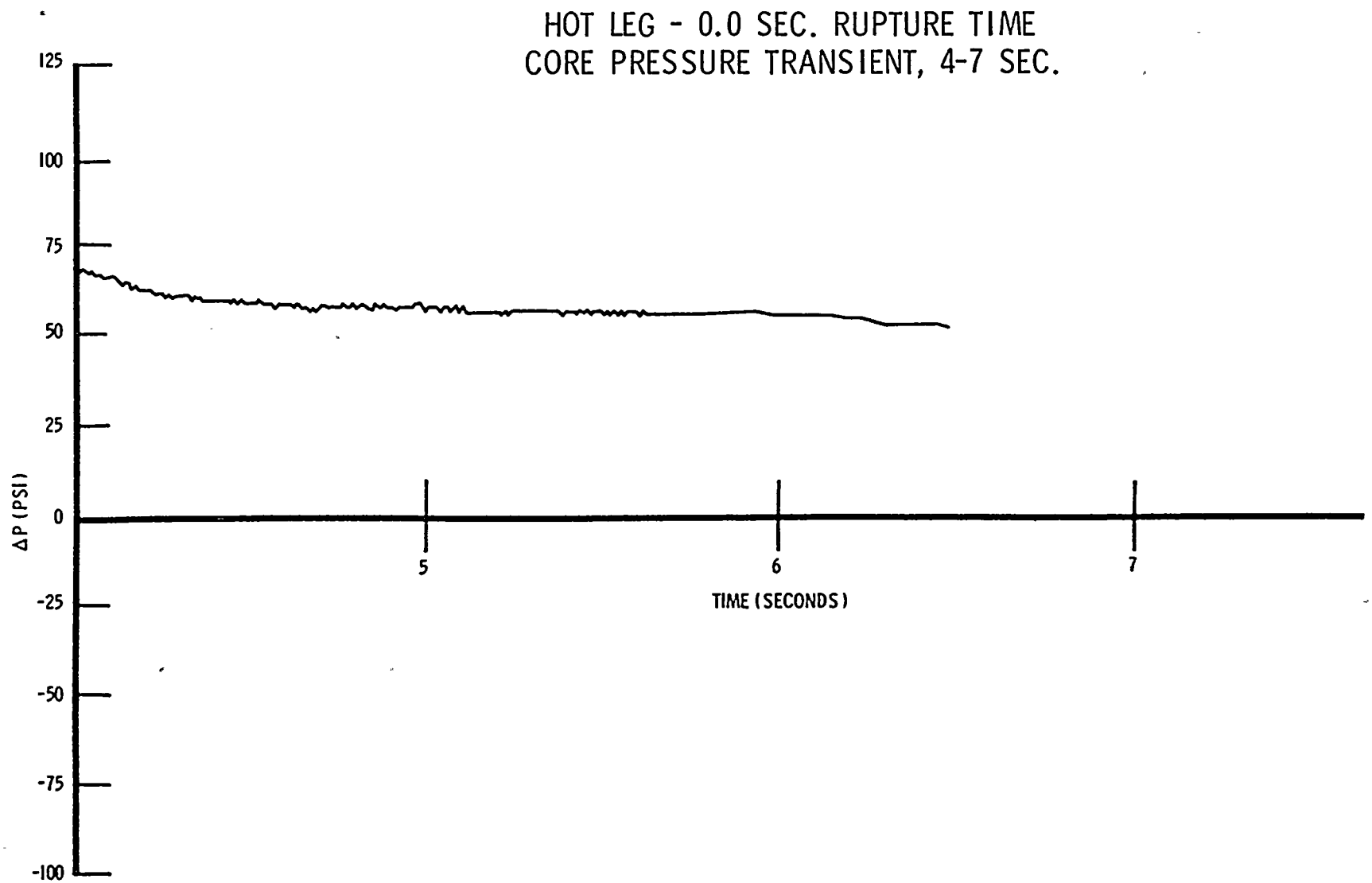
HOT LEG - 0.0 SEC. RUPTURE TIME
CORE PRESSURE TRANSIENT, 4-7 SEC.
125
100
75
50
25
0
-25
-50
-75
-100
ΔP (PSI)
5
6
7
TIME (SECONDS)

FIG. 12-10

HOT LEG - 0.0 SEC. RUPTURE TIME
CORE BARREL PRESSURE TRANSIENT, 0-4 Sec.

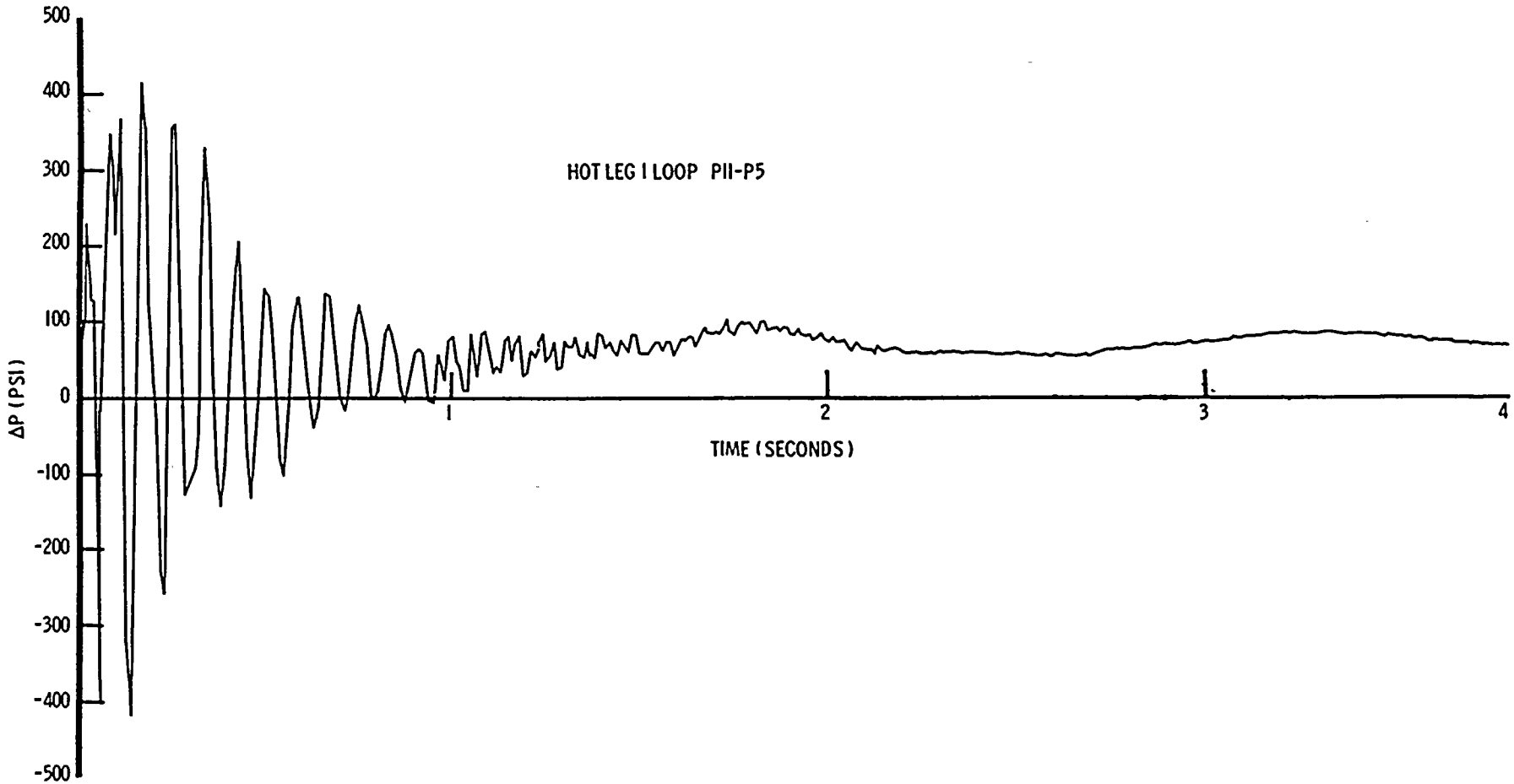

FIG. 12-11

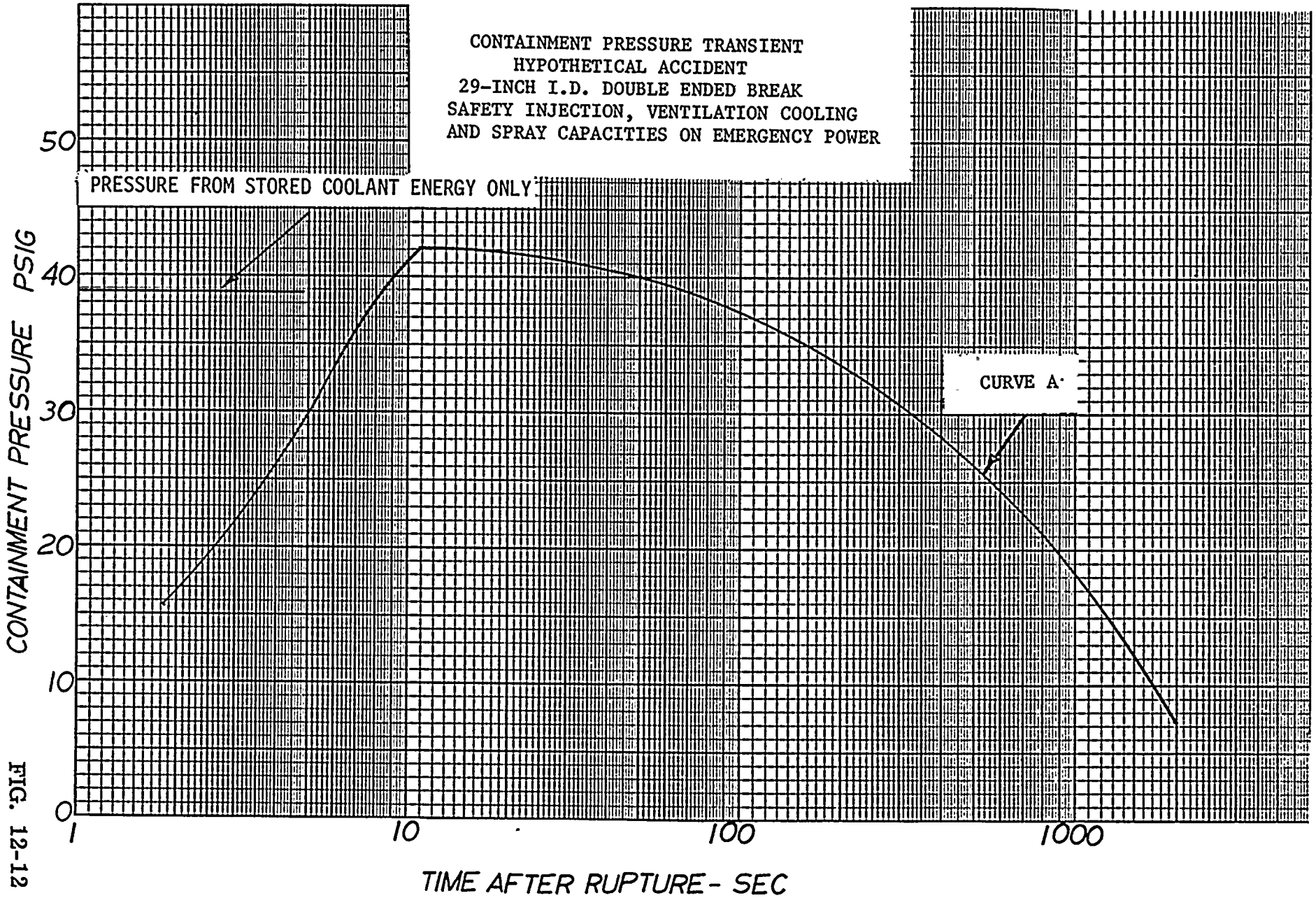
CONTAINMENT PRESSURE TRANSIENT
HYPOTHETICAL ACCIDENT
29-INCH I.D. DOUBLE ENDED BREAK
SAFETY INJECTION, VENTILATION COOLING
AND SPRAY CAPACITIES ON EMERGENCY POWER
PRESSURE FROM STORED COOLANT ENERGY ONLY
CURVE A
CONTAINMENT PRESSURE PSIG
50
40
30
20
10
0
1
10
100
1000
TIME AFTER RUPTURE - SEC

FIG. 12-12

CONTAINMENT PRESSURE TRANSIENT WITH
SAFETY INJECTION, VENTILATION COOLING
AND SPRAY CAPACITIES ON EMERGENCY POWER

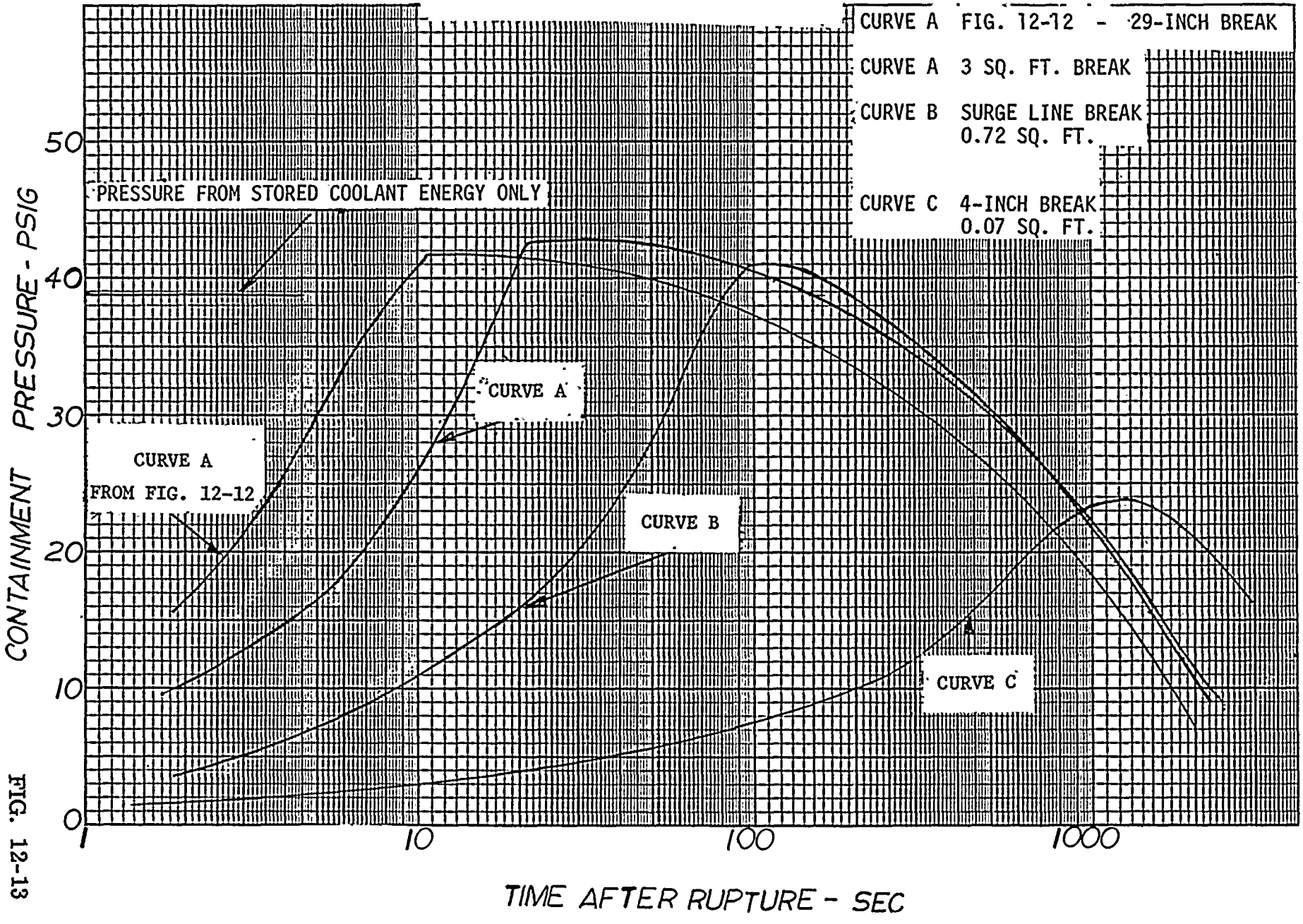

FIG. 12-13

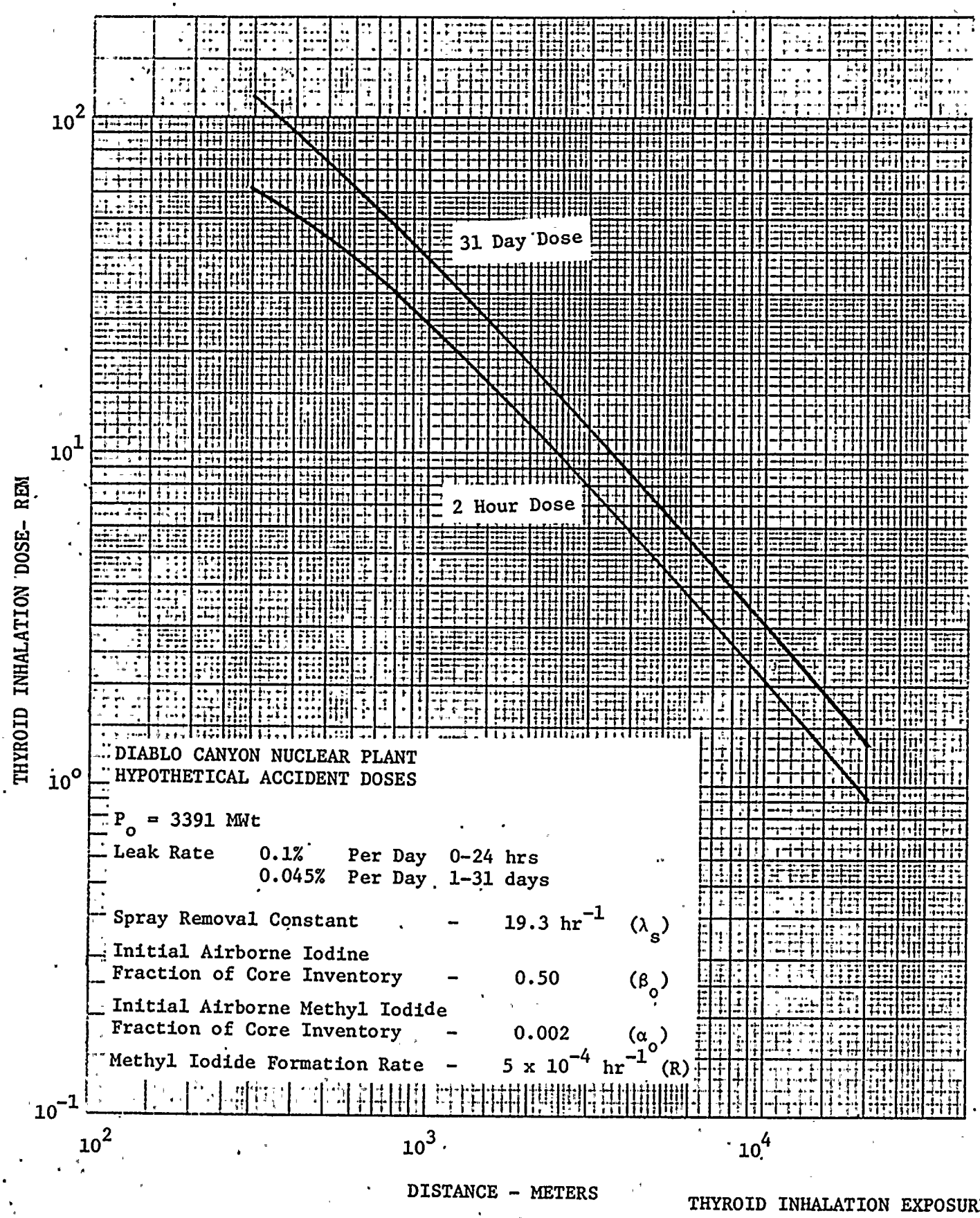

THYROID INHALATION EXPOSURE
FIGURE 12-14
(Revised 7-31-67)

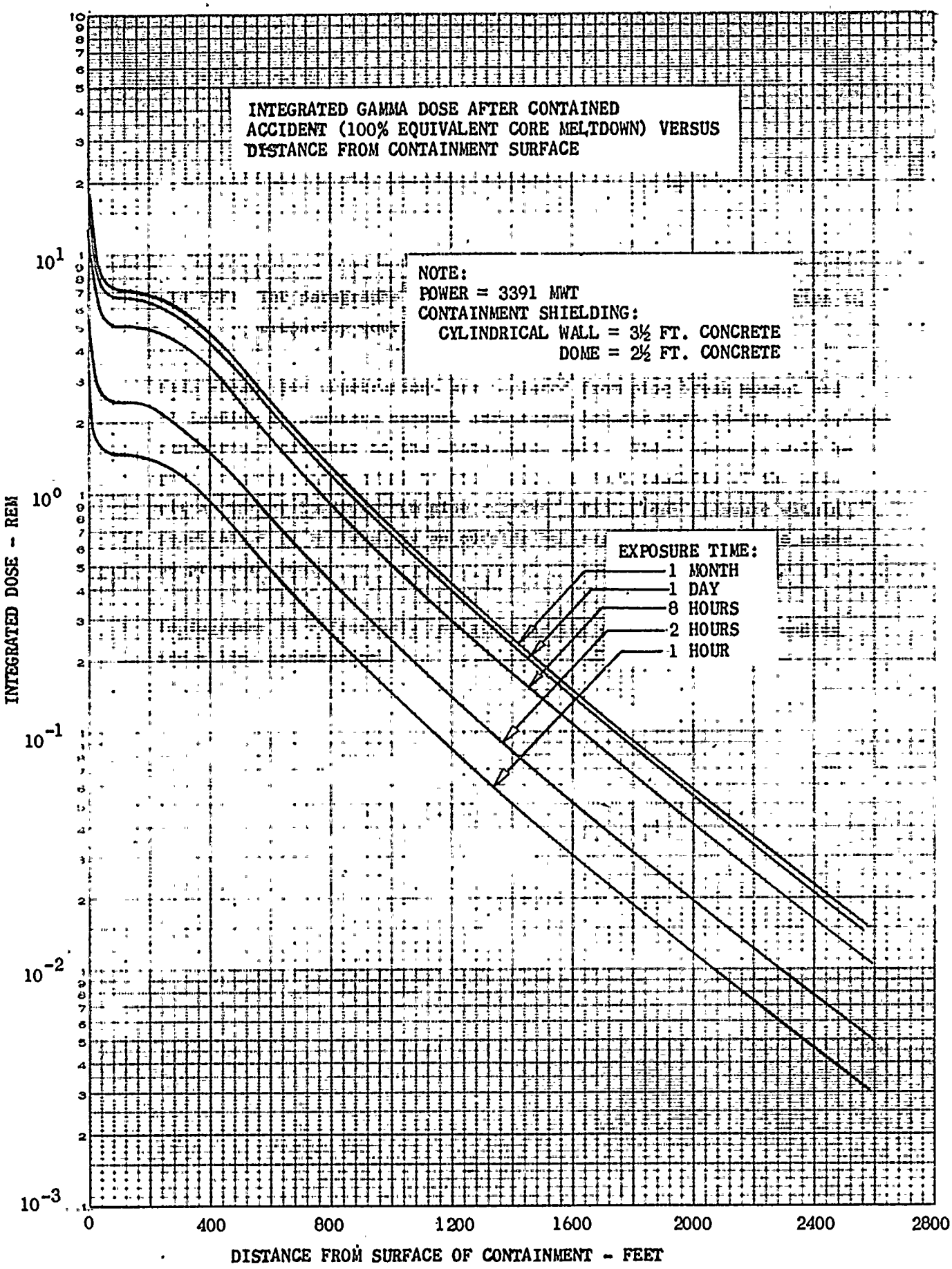

FIG. 12-15 (Revised 11-6-67)

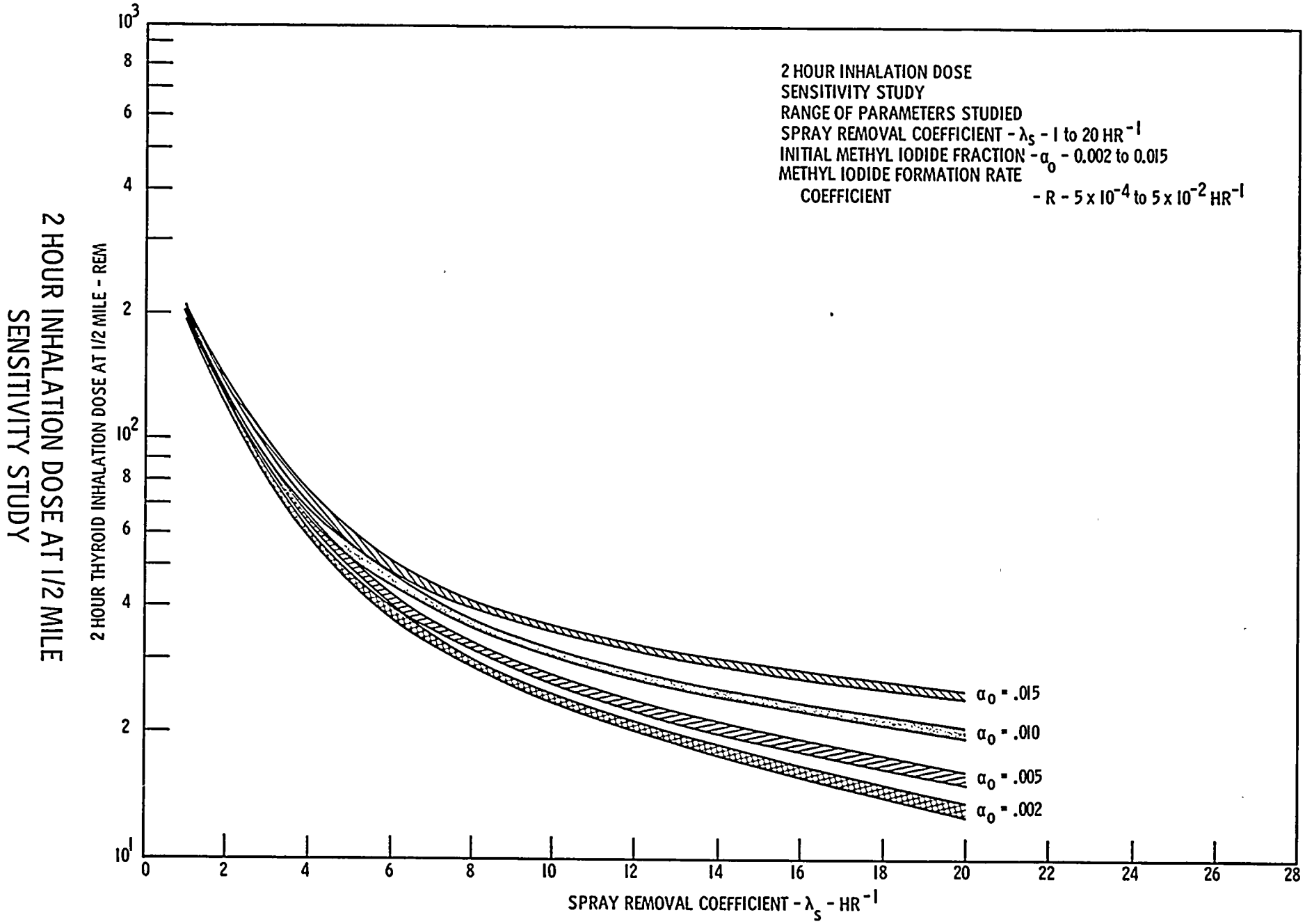
2 HOUR INHALATION DOSE AT 1/2 MILE
SENSITIVITY STUDY
2 HOUR THYROID INHALATION DOSE AT 1/2 MILE - REM
2 HOUR INHALATION DOSE
SENSITIVITY STUDY
RANGE OF PARAMETERS STUDIED
SPRAY REMOVAL COEFFICIENT - λ_S - 1 to 20 HR^{-1}
INITIAL METHYL IODIDE FRACTION - α_0 - 0.002 to 0.015
METHYL IODIDE FORMATION RATE
COEFFICIENT - R - 5×10^{-4} to 5×10^{-2} HR^{-1}
α_0 = .015
α_0 = .010
α_0 = .005
α_0 = .002
10^3
8
6
4
2
10^2
8
6
4
2
10^1
0
2
4
6
8
10
12
14
16
18
20
22
24
26
28
SPRAY REMOVAL COEFFICIENT - λ_s - HR^{-1}

FIG. 12-16

31 DAY INHALATION DOSE AT 1/2 MILE
SENSITIVITY STUDY

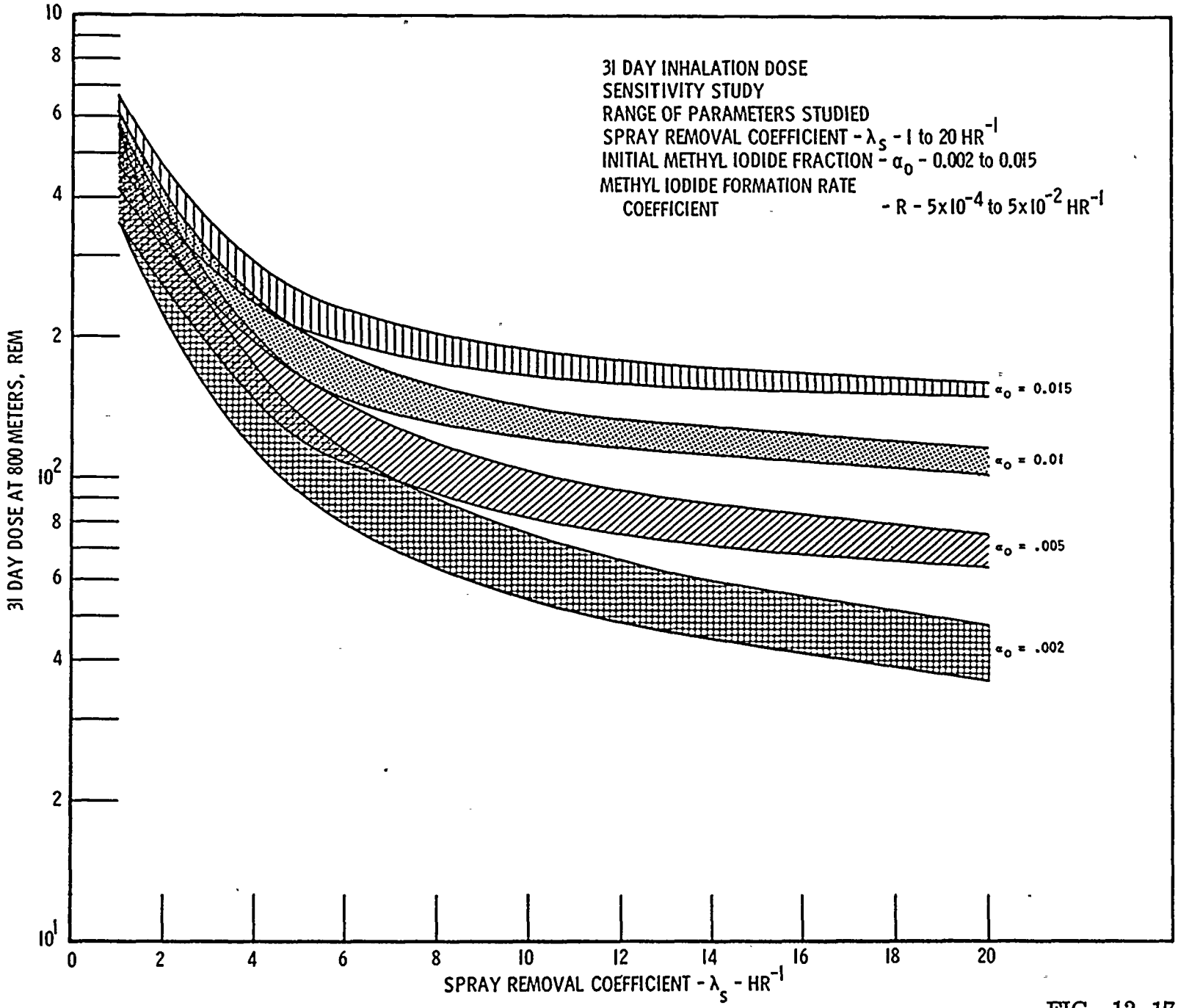

FIG. 12-17

TABLE OF CONTENTS

Section	Title	Page
CHAPTER 13	OPERATION	
13.1	Introduction	13-1
13.2	Organization and Responsibility	13-1
13.3	Personnel Training	13-2
13.4	Written Procedures	13-4
13.5	Records	13-4
13.6	Review and Operational Audit Procedure	13-5
13.7	Initial Tests and Operation	13-5

CHAPTER 13 OPERATION

13.1 INTRODUCTION

The purpose of this chapter is to describe the general manner in which the Company intends to operate and maintain the plant. The Company has been involved in the operation of nuclear power plants during the past ten years. An approach to the operation of nuclear power plants has been developed during this period which is compatible with the Company's organizational concepts and the operational philosophy which has been successfully employed for many years in its conventional thermal power plants. The Atomic Energy Commission has had the opportunity to observe this operational approach over the past four years in the operation of the Humboldt Bay Nuclear Unit. The successful operation of this unit demonstrates that the Company has technically competent and safety-oriented nuclear design and operating organizations.

13.2 ORGANIZATION AND RESPONSIBILITY

The anticipated ultimate organization for routine operations of the plant is shown in Figure 13-1. This organization is in accordance with the Company's organizational practices for conventional generating plants, with increased emphasis on the technical functions required in the operation of a nuclear unit. The organization is generally similar to the Humboldt Bay Power Plant organization. It has been possible to reduce the size of the plant maintenance force because of the proximity of the Morro Bay Power Plant. Personnel from this plant will be available to assist in major overhaul work.

The Plant Superintendent will be responsible for all on-site activities in connection with operation and maintenance of the plant. The plant organization will be under the functional direction of, and will receive technical support from the Company's General Office Department of Steam Generation in San Francisco. Consulting services from Westinghouse Electric Corporation or others will be used as required.

The operating organization shown in Figure 13-1 will be augmented during the period of the plant startup by adding additional Shift Foremen and increasing the number of Nuclear Engineers to provide for necessary shift coverage of startup operations. In the startup organization, the radiation protection and chemistry functions will be handled by two engineers. Consolidation of the duties and responsibilities of these two positions into a single position of Radiation Protection - Chemical Engineer will take place some time after the initial operating period.

The key positions in the plant organization will be filled by individuals who have been actively involved in the Company's nuclear power program. The experience of senior supervisory personnel in nuclear power plant operation and maintenance will generally be in the range of five to fifteen years at the time of the plant startup.

Each of the professional positions in the operating organization - Power Plant Engineer, Nuclear Engineer, Instrument Engineer, Radiation Protection Engineer and Chemical Engineer - will be filled by a graduate engineer with appropriate experience in the nuclear power field. The background of these individuals will be sufficiently broad so that at least two individuals will be qualified to fill each functional position.

It is expected that about half of the non-supervisory operations personnel and all of the Control Technicians will come from the Humboldt Bay Nuclear Unit.

13.3 PERSONNEL TRAINING

A training program similar to the program which the Company developed and carried out to train personnel prior to the startup of the Humbolt Bay Nuclear Unit will be used to provide plant personnel with the required knowledge to safely and efficiently operate and maintain the plant. It is planned that the Plant Superintendent, the Supervisor of Operations,

the Power Plant Engineer, the Nuclear Engineers and the Shift Foremen will receive AEC Senior Operator Licenses prior to the initial fuel loading. Other personnel shown as licensed in Figure 13-1 (Senior Control Operator and Control Operators) will not be licensed until they receive appropriate operating experience during the initial operation of the plant.

Approximately 18 months prior to startup, a group comprised of key supervisory and technical personnel for the plant operating organization will be established to prepare training material for the plant personnel training program. Other functions of this group will include the preparation of the startup program for the plant in collaboration with personnel from the Company's Construction Department, preparation of an operating manual for the plant, participation in the preparation of AEC license material including the operational aspects of the Technical Specifications, and review of the design of the plant to determine that it meets all operating requirements. Individuals from this group will attend a special course of approximately four weeks duration presented by design engineers of the reactor manufacturer covering the design operation and safeguards of the nuclear steam supply system. Although members of this group will all have had considerable boiling water reactor experience, it is planned that selected individuals will spend appropriate periods of time at operating pressurized water reactor plants to obtain operating experience in their fields of specialty.

Approximately eight months prior to initial fuel loading, supervisory and technical personnel will be assigned to the plant. During the period prior to initial fuel loading, the various groups of plant physical personnel will be assigned and will begin their formal classroom training programs. All personnel will receive a course in radiation protection. Operating personnel will receive a course in the design and operation of the plant based on the Operating Manual. They will also carry out the pre-operational testing program of the plant's systems and equipment as a part of their training program. Control Technicians will receive courses in radiation monitoring, instrumentation and chemical procedures and will participate in the pre-operational testing of the plant's chemical systems and control and instrumentation system.

After routine operation of the plant begins, a continual on-the-job training program will be established in accordance with normal Company practice. This program will provide a reserve of replacement personnel as vacancies occur in the plant organization as well as providing "refresher" training for all plant personnel. Operators at the Auxiliary Operator level will complete reactor operations training and receive an AEC Operators License before qualifying for advancement to Control Operator. Similarly, Senior Control Operators will be qualified for advancement to Shift Foremen only after obtaining an AEC Senior Operators License. Technicians and mechanical and electrical personnel will be required to complete appropriate apprentice programs varying in length from 24 to 42 months before qualifying for journeyman status.

13.4 WRITTEN PROCEDURES

Detailed written procedures for all normal operations and for abnormal and emergency situations will be prepared prior to initial startup in accordance with normal Company practice. These procedures will include a Site Emergency Plan. This plan will provide the necessary prearrangement and organization of personnel to deal effectively with any foreseeable emergency at the plant site. The plant design is such that none of the credible nuclear accidents would create an undue hazard to the public; however, organization for action in various types of emergencies will be prearranged.

The Site Emergency Plan will be coordinated with the State of California and local disaster organizations similar to the Humboldt Bay Plant Plan. Drills will be staged prior to initial operation of the plant and periodically after operation of the plant commences to assure that all plant personnel are thoroughly familiar with the Plan.

13.5 RECORDS

Records documenting the operation and maintenance of the plant will be maintained in accordance with established Company procedure. Experience in the operation of the Humboldt Bay Nuclear Unit indicates that our approach to

record keeping has been satisfactory to the Commission. Operating records will include appropriate log books, log sheets, and recorder charts covering all aspects of operation. Detailed records of the routine operational testing of nuclear safeguards systems and components will also be maintained. Maintenance records will be kept documenting the inspection, preventive maintenance, and repair of mechanical, electrical and instrumentation systems.

13.6 REVIEW AND OPERATIONAL AUDIT PROCEDURE

A review procedure similar to that in use for the Humboldt Bay Nuclear Unit will be used in connection with (1) proposed design modifications (2) proposed changes in operating procedures and (3) proposed tests. Two review committees will be used for this purpose: an On-Site Review Committee and the General Office Nuclear Plant Review Committee in the Company's General Office in San Francisco.

A procedure will be established for auditing the operation of the plant similar to the one used for the Humboldt Bay Nuclear Unit. This procedure will involve review of operating experience by the On-Site Review Committee and at the Company's General Office level.

13.7 INITIAL TESTS AND OPERATION

Pre-operational testing of the plant, initial loading and low level testing of the reactor, and power operation testing of the plant will be carried out in a manner generally similar to the program conducted for the Humboldt Bay Nuclear Unit. Company Construction and Operating Department personnel will prepare and carry out the program with technical assistance from the reactor manufacturer and other equipment suppliers. Experience gained in the start-up of similar pressurized water reactors will be available at the time the startup program for this plant is prepared. This experience should be extremely useful in defining areas in which particular emphasis is required to demonstrate that the plant meets its design criteria.

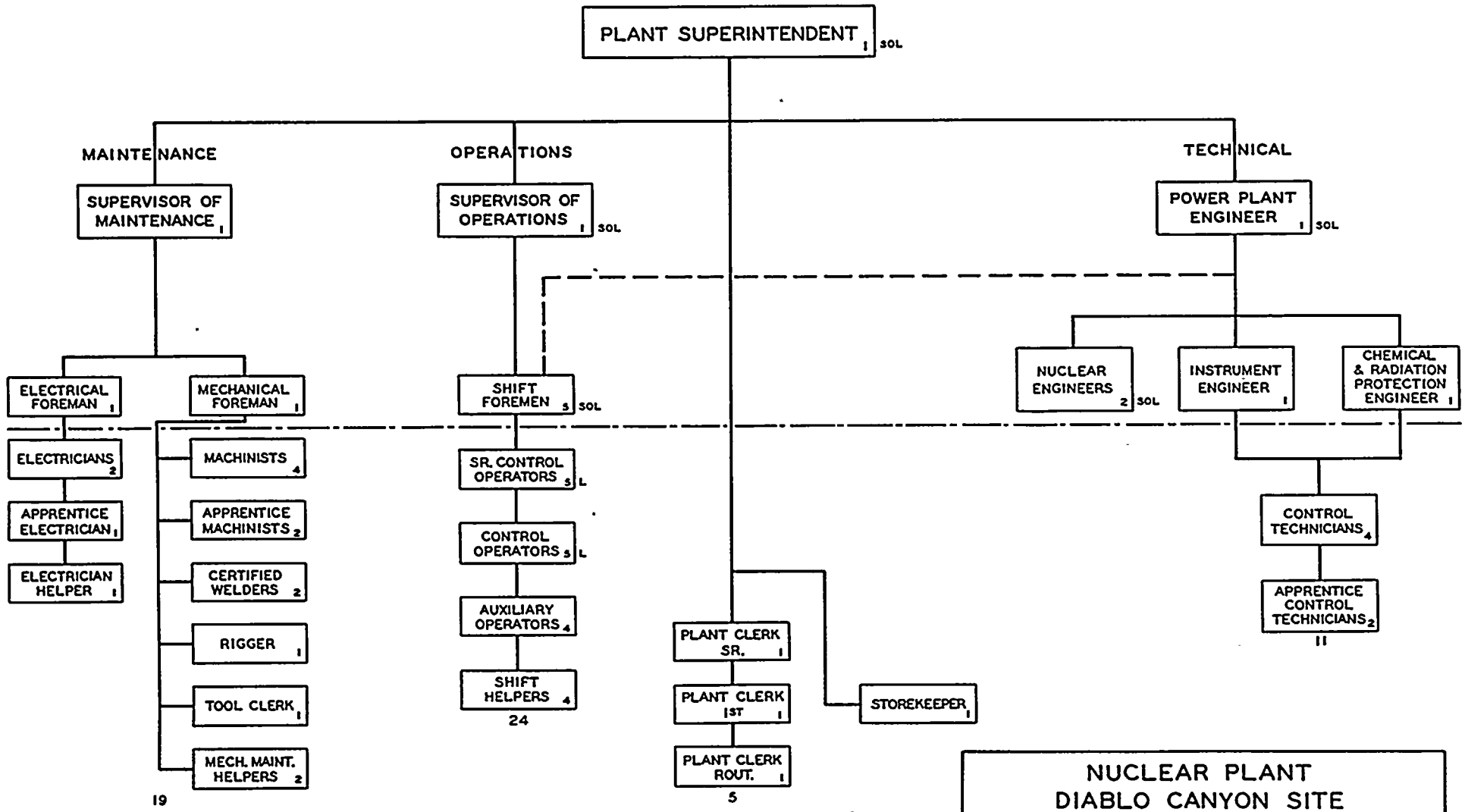

LEGEND:

SOL - AEC SENIOR OPERATOR LICENSE REQUIRED

L - AEC OPERATOR LICENSE REQUIRED

TOTAL PLANT COMPLEMENT = 59

NUCLEAR PLANT
DIABLO CANYON SITE
SAFETY ANALYSIS REPORT

FIG. 13-1 ULTIMATE OPERATING ORGANIZATION

GEOLOGY OF THE
DIABLO CANYON
POWER PLANT SITE

SAN LUIS OBISPO COUNTY

CALIFORNIA

CONTENTS

	Page
Introduction	1
Geologic setting	3
Bedrock units	6
Obispo tuff	6
Monterey formation	9
Diabasic intrusive rocks	11
Structure	12
Folds	12
Faults	14
Masses of brecciated rocks	18
Surficial deposits	20
Coastal terrace deposits	20
Stream-terrace deposits	22
Landslide deposits	23
Slump, creep, and slope-wash deposits	24
Talus and beach deposits	25
Stream-laid alluvium	26
Other deposits	26
Geologic relationships at the plant site	27
Surficial deposits	27
Bedrock	28
Faults	29
Seismicity	31
Groundwater	31

CONTENTS

(continued)

	Page
Recommended exploration at the plant site	32
Conclusions	34

GEOLOGY OF THE DIABLO CANYON POWER PLANT SITE
SAN LUIS OBISPO COUNTY, CALIFORNIA

INTRODUCTION

The area described in this report is a coastal tract in San Luis Obispo County approximately 6½ miles northwest of Point San Luis. It lies immediately southeast of the mouth of Diablo Canyon, a major westward-draining feature of the San Luis Range, and it is about a mile southeast of Lion Rock, a prominent offshore element of the highly irregular coastline.

The ground under consideration as a power plant site occupies an extensive topographic terrace about 1,000 feet in average width. The gently undulating surface of this terrace slopes gradually southwestward to an abrupt termination along a cliff fronting the ocean; in a landward, or northeasterly, direction it rises with progressively increasing slope to merge with the much steeper front of a foothill ridge of the San Luis Range. The surface ranges in altitude from 65 to 80 feet along the coastline to a maximum of nearly 300 feet along the base of the hillslope to the northeast, but nowhere is its local relief greater than 10 feet. It is marked by only one major interruption, the steep-walled canyon of lower Diablo

Creek; this gash is about 75 feet in average depth.

The geology of the subject area was studied by the writer during the period December 1965 - July 1966. A total of five days was devoted to field investigation that included mapping at scales of 100 feet and 200 feet to the inch. The geologic map accompanying this report was prepared from a topographic base that was provided at the smaller of these scales and with a contour interval of 5 feet.

Bedrock and overlying surficial deposits are exposed almost continuously along the seacliff and much less extensively along the walls of Diablo Canyon and on the main hillslope in the northeastern part of the area. The prominent points and ridges along the coastline, as well as the offshore rocks and shoals, are essentially bare bedrock. Man-made exposures are limited to a few shallow roadcuts in and near Diablo Canyon. In the fall of 1965 two exploratory trenches were dug beneath the terrace surface a short distance northwest of triangulation point Coon at the northwestern edge of the map area, but these had been backfilled prior to the writer's initial visit. No other subsurface exploration has been attempted as yet, and the depth, lithology, and structure of the bedrock section concealed beneath the continuous blanket of surficial deposits that underlies the main terrace surface therefore must be inferred from adjacent pertinent expo-

sures among those noted above (see accompanying geologic map and section).

The present investigation was directed toward determining the feasibility, in terms of geologic conditions, of this coastal area as a site for a nuclear power plant of large capacity. As indicated in preliminary memoranda of opinion submitted under dates of December 11, 1965, January 17, 1966, and May 18, 1966, the area is regarded as feasible for this purpose. Further, it is expected that detailed subsurface exploration as recommended in this report, together with testing of the natural materials and final analysis of geologic and seismic data, will firmly establish its suitability for such use and will provide a basis for determining appropriate design criteria for a plant.

GEOLOGIC SETTING

The entire subject area is underlain by a complex sequence of stratified marine sedimentary rocks and tuffaceous volcanic rocks, all of Tertiary (Miocene) age. Diabasic intrusive rocks are locally exposed high on the walls of Diablo Canyon at the edge of the area. Both the sedimentary and volcanic rocks have been folded and otherwise disturbed over a considerable range of scales.

Surficial deposits of Quaternary age are widespread; in a few places they are as thick as 50 feet, but their

average thickness probably is on the order of 20 feet over the terrace areas and 10 feet or less over the entire mapped ground. By far the most extensive deposits underlie the main topographic terrace, and their nature and thickness are highly significant with respect to further exploration and appraisal of the site.

Like many other parts of the California coast, the Diablo Canyon area is characterized by several wave-cut benches of Pleistocene age. These surfaces of irregular but generally low relief can be likened to broad steps in a gently rising staircase. They were developed across bedrock by marine erosion, and they are ancient analogues of the benches now being cut approximately at sea level along the present coast (see geologic map). They were formed during periods when sea level was higher than it is now and/or when the land was lower than it is now. Each is thinly and discontinuously mantled with marine sand, gravel, and rubble similar to the beach and offshore deposits that are accumulating along the present coastline. Along its landward margin each bears thicker and more localized coarse deposits similar to the modern talus along the base of the present seacliff.

Both the ancient wave-cut benches and their overlying marine and shoreline deposits have been buried beneath gravelly detritus derived from landward sources after the benches were in effect abandoned by the ocean. This non-

marine cover is essentially an apron of coalescing alluvial fans, and it is thickest adjacent to the mouths of major canyons. Where it has been deeply trenched by subsequent erosion, as along Diablo Canyon in the map area, it can be seen to have buried some of the benches so heavily that their individual identities are not reflected by the present rather smooth terrace topography. Thus the main terrace is basically a depositional feature, and its nonmarine deposits conceal both the older benches of marine erosion and some of the abruptly rising ground that separates them (see map and section).

The observed and inferred relationships among the terrace surfaces and the wave-cut benches buried beneath them can be summarized as follows:

Wave-cut bench		Terrace surface	
Altitude (feet)	Location	Altitude (feet)	Location
170 - 175	Small remnants on sides of Diablo Canyon	Mainly 170-190	Sides of Diablo Canyon and upper parts of main terrace; in places separated from lower parts of terrace by scarps
145 - 155	Very small remnants on sides of Diablo Canyon	Mainly 150 - 170	
120 - 130 90 - 95 65 - 80	Subparallel benches elongate in a northwest-southeast direction but with considerable aggregate width; wholly beneath main terrace	Mainly 70 - 160	Most of main terrace, a widespread surface on a composite section of nonmarine deposits; no well-defined scarps

(continued)

30 - 45	Small remnants above modern seacliff	50 - 100	Small remnants above modern seacliff
Approx. 0	Small to moderately large areas along present coastline	No depositional terrace	

Within the subject area the wave-cut benches increase progressively in age with increasing elevation above present sea level, hence their order in the above list is one of decreasing age.

BEDROCK UNITS

Obispo tuff

The Obispo tuff, commonly regarded as a member of the Miocene Monterey formation, is the oldest bedrock unit exposed in the area of investigation. It is relatively resistant to erosion, in general is well exposed, and appears extensively in the coastward parts of the area. This rock forms nearly all of the offshore prominences and shoals (see map).

The tuff is dense to highly porous, and thinly layered to almost massive. It ranges in color from white to buff where fresh, and from yellowish to reddish brown where weathered; most exposures are variegated in shades of brown. Many of the weathered surfaces have a "punky" appearance, but the rock is tough and cohesive.

Several pyroclastic rock types constitute the Obispo tuff (To on map) in and near the subject area. By far the most widespread is fine-grained vitric tuff with rare to moderately abundant tabular crystals of sodic plagioclase. The constituent glass commonly appears as fresh shards, but in many places it has been partly or completely devitrified. Crystal tuffs are locally prominent, and some of these are so crowded with 1/8- to 3/8-inch crystals of plagioclase that they superficially resemble granitoid plutonic rocks. Other observed rock types include pumiceous tuffs, pumice-pellet tuff breccias, perlitic vitreous tuffs, tuffaceous siltstones and mudstones, and fine-grained tuff breccias with fragments of glass and various Monterey rocks. No massive flow rocks were recognized anywhere in the exposed volcanic section.

In terms of bulk composition, the pyroclastic rocks appear to be chiefly soda rhyolites and soda quartz latites. Their plagioclase, which ranges from calcic albite to sodic oligoclase, commonly is accompanied by lesser amounts of quartz as small rounded crystals and irregular crystal fragments. Biotite, zircon, and apatite also are present in many of the specimens that were examined under the microscope. Most of the tuffaceous rocks, and especially the more vitreous ones, have been locally to pervasively altered. Products of silicification, zeolitization, and pyritization are readily recognizable in many exposures;

where the rocks generally are traversed by numerous thin, irregular veinlets and layers of cherty to opaline material. Veinlets and thin pod-like concentrations of gypsum also are widespread. Where pyrite is present, the rocks characteristically weather yellowish to brownish with gossan-like crusts.

The various contrasting rock types are simply interlayered in only a few places; much more typical are abutting, intertonguing, and irregularly interpenetrating relationships over a wide range of scales. Septa and inclusions of Monterey rocks are abundant, and some of them are large enough to be shown separately on the accompanying map. Highly irregular inclusions, a few inches to several feet in maximum dimension, are locally so densely packed together that they form breccias with volcanic matrices.

The Obispo tuff is underlain by mudstones of Lower Miocene (pre-Monterey) age, on which it rests with a highly irregular contact that appears to be intrusive. This contact lies offshore in the vicinity of the subject area, but is exposed along the seacoast to the southeast. In a gross way, the Obispo forms the basal part of the Monterey formation, but many of its contacts with these sedimentary rocks are plainly intrusive. Moreover, individual sills and dikes of slightly to thoroughly altered tuffaceous rocks appear here and there in the Monterey section, not uncommonly at stratigraphic levels well above its base (see

map). The observed physical relationships, together with the local occurrence of diatoms and foraminifera within the principal masses of volcanic rocks, indicate that most of the Obispo tuff probably was emplaced at shallow depths beneath the Miocene seafloor during accumulation of the Monterey strata. The tuff unit does not appear to represent a single, well-defined eruptive event, nor is it likely to have been derived from a single source conduit.

Monterey formation

Stratified rocks of the marine Monterey formation (Tm on map) underlie most of the subject area, including all of that portion intended for power-plant location. They are almost continuously exposed along the crescentic seacliff that borders Diablo Cove (see map), and elsewhere they appear in much more localized outcrops.

The observed rock types, listed in general order of decreasing abundance, are silty and tuffaceous sandstone, siliceous shale, shaly siltstone and mudstone, diatomaceous shale, sandy to highly tuffaceous shale, calcareous shale and impure limestone, bituminous shale, fine- to coarse-grained sandstone, impure vitric tuff, silicified limestone and shale, and tuff-pellet sandstone. Dark-colored and relatively fine-grained strata are most abundant in the lowest part of the section, as exposed along the east side of Diablo Cove, whereas lighter-colored sandstones

and siliceous shales are dominant at stratigraphically higher levels farther north. In detail, however, the different rock types are interbedded in various combinations, and intervals of uniform lithology rarely are thicker than 30 feet. Indeed, the closely-spaced alternations of contrasting strata yield a prominent rib-like pattern of outcrop along much of the seacliff and shoreline bench forming the margin of Diablo Cove.

The sandstones are mainly fine to medium grained, and most are distinctly tuffaceous. Shards of volcanic glass generally are recognizable under the microscope, and the very fine-grained siliceous matrix may well have been derived largely through alteration of original glassy material. Some of the sandstone contains small but megascopically visible fragments of pumice, perlitic glass, and tuff, and a few beds grade along strike into submarine tuff breccia. The sandstones are thinly to very thickly layered; individual beds 6 inches to 4 feet thick are fairly common, and a few appear to be as thick as 15 feet. Some of them are hard and very resistant to erosion, and they typically form subdued but nearly continuous elongate projections on major hillslopes (see map).

The siliceous shales are buff to light gray platy rocks that are moderately hard to extremely hard according to their silica content, but they tend to break readily along bedding and fracture surfaces. The bituminous rocks and

the siltstones and mudstones are darker colored, softer, and grossly more compact. Most of them are very thinly bedded or laminated, but in general planar structure is not conspicuous. The diatomaceous, tuffaceous, and sandy rocks are lighter colored. The more tuffaceous types are softer, and the diatomaceous ones are soft to the degree of punkiness; both kinds of rocks are easily eroded, but are markedly cohesive and tend to retain their gross positions on even the steepest of slopes.

The siliceous shale and most of the hardest, highly silicified rocks weather to very light gray, and the dark-colored, fine-grained rocks tend to bleach when weathered. The other types, including the sandstones, weather to various shades of buff and light brown. Stains of iron oxides are widespread on exposures of nearly all the Monterey rocks, and are especially well developed on some of the finest-grained shales that contain disseminated pyrite. All but the hardest and most thick-bedded rocks are considerably broken to depths of as much as 6 feet in the zone of weathering on slopes other than the present seacliff, and the broken fragments have been separated and displaced by surface creep to somewhat lesser depths.

Diabasic intrusive rocks

Small, irregular bodies of diabasic rocks are poorly exposed high on the walls of Diablo Canyon at and beyond

the northeasterly edge of the map area. Contact relationships are not readily determined, but these rocks evidently are intrusive into the Monterey formation. They are considerably weathered, but an ophitic texture is recognizable. They consist chiefly of calcic plagioclase and augite, with some olivine, opaque minerals, and zeolitic alteration products.

STRUCTURE

Folds

The bedrock units within the entire subject area form part of the southerly flank of a very large syncline that is a major feature of the San Luis Range. The northerly-dipping sequence of strata is marked by several smaller folds with subparallel trends and flank-to-flank dimensions measured in hundreds of feet. One of these, a syncline with gentle to moderate westerly plunge, is the largest flexure recognized within the mapped area. Its axis lies a short distance north of the power-plant site and about 450 feet northeast of the mouth of Diablo Canyon (see geologic map and section). East of the canyon this fold appears to be rather open and simple in form, but farther west it probably is complicated by several large wrinkles and may well lose its identity as a single feature. Some of this complexity is clearly revealed along the northerly margin of Diable

Cove, where the beds exposed in the seacliff have been closely folded along east to northeast trends. Here a tight syncline (shown on map) and several smaller folds can be recognized, and steep to near-vertical dips are dominant in several parts of the section.

The southerly flank of the main syncline within the map area steepens markedly as traced southward away from the fold axis. Most of this steepening is concentrated within an across-strike distance of about 300 feet as revealed by the strata exposed in the seacliff southeastward from the mouth of Diablo Canyon; farther southward the beds of sandstone and finer-grained rocks dip rather uniformly at angles of 70 degrees or more. A slight overturning through the vertical characterizes the several hundred feet of section exposed immediately north of the Obispo tuff that underlies South Point and the north shore of South Cove (see map). Thus the main syncline, though simple in gross form, is distinctly asymmetric. The relative steepness of its southerly flank may well have resulted from buttressing, during the folding, by the relatively massive and competent unit of tuffaceous rocks that adjoins the Monterey strata at this general level of exposure.

Smaller folds, corrugations, and highly irregular convolutions are widespread among the Monterey rocks, especially the finest-grained and most shaly types. Some of these flexures trend east to southeast and appear to be drag features systematically related to the larger-scale folding

in the area. Most, however, reflect no consistent form or trend, range in scale from inches to only a few feet, and evidently are confined to relatively soft rocks that are flanked by intervals of harder and more massive strata. They constitute crudely tabular zones of contortion within which individual rock layers can be traced for short distances but rarely are continuous throughout the deformed ground. Some of this contortion appears to have derived from slumping and sliding of unconsolidated sediments on the Miocene seafloor during accumulation of the Monterey section. Most of it, in contrast, plainly occurred at much later times, presumably after conversion of the sediments to sedimentary rocks, and it can be most readily attributed to highly localized deformation during the ancient folding of a section that comprises rocks with contrasting degrees of structural competence.

Faults

Numerous faults with total displacements ranging from a few inches to several feet cut the exposed Monterey rocks. Most of these occur within, or along the margins of, the zones of contortion noted above. They are sharp, tight breaks with highly diverse attitudes, and they typically are marked by 1/16 inch or less of gouge or microbreccia. Nearly all of them are curving or otherwise somewhat ir-

regular surfaces, and many can be seen to terminate abruptly or to die out gradually within masses of tightly folded rocks. These small faults appear to have been developed as end products of localized intense deformation caused by folding of the bedrock section. Their unsystematic attitudes, small displacements, and limited effects upon the host rocks identify them as second-order features, i.e., as results rather than causes of the localized folding and convolution with which they are associated.

Three distinctly larger and more continuous faults also were recognized within the mapped area. They are well exposed on the seacliff that fringes Diablo Cove (see map), and each lies within a zone of moderately to severely contorted fine-grained Monterey strata. Each is actually a zone, 6 inches to several feet wide, within which two or more subparallel tight breaks are marked by slickensides, 1/4 or less of gouge, and local stringers of gypsum. None of these breaks appears to be systematically related to individual folds within the adjoining rocks. None of them extends upward into the overlying blanket of Quaternary terrace deposits.

One of these faults, exposed on the north side of the cove, trends north-northwest essentially parallel to the flanking Monterey beds, but it dips more steeply that these beds. Another, exposed on the east side of the cove, trends

east-southeast and is essentially vertical; thus it is essentially parallel to the structure of the host Monterey section. Neither of these faults projects toward the ground intended for power-plant construction. The third fault, which appears on the seacliff at the mouth of Diablo Canyon, trends northeast and projects toward ground immediately north of the power-plant site. It dips northward somewhat more steeply than the adjacent strata.

Total displacement is not known for any of these three faults, but it could amount to tens or even to a few hundreds of feet. That these breaks are not major features, however, is strongly suggested by their sharpness, by the thinness of gouge along individual surfaces of slippage, and by the essential lack of correlation between the highly irregular geometry of deformation in the enclosing strata and any directions of movement along the slip surfaces.

The possibility that these surfaces are late-stage expressions of much larger-scale faulting at the same general sites was tested by careful examination of the deformed rocks that they transect. On megascopic scales the rocks appear to have been deformed much more by flexing than by rupture and slippage, as evidenced by local continuity of numerous thin beds that denies the existence of pervasive faulting within much of the ground in question. That the finer-grained rocks are not themselves fault gouge was confirmed by examination of 34 samples under the microscope.

Sedimentary layering, recognized in 27 of these samples, was observed to be grossly continuous even though dislocated here and there by tiny fractures. Moreover, nearly all the samples were found to contain shards of volcanic glass and/or the tests of foraminifera; some of these delicate components showed effects of microfracturing and a few had been offset a millimeter or less along tiny shear surfaces, but none appeared to have been smeared out or partially obliterated by intense shearing or grinding. Thus the three larger faults in the area evidently were superimposed upon ground that already had been deformed primarily by small-scale and locally very intense folding rather than by pervasive grinding and milling.

It is not known whether these faults were late-stage results of major folding in the region or were products of independent tectonic activity. In either case they are relatively ancient features, as they are capped without break by the Quaternary terrace deposits exposed along the upper part of the seacliff. They probably are not large-scale elements of regional structure, as examination of the nearest areas of exposed bedrock along their respective landward projections revealed no evidence of substantial offsets among recognizable stratigraphic units. Seaward projection of one or more of these faults might be taken to explain a possible large offset of the Obispo tuff units exposed on North Point and South Point. The notion of such an offset, however, would rest upon the assumption that

these two units are displaced parts of an originally continuous body, for which there is no real evidence. Indeed, the two tuff units are bounded on their northerly sides by lithologically different parts of the Monterey formation, hence clearly were originally emplaced at different stratigraphic levels and are not directly correlative.

Masses of brecciated rocks

Highly irregular masses of coarsely brecciated rocks, a few feet to many tens of feet in maximum dimension, are present in some of the relatively siliceous parts of the Monterey section that adjoin the principal bodies of Obispo tuff. The fracturing and dislocation is not genetically related to any recognizable faults, but instead seems to have been associated with emplacement of the volcanic rocks; it evidently was accompanied or soon followed by extensive silicification. Many adjacent fragments in the breccias are closely juxtaposed and have matching opposed surfaces, so that they plainly represent no more than coarse crackling of the brittle rocks. Other fragments, though angular or subangular, are not readily matched with adjacent fragments and hence may represent significant translation within the entire rock masses.

The ratio of matrix materials to coarse fragments is very low in most of the breccias, and nowhere was observed to exceed about 1:3. The matrices generally comprise

smaller angular fragments of the same Monterey rocks that are elsewhere dominant in the breccias, and they characteristically are set in a siliceous cement. Tuffaceous matrices, with or without Monterey fragments, also are widespread and commonly show the effects of pervasive silicification. All the exposed breccias are firmly cemented, and they rank among the hardest and most resistant units in the entire bedrock section.

A few 3- to 18-inch beds of sandstone have been pulled apart to form separate tabular masses along specific stratigraphic horizons in higher parts of the Monterey sequence. Such individual tablets, which are boudins rather than ordinary breccia fragments, are especially well exposed in the seacliff at the northern corner of Diablo Cove. They are flanked by much finer-grained strata that converge around their ends and continue essentially unbroken beyond them. This boudinage, or separation and stringing out of sandstone beds that lie within intervals of much softer and more shaly rocks, has resulted from compression during folding of the Monterey section. Its distribution is stratigraphically controlled and is not systematically related to recognizable faults in the area.

SURFICIAL DEPOSITS

Coastal terrace deposits

The coastal wave-cut benches of Pleistocene age, referred to on page 4, are almost continuously blanketed by terrace deposits (Qter on map) of several contrasting types and modes of origin. The oldest of these deposits are relatively thin and patchy in their occurrence, and were laid down along and adjacent to ancient beaches during Pleistocene time. They are covered by considerably thicker and more extensive nonmarine accumulations of detrital materials derived from various landward sources.

The marine deposits consist of silt, sand, gravel, and cobbly to bouldery rubble. They are approximately 2 feet in average thickness over the entire terrace area, and reach a maximum observed thickness of about 8 feet. They rest directly upon bedrock, some of which is marked by numerous holes attributable to the action of boring marine mollusks, and they commonly contain large rounded cobbles and boulders of Monterey and Obispo rocks that have been similarly bored. Lenses and pockets of highly fossiliferous sand and gravel are present locally.

The marine sediments are poorly to very well sorted, and loose to moderately well consolidated. All of them have been naturally compacted; the degree of compaction varies according to the material, but it is consistently

greater than that observed in any of the associated surficial deposits of other types. Near the inner margins of individual wave-cut benches the marine deposits merge landward into coarser and less well-sorted debris that evidently accumulated along the bases of ancient seacliffs or other shoreline slopes. This debris is locally as much as 12 feet thick; it forms broad but very short aprons, now buried beneath younger deposits, that are ancient analogues of the talus accumulations along the inner margin of the present beach in Diablo Cove. One of these occurrences, identified as "fossil Qtb" on the geologic map, is well exposed high on the northerly wall of Diablo Canyon.

A younger, thicker, and much more continuous nonmarine cover is present over most of the coastal terrace area. It consistently overlies the marine deposits noted above, and where these are absent it rests directly upon bedrock. It is composed mainly of stream-laid detritus contributed during Pleistocene time from Diablo Canyon and several smaller drainage courses, and it thickens markedly as traced sourceward toward these canyons. It constitutes a series of alluvial fans, some of which appear to have partly coalesced with adjacent ones. The fan debris is chiefly fine- to moderately coarse-grained gravel and rubble characterized by tabular fragments of Monterey rocks in a rather abundant silty to clayey matrix. Most of it is thinly and regularly stratified, but the distinctness of this layering varies

greatly from place to place.

Slump, creep, and slope-wash deposits, derived from adjacent hillsides by relatively slow downhill movement over long periods of time, also form parts of the nonmarine terrace cover. All are loose and uncompacted. They comprise fragments of Monterey rocks in a dark-colored clayey matrix, and their internal structure is essentially chaotic. In some places they are crudely interlayered with the alluvial-fan deposits, but they ordinarily overlie these bedded sediments. On parts of the main terrace area not reached by any of the alluvial fans, a cover of slump, creep, and slope-wash deposits, a few inches to nearly 10 feet thick, rests directly upon either marine terrace deposits or bedrock.

Thus the entire section of terrace deposits that caps the coastal benches of Pleistocene marine erosion is heterogeneous and internally complex; it includes contributions of detritus from contrasting sources, from different directions at different times, and via several basically different modes of transport and deposition.

Stream-terrace deposits

Several narrow, irregular benches along the walls of Diablo Canyon are veneered by a few inches to 6 feet of silty gravels that are somewhat coarser but otherwise similar to the alluvial-fan deposits described above. These

stream-terrace deposits (Qst) originally occupied the bottom of the canyon at a time when the lower course of Diablo Creek had been cut downward through the alluvial-fan sediments of the main terrace and well into the underlying bedrock. Subsequent deepening of the canyon left remnants of the deposits as cappings on scattered small terraces.

Landslide deposits

The walls of Diablo Canyon also are marked by tongue- and bench-like accumulations of loose, rubbly landslide debris (Qls), consisting mainly of highly broken and jumbled Monterey rock masses with abundant silty and soily matrix materials. These landslide bodies represent localized failure on naturally oversteepened slopes, generally confined to fractured bedrock in and immediately beneath the zone of weathering. Individual bodies within the mapped area are small, with probable maximum thicknesses no greater than 20 feet. All of them lie outside the area intended for power-plant construction.

Landslide deposits along the seacliff have been recognized at only one locality, on the north side of Diablo Cove about 400 feet northwest of the mouth of Diablo Canyon. Here slippage has occurred along bedding and fracture surfaces in siliceous Monterey rocks, and it has been confined essentially to the axial region of a well-defined syncline (see map). Several episodes of sliding are at-

tested by thin, elongate masses of highly broken ground separated from one another by well-defined zones of dislocation. Some of these masses are still capped by terrace deposits. The entire composite accumulation of debris is not more than 35 feet in maximum thickness, and ground failure at this locality does not appear to have resulted in major recession of the cliff. Elsewhere within the mapped area landsliding along the seacliff evidently has not been a significant process.

Large landslides, some of them involving substantial thicknesses of bedrock, are present on both sides of Diablo Canyon not far northeast of the mapped area. These occurrences need not be considered in connection with the powerplant site, but they will constitute highly significant factors in establishing a satisfactory grading design for a switchyard or any other up-canyon installation. They are not dealt with in this report.

Slump, creep, and slope-wash deposits

As noted earlier, slump, creep, and slope-wash deposits (Qsw) form parts of the nonmarine sedimentary blanket on the main terrace. These materials are shown separately on the geologic map only in those limited areas where they have been considerably concentrated along well-defined swales. Their actual distribution is much wider, and they undoubtedly are present over a large fraction of

the areas designated as Qter; their average thickness in such areas, however, probably is less than 5 feet.

Angular fragments of Monterey rocks are sparsely to very abundantly scattered through the slump, creep, and slope-wash deposits, whose most characteristic feature is a fine-grained matrix that is dark-colored, moderately rich in clay minerals, and extremely soft when wet. Internal layering is rarely observable and nowhere is sharply expressed. The debris seems to have been rather thoroughly intermixed during its slow migration down hillslopes in response to gravity. That it was derived mainly from broken materials in the zone of weathering is shown by several exposures in which it grades downward through soily debris into highly disturbed and partly weathered bedrock, and thence into progressively fresher and less broken bedrock.

Talus and beach deposits

Much of the present coastline in the subject area is marked by bare rock, but Diablo Cove and a few other large indentations are fringed by narrow, discontinuous beaches and irregular concentrations of seacliff talus. These deposits (Qtb) are very coarse grained. Their total volume is small, and they are of interest mainly as modern analogues of much older deposits at higher levels beneath the main terrace surface.

The beach deposits consist chiefly of well-rounded

cobbles. They form thin veneers over bedrock, and in Diablo Cove they grade seaward into patches of coarse pebbly sand. The floors of both Diablo Cove and South Cove probably are irregular in detail and are featured by rather hard, fresh bedrock that is discontinuously overlain by irregular thin bodies of sand and gravel. The distribution and abundance of kelp suggest that bedrock crops out over large parts of these cove areas where the seabottom cannot be observed from onshore points.

Stream-laid alluvium

Stream-laid alluvium (Qal) occurs as a strip along the present narrow floor of Diablo Canyon, where it is only a few feet in average thickness. It is composed of irregularly intertongued silt, sand, gravel, and rubble. It is crudely to sharply stratified, poorly to well sorted, and in general somewhat compacted. Most of it is at least moderately porous.

Other deposits

Earlier inhabitation of the area by Indians is indicated by several midden deposits that are rich in charcoal and fragments of shells. The most extensive of these occurrences marks the site of a long-abandoned village along the edge of the main terrace immediately northwest of Diablo Canyon. Others have been noted on the main terrace

just east of the mouth of Diablo Canyon, on the shoreward end of South Point, and at several places in and near the power-plant site. Maximum inferred thickness of these extremely loose-textured deposits is about 6 feet.

Artificial (man-made) fill is present within the area as low benches along unimproved sidehill roads, as small abutment prisms at an old road crossing in Diablo Canyon, and as numerous small piles of rocks rejected from parts of the main terrace surface that formerly were under cultivation.

GEOLOGIC RELATIONSHIPS AT THE PLANT SITE

The site for the proposed power plant lies on the part of the main terrace surface that extends southward and southeastward from Diablo Canyon. It is not specifically delineated on the accompanying geologic map, but the center of the initial reactor unit corresponds approximately in position to the map designation Qter about 650 feet east of the mouth of Diablo Canyon.

Surficial deposits

The site area is underlain by terrace deposits that probably range in thickness from as little as 4 feet to as much as 35 feet in the vicinity of the reactor-unit position. Dominant among these deposits is ancient alluvial-fan detritus derived from the Diablo Canyon drainage.

Slump, creep, and slope-wash deposits also are present, and these are likely to increase in relative abundance as the terrace cover is traced in a southeasterly direction. Marine sediments should be present at the base of the terrace section, but nowhere in thicknesses greater than 5 feet.

Bedrock

No bedrock is exposed within the area of the plant site, but the lithology and structure of the section beneath the terrace deposits can be inferred from nearby outcrops in Diablo Canyon, along the seacliff on the east side of Diablo Cove, and on the major hillslope east of the site. The bedrock should be a part of the Monterey formation in which thin- to thick-bedded, moderately hard to very hard sandstone is dominant. Much of this rock is tuffaceous. Some of the hardest and thickest-bedded sandstone is likely to be encountered at the site of the reactor unit. All the strata probably lie on the southerly side of the syncline that was described earlier, and moderate to rather steep northerly dips should be characteristic. The prevailing angle of dip can be expected to increase as the strata are crossed from north and northwest to south and southeast within the site.

The bedrock surface beneath the terrace deposits almost certainly is not a simple planar or near-planar feature.

Instead, it is likely to be featured by two or more relatively smooth and level domains at different levels, separated by one or more moderately steep slopes with northwestward trend. Further, the presence of exceptionally hard and massive sandstone units probably is expressed by local upward protuberances from the otherwise smooth surfaces, or by outward projections along any moderately steep slope.

Subsurface installations extending southward from the plant site will cross the major boundary between Monterey strata and the large unit of Obispo tuff before reaching the ocean at South Cove. The floor of the cove itself is underlain by the tuff, possibly with local septa and inclusions of silicified Monterey rocks. A thin cover of sand and gravel is present locally, but this is not likely to be a serious obstacle to establishing suitable foundations for a breakwater or other offshore works.

Faults

Detailed study of all bedrock exposures within and immediately adjacent to the map area indicates that no major fault should be present within the ground beneath the powerplant site. Scattered small breaks can be expected there, however, and it also is possible that an eastward extension of the minor fault exposed in the seacliff at the mouth of Diablo Canyon might lie beneath the extreme northerly part

of the site area.

None of the faults observed in the mapped area extends upward from the bedrock section into overlying terrace deposits, nor have any of the wave-cut benches beneath these deposits been offset by such faults. These important relationships, which were positively identified by examining freshly hand-trenched exposures of the basal terrace deposits above all faults recognized along the seacliff, indicate that the most recent fault displacements occurred prior to marine planation of the bedrock and deposition of the overlying marine and nonmarine terrace sediments. These elements of terrace development have not been dated within this area, but they assuredly are Pleistocene rather than Recent in age, as evidenced by the elevation of the main wave-cut bench 50 feet or more above present sea level. Further, they must date back to a period of relatively high sea level in Pleistocene time, and hence back to pre-Wisconsin time (i.e., they antedate at least the youngest major episode of Pleistocene glaciation in North America). Thus their age is at least 100,000 years, and more probably at least 120,000 years; both these estimates are compatible with radiometrically determined ages for similarly elevated marine terrace deposits at localities both northward and southward along the California coast.

If faults are encountered within the ground beneath the plant site, they should be minor features confined wholly

to bedrock. It can be anticipated that examination of their relationships with the overlying terrace deposits will show that their youngest displacements occurred at least 100,000 years ago. Moreover, an age thus determined would be minimal, as the latest fault movements could have occurred millions of years ago.

Seismicity

No large or active fault is known to exist within the general area of the San Luis Range, and available records of earthquake epicenters in California indicate that this area is not characterized by a high level of seismic activity. However, moderately severe to severe ground shaking at the power-plant site can be expected from a major earthquake along a relatively distant large fault. In this connection, the Nacimiento fault zone lies about 18 miles to the northeast, and the San Andreas fault zone nearly 50 miles to the northeast. Analysis of such possible seismic effects is beyond the scope of this report.

Groundwater

The level of permanent groundwater beneath the main terrace area probably lies at levels little above those of the bottom of lower Diablo Canyon. Some seepage might be encountered in deep cuts, but unless such cuts were extended downward to points near sea level subsurface water should

constitute no more than a minor and temporary nuisance.

RECOMMENDED EXPLORATION AT THE PLANT SITE

Excavation of trenches beneath the main terrace surface at the plant site is strongly recommended as a necessary means for exposing the terrace deposits and underlying bedrock in order to determine:

1. Nature and thickness of the surficial deposits, together with their bearing strengths and stability on slopes.
2. Configuration of the bedrock surface.
3. Lithology, gross structure, and bearing strength of the bedrock.
4. Distribution and nature of any faults, shear surfaces, and zones of rupture present in the bedrock.

Most of these factors already have been appraised in advance of subsurface exploration, but these appraisals necessarily were based almost wholly upon projection and inference from features observed outside the site area itself. They now require direct confirmation or rejection at the site. Most critical on this score is conclusive demonstration that no major fault exists within the ground in question, and that no lesser fault that does exist extends upward from bedrock into the overlying terrace deposits.

Accordingly, it is suggested that two pairs of exploratory trenches be developed across the plant site. One pair, comprising parallel trenches about 150 feet apart and each at least 400 feet long, should be aligned nearly east-west. The other pair should be similar, but aligned at right angles to the first; the four trenches should cross one another to form an essentially symmetrical pattern. One of the north-south pair could well be extended southward for an additional several hundred feet to provide information on some of the terrace ground between the plant site and South Cove.

All trenches should be excavated at least three feet into bedrock throughout their entire lengths, and each should be sufficiently wide along its bottom to permit ready observation and photographic recording of the materials exposed along its walls. The lower part of one wall in each trench should be trimmed to an essentially vertical slope to facilitate detailed mapping and study of the continuously exposed contact between bedrock and the overlying cover of surficial deposits.

Test borings could yield useful information concerning the depth distribution of bedrock in advance of trenching, but under no circumstances should such holes be regarded as a satisfactory substitute for a program of trenching.

CONCLUSIONS

On the basis of all known geologic factors, as outlined and discussed in the foregoing pages of this report, it is the writer's judgment that the Diablo Canyon Power Plant Site is a feasible one for the use under consideration. Owing to the nature, distribution, and structure of the bedrock and surficial deposits that are present, no special problems involving bearing strengths or ground stability are anticipated. Subsurface water should impose no serious difficulties during excavation and construction on this property.

Results of the investigations completed to October 1, 1966, suggest that a program of detailed subsurface studies based upon the exploratory trenches recommended on the foregoing page, if coordinated with appropriate testing of materials and a geologic-seismic analysis, will lead to a favorable judgment regarding suitability and to the establishment of satisfactory design criteria for the plant. With reference to future earthquakes and fault movements, it is expected that such additional investigation and analysis will provide a basis for earthquake-resistant design, and that it will justify the conclusion that the possibility of permanent ground displacement beneath the site during the useful life of the power plant is sufficiently remote to be safely disregarded.

CERTIFICATION

The foregoing report was prepared and submitted according to the following time schedule:

Draft prepared without recommendations concerning subsurface exploration, August 15, 1966

Section on recommended exploration prepared, September 25, 1966

Report expanded to include results of laboratory investigations, November 15, 1966

Complete report transmitted December 5, 1966, without substantive modifications relative to the original draft

Richard H. Jahns

Richard H. Jahns

Geologist

GEOLOGIC MAP OF DIABLO CANYON COASTAL AREA

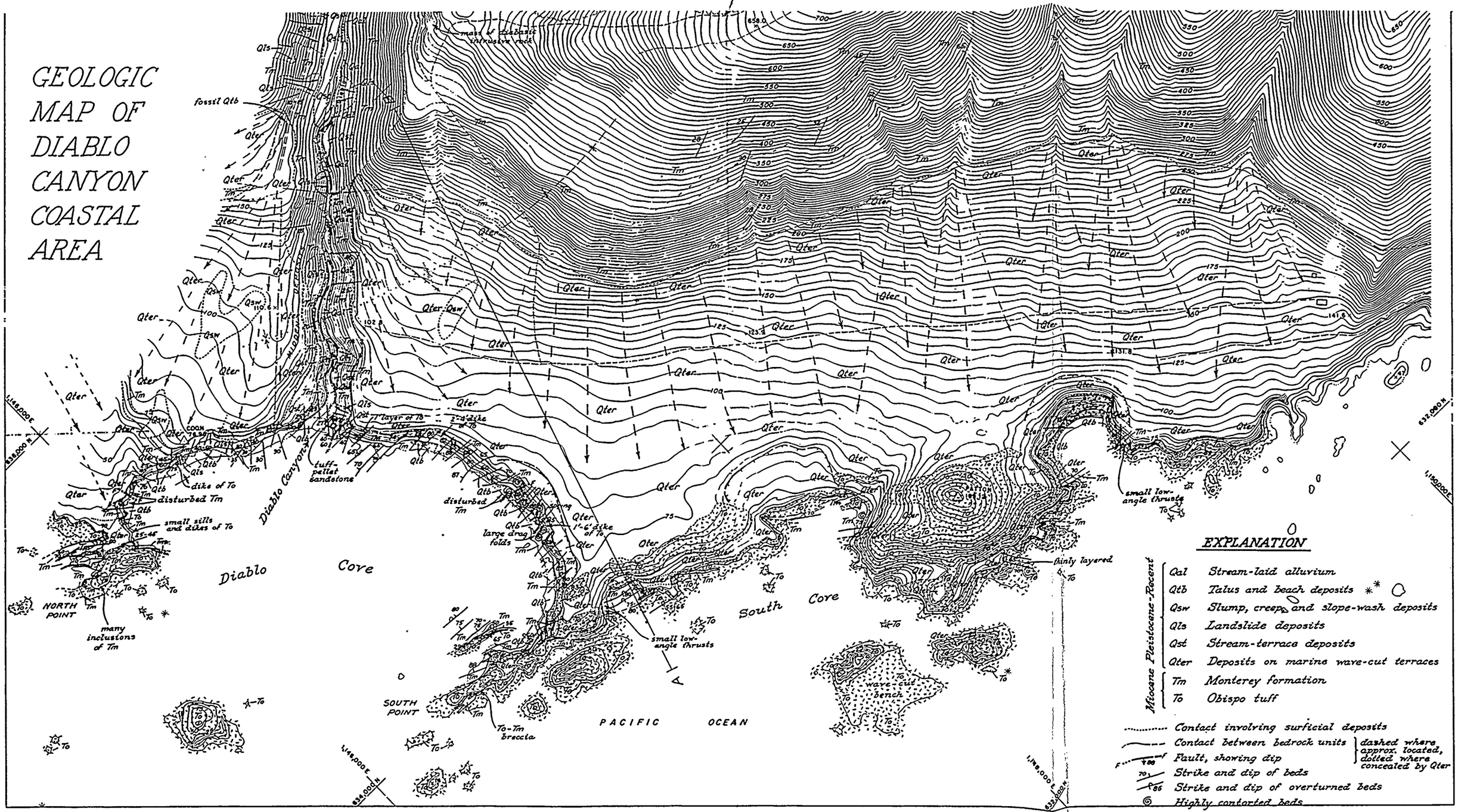

EXPLANATION

Holocene-Recent	Qal	Stream-laid alluvium
	Qtb	Talus and beach deposits
	Qsw	Slump, creep, and slope-wash deposits
	Qls	Landslide deposits
	Qst	Stream-terrace deposits
	Qter	Deposits on marine wave-cut terraces
Miocene-Pleistocene	Tm	Monterey formation
	To	Obispo tuff

- Contact involving surficial deposits
- Contact between bedrock units (dashed where approx. located, dotted where concealed by Qter)
- Fault, showing dip
- Strike and dip of beds
- Strike and dip of overturned beds
- Highly contorted beds
- Axis of syncline
- Boundary between different generations of Qter
- General trend of alluvial-fan deposition
- Surface trace of resistant horizon in Tm

200 0 200 400 600 800 1000

CONTOUR INTERVAL 5' & 10'

Photogrammetric map by
R.M. TOWILL, Inc.
612 Howard Street, San Francisco, California
Date of Photography July 2, 1965

Grid is based on California Coordinate System, Zone 5
Mean Sea Level Datum, 1929 Adj.

Geology mapped by R.H. Jahns
12/65, 3/66, 7/66

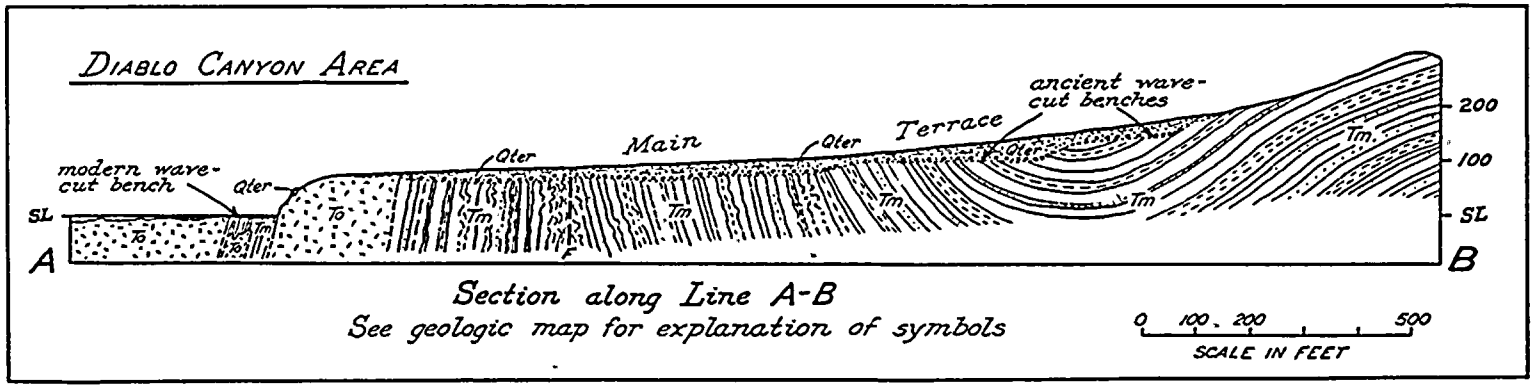
DIABLO CANYON AREA
modern wave-cut bench
Qter
Qter
Main
Qter
Terrace
ancient wave-cut benches
Qter
Tm
Tm
Tm
Tm
To
To
To
SL
200
100
SL
A
B
Section along Line A-B
See geologic map for explanation of symbols
0 100 200 500
SCALE IN FEET

GEOLOGY OF THE
DIABLO CANYON
POWER PLANT SITE

SAN LUIS OBISPO COUNTY

CALIFORNIA

SUPPLEMENTARY REPORT

CONTENTS

	Page
Introduction	1
The exploratory trenches	3
Bedrock	4
Bedrock structure	5
Terrace deposits	7
The interface between bedrock and surficial deposits	9
Final conclusions	12

GEOLOGY OF THE DIABLO CANYON POWER PLANT SITE
SAN LUIS OBISPO COUNTY, CALIFORNIA

SUPPLEMENTARY REPORT

INTRODUCTION

The geology of the Diablo Canyon Coastal Area, San Luis Obispo County, was investigated in detail by this writer during the period December 1965-December 1966. In a report submitted under date of December 5, 1966, he concluded that the area is feasible, in terms of geologic conditions, as a site for a nuclear power plant of large capacity. This general conclusion, based upon the results of field and laboratory investigations completed as of November 15, 1966, was accompanied by a summary of earlier informal recommendations for a program of exploratory trenching at the power-plant site. The chief purpose of such subsurface exploration of unconsolidated deposits and underlying bedrock was to determine whether the initial conclusion of geologic feasibility could be properly translated into one of geologic suitability.

The broad terrace surface at the power-plant site has been deeply trenched according to a plan recommended in September 1966 and subsequently set forth on page 33 of the geologic report noted above. The continuous exposures thus

provided were examined, studied, and mapped by the writer during periods aggregating six days in October and November 1966; throughout the four days of field work in November, Dr. Arvid M. Johnson of the Department of Geology, Stanford University, participated in the project and made independent judgments concerning the exposed geologic features.

One wall of each trench was mapped from end to end at a scale of approximately 2½ feet to the inch. The geologic data were plotted directly on series of overlapping photographs provided by Pacific Gas and Electric Company, and from this composite base four sections were prepared at a scale of 20 feet to the inch. Survey control, established by engineers of Pacific Gas and Electric Company, comprised points on the original ground surface, points along the floors of the cuts, and points at 10-foot intervals along one wall of each cut.

The purposes of this supplementary report are (1) to outline the geologic relationships revealed in the exploratory trenches and to indicate their bearing on specific appraisals noted in the earlier report, (2) to provide documentation in the form of photographs, detailed sketches, and geologic sections, and (3) to present final conclusions based upon the entire geologic investigation of the Diablo Canyon Coastal Area and the included power-plant site.

THE EXPLORATORY TRENCHES

Four exploratory trenches have been cut beneath the main terrace surface at the power-plant site, as shown in Plate 1. Trench A, about 1,080 feet long, extends in a north-northwesterly direction and thus is roughly parallel to the nearby margin of Diablo Cove. Trench B, 380 feet long, is parallel to A and lies about 150 feet east of the northerly one-third of the longer trench. Trenches C and D, respectively 450 and 490 feet long, are nearly parallel to each other, 130 to 150 feet apart, and are essentially normal to Trenches A and B. The two pairs of trenches cross each other to form a # pattern that would be symmetrical were it not for the long southerly extension of Trench A. They cover the area intended for power-plant construction, and the intersection of Trenches B and C coincides in position with the center of the nuclear reactor structure.

All four trenches, throughout their aggregate length of approximately 2,400 feet, reveal a section of surficial deposits and underlying Monterey bedrock that corresponds to the "two-ply" sequence of surficial deposits and Monterey strata exposed along the seacliff in nearby Diablo Cove (Plate 2). The trenches range in depth from 10 feet to nearly 40 feet, and all have sloping sides that give way downward to essentially vertical walls in the bedrock encountered 3 to 8 feet above their wide floors (Plates 3, 4, 5, 9). To facilit-

ate detailed geologic mapping, the easterly walls of Trenches A and B and the southerly walls of Trenches C and D were trimmed to near-vertical slopes extending upward from the trench floors to levels well above the top of bedrock (Plates 5, 6, 7, 8). These walls subsequently were scaled back by means of hand tools in order to provide fresh, clean exposures prior to mapping of the contact between bedrock and overlying unconsolidated materials.

BEDROCK

The bedrock that is continuously exposed in the lowest parts of all the exploratory trenches lies within a portion of the Monterey formation characterized by a preponderance of sandstone. It corresponds to the part of the section that crops out in lower Diablo Canyon and along the seacliff southeastward from the canyon mouth. The sandstone ranges from light gray through buff to light reddish brown, from silty to markedly tuffaceous, and from thin-bedded and platy to massive. The distribution and thickness of beds can be readily appraised from the sections along Trenches A and B (Plate 1), which show nearly all individual bedding surfaces that could be recognized on the ground.

The sandstone ranges from very hard to moderately soft, and some of it feels slightly punky when struck with a pick. All of it, however, is firm and very compact. In general the

most platy parts of the sequence are also the hardest, but plainly the soundest rock in the area is almost massive sandstone of the kind that underlies the site of the intended reactor structure. This rock is well exposed on the nearby hillslope adjoining the main terrace area, where it has been markedly resistant to erosion and stands out as distinct low ridges (ref. earlier report and accompanying map).

Tuff, consisting chiefly of altered volcanic glass, forms irregular sills and dikes in several parts of the bedrock section. This material, generally light gray to buff, is compact but distinctly softer than the enclosing sandstone. Individual bodies are half an inch to four feet thick. They are locally abundant in Trench C west of Trench A, and in Trench A southward beyond the end of the section in Plate 1. They are very rare or absent in Trenchs B and D, and in the easterly parts of Trench C and the northerly parts of Trench A. These volcanic rocks probably are related to the Obispo tuff as described in the earlier report, but all known masses of typical Obispo tuff in this area lie at considerable distances west and south of the ground occupied by the trenches.

BEDROCK STRUCTURE

The stratification of the Monterey rocks dips northward wherever it can be observed in the trenches, in general at angles of 35 to 55 degrees. Thus the bedrock beneath the power-plant site evidently lies on the southerly flank of the

major syncline noted in the earlier geologic report. Zones of convolution and other expressions of locally intense folding were not recognized, and probably are much less common in this general part of the section than in other, previously described parts that include intervals of softer and more shaly rocks.

Much of the sandstone is traversed by fractures. Planar, curving, and irregular surfaces are well represented, and in places they are abundant and closely spaced. All prominent fractures and many of the minor and discontinuous ones are shown in the sections of Plate 1. Also shown in these sections are all recognized "slip joints," shear surfaces, and faults, i.e., all surfaces along which the bedrock has been displaced. Such features are most abundant in Trenches A and C near their intersection, in Trench D west of the intersection with Trench A, and near the northerly end of Trench B.

Most of the surfaces of movement are "hairline" features with or without thin films of clay and/or gypsum. Displacements range from a small fraction of an inch to several inches. The other surfaces are more prominent, with well-defined zones of gouge and fine-grained breccia ordinarily 1/8 inch or less in thickness. Such zones were observed to reach a maximum thickness of nearly 1/2 inch along two small faults, but only as local lenses or "pockets." Exposures are not sufficiently extensive in three dimensions for definitely determining the magnitude of slip along the more prominent

faults, but all of these breaks appear to be minor features. Indeed, no expressions of major faulting were recognized in any of the trenches despite careful search, and the continuous bedrock exposures preclude the possibility that such features could be readily overlooked.

A northeast-trending fault that appears on the seacliff at the mouth of Diablo Canyon projects toward ground immediately north of the power-plant site, as noted in the previous report. No zone of breaks as prominent as this one was identified in the trench exposures, and any distinct northeastward continuation of the fault may indeed lie north of the trenched ground. Alternatively, this fault might well separate northeastward into several smaller faults; some or all of these could correspond to some or all of the breaks mapped in the northerly parts of Trenches A and B.

TERRACE DEPOSITS

Marine terrace deposits of Pleistocene age form a cover, generally 2 to 5 feet thick, over the bedrock that lies beneath the power-plant site. This cover is continuous in Trench C and the northerly part of Trench A, and it is nearly continuous in the other two trenches (Plate 1). Its lithology is highly variable (Plates 7, 9), and includes bouldery rubble, loose beach sand, pebbly silt, silty to clayey sand with abundant shell fragments, and soft clay derived from underlying

tuffaceous rocks. Nearly all of these deposits are at least sparsely fossiliferous, and in a few places they consist mainly of shells and shell fragments. Vertebrate fossils, chiefly vertebral and rib materials representing large marine mammals, are present locally (Plate 8); recognized occurrences are designated by the symbol X on the sections of Plate 1.

At the easterly ends of Trenches C and D the marine deposits intergrade and intertongue in a landward direction with thicker and coarser accummulations of poorly-sorted debris. This material evidently is talus that was formed along the base of an ancient seacliff or other shoreline slope (ref. pl. 4, 21 of earlier report). In some places the marine deposits are overlain by nonmarine terrace sediments with a sharp break, but elsewhere the contact between these two kinds of deposits is a dark-colored zone, a few inches to as much as two feet thick, that appears to represent a soil developed on the marine section (Plate 9). Fragments of these soily materials appear here and there in the basal parts of the nonmarine section.

The nonmarine sediments exposed in Trenches B, C, and D and in the northerly part of Trench A are mainly alluvial-fan gravels derived in ancient times from Diablo Canyon. They consist of numerous tabular fragments of Monterey rocks in a relatively dark-colored silty to clayey matrix, and in general they are distinctly bedded and moderately to highly compact. As indicated on the sections of Plate 1, they thicken progres-

sively in a north-northeastward direction, i.e., toward their principal source, the ancient mouth of Diablo Canyon.

Slump, creep, and slope-wash deposits, which constitute the youngest major element of the terrace section, overlie the alluvial-fan gravels and locally are interlayered with them. Where the gravels are absent, as in the southerly part of Trench A, this younger cover rests directly upon bedrock. It is loose and uncompacted, internally chaotic, and is composed of fragments of Monterey rocks in an abundant dark-colored clayey matrix.

All the terrace deposits are soft and unconsolidated, and hence are much less resistant to erosion than is the underlying bedrock. Those appearing along the walls of the exploratory trenches have been exposed to heavy rainfall during two recent fall storms, and have shown some tendency to wash and locally to rill. Little slumping and no gross failure has been noted in the trenches, however, and it is not anticipated that these materials would cause special problems during construction of a power plant.

THE INTERFACE BETWEEN BEDROCK AND SURFICIAL DEPOSITS

As exposed continuously in the exploratory trenches, the contact between bedrock and overlying terrace deposits represents a broad wave-cut platform of Pleistocene age. This

buried surface of ancient marine erosion ranges in altitude between extremes of 82 and 100 feet, and more than three-fourths of it lies within the much more limited range of 90 to 95 feet. As noted in the previous report (p. 4-6), it is one of several wave-cut benches that can be likened in this coastal area to broad steps in a gently rising staircase. It terminates eastward against a moderately steep shoreline slope, the lowest parts of which are exposed at the extreme easterly ends of Trenches C and D, and beyond this slope is an older buried bench at altitudes of 120 to 130 feet.

Available exposures indicate that the configuration of the erosional platform is markedly similar, over a wide range of scales, to that of the platform now being cut approximately at sea level along the present coast (Plate 2). Grossly viewed, it slopes very gently in a seaward (westerly) direction and is marked by broad, shallow channels and by upward projections that must have appeared as low spines and "reefs" when the bench was being formed (Plate 1). The most prominent "reef," exposed in Trenches B and D at and near their intersection, is a wide, westerly-trending projection that rises 5 to 15 feet above neighboring parts of the bench surface. It is composed of massive sandstone that was relatively resistant to the ancient wave erosion.

As shown in the sections and sketches of Figure 1, the surface of the platform is nearly planar in some places but elsewhere is highly irregular in detail. The small-scale

irregularities, generally 3 feet or less in vertical extent, include knob-, spine-, and rib-like projections and various wave-scoured pits, crevices, notches, and channels. The upward projections clearly correspond to relatively hard, resistant beds or parts of beds in the sandstone section. The depressions consistently mark the positions of relatively soft silty or shaly sandstone, of very soft tuffaceous rocks, or of extensively jointed rocks. The surface traces of most faults and some of the most prominent joints are in sharp depressions, some of them with overhanging walls. All these irregularities of detail have modern analogues that can be recognized on the bedrock bench now being cut along the margins of Diablo Cove.

The interface between bedrock and overlying surficial deposits is of particular interest in the trenched area because it provides information concerning the age of fault movements within the bedrock section. This interface is nowhere offset by faults exposed in the trenches, but instead has been developed irregularly across these faults after their latest movements. The consistency of this general relationship was established by highly detailed tracing and inspection of the contact as freshly exhumed by scaling of the trench walls. Gaps in exposure of the interface necessarily were developed at the four intersections of trenches; at these localities the bedrock was carefully exposed so that all joints and faults could be recognized and traced along the trench floors to

points where their relationships with the exposed interface could be determined.

Corroborative evidence concerning age of the most recent fault displacements stems from the marine deposits that overlie the bedrock bench and form the basal part of the terrace section. That these deposits rest without break across the traces of faults in the underlying bedrock is shown by the continuity of individual sedimentary beds and lenses that can be clearly recognized and traced. Further, some of the faults are directly capped by individual boulders, cobbles, pebbles, shells, and fossil bones, none of which have been affected by fault movements. Thus the most recent fault displacements in the plant-site area occurred prior to marine planation of the bedrock and deposition of the overlying terrace sediments. As pointed out in the earlier report (p. 30-31), the age of the most recent faulting in this area is therefore at least 100,000 years, and more probably at least 120,000 years. It might be millions of years.

FINAL CONCLUSIONS

Geologic investigation of the Diablo Canyon Coastal Area, including detailed mapping of all natural exposures and exploratory trenches, yields the following basic conclusions concerning the nature, distribution, and relationships of existing bedrock and surficial deposits:

1. The area is underlain by sedimentary and volcanic bedrock units of Miocene age. Within this area, the power-plant site is underlain almost wholly by sedimentary strata of the Monterey formation, which dip northward at moderate to very steep angles. More specifically, the reactor site is underlain by thick-bedded to almost massive Monterey sandstone that is well indurated and firm. Where exposed on the nearby hillslope, this rock is markedly resistant to erosion.
2. The bedrock beneath the main terrace area, within which the power-plant site has been located, is covered by 3 to 35 feet of surficial deposits. These include marine sediments of Pleistocene age and nonmarine sediments of Pleistocene and Recent age. In general they are thickest in the vicinity of the reactor site.
3. The interface between the unconsolidated terrace deposits and the underlying bedrock comprises flat to moderately irregular surfaces of Pleistocene marine planation and intervening steeper slopes that also represent erosion in Pleistocene time.

4. The bedrock beneath the power-plant site occupies the southerly flank of a major syncline that trends west to northwest. No evidence of a major fault has been recognized within or near the coastal area, and bedrock relationships in the exploratory trenches positively indicate that no such fault is present within the area of the power-plant site.

5. Minor surfaces of disturbance, some of which plainly are faults, are present within the bedrock that underlies the power-plant site. None of these breaks offsets the interface between bedrock and the cover of terrace deposits, and none of them extends upward into the surficial cover. Thus the latest movements along these small faults must have antedated erosion of the bedrock section in Pleistocene time.

6. No landslide masses or other gross expressions of ground instability are present within the power-plant site or on the major hillslope east of the site. Some landslides have been identified in adjacent ground, but these are minor features confined to the naturally oversteepened walls of Diablo Canyon.

7. No water of subsurface origin was encountered in the exploratory trenches, and the level of permanent groundwater beneath the main terrace area probably is little different from that of the adjacent lower reaches of the deeply incised Diablo Creek.

Additional conclusions, based upon interpretation and analysis of available data, can be offered as follows:

1. No special problems involving bearing strength or lateral stability of the bedrock beneath the power-plant site need be anticipated.
2. Cuts in surficial deposits should be stable if they are designed and developed in accordance with modern soils engineering practice, including proper application of testing procedures during the course of grading.
3. Subsurface water should impose no serious difficulties during excavation and construction at the site.
4. Moderately severe to severe ground shaking can be expected at this locality during the useful lifetime of a power plant. Such motion, probably deriving from one

or more earthquakes associated with distant large faults, should be provided for in design of the plant.

5. The absence of major faults within the power-plant area, the highly probable absence of such breaks in nearby parts of the region, and an established age of at least 100,000 years for the latest displacements along the few small breaks that are present in the bedrock of the site area indicate that the possibility of fault-induced permanent ground displacement within the subject property during the useful life of a power plant is sufficiently remote to be safely disregarded.

On the basis of all known geologic factors, as outlined and discussed in this supplementary report and its antecedent, it is the writer's judgment that the Diablo Canyon Power Plant Site is both feasible and suitable for the use under consideration.

Richard H. Jahns

Richard H. Jahns
Geologist

Menlo Park, California
January 3, 1967

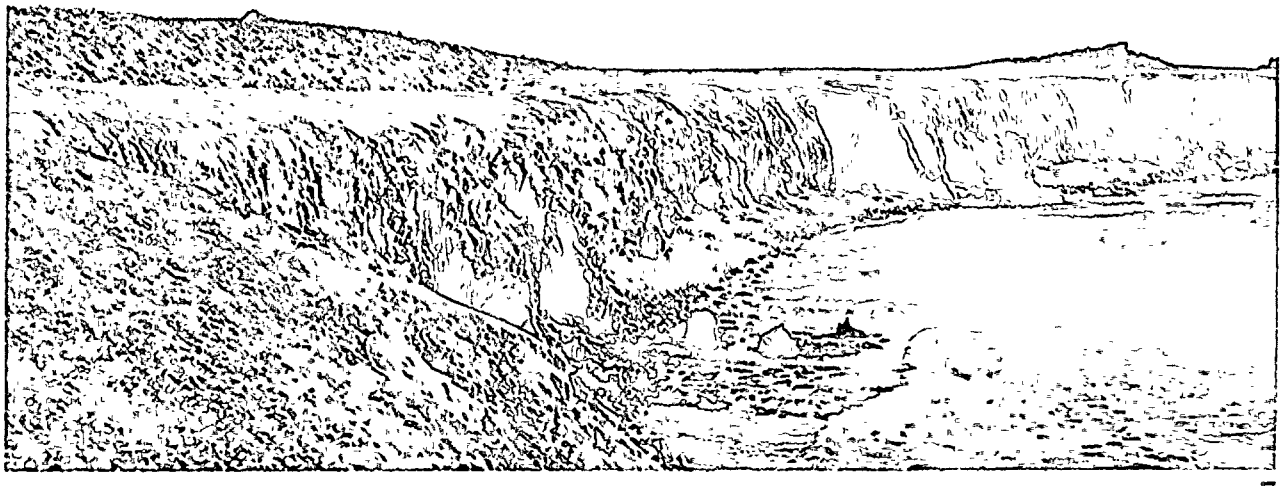

Plate 2. The seacliff and narrow beach along the easterly margin of Diablo Cove, as viewed in a southeastward direction. Exposed on the cliff are steeply-dipping strata of the Monterey formation, thinly and almost horizontally capped by Pleistocene terrace deposits. The break in slope and accompanying change in color along the top of the cliff mark the position of a wave-cut surface developed across the bedrock during Pleistocene time; this surface is overlain by the relatively dark-colored terrace deposits. Note the ribbed surface of the modern wave-cut bench approximately at sea level in center foreground.

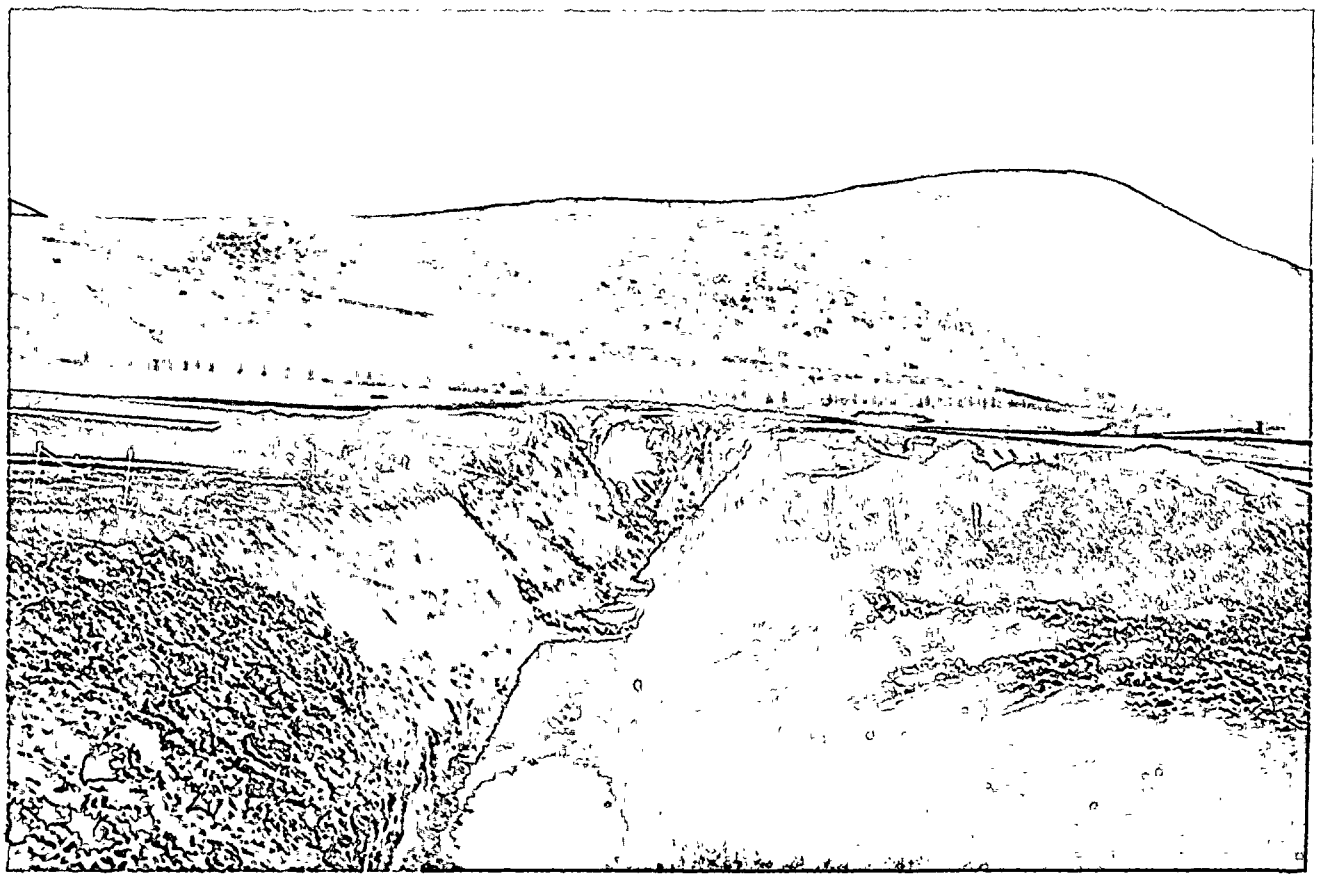

Plate 3. Trench C, looking eastward. The smoothly sloping main walls expose terrace deposits, and the underlying bedrock is continuously exposed along the low vertical walls near the bottom of the trench. Plate 9 shows relationships along the left-hand vertical wall in extreme foreground.

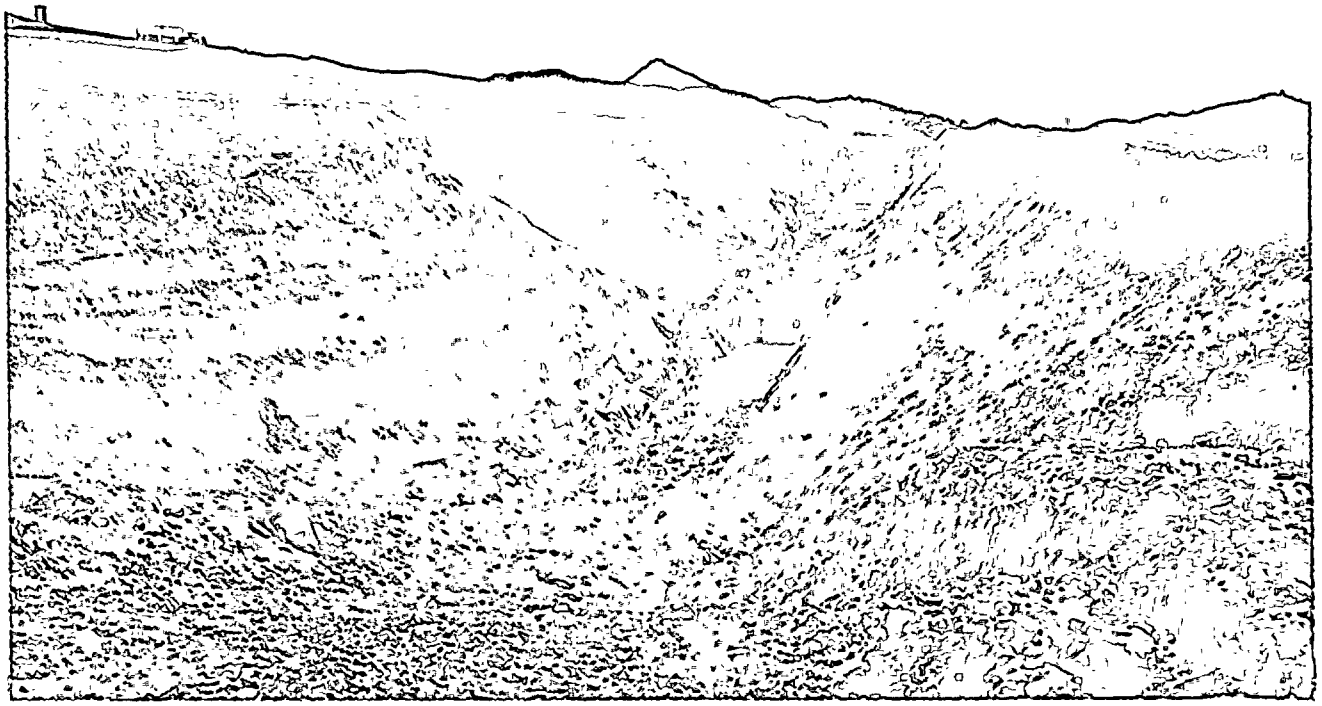

Plate 4. Trench B, looking southward across intersections with Trenches C and D. Here the terrace deposits are mainly alluvial-fan gravels, overlain by darker-colored slump, creep, and slope-wash debris. This nonmarine section is underlain by a much thinner section of Pleistocene marine deposits, which in turn rest upon bedrock near the bottom of the trench. Detailed relationships at the near left-hand corner of the trench intersection marked by standing water are shown in Plate 8.

Plate 5. Trench B, looking southeastward at intersections with Trenches C and D. Monterey sandstone is clearly recognizable beneath the thick cover of terrace deposits, and a prominent upward projection of massive, resistant sandstone can be seen along the left-hand wall of the trench in middle distance (ref. section along Trench B in Plate 1). Note how the contact between bedrock and overlying surficial deposits has been continuously exposed by hand-tool scaling of the trench walls.

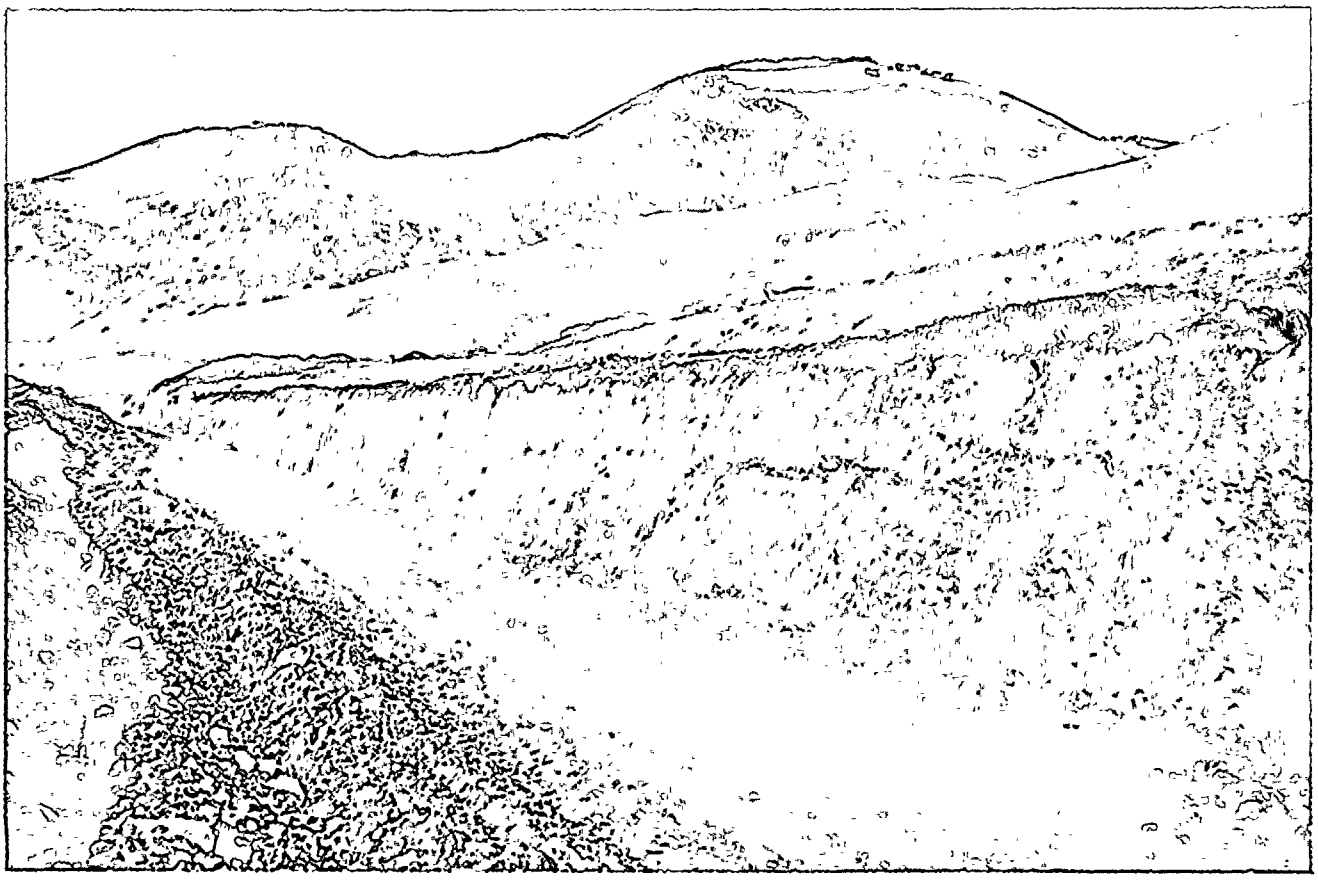

Plate 6. Northward view along Trench A, showing slightly undulatory contact between surficial deposits and underlying lighter-colored Monterey rocks.

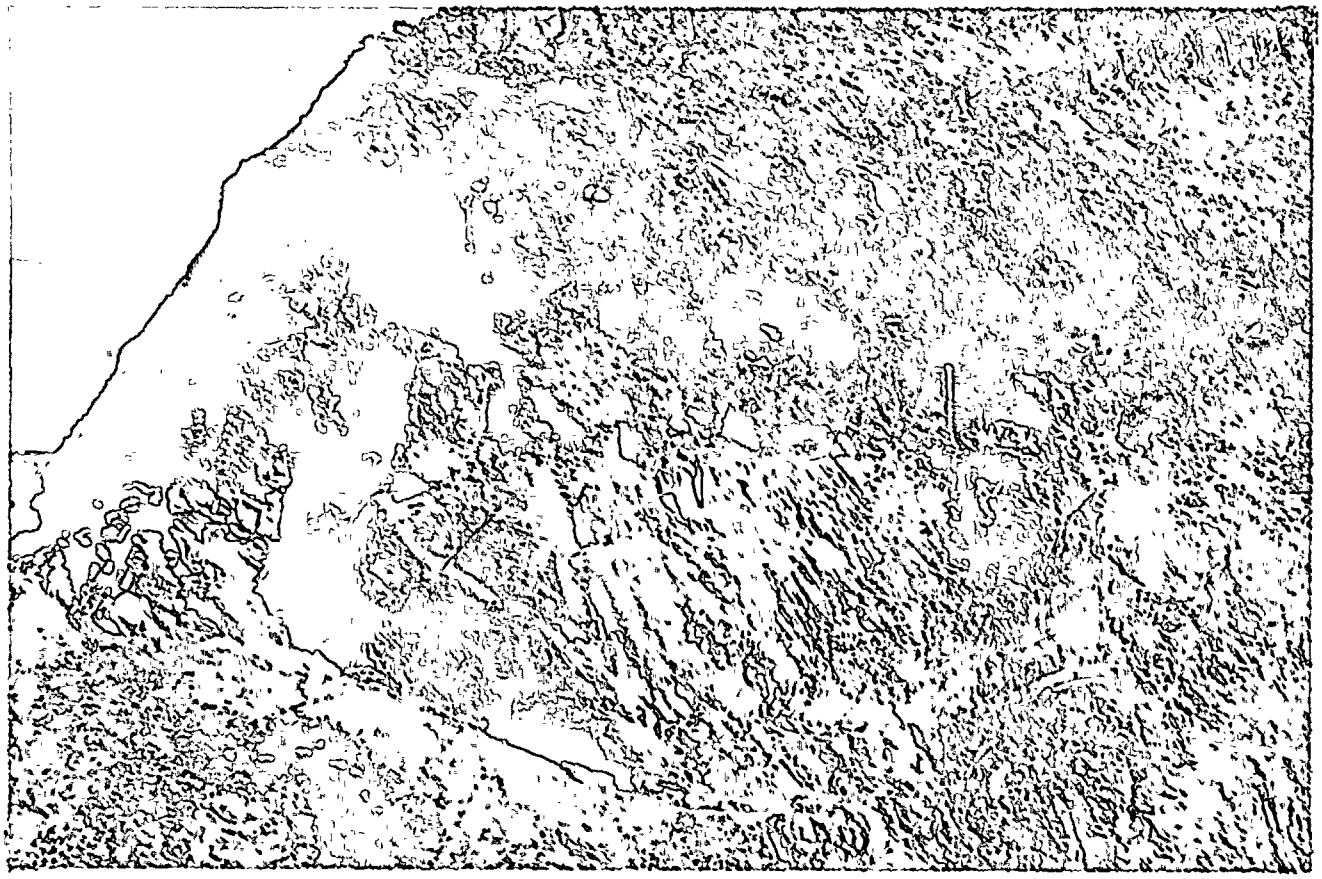

Plate 7. Typical sharp contact between Monterey sandstone and overlying marine terrace deposits of Pleistocene age, east wall of Trench A at intersection with Trench C. The nearly planar surface of the bedrock bench is interrupted by an abrupt protuberance (to right of knife) that marks the position of an unusually hard and resistant part of the sandstone.

Plate 8. Northeastward view of exposure at intersection of Trenches B and C. The whitish mass to left of the mattock head is a large fossil bone embedded in coarse-grained marine terrace deposits a few inches above their very gently sloping contact with Monterey sandstone (ref. section along Trench B, Plate 1; also Plate 4).

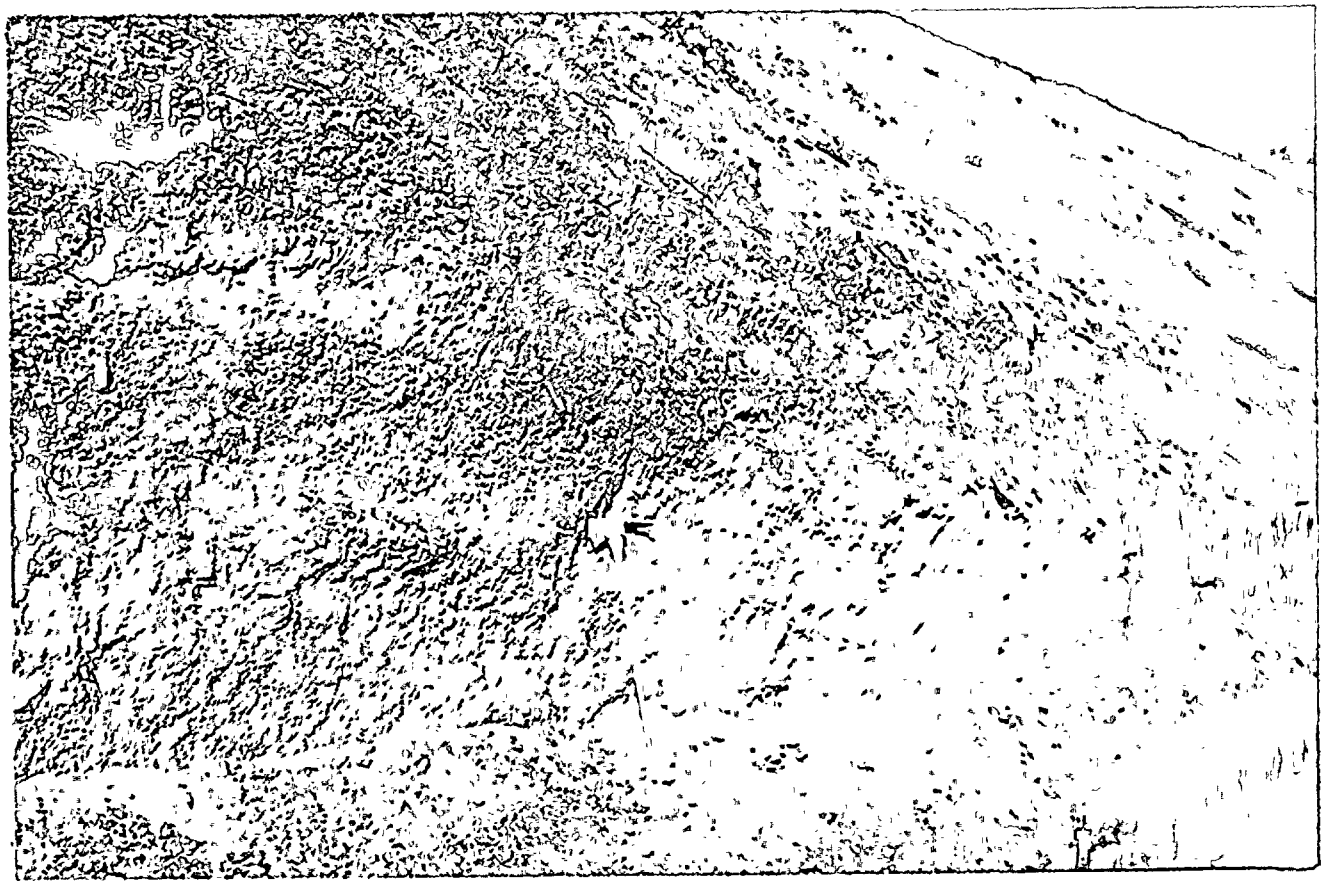

Plate 9. Northeastward view of exposure near the west end of Trench C (ref. Plate 3). Here a surface of Pleistocene erosion developed across Monterey strata (concealed beneath loose detritus in trench) is overlain by 3 to 5 feet of gravelly marine terrace deposits. At the top of these deposits is a soil horizon (dark-colored band at general level of mattock head), which in turn is overlain by nonmarine terrace deposits of alluvial-fan origin.

E. C. MARLIAVE
CONSULTING GEOLOGIST
4466 NORTH PARK DRIVE
SACRAMENTO 21, CALIF.
IVANHOE 9-4516

December 8, 1966

Mr. B. W. Shackelford
Chief Civil Engineer
Pacific Gas and Electric Company
245 Market Street
San Francisco, California

Subject: Nuclear Power Plant
Diablo Canyon Site

Dear Mr. Shackelford:

I have visited the subject plant area on three occasions and have spent a total of about six days in field examination of the area proposed for the reactor site, switchyard site, and transmission line immediately adjacent to the proposed plant site.

I have reviewed various reports and maps that are generally available on this area. I have also reviewed the geological reports of Mr. M. Micheli and Dr. Richard H. Jahns, and have also spent several days in the field with Mr. Micheli. I concur in their thinking concerning this site, and must say that I find it to be admirably suited to your purpose.

The site is located on a marine cut terrace, which is now covered with slope wash and alluvium overlying the consolidated rocks to depths of from a few feet to about 40 feet. The underlying consolidated rocks consist of fine-grained shale and sandstones and Obispo tuff and are of the Miocene Age. However, only shale and sandstones underlie the immediate plant area. These rocks have been folded and faulted to a considerable degree and are, therefore, sheared and broken, but are still firm and compact and capable of carrying any of the proposed loads.

We must always consider the matter of faulting, which is common to almost all of California's rocks, and particularly to those of the Coast Ranges. These rocks, which are on the order of 50 to 70 million years in age, have been frequently folded and, as a result, many bedding shears and small faults have been developed

over this period of time. These small faults do not indicate any recent or active faulting. Much of the shearing and faulting probably originated in the orogenic or mountain building movement that elevated this block of sediments from under the sea by slow folding and uplifting. It was not caused by sudden block faulting, but by slow deformation which produced minor shears and faults in the least resistant beds.

These rocks were probably principally folded and sheared millions of years ago, and during that time, have been elevated hundreds to thousands of feet above existing sea level. The marine cut terrace, presently 60 to 80 feet above sea level, has a small amount of marine deposition at the terrace surface, and later the slope wash and Recent alluvium have been deposited over the marine material.

The generally accepted estimate for the time of occurrence of wave cut terraces, such as are found in this area, is about 100,000 years ago.

The trenches excavated at the site have been thoroughly examined, and there is no evidence of faulting by cutting of any of the marine materials or the alluvium or slope wash. This shows, therefore, that there has been no fault movement in this area for at least 100,000 years. The period of any fault activity in this area might well be gauged in terms of millions of years.

There are no potential landslides that threaten the reactor site. Very small slide problems may exist in the switchyard area, but these can be minimized by appropriate slope stabilization and should be considered a negligible problem.

The area is generally seismically inactive, although it is expected that the area would be shaken severely once or twice in 100 years by activity on the San Andreas Fault, many miles to the east. This portion of the subject should be covered by the seismologists engaged in this study.

As a result of examining this site, I have the following conclusions:

1. The site is admirably suited to your purposes.

2. The proposed foundation materials are adequate to support any structure you propose to place upon it.

3. The possibility of fault rupture under this area is extremely remote.

4. The site may be shaken severely on possibly one or two occasions in 100 years.

5. The switchyard lies in the path of small potential landslides, but if suitable precautions are taken in design, the site can be adequately and properly developed to provide a suitable and safe area.

6. The ground to be occupied by the first few miles of the transmission line is geologically stable.

I, therefore, particularly believe that this site is geologically suitable, and an excellent one for your purposes.

Very truly yours,

E C Marliave

E. C. Marliave
Consulting Geologist

ECM:mem

Report Issued: January 25, 1966 Report No. 5326-65

Pacific Gas and Electric Company
Department of Engineering Research

DIABLO CANYON NUCLEAR PLANT SITE
PRELIMINARY GEOLOGIC INVESTIGATION

I. INTRODUCTION

This investigation was undertaken to explore the surface geology at Diablo Canyon, San Luis Obispo County, for a proposed nuclear plant site. The attached geologic maps and cross sections designated as DC-1, DC-2, DC-3, and DC-4, show the major geological and structural features of the area covered. A geologic description, photos, an earthquake & fault map of California, and conclusions and recommendations are also included in this report.

Although there is evidence of old and inactive faults in the area, the Diablo Canyon location appears geologically suitable for a Nuclear Generating Plant.

II. LOCATION AND ACCESSIBILITY

The Diablo Canyon area is located on the coast, approximately ten miles southwest of San Luis Obispo. Access to the area is via Highway 101 to Avila Beach and then via a rugged private dirt road, approximately one hour's ride. The proposed site is located near the mouth of Diablo Canyon, which is the only named topographic feature in the mapped area. The area is covered with low grazing grass (pasture) and can be easily traversed on foot.

It is proposed to locate the reactors, turbine generator, and related facilities on the terrace in the immediate vicinity of Diablo Cove on the south side of Diablo Creek, and to locate the switchyard in a widened section of Diablo Canyon about a quarter mile upstream from the mouth of the canyon.

III. GEOLOGY

The mapped area is underlain by sedimentary rocks, marine terrace deposits, and minor occurrence of basic intrusive rocks. The sedimentary rocks occur in the upper Miocene Point Sal Formation and lower Miocene Obispo Formation. The minor igneous rock, which instrudes the Point Sal Formation, is also Miocenic in age. These geologic units are best exposed in the sea cliffs along the ocean. Exposures are poor on the adjacent hillside. At the proposed plant site, the bedrock units are overlain by a shallow veneer of terrace deposits.

1. Tectonic

The major structural features of the area intercept the coast line almost at right angles and are readily seen in the cliffs around Diablo Cove.

The formations in the area of the reactor site appear to have been intensely folded in post-Miocene time. Numerous sheared and faulted areas in the Point Sal and Obispo Formations are visible in the near vertical sea cliffs. The faults are usually very small and only those of significance were mapped. The fault planes dip at various angles with small horizontal and vertical displacements, at times measurable in the order of one to three feet. All the mapped faults appear to be old and inactive and of the fold-fault type, originated by a close-folding movement. The folding thrusts are considered a combination of uplifting and subsequent lateral movements in a probable south-north direction. The occurrence of this type of tectonic movement in the area was probably contemporaneous with the Pilocene orogenic movements of the West Coast.

2. Point Sal Formation

The Point Sal Formation overlies the Obispo Formation and is overlain in part by marine terrace deposits. The major rock types are dark gray and light brown silty and clay shale and mudstones, light-colored tuff and limestone. Occasional nodules and thin beds of black chert and thin beds of fine-grained sandstone are present. These various rock types are clearly exposed in the sea cliff to the west and east of Diablo Canyon. On the hillside to the northeast only outcrops of hard shale and limestone are visible. The various members are well bedded and fairly hard. The predominant rock type is shale which is exposed in the sea cliffs in alternating beds of nearly uniform thickness, varying from very hard, firm and sparsely fractured, to weak and minutely fractured, and crushed at times. The apparent strike of the bedding planes is in a general east-west direction, with local variations due to folding. The beds dip at a high angle, almost vertical at times, where exposed in the sea cliffs. Some unrecognizable microfossils including fish bones microfragments, supposedly abundant in this formation, were detected in hand specimen and in one thin section.

3. Obispo Formation

The Obispo Formation crops out along the coast, south of the plant site and underlies the Point Sal Formation. The major rock types in the formation are light colored, buff and gray tuff, and black shale. Black chert interbeds are present in minor amounts.

The tuff, which is the predominant rock type, is generally hard. White when fresh, it weathers to an orange-brown color that makes it clearly distinguishable in outcrop. The tuff seems to be basically vitric with presence of crystal fragments. Different types of hard, welded tuff are also present. The black shale, generally well-indurated, seems to be more abundant in the outcrops west of Diablo Canyon.

Both the tuff and the shale have undergone some degree of crystallization which, at times, renders the shale very hard. These rocks have been subjected to extensive folding movements and like the Point Sal Formation vary from extensively to moderately fractured. The tuff and the shale are generally well-bedded and trend east-west with a high angle of dip. When the tuff predominates, the shale occurs as interbedded streaks and lenses.

The contact with the overlying Point Sal Formation is clearly distinguishable along the ocean front. The two formations appears to be in fault contact along a surface roughly paralleling the coast. The fault contact probably lies approximately along the dotted contact line shown on drawing DC-1, but its exact location and extent, if it exists, cannot be determined by surface examination.

4. Terrace Deposits

Terrace deposits overlie more than half of the mapped area. Although mapped as a single unit, they include marine deposits, non-marine talus and slope wash. The deposits range in thickness from a few feet to 30 or perhaps 40 feet at the base of the hill to the northeast. Slope wash and talus material from the nearby hills account for some of the greater thickness near the hills. Over most of the area, these sediments occur as a black adobe-like material that contain occasional fragments of rocks of the Point Sal Formation.

Morphologically, this area appears to be a cut terrace. The gentle slope might also indicate a slow rise of the land from the sea with contemporary marine sedimentation.

Typical marine terrace deposits overlying the Obispo Formation are visible only in a few small and localized parts of the mapped area. They contain essentially flat lying, crudely stratified thin beds of small pebbles alternating with thicker beds of sandy and silty material containing some small rock fragments. Outside the mapped area, especially west of Diablo Canyon these stratified marine terrace deposits are clearly and continuously exposed along the sea cliff. They were thoroughly explored, but no sign of any fault movement was detected. Any minor displacement (due to faulting) in these stratified deposits, if present, would have been easily observed. In the immediate vicinity of the proposed reactor site the fields have been cultivated and surface features have been obliterated.

5. Igneous Intrusive

A small intrusive body crops out to the east of Diablo Canyon. The rock which is highly weathered appears to have relict granitic texture.

6. Landslides

On the south facing hillside, immediately above the reactor site, bedding planes of the Point Sal Formation dip into the hill. This situation is very favorable to avoidance of slides, and no sliding is to be anticipated in this area.

Several old slides were noted on the north facing slope of Diablo Canyon in an area beginning approximately 1000 ft. upstream from the mouth. The slides appear to be partially stabilized and there is no evidence of any particularly recent movement. The cross sections shown on Drawing DC-4 indicate the general dips found near the crest and on the south side of the hill, but some surface visual indications would suggest that the dips might be somewhat flatter. These hillsides can be so treated that they will not threaten the proposed switchyard.

This section of Diablo Canyon appears to be the only feasible location for the switchyard, but certain precautions should be observed in design and construction. Sizeable hill cuts should be avoided. Whatever level land is required for the switchyard should be created by filling with provisions for drainage. Considering the area between Sections C-C and E-E, drawing DC-4, an area approximately 1000 feet square, could be made with a fill extending across Diablo Canyon whose maximum height would not exceed 80 or 90 feet. Such a fill, if desired, could be used as a dam to store water on Diablo Creek.

IV. SEISMICITY

This area has not been the source of any strong earthquakes. See enclosed map from Bulletin No. 116-2, by the Department of Water Resources.

V. EXPLORATORY TRENCHING

On the enclosed aerial photo, the terrace deposits, overlying the fault immediately west of Diablo Canyon, showed indications that might have been suggestive of recent faulting.

To clarify these conditions, only partly visible on the ground, two exploratory trenches were excavated transversally to the projection of the fault line. These trenches were so located that any faulting in the terrace material, if it existed, was certain to be intercepted.

The first trench was excavated approximately 100 feet north of the sea cliff. The trench was dug to an average depth of 4-1/2 to 5 feet with a maximum of 11 feet at one point. Exposed in the trench was a black, organic, clayey, adobe-like material that grades uniformly downward into a gray-greenish type of fat clay.

The second trench was located north of the first, approximately 400 feet from the sea. It was excavated to an average depth of 4-1/2 to 5 feet with a maximum of 9 feet. The trench was in black, silty, organic, partly clayey, adobe-like material which directly overlies the westerly sloping surface of the Point Sal Formation. No sign of any fault movement in the terrace deposits was detected in either trench.

VI. RECOMMENDATIONS

In the event that this site is to be used, and layout and design work is to proceed, a seismic investigation in combination with a drilling and trenching program should be carried out. These investigations will determine the thickness of the terrace deposits and the extent and location of contacts, faults, and sheared zones in the older rocks.

Approximately five or six continous core bore holes should be drilled in the area of the reactor site to an approximate depth of 60 to 70 feet. Additional holes may be required. Some underwater geologic mapping in the immediate vicinity of the coast line should be done for planning of offshore construction.

VII. CONCLUSIONS

There are no apparent geological conditions which would preclude the construction of a nuclear reactor at this site.

No slide problems are anticipated at the reactor site. There are minor faults present in the older rocks that appear to be old and inactive. No evidence of faulting was detected on the hillsides or in the recent terrace deposits. While moderate seismic shaking may be anticipated, rupture is not to be expected.

Massimo Micheli

M. Micheli, Geologist

W.O. 21935

Distribution: FFMautz

Encl. Cross Sections 2 Sheets
Geologic Maps 2 Sheets
Earthquake & Fault Map
Photos 5 Sheets

sd

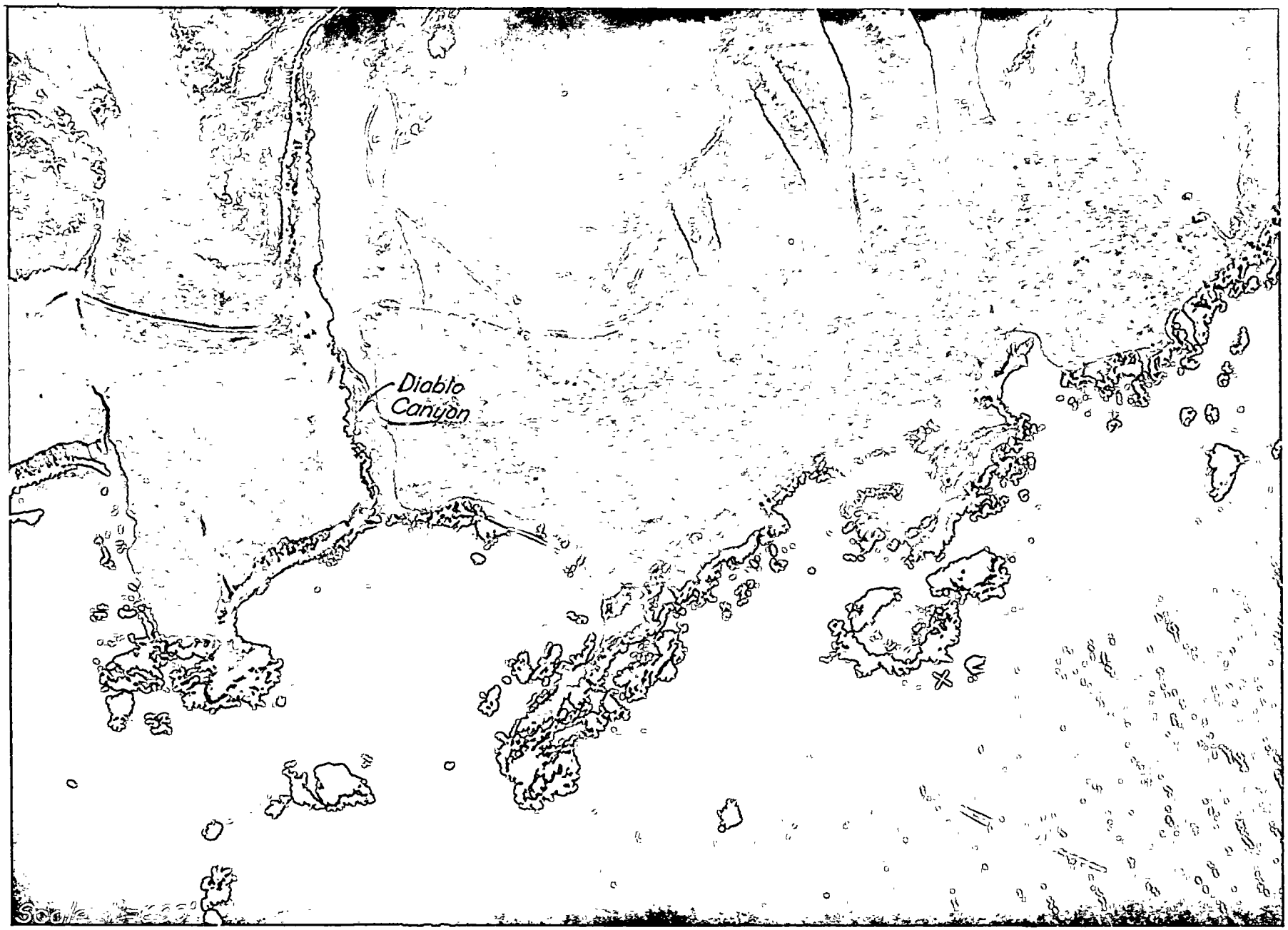
Diablo
Canyon

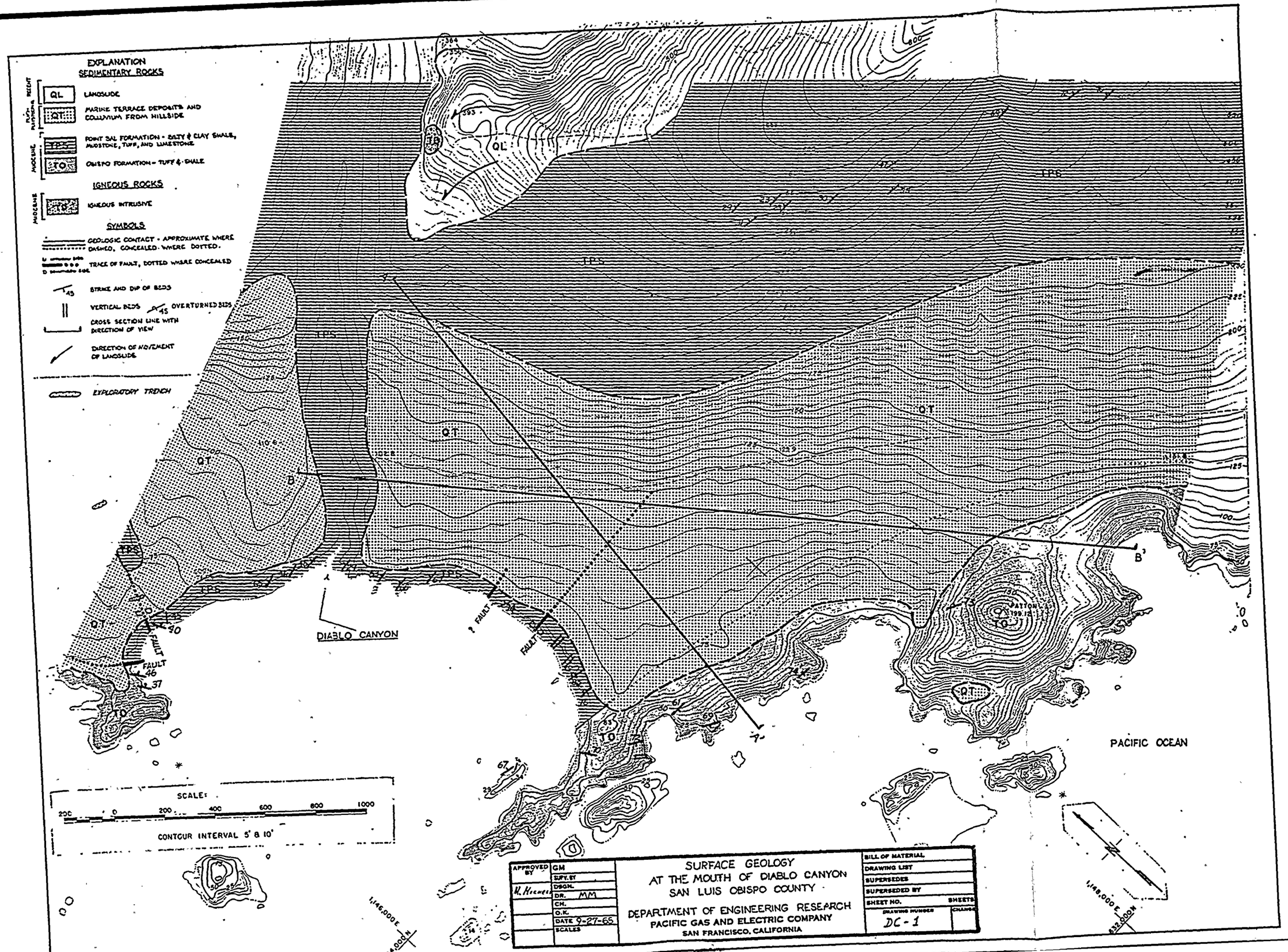
EXPLANATION
SEDIMENTARY ROCKS
RECENT
QL LANDSLIDE
PLEISTOCENE
QT MARINE TERRACE DEPOSITS AND COLLUVIUM FROM HILLSIDE
MIOCENE
TPS POINT SAL FORMATION - SALTY & CLAY SHALE, MUDSTONE, TUFF, AND LIMESTONE
TO OBISPO FORMATION - TUFF & SHALE
IGNEOUS ROCKS
MIOCENE
TD IGNEOUS INTRUSIVE
SYMBOLS
GEOLOGIC CONTACT - APPROXIMATE WHERE DASHED, CONCEALED WHERE DOTTED.
TRACE OF FAULT, DOTTED WHERE CONCEALED
STRIKE AND DIP OF BEDS
VERTICAL BEDS
OVERTURNED BEDS
CROSS SECTION LINE WITH DIRECTION OF VIEW
DIRECTION OF MOVEMENT OF LANDSLIDE
EXPLORATORY TRENCH
DIABLO CANYON
FAULT
PACIFIC OCEAN
PATTON
SCALE:
200 0 200 400 600 800 1000
CONTOUR INTERVAL 5' & 10'
1,146,000 E
634,000 N
1,148,000 E
632,000 N
APPROVED BY
GM
SUPV. BY
DSGN.
DR. MM
CH.
O.K.
DATE 9-27-65
SCALES
SURFACE GEOLOGY
AT THE MOUTH OF DIABLO CANYON
SAN LUIS OBISPO COUNTY
DEPARTMENT OF ENGINEERING RESEARCH
PACIFIC GAS AND ELECTRIC COMPANY
SAN FRANCISCO, CALIFORNIA
BILL OF MATERIAL
DRAWING LIST
SUPERSEDES
SUPERSEDED BY
SHEET NO.
SHEETS
DRAWING NUMBER
DC-1
CHANGE

APPROVED BY	GM
	SPECN. BY
	DSGN. N.M.
M. Nicolau	DR. N.M.
	CH.
	O.K.
	DATE
	SCALE

Surface Geology - Switch Yard Area
Diablo Canyon Nuclear Plant Site
San Luis Obispo County

DEPARTMENT OF ENGINEERING RESEARCH
PACIFIC GAS AND ELECTRIC COMPANY
SAN FRANCISCO, CALIFORNIA

BILL OF MATERIAL	
DRAWING LIST	
SUPERSEDES	
SUPERSEDED BY	
SHEET NO.	SHEETS
DRAWING NUMBER DC-3	CHANGE

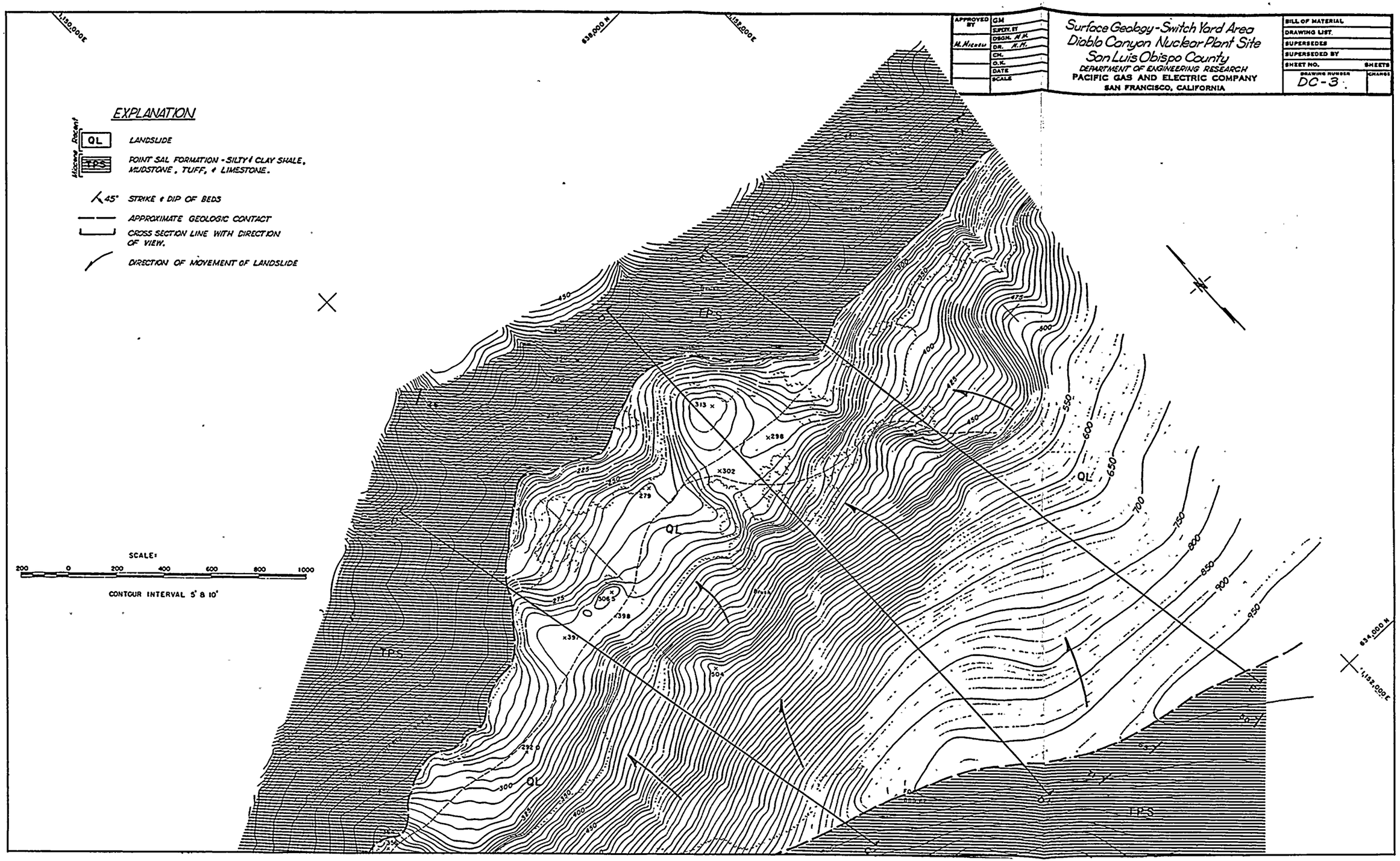

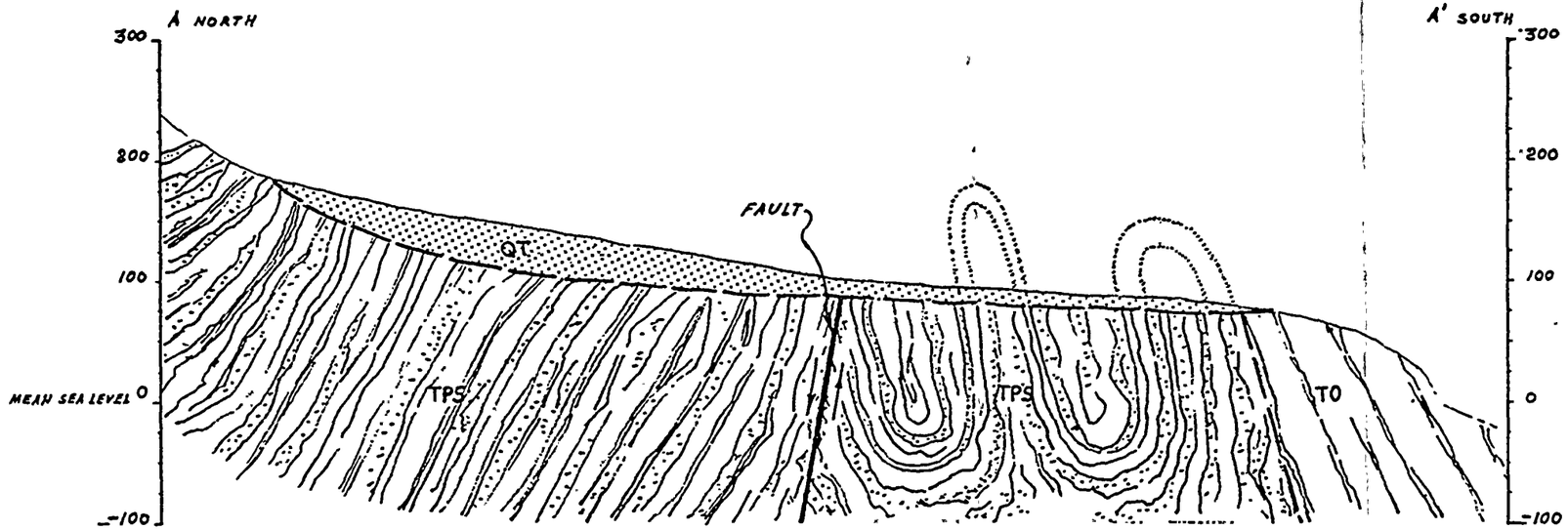

EXPLANATION

QT - TERRACE DEPOSITS

TPS - POINT SAL FORMATION

TO - OBISPO FORMATION

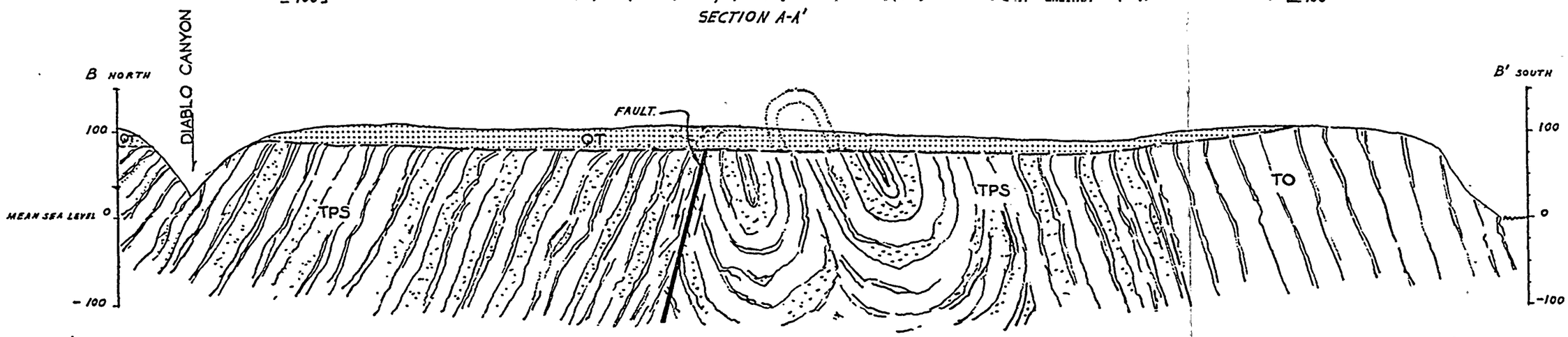

NO.	DATE	DESCRIPTION	GM	BY	CH	APPD.

TABLE OF CHANGES

APPROVED BY	GM
	SUPV. BY
	DSGN.
R. Liebel	DR. REL
	CH.
	O.K. MM
	DATE 7-31-65
	SCALES HORIZONTAL: 1" = 200' VERTICAL: 1" = 100'

GEOLOGIC SECTIONS
DIABLO CANYON NUCLEAR PLANT SITE
SAN LUIS OBISPO COUNTY, CALIFORNIA

DEPARTMENT OF ENGINEERING RESEARCH
PACIFIC GAS AND ELECTRIC COMPANY
SAN FRANCISCO, CALIFORNIA

BILL OF MATERIAL	
DRAWING LIST	
SUPERSEDES	
SUPERSEDED BY	
SHEET NO.	SHEETS
DRAWING NUMBER DC-2	CHANGE

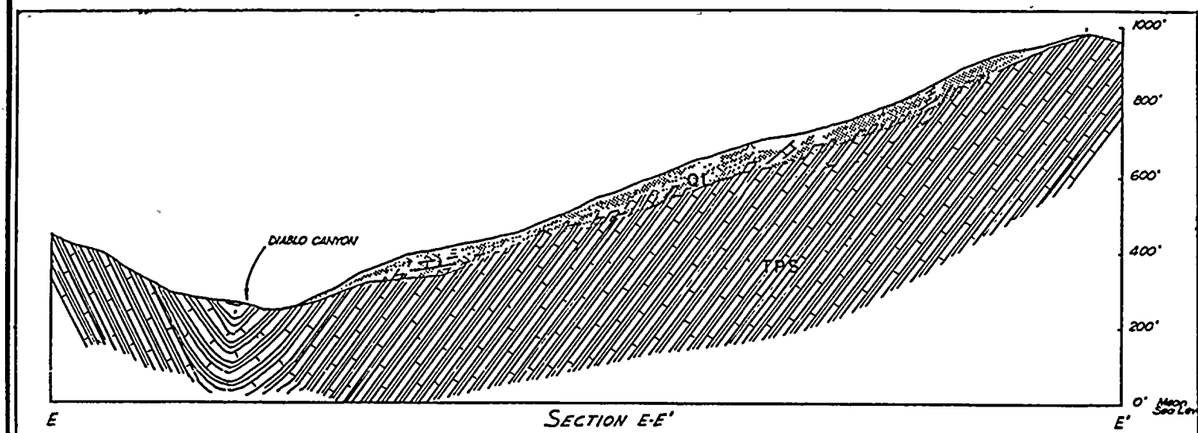

SECTION E-E'

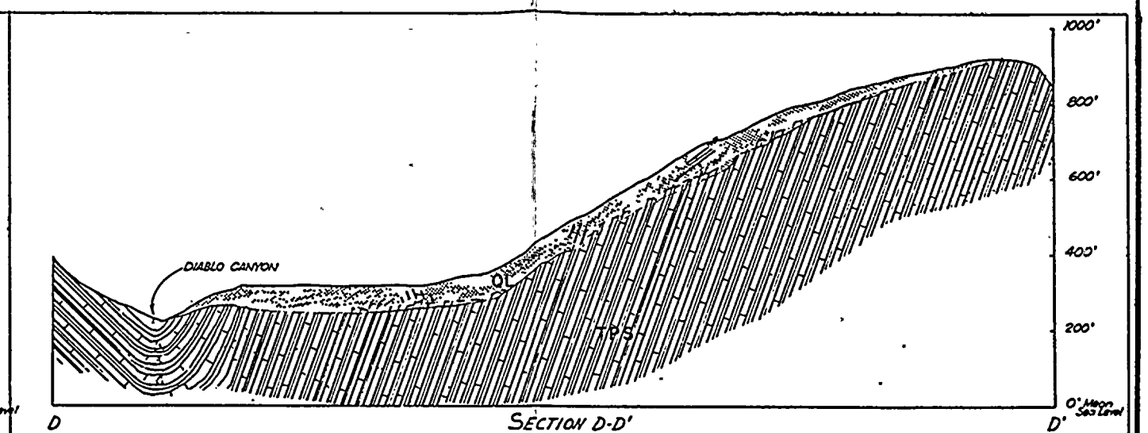

SECTION D-D'

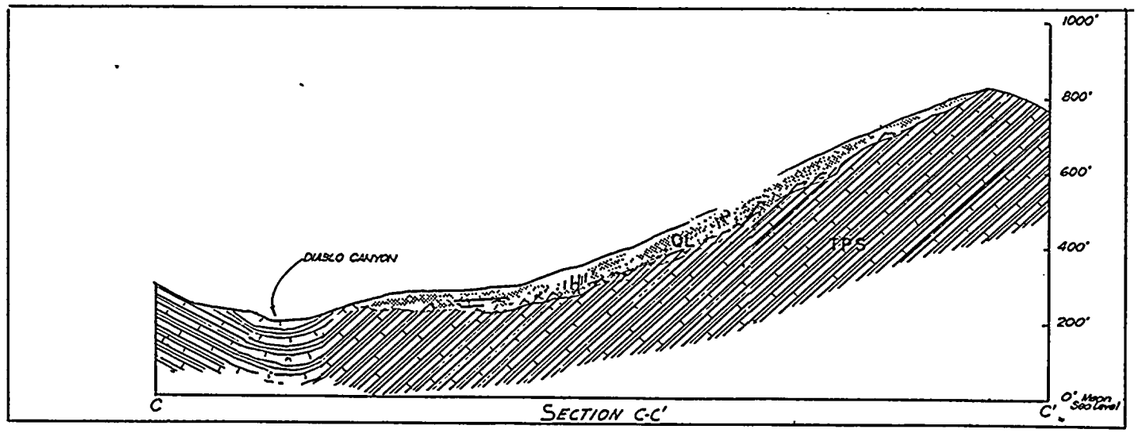

SECTION C-C'

EXPLANATION

TPS — POINT SAL FORMATION

OL — LANDSLIDE

0 100' 200' 400'
SCALE

APPROVED BY	GM	Geologic Section - Switch Yard Area Diablo Canyon Nuclear Plant Site San Luis Obispo County DEPARTMENT OF ENGINEERING RESEARCH PACIFIC GAS AND ELECTRIC COMPANY SAN FRANCISCO, CALIFORNIA	BILL OF MATERIAL
	SUPV. BY		DRAWING LIST
M. Mikola	DSGN. M.M.		SUPERSEDES
	DR. T. Bosko		SUPERSEDED BY
	CH.		SHEET NO. / SHEETS
	O.K.		DRAWING NUMBER / CHANGE
	DATE 12-6-65		DC-4
	SCALES As Shown		

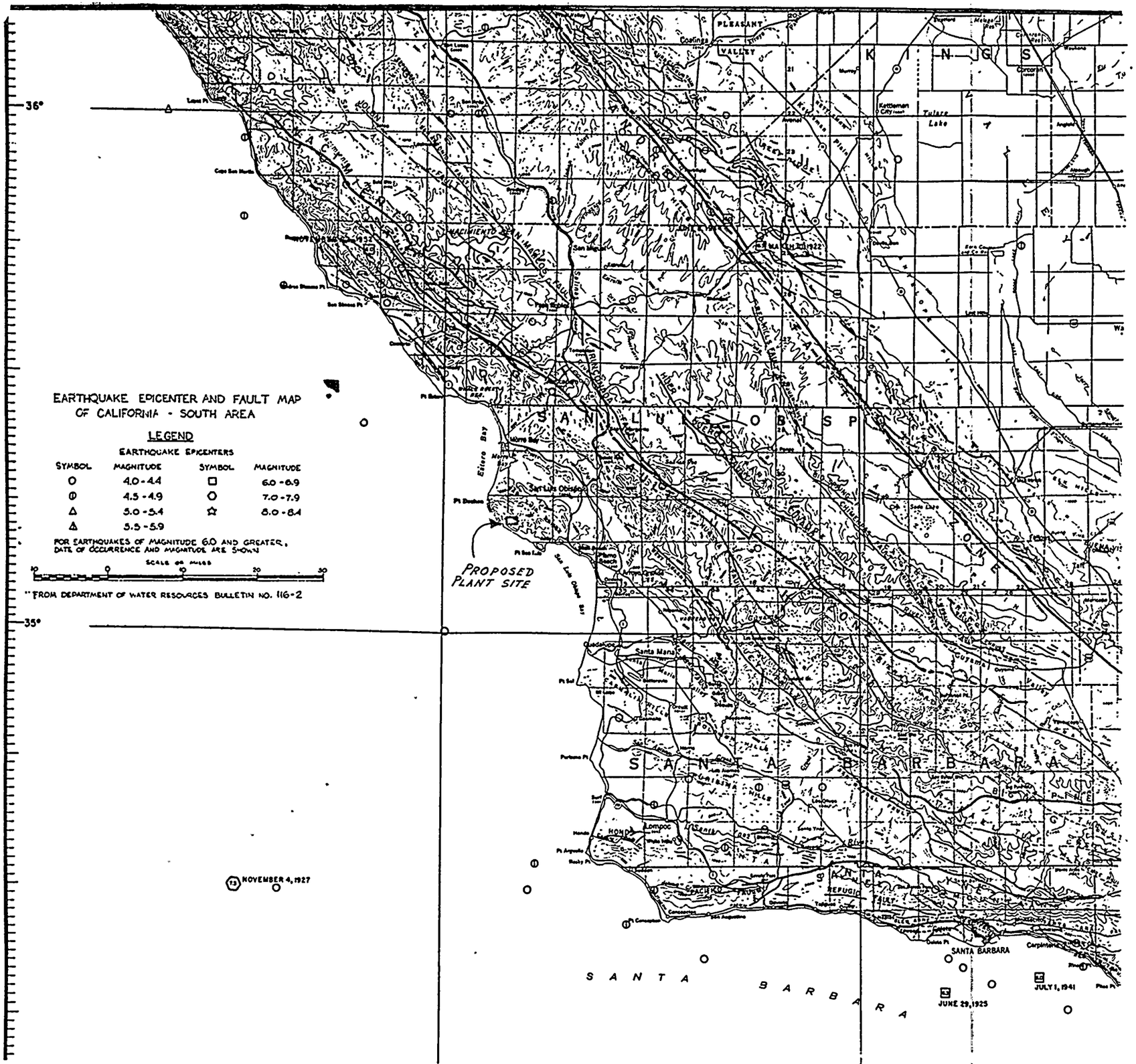
EARTHQUAKE EPICENTER AND FAULT MAP
OF CALIFORNIA - SOUTH AREA
LEGEND
EARTHQUAKE EPICENTERS
SYMBOL MAGNITUDE SYMBOL MAGNITUDE
4.0 - 4.4
4.5 - 4.9
5.0 - 5.4
5.5 - 5.9
6.0 - 6.9
7.0 - 7.9
8.0 - 8.4
FOR EARTHQUAKES OF MAGNITUDE 6.0 AND GREATER, DATE OF OCCURRENCE AND MAGNITUDE ARE SHOWN
SCALE OF MILES
10 0 10 20 30
"FROM DEPARTMENT OF WATER RESOURCES BULLETIN NO. 116-2
36°
35°
PROPOSED PLANT SITE
NOVEMBER 4, 1927
JUNE 29, 1925
JULY 1, 1941
SANTA BARBARA
SANTA BARBARA
SAN LUIS OBISPO
KINGS
PLEASANT VALLEY
Tulare Lake
Kettleman City
Estero Bay
San Luis Obispo Bay
Morro Bay
Santa Maria
Lompoc
HOPE
REFUGIO FAULT
Cuyama
Carpinteria

FAULT ZONE IN POINT SAL FORMATION EXPOSED IN SEA CLIFF EAST OF DIABLO CANYON. NOTE CHANGE IN ATTITUDE OF BEDS ON EITHER SIDE OF FAULT AND CRUMPLED BEDS IN FAULT ZONE. HAMMER IN CENTER OF PHOTO FOR SCALE.

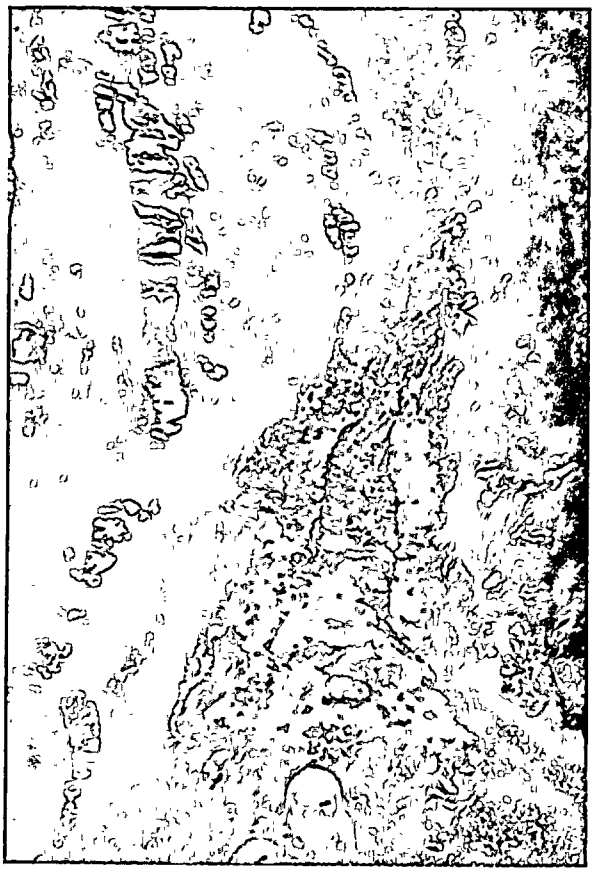

SMALL SHEAR ZONE IN POINT SAL FORMATION EXPOSED ALONG SEA CLIFF EAST OF DIABLO CANYON.

CLOSE-UP OF MASSIVE MUDSTONE AND THINLY-LAMINATED SHALE INTERBED, IN POINT SAL FORMATION. SEA CLIFF EAST OF DIABLO CANYON.

BEDS OF TUFF AND SHALE IN OBISPO FORMATION OFFSET BY SMALL LOCAL FAULT WEST OF DIABLO CANYON.

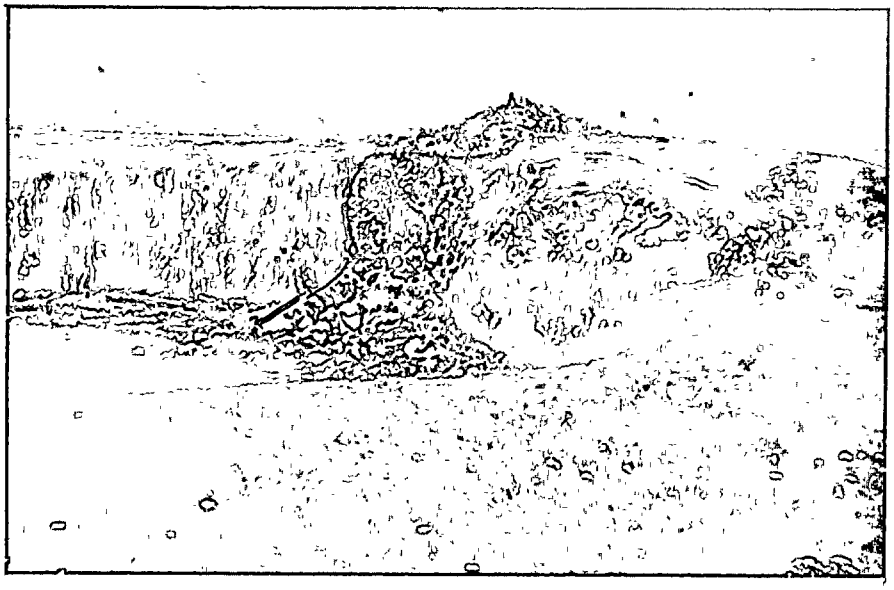

CONTACT (MARKED IN BLACK) BETWEEN POINT SAL FORMATION (LEFT) AND OLDER OBISPO FORMATION. SEA CLIFF EAST OF DIABLO CANYON.

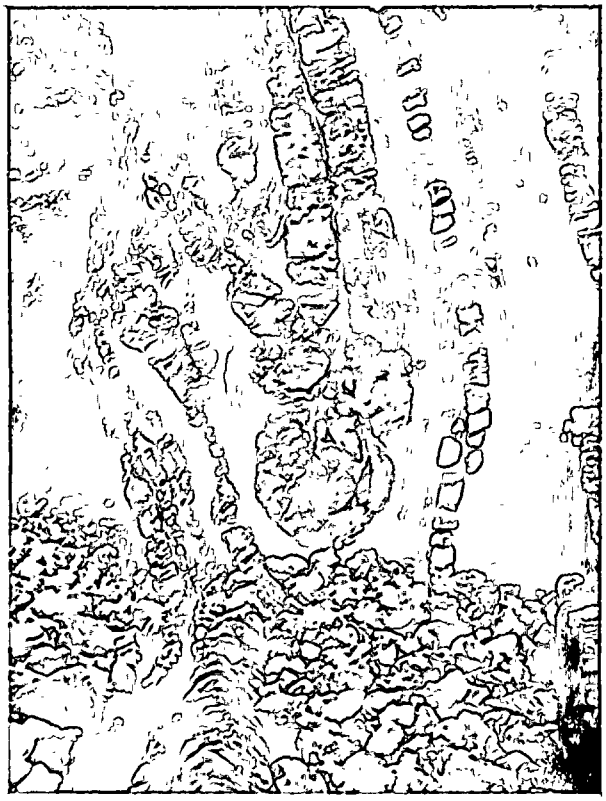

TIGHT SYNCLINAL FOLD IN POINT
SAL FORMATION.
SEA CLIFF EAST OF DIABLO CANYON.

GENTLE FOLD IN POINT SAL FORMATION.
SEA CLIFF EAST OF DIABLO CANYON.

January 9, 1967

Mr. Gordon V. Richards
Pacific Gas and Electric Company
245 Market Street
San Francisco, California 94106

Dear Mr. Richards:

Enclosed is the text for a report entitled, "Seismic evaluation of the Diablo Canyon site," written by Hugo Benioff and myself. The report is complete except for a portion of the Earthquake and Epicenter Fault map, which I understand is being reproduced at your facility.

Sincerely yours,

Stewart W. Smith

Stewart W. Smith
220 N. San Rafael
Pasadena, California 91105

SWS:vg

Encls.

SEISMIC EVALUATION OF THE DIABLO CANYON SITE

Hugo Benioff and Stewart Smith

Objectives

The objectives of this report are: 1) to provide a historical summary of earthquake activity in the immediate vicinity of the reactor site and in adjacent areas where an earthquake might be expected to produce secondary effects within the site area, and 2) to provide an estimate of the "size" of earthquakes that can be expected to occur in these regions during the lifetime of the reactor.

The results that such earthquakes may be expected to produce in the site area due to shaking or seismic sea waves will be treated in separate reports by others.

Methods

Historical and instrumental records of seismic activity in a region are important for the prediction of future occurrences of earthquakes in that region. The distribution of number of earthquakes versus their magnitude provides one convenient way of summarizing the seismic activity of a region. Use of such data, however, can produce misleading results if the region considered is too small or if the data cover too short a span of time. In particular, extrapolations from data on small earthquakes to predict the occurrence of larger ones are unreliable. To avoid some of these problems, and provide an estimate of the largest possible earthquakes that can be expected, we have used the following approach. On faults where there is seismic activity and evidence of large earthquakes in the past, we assume that the largest of such events will recur in the near future. On faults where there is no evidence of major seismic activity in the historic record, we assume that a large earthquake, although unlikely, cannot be ruled out.

In the case of such a fault, two methods can be used to estimate the maximum "size" earthquake that can occur, the known behavior of other faults of similar dimensions and the observations of the maximum aftershock that might be induced on a minor fault due to a great earthquake on a nearby major fault.

In this report the terms fault, or fault system, are applied to discontinuities in the earth along which regional or large-scale stresses are relieved in connection with the occurrence of earthquakes. Discontinuities due to the folding of sedimentary rocks, gravity sliding, or other local effects are not pertinent to the seismic evaluation of the site.

Earthquake Size

The size of an earthquake can be described by its magnitude on the Gutenberg-Richter scale, total energy, maximum acceleration, frequency spectrum, fault length and slip, region of severe shaking, duration of shaking, stress drop or strain release. Although magnitude is the most common way of classifying earthquakes, it is not necessarily the best measure of those earthquake characteristics, such as the frequency spectrum, which are most important for engineering purposes. This is true because the magnitude measurement is essentially an estimate of the seismic energy at only a single frequency. No means are available for predicting the effect of a magnitude change on the over-all frequency spectrum. For this reason the "design" earthquake described in this report will be given in terms of those parameters which are most closely related to the frequency spectrum; they are fault length, depth, slip, and duration of strong shaking.

Seismicity

During the time covered by available historic records, seismic activity

within about 20 miles of the Diablo Canyon site has been very low. In the "Catalog of California Earthquakes" by H. O. Wood,[1/] only one earthquake is listed as having caused damage within this area. This was a shock in 1830 which damaged a church in San Luis Obispo. Since no other damage is reported, this earthquake was probably quite small. The Earthquake and Epicenter Fault Map prepared by the Department of Water Resources, State of California,[2/] a portion of which is appended to this report, shows several small shocks of magnitude 4 to 4.4 with epicenters distant about 20 miles from the site. On November 4, 1927 a fairly large earthquake, listed by Gutenberg and Richter[3/] with a magnitude of 7.3, occurred off the coast some 60 miles southwest of the site, presumably on the western extension of the east-west trending fault system which includes the Santa Ynez Fault on land and the source of the June 29, 1925 (magnitude 6.3) and July 1, 1941 (magnitude 6.1) Santa Barbara earthquakes offshore.

The nearest seismically significant fault system to the site, the Nacimiento Fault, is some 20 miles distant. The largest earthquake known to have been associated with this fault occurred on November 22, 1952 at an epicentral distance to the site of about 44 miles. It is listed with a magnitude of 6.0. Although the activity of the Nacimiento fault system has thus been very low during the past century and a half, we have no means as yet of determining the character of its behavior pattern, and consequently, it must be assumed that an earthquake of significant size may have its origin on

---

1/ Bulletin Seismological Society of American, Vol. VI, pages 1 - 180, 1916

2/ Dept. of Water Resources Bulletin No. 116-2, Crustal Strain and Fault Movement Investigation, January, 1964.

3/ Seismicity of the Earth, Princeton University Press, Princeton, N.J., 1949

this fault during the life of the reactor. Considering the length of the fault system -- about 120 miles -- and the behavior of other similar minor faults in California and Nevada, the largest earthquake which can be expected to be generated on this fault would be similar to the 1952 Tehachapi or the 1954 Fairview Peak earthquakes. Thus it would have a fault displacement of 3 to 10 feet at its maximum point, a break of about 60 miles in length and a duration of about 10 seconds. This corresponds to a shock of about 7-1/4 magnitude on the Gutenberg-Richter scale. However, since for earthquakes greater than about 6.5 the magnitude scale is indeterminate within ± 1/2 magnitude, and as previously noted the physical effects are not necessarily predictable from the magnitude, we prefer to specify the estimated fault slip, length of break and duration of strong shaking rather than to specify a particular magnitude.

At its closest point the San Andreas fault passes some 48 miles from the site. This point is also the approximate northern terminus of the 1857 earthquake break. The 150-mile-long segment extending from here north to San Juan Bautista has had no major slip since the advent of the white man. Two small shocks, March 10, 1922, magnitude 6.5, and June 8, 1934, magnitude 6, occurred on this segment. The most recent significant earthquake in this region was the June 28, 1966, event at Cholame of magnitude about 5.4 which produced several inches of fault displacement. None of these events was large enough to relieve any significant amount of strain. Since the strain on this segment has been accumulating for more than 150 years, it is very likely greater on this segment than on any other, and consequently this is the segment most likely to be involved in the next great earthquake on the

San Andreas fault. Therefore, we must assume that during its life the reactor will be subjected to an earthquake due to movement on the San Andreas fault similar to the movement that occurred in 1857 and 1906. In these shocks the maximum fault offset was about 20 feet in the horizontal direction and 3 feet in the vertical direction. The fault break was about 200 miles long and the duration of strong shaking was about 40 seconds.

An earthquake of this size can be expected to produce numerous aftershocks on adjacent faults ranging in size up to about one magnitude less than the principal shock. Thus such a maximum aftershock could occur on the Nacimiento fault system and thus account for the maximum shock considered in the previous paragraph for this fault. Should a great earthquake occur on the San Andreas fault there might be a wide distribution of aftershocks extending out to distances of about 50 miles from the San Andreas fault. These aftershocks may occur either on or away from existing fault systems. Those occurring on existing fault systems could have magnitudes ranging up to about 7-1/2 and could produce surface faulting along existing faults. Those occurring away from existing faults would have magnitudes ranging up to about 6-3/4. The probability that these particular aftershocks would produce new surface faults where none now exist is extremely remote. Experience with California and Nevada earthquakes indicates that such aftershocks not associated with existing fault systems will be restricted to depths of about 6 miles or more. Thus, in the event of a great earthquake on the San Andreas fault, large aftershocks may occur anywhere within about 50 miles of the San Andreas fault, but those which are not located on existing faults would be restricted to depths of about 6 miles or more and magnitudes of about 6-3/4 or less.

Offshore Earthquakes

The seaward extension of the Santa Ynez fault is the closest significant fault system that may be responsible for large offshore earthquakes. Using earthquake epicenters and submarine topography to determine the western limit of this fault, the maximum offshore fault length is found to be about 80 miles. This fault's point of closest approach to the site is fifty miles. Using the methods previously described, we estimate that an 80 mile fault break with a horizontal slip of 10 feet could occur offshore on this system, producing an earthquake of magnitude 7-1/2.

The offshore extension of the San Andreas fault northwest of Cape Mendocino, although a distance of more than 420 miles from the site, may have to be considered for possible seismic sea wave generation. There are two distinct concentrations of offshore seismic activity in this region: One zone trends northwesterly along an extension of the San Andreas fault and the other trends east-west along the Gorda Escarpment. Using earthquake epicenters to estimate the length of the fault system that is active, we estimate that a 100 mile fault with horizontal offsets of about 10 feet could occur on the northwesterly extension of the San Andreas fault equivalent to a magnitude 7-1/2 earthquake. The largest offshore earthquake recorded in this region was a magnitude 7.3 event of 1 February 1922. There were no reports of a seismic seawave due to the earthquake.

The activity on the Gorda Escarpment appears to be limited to magnitudes of about 6.0 and below; however, the zone of activity is large enough to support a 40 mile fault break with offsets of about 5 feet equivalent to a magnitude 7 earthquake. In view of the submarine topography in this region,

it is possible that the offset for such an earthquake could be in the vertical direction.

The possible generation of seismic sea waves by such earthquakes and the resulting effects at the reactor site will be treated in a separate report by others.

Summary and Conclusions

The maximum size earthquakes that can be expected to occur during the life of the reactor are listed below:

1) A great earthquake may occur on the San Andreas fault at a distance from the site of more than 48 miles. It would be likely to produce surface rupture along the San Andreas fault over a distance of 200 miles with a horizontal slip of about 20 feet and a vertical slip of 3 feet. The duration of strong shaking from such an event would be about 40 seconds, and the equivalent magnitude would be 8-1/2.

2) A large earthquake on the Nacimiento fault at a distance from the site of more than 20 miles would be likely to produce a 60 mile surface rupture along the Nacimiento fault, a slip of 6 feet in the horizontal direction, and have a duration of 10 seconds. The equivalent magnitude would be 7-1/4.

3) Possible large earthquakes occurring on offshore fault systems that may need to be considered for the generation of seismic sea waves are listed below:

Location	Length of Fault Break	Slip	Magnitude	Distance to Site
Santa Ynez Extension	80 miles	10' horizontal	7-1/2	50 miles
Cape Mendocino, NW Extension of San Andreas Fault	100 miles	10' horizontal	7-1/2	420 miles
Gorda Escarpment	40 miles	5' vertical or horizontal	7	420 miles

4) Should a great earthquake occur on the San Andreas fault as described in paragraph 1) above, large aftershocks may occur out to distances of about fifty miles from the San Andreas fault, but those aftershocks which are not located on existing faults would not be expected to produce new surface faulting, and would be restricted to depths of about 6 miles or more and magnitudes of about 6-3/4 or less. The distance from the site to such aftershocks would thus be more than 6 miles.

STATE OF CALIFORNIA
DEPARTMENT OF WATER RESOURCES

EARTHQUAKE EPICENTER AND FAULT MAP

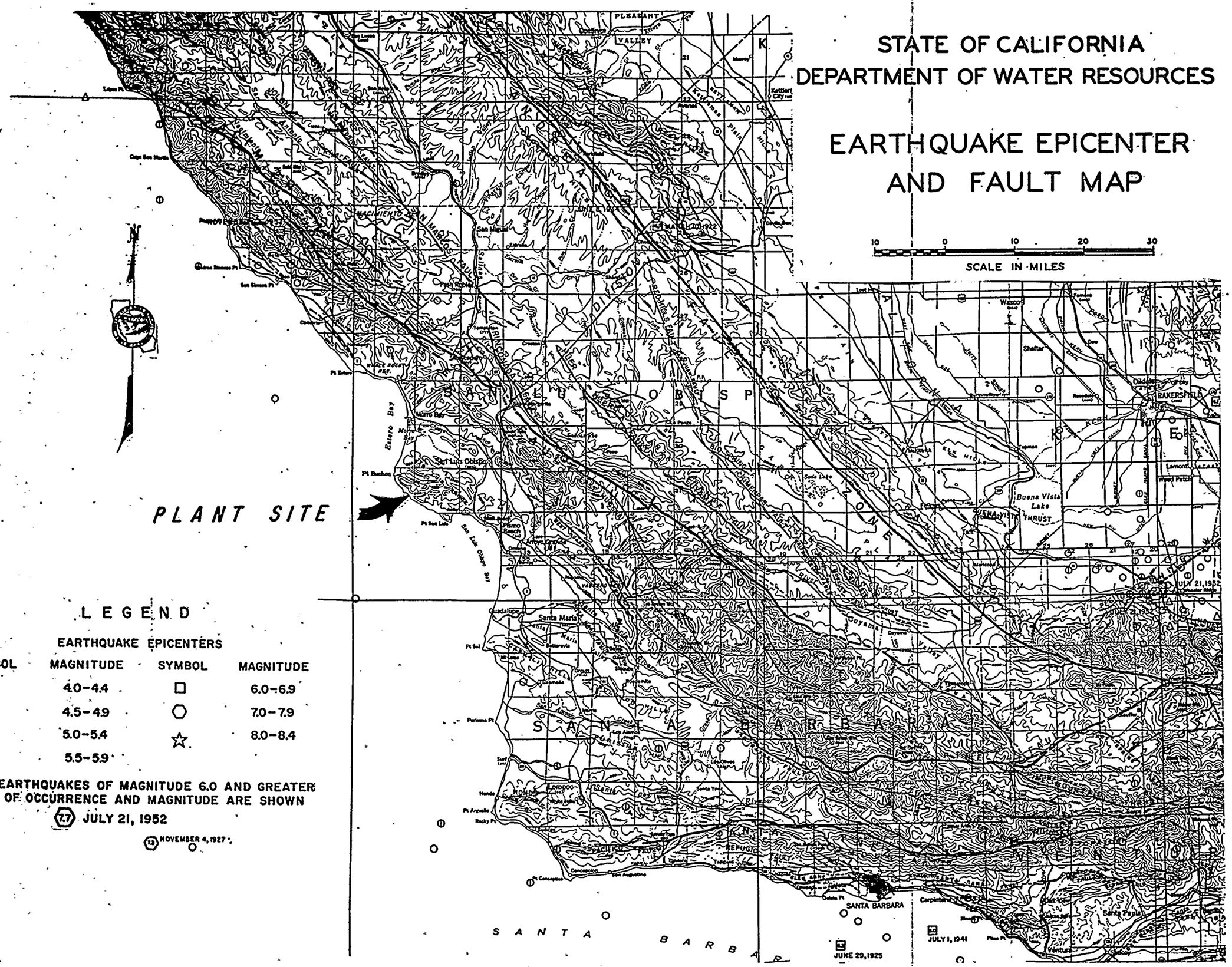
10 0 10 20 30
SCALE IN MILES
PLANT SITE
SANTA BARBARA
JUNE 29, 1925
JULY 1, 1941
JULY 21, 1952
NOVEMBER 4, 1927
Buena Vista Lake
Bakersfield
Lompoc
Santa Maria
San Luis Obispo
Pt Buchon
Pt Sal
Pt Arguello
Pt Conception
Estero Bay
San Luis Obispo Bay
Santa Barbara Channel
Santa Ynez Mts
Santa Barbara Mts
Tehachapi Mts
Carpinteria
Ventura
Santa Paula
Taft
Maricopa
Wasco
Shafter
Lamont
Weed Patch
Guadalupe
Orcutt
Los Alamos
Los Olivos
Solvang
Buellton
Guyama
Cuyama
Sisquoc
Cuyama Valley
Cuyama Range
Sisquoc Range
Pleasant Valley
Kettleman City
Avenal
Coalinga
Paso Robles
San Miguel
Atascadero
Morro Bay
Cayucos
Cambria
Los Osos
Nipomo
Arroyo Grande
Pismo Beach
Oceano
Guadalupe
Santa Maria
Santa Ynez
Lompoc
Refugio
Gaviota
Goleta
Carpinteria
Ventura
Santa Paula
Taft
Maricopa
Wasco
Shafter
Lamont
Weed Patch
Bakersfield
Buena Vista Lake
Buena Vista Thrust
Kettleman Plain
Kettleman Hills

JOHN A. BLUME
J. P. NICOLETTI
H. J. SEXTON
R. L. SHARPE
D. M. TEIXEIRA

JOHN A. BLUME & ASSOCIATES, ENGINEERS
612 HOWARD STREET • SAN FRANCISCO, CALIFORNIA 94105 • (415) 397-2525

January 12, 1967

Pacific Gas & Electric Company
245 Market Street
San Francisco, California

Attention: Mr. Gordon Richards

Subject: Earthquake Design Criteria for the Nuclear Power Plant - Diablo Canyon Site

Gentlemen:

Transmitted herein is the report on the earthquake design criteria for the subject site. This report presents the recommended design earthquake and corresponding response spectra to be used in the design of components of the plant.

Very truly yours,

JOHN A. BLUME & ASSOCIATES, ENGINEERS

John A. Blume

Dr. John A. Blume
President

Edward J. Keith

Edward J. Keith
Assistant Vice President

EARTHQUAKE DESIGN CRITERIA
FOR THE
NUCLEAR POWER PLANT - DIABLO CANYON SITE

INTRODUCTION

The purpose of this report is to present recommended earthquake design criteria for the proposed Nuclear Power Plant at Diablo Canyon. Specifically, the report establishes the maximum design ground acceleration at the proposed site, the design earthquakes and corresponding response spectra to be used in the design of components of the plant, and an outline of the recommended earthquake design procedures. The results set forth herein are based on the information presented in other reports: geology and tectonics as presented in Reference 1; seismology and seismicity as presented in Reference 2.

The proposed plant is located in San Luis Obispo County, California. The site lies twelve miles west southwest of the City of San Luis Obispo, the county seat, just south of the mouth of Diablo Creek. It is assumed that the major structures for the facility will be founded directly on rock.

SEISMIC FIELD INVESTIGATIONS

In order to evaluate the seismic characteristics of the site, a field investigation was made to determine the dynamic physical properties of the founding rock material. This investigation was carried out by personnel of John A. Blume & Associates on October 17, 1966. Compressional and shear velocities were determined with the aid of geophones spaced known distances apart. Based on this investigation, the average compressional and shear wave velocities were found to be 6,500 feet per second, and 2,500 feet per second respectively. The density of the rock was determined to be 143 pounds per cubic foot. The dynamic modulus of elasticity and Poisson's ratio were calculated

from the field determined compressional and shear wave velocities and were found to be 545,000 pounds per square inch and 0.41 respectively. The value of dynamic modulus indicated above suggests that rocking of the reactor building will contribute to the overall response of the structure and will have to be considered in the dynamic analysis.

MAXIMUM GROUND ACCELERATION

Reference 2 sets forth the following postulated earthquakes:

Earthquake A: A great earthquake on the San Andreas fault at a distance of 48 miles producing surface faulting over a distance of 200 miles with a slip of about 20 feet; duration of strong shaking about 40 seconds; equivalent Gutenberg-Richter magnitude equal to 8-1/2.

Earthquake B: A large earthquake on the Nacimiento fault at a distance of 20 miles producing surface faulting over a distance of 60 miles with a slip of about 6 feet; duration of strong shaking of about 10 seconds; equivalent Gutenberg-Richter magnitude equal to 7-1/4.

Earthquake C: Large offshore earthquakes, the most significant of which is on the extension of the Santa Ynez fault at a distance of 50 miles producing surface faulting over a distance of 80 miles; equivalent Gutenberg-Richter magnitude equal to 7-1/2. This earthquake was postulated to indicate a possible source of seismic sea waves.

Earthquake D: An aftershock of Gutenberg-Richter magnitude 6-3/4 centered anywhere at the site and at a depth of 6 miles. The 6 mile focus depth of the earthquake is the vertical distance to the point of initial rupture. Since the possibility of surface faulting due to this shock is considered extremely remote, the focus must be assumed to occur at the uppermost extent of the sub-surface fault plane. (It is assumed that the "tearing" of the fault plane extends downward.) The estimated depth to the center of the fault plane is 12 miles for Earthquake D.

Based on the above postulated earthquakes, the maximum anticipated ground acceleration at the site can be estimated using the methods set forth in References 4 and 5. The site accelerations are primarily dependent on the following parameters: Gutenberg-Richter magnitude and released energy, distance from the earthquake focus to the site, shear and compressional velocities of the rock media, and density of the rock. Since all of these parameters are known the maximum rock accelerations at the site are estimated as follows:

Earthquake A. 0.10g	Earthquake C. 0.05g
Earthquake B. 0.12g	Earthquake D. 0.20g

DESIGN EARTHQUAKES AND RESPONSE SPECTRA

The acceleration values presented in the previous sections cannot be used alone in establishing the design earthquakes for the site. Not only must maximum acceleration be considered, but the frequency distribution of the accelerations must also be investigated. In general, the parameters affecting the frequency distribution of an earthquake are distance, properties of the transmitting media, length of faulting, focus depth, and total energy release. Earthquakes which reach the site after traveling over great distances tend to have their high frequency waves filtered out. Earthquakes centered close to the site tend to produce wave forms at the site having minor low frequency characteristics.

In order to evaluate the frequency distribution of earthquakes, the concept of the response spectrum is used. For close-by earthquakes, the resulting response spectrum peaks sharply at short periods and the accelerations decay rapidly at longer periods. Earthquake D is the type of earthquake which would produce such a response spectrum. The March 1957 San Francisco earthquake as recorded in Golden Gate Park (S 80° E component) is the same type of earthquake. This shock produced a maximum recorded ground acceleration of 0.13g (on rock) at a distance of about 8 miles from the epicenter. Since Earthquake D has an assigned hypocentral distance of 12 miles, it can be expected to produce a response spectrum quite similar

in shape to the 1957 event. Thus, the smoothed response spectra for Earthquake D were constructed by normalizing the 1957 spectra to the predicted maximum ground acceleration of 0.20g. These spectra are shown on Plates 1 and 2 in arithmetic and logarithmic form respectively.

Large earthquakes centered at some distance from the site tend to produce response spectra that peak at longer periods than those for near-by smaller shocks. Such spectra maintain a higher spectral acceleration throughout the period range beyond the peak period. Earthquakes A and C are events which would tend to produce this type of response spectra. The intensity of shaking as indicated by the maximum predicted ground accelerations shows that Earthquake C will always have lower spectral accelerations than Earthquake A. Since the two shocks will have approximately the same shape spectra, Earthquake C is clearly not critical as far as ground motion at the site is concerned and will therefore be neglected in this analysis. The north-south component of the 1940 El Centro earthquake produced response spectra which emphasized the long period characteristics described above. Earthquake A, because of its distance from the site, is expected to produce response spectra similar in shape to those produced by the El Centro event. Thus, smoothed response spectra for Earthquake A were constructed by normalizing the El Centro spectra to 0.10g. These spectra, however, result in smaller accelerations than the spectra from Earthquake B for all building periods. They are not presented herein since they do not govern the seismic design.

Earthquake B is an event which tends to produce response spectra that emphasize the intermediate period range; i.e., the epicenter is not close enough to the site to produce large high frequency (short period) effects, and it is too close to the site and too small a magnitude to produce large low frequency (long period) effects. The N 69° W component of the 1952 Taft earthquake produced response spectra having the above characteristics. This shock was therefore used as a guide in establishing the shape of the expected response spectra for Earthquake B. Thus, the smoothed response spectra for Earthquake B were constructed by normalizing the

Taft spectra to the predicted maximum ground acceleration of 0.12g. These spectra are shown on Plates 3 and 4 in arithmetic and logarithmic form respectively.

Based on the information presented above, it is our recommendation that two different earthquakes be used for design purposes. The response spectra for these two earthquakes are shown on Plates 1 and 3, and correspond, respectively, to the earthquake wave forms of the S 80° E component of the 1957 Golden Gate Park, San Francisco earthquake normalized to 0.20g; and the N 69° W component of the 1952 Taft earthquake normalized to 0.12g. Both of these earthquakes should be considered in the seismic analysis, and the most severe results used in the design. In addition, in order to assure adequate reserve energy capacity of the structures, the facility should be reviewed for twice the design accelerations.

RECOMMENDED EARTHQUAKE DESIGN PROCEDURES

For purposes of design, structures (buildings or equipment) are divided into three classes:

Type I. Those structures whose failure might cause a nuclear incident or structures whose failure may damage vital equipment and thus might cause a nuclear incident.

Type II. Those structures and components whose failure could cause no nuclear incident but are important to the generation of power.

Type III. Other structures.

Recommended Procedures for Type I Structures and Equipment

1. For structures or equipment founded directly on soil or rock, a structural design shall first be executed based on estimated seismic shears, moments, and displacements. The structures thus designed shall then be subjected to a dynamic analysis using the spectra on Plate 1 and Plate 3. The earthquake producing the most severe results shall be used in the final design of each structural element. Damping values shall be taken from Table 1. Sufficient modes shall be included to assure participation of all modes having a period greater than 0.08 second. For the "spectral" method of analysis, modes may be combined by taking the square root of the sum of the squares. Rocking of the structure on its foundation shall also be included. The vertical ground acceleration shall be a constant value equal to two-thirds the maximum horizontal ground acceleration, and resulting stresses due to horizontal and vertical accelerations shall be considered to act simultaneously and shall be added directly. When combined with stresses from other loadings the resulting stresses shall comply with applicable codes without the usual fractional increase for short-term loadings. If the Ultimate Strength method of design is used, appropriate load factors should be used which reflect the relative contributions of the various types of loadings, and provide safety factors consistent with those of the working stress method. The final design shall be reviewed for compliance with local requirements.

If computerized methods of dynamic analysis are used, the mathematical model may be subjected to the ground motion of both the S 80° E component of the 1957 Golden Gate Park, San Francisco earthquake (normalized to 0.20g); and the N 69° W component of the 1952 Taft earthquake (normalized to 0.12g). The resulting maximum shears, moments, displacements, and accelerations shall be used in the design without reference to which of the design earthquakes produced the maximum response.

After the above have been satisfied, the structure shall be examined under twice the design accelerations determined from the "spectral" approach (or computer analysis). As before, horizontal and vertical seismic components shall be considered simultaneously with other appropriate loads, and in this case the vertical coefficient shall be equal to two-thirds the doubled maximum horizontal ground acceleration. Under this loading there shall be no failure that would prevent a safe shutdown during or after the earthquake.

2. Structures or equipment supported in or on other structures or equipment are placed into three categories based on their natural frequency and the predominant frequency of the supporting structure:

(1) Rigid category: $\frac{fm}{f} > 2.0$

(2) Resonance category: $0.5 \leq \frac{fm}{f} \leq 2.0$

(3) Flexible category: $\frac{fm}{f} < 0.5$

Where:

fm is the natural frequency of the mechanical structure or equipment, and f is a predominant frequency of supporting structure at the location of installation.

(1) For Rigid Category: Because of the high frequency, the design shall be based on an acceleration corresponding to the maximum acceleration experienced by the supporting structure at the location of equipment support.

(2) For Resonance Category: Elimination of resonance phenomena is one of the principles of the design. In order to eliminate resonance vibration some structural modification may be required. In case the resonance vibration cannot be avoided, prevention of large amplitudes by means of damping devices is required or dynamic design considering resonance vibration is required. Should the restriction of vibration be enough to make the object rigid, examination for rigid category is also required.

(3) For Flexible Category: Those items which are designated as flexible will be designed for accelerations corresponding with their frequencies using Plates I or 3 as though they were supported directly on the ground. Careful examinations will be made concerning objects coming into contact because of excessive displacements.

Except as modified above, structures or equipment supported in or on other structures or equipment shall meet the requirements of the "single" and "double" earthquake criteria set forth for structures or equipment founded on soil or rock.

TABLE I

RECOMMENDED DAMPING VALUES

Item	Percent Critical Damping
Containment structure and all internal concrete structures	2.0
Conventionally reinforced concrete structures above ground such as shear walls or rigid frames	5.0
Steel structures	
Welded steel structures	1.0
Bolted or riveted steel structures	2.0
Vital piping systems	0.5

Recommended Procedures for Type II Structures and Equipment

It is recommended that Type II structures and equipment be designed on the basis of a minimum seismic horizontal coefficient of 0.20 in accordance with applicable local building requirements. All equipment should be so bolted or fastened that its displacement will not occur if friction is non-existent.

Recommended Procedures for Type III Structures

It is recommended that Type III structures be designed in accordance with local building requirements.

REFERENCES

1. Richard H. Jahns, Geology of the Diablo Canyon Plant Site, December 5, 1966, and Supplement, January 4, 1967.

2. Benioff, Hugo and Smith, Stewart, Seismic Evaluation of the Diablo Canyon Site, December 2, 1966.

3. Swain, R. J., Recent Techniques for Determination of "In-Situ" Elastic Properties and Measurement of Motion Amplified in Layered Media, Geophysics, Vol. XXVII, No. 2 (April 1962).

4. Wiggins, John H., Jr., Effect of Site Conditions on Earthquake Intensity, ASCE Proceedings, Vol. 90, No. ST2, Part I (1964).

5. Blume, John A., Earthquake Ground Motion and Engineering Procedures for Important Installations Near Active Faults, Third World Conference on Earthquake Engineering, New Zealand, 1965.

JOHN A. BLUME AND ASSOCIATES, ENGINEERS
612 HOWARD STREET SAN FRANCISCO

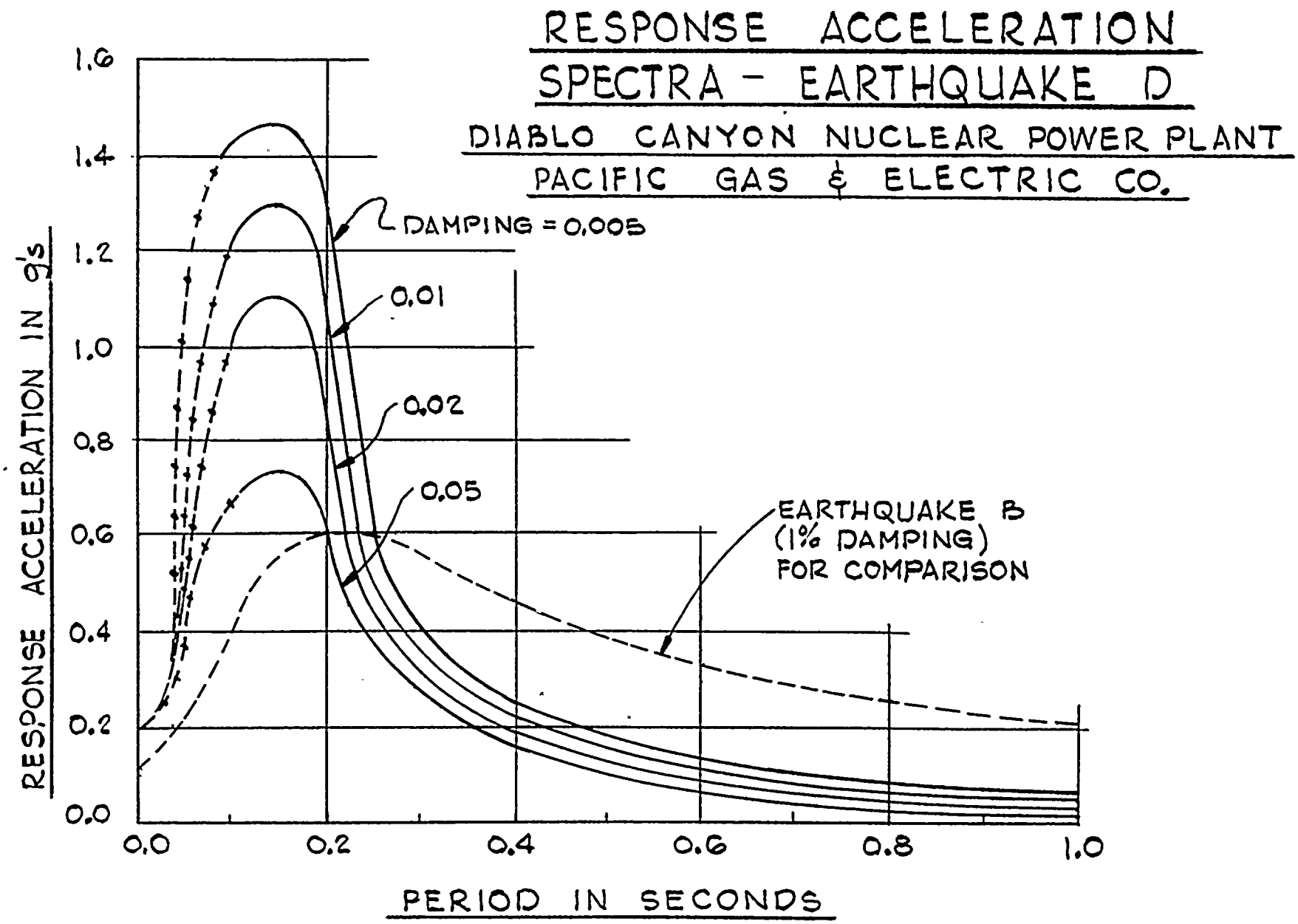

PLATE 1

JOHN A. BLUME AND ASSOCIATES, ENGINEERS

612 HOWARD STREET SAN FRANCISCO

RESPONSE ACCELERATION SPECTRA - EARTHQUAKE D

DIABLO CANYON NUCLEAR POWER PLANT

PACIFIC GAS & ELECTRIC CO.

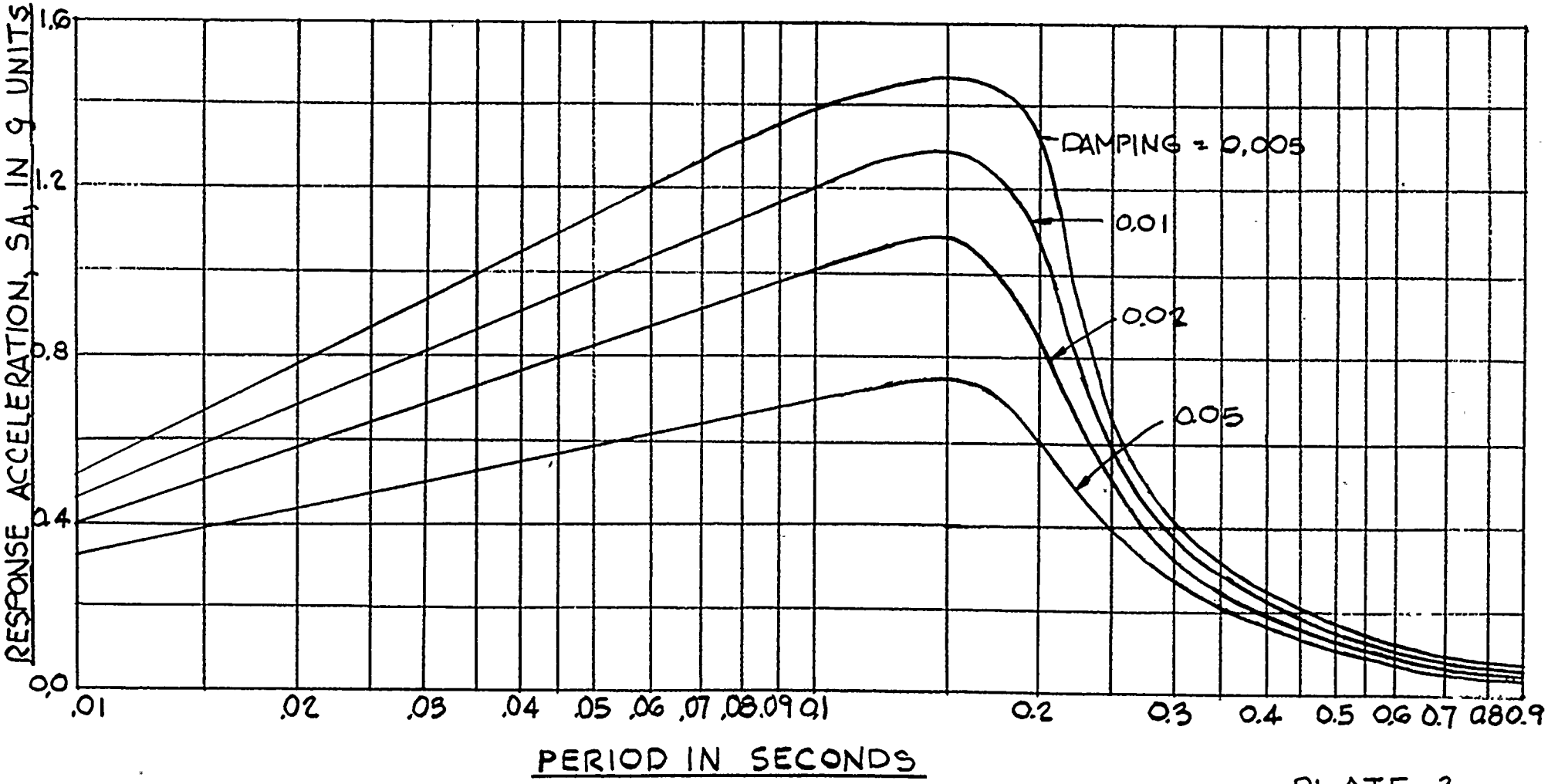

PLATE 2

JOHN A. BLUME AND ASSOCIATES, ENGINEERS
612 HOWARD STREET SAN FRANCISCO

RESPONSE ACCELERATION SPECTRA - EARTHQUAKE B

DIABLO CANYON NUCLEAR POWER PLANT
PACIFIC GAS & ELECTRIC CO.

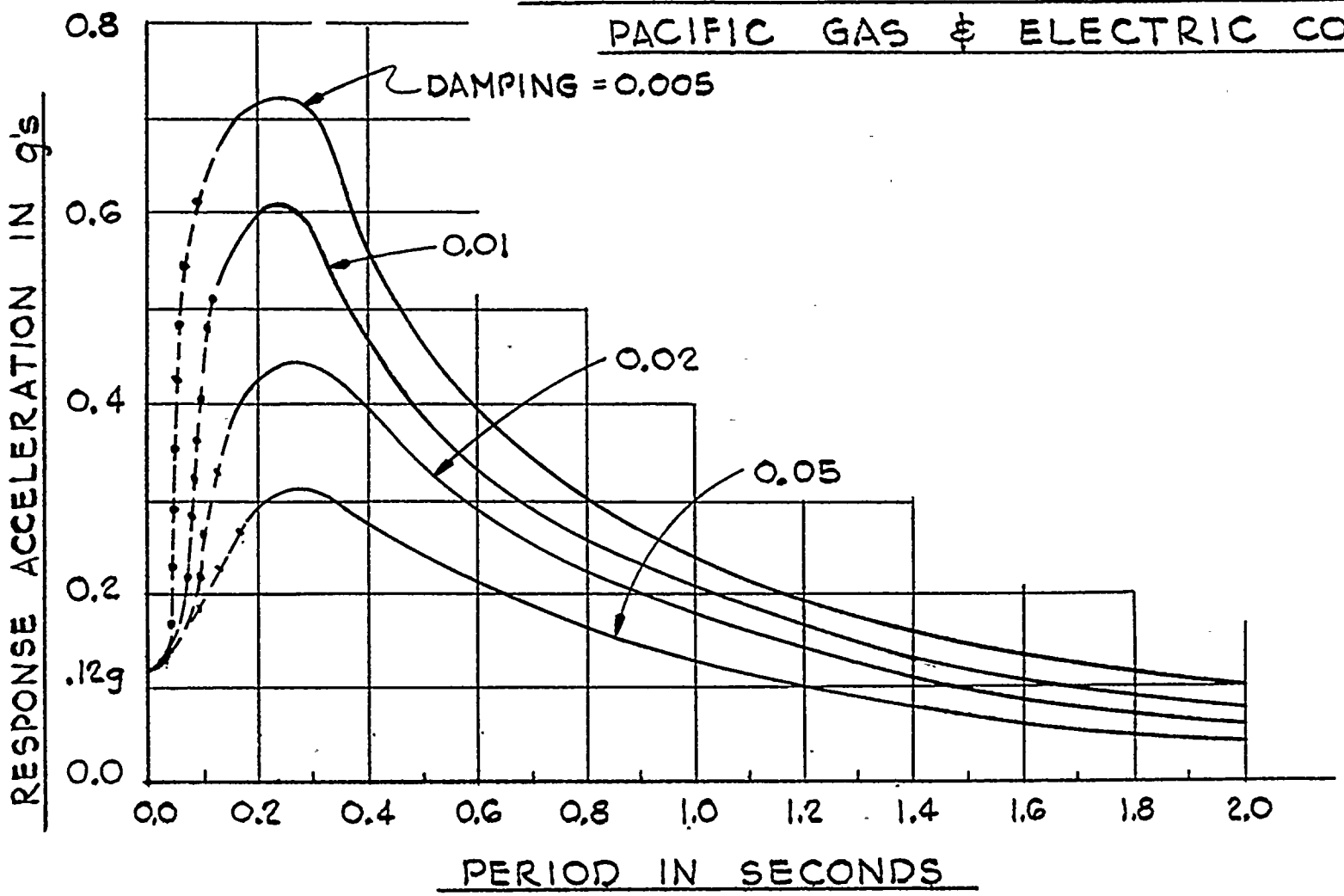

PLATE 3

JOHN A. BLUME AND ASSOCIATES, ENGINEERS
612 HOWARD STREET SAN FRANCISCO

RESPONSE ACCELERATION SPECTRA - EARTHQUAKE B

DIABLO CANYON NUCLEAR POWER PLANT

PACIFIC GAS & ELECTRIC CO.

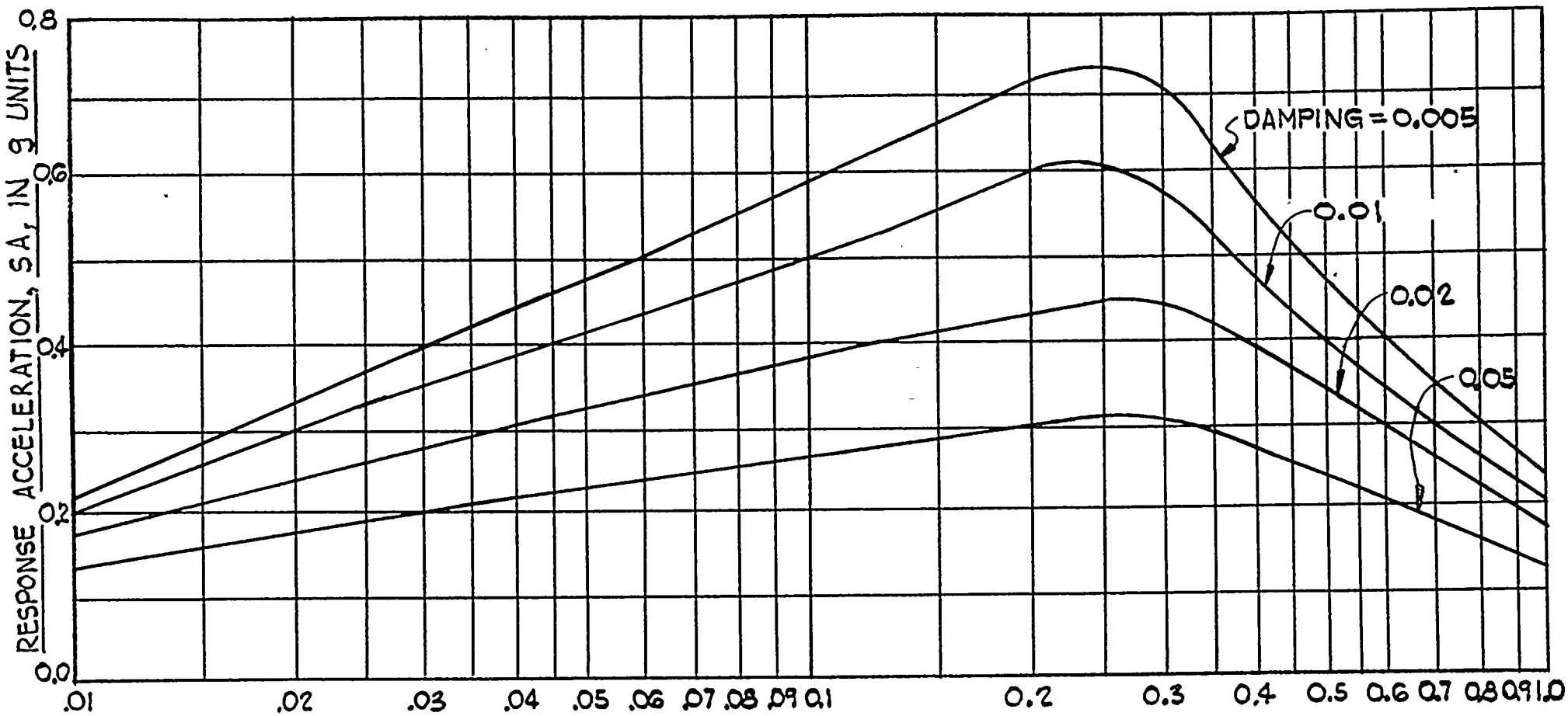

PLATE 4

AN EVALUATION OF TSUNAMI POTENTIAL AT THE DIABLO CANYON SITE

Prepared for

Pacific Gas and Electric Company
245 Market Street
San Francisco, California

By

Marine Advisers, Inc.
La Jolla, California

Report A-253

December 1966

INTRODUCTION

This report discusses the potential magnitude of future tsunamis in the vicinity of the Pacific Gas and Electric Company's proposed nuclear power plant site at Diablo Canyon. The site is located approximately 200 miles north of Los Angeles between the two small towns of Avila Beach and Morro Bay in San Luis Obispo County.

Assessment of an area for tsunami potential requires an empirical knowledge of the variable parameters involved in the generation, propagation and dissipation of the waves. Tsunami theory has not yet reached a state where rigorous solutions employing accurately known variables are attainable, for the simple reason that the paucity of tsunamis makes observational study difficult. Similarly, a convincing statistical treatment of the probability of occurrence is inhibited by the short recorded history of tsunamis.

Most of the empirical studies have been done in Japan and Russia primarily because the frequency of occurrence of tsunamis is considerably higher there. While it is true there are differences in geography, geology, and culture between these two countries and the west coast of the United States, many of their findings and techniques may be applied, with judicious care, to the United States west coast.

The Japanese have really done more to determine the correlations between the parameters. This correlation procedure by such authors as Iida (1963a,b) allows a more general application of the findings to other areas where

one may determine the extent of similarity between that area and the Japanese coast.

Perhaps the best guide to the application of current knowledge of tsunamis to the California coast is the result of the tsunami conference (January 29-30, 1965) convened by Marine Advisers, Inc. The conferees included prominent representatives of the specialties relating to tsunamis. Following their comments and suggestions (Marine Advisers, Inc., 1965), the investigations of the Diablo Canyon site assumed the following mode:

1. A review of the tsunami history of the area from personal interviews, newspaper articles, local histories, and tide records.
2. A comparison of the Diablo Cove background spectra to that of nearby areas of known response.
3. An evaluation of the geography and hydrography as it relates to tsunami theory.
4. A consideration of the probability of occurrence based on seismicity, both local and distant.

An extrapolation to the Diablo Canyon site prototype from model studies of tsunamis by both Kaplan (1955) and Van Dorn (1965), not included in the conferees' suggestions, has been explored, but application was ruled out because model studies of runup have not been successful for slopes representative of those found at the Diablo Canyon site.

I. HISTORICAL REVIEW

No natural historical treatment for the Diablo Canyon site itself exists because the site is remote from populated areas. Morro Bay and Avila Beach, the two nearest communities, were selected for a review of tsunami history, but both are situated on the shores of large embayments. Cambria, 13 miles north of Morro Bay, is a nearby community with coastal features more nearly approximating the Diablo Canyon site area.

Morro Bay was founded in 1870 by Franklin Riley. Historical records remark on the residents' dependence on the sea for food and recreation, and that each family owned its own boat. Dock and pier facilities were constructed early in that community's history to ship the grains and other agricultural goods produced in the inland areas. Residents were naturally concerned with the state of the sea, particularly with uncommon sea levels or damaging waves, so that such occurrences of any significance should be easily traceable. Separated from the Diablo Canyon site by only 11 miles, an event at Morro Bay would indicate the occurrence and, in some proportion, the intensity of such events as tsunamis at the neighboring location.

Mr. D. Pereira was the source of information in Morro Bay. He has resided there since 1910 and has operated a small business within 300 yards of the shore since 1923. His location has caused him to observe the sea's changes with more than casual interest.

Avila Beach, located approximately 10 miles to the south of the Diablo Canyon site, owes its beginning early in the eighteenth century to Juan Avila.

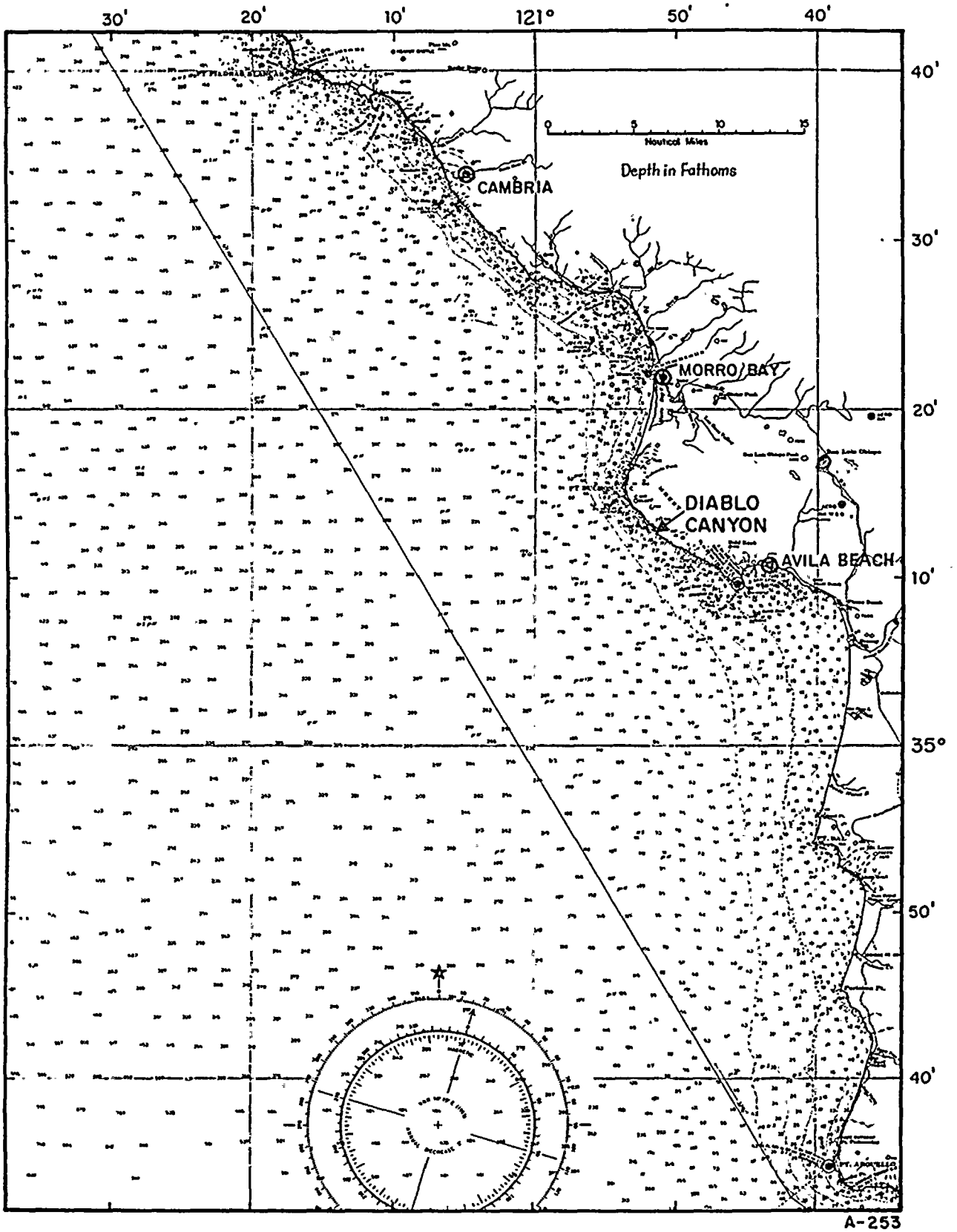

Figure 1. Location map of Diablo Canyon.

It too is nestled close to the shore and, like Morro Bay, has relied for its existence on the sea- - particularly on shipping. It differs from Morro Bay in the configuration of the embayment which it borders. The retired postmaster, Mr. Canet, offered what information he had accrued in his 68 years in the area. His interest in the area history has resulted in a large collection of pictures, newspaper articles, and handwritten accounts.

Cambria approximates the situation at the Diablo Canyon site because the coastlines of the two areas are similar in their gross features and are sparsely populated. Cambria had attempted in her early years to become a major shipping port, and a large pier was constructed there in 1907. After nine months' use, the pier was destroyed by a southeast storm, and the community subsequently turned inland and developed away from the coastal area. In Cambria, the main source of information was a long-time resident, Mr. Paul Squibb, who is a retired teacher with an active personal interest in local history. Families owning coastal properties gave freely what help they could offer. Other persons in each area were contacted but generally were not qualified to recount events first hand.

Following is a list of sea-level disturbances of sufficient significance to have been noted by human observation* since 1878.

---

*An earlier disturbance that has received considerable attention is the Santa Barbara earthquake and the accompanying tsunami. Some accounts mention water levels of nearly 30-35 feet at Santa Barbara and perhaps 15 feet at Ventura, but a thorough investigation (Marine Advisers, Inc., 1965) has presented evidence of much lower levels.

Place of Observation	Date and Generator	Form and Degree of Disturbance	Source of Observation*
Avila Beach	Nov. 2., 1878 Source unknown	Occurred at low tide. Down surge 3 feet. Slow rise to high tide level. Tore out pier.	San Luis Obispo Telegram and Telegraph. Mr. Canet.
Avila Beach	Dec. 10, 1907 Probably a storm.	Some accounts refer to a tidal wave. It accompanied a severe storm. Tore out the pier.	San Luis Obispo Telegram and Telegraph. Mr. Canet.
Avila Beach	Nov. 4, 1927 Earthquake west of Pt. Arguello.	1. Termed an unusual high tide reaching almost to sea wall. 2. A six-foot wave was reported at Pismo. 3. A four-foot rise and fall reported at Pt. San Luis.	1. San Luis Obispo Telegram and Telegraph. 2. Pacific Coast Agent 3. Lightkeeper, San Luis Obispo.
Avila Beach	April 1, 1946 Aleutian Islands 53.5°N, 163°W.	About a five-foot maximum rise occurring just after high tide maximum.	C&GS tide record. C.K. Green (Trans. AGU, 1946).
Cambria Morro Bay	Dec. 12, 1953 Peruvian 7 3/4MM.	1. Morro Bay drained by down surge. No bore followed. Water rose to normal level. 2. Cambria had no evident result.	1. San Luis Obispo Telegram and Telegraph. 2. Mr. Paul Squibb.
Avila Beach	Feb. 9, 1960 Apparently a storm centered well out to sea.	A heavy ground swell tore out a section of dock.	San Luis Obispo Telegram and Telegraph. Mr. Canet.
Avila Beach Morro Bay Cambria	May 22, 1960 Earthquake - coast of Chile, 39 1/2°S, 74 1/2°W.	1. A tsunami disturbance of perhaps three feet down surge at Avila. 2. Morro Bay had a slight down surge with rather strong currents accompanying. 3. Cambria showed no effect.	1. Mr. Canet 2. Mr. Pereira 3. Mr. Squibb

* Observer qualification will not be included but is available for reference.

Place of Observation	Date	Form and Degree of Disturbance	Source of Observation
Avila Beach Morro Bay Cambria	Mar. 28, 1964 Earthquake, Prince William Sound, Alaska.	1. Avila C & GS tide gauge recorded a down surge greater than elevan feet. 2. Morro Bay residents reported a down surge of about six feet - - strong currents. 3. Cambria residents felt there was at most a three-foot change in sea level but were not certain it really occurred.	1. C & GS records. 2. San Luis Obispo Telegraph and Telephone. Mr. Pereira and other residents. 3. Mr. Squibb, Mrs. Tartella.

The preceding list of events is notable for two points: (1) that over a period of at least 80 years the range of the most serious observed disturbances of water level has been within the normal astronomical tide range (approximately six feet) at Morro Bay and Cambria, and (2) the disturbances at the Cambria and Morro Bay areas have been less frequent and of less range, although they are very near Avila Beach in geographic distance. This is a strong argument that the local configurations play a large part in the ultimate character of the tsunami. The second point will be further explored in Section II.

Severe earthquakes which occurred with no accompanying tsunami at the area of interest are worth noting. In the search for references to disturbances of the sea level at these locales, the dates of known local earthquakes were explored specifically.

Date	Epicenter	Remarks
January 22, 1923	Off Cape Mendocino	Rossi-Forel Scale IX, Submarine.

Date	Epicenter	Remarks
June 17, 1928	14°N, 97°W	La Jolla (6.0 inches max) and San Francisco (2.25 inches max) tsunami.
August 31, 1930	Santa Monica Bay	Social news reports large crowds at Pismo Beach, Avila Beach and Morro Bay. No notice of tsunami. Tremors felt at San Luis Obispo. Intensity maximum VII-VIII, (Modified Mercalli Scale) (M-M).
March 10, 1933	Long Beach	Tremors at Avila Beach, no wave. Intensity at Avila Beach, III (M-M).
March 29, 1947	Fifteen miles off Cape Mendocino.	Maximum VI (M-M) at San Nicolas Island.

In the period 1956-1963, which does not include the more recent occurrence of March 1964 disturbance, 24 tsunamis are known to have been generated in the Pacific Ocean (C & GS report, April 17, 1965). The sources were distributed broadly, with six off the coast of South America, five near Japan, four in the Kurils, three off Central America and Mexico, two off Kamchatka, one in the South Pacific, one in the Aleutians, one in the New Hebrides, and one in Alaska. Some were of destructive proportions. Others were recorded widely but did not have the capability for destruction. Only the 22 May 1960 disturbance was noticed by residents at Avila Beach, Morro Bay or Cambria.

Historically then, the evidence implies that the area of interest is relatively insensitive to tsunamis. The tsunamis that have occurred at the three specific areas have been notable for their mild nature and the small

range of disturbance. Of particular interest is the fact that there is no recorded occurrence of a bore; the waves usually assume the nature of an unusually high or low tide.

This short history of the area agrees in nature with the longer history of the entire California coast. Tsunamis have been shown to affect most of the California coast only moderately, (Marine Advisers, Inc., 1965; C & GS, 1960; C & GS, 1964) with a few small areas excepted. The problem of these small areas of exception will be considered in Section II.

II. DISTANTLY-GENERATED TSUNAMIS

The importance of distinguishing between distantly-generated tsunamis (generally defined by a distance greater than several times the principal source dimension) and locally-generated tsunamis has been rather well established. This distinction is particularly pertinent in reference to the California coast because the coast generally shows a very moderate reaction to tsunamis from distant sources, certain "sensitive" areas to the contrary. Locally-generated tsunamis, on the other hand, offer a combination of parameters which must be weighted to individual areas, for any postulated occurrence, through simultaneous regard for seismicity, geography and offshore hydrography of that area. Seismicity of the local area will usually determine the tsunami-generating sources, and from that the limits of the other parameters may be derived.

A complete development of the current knowledge of tsunamis by Van Dorn (1965) and Munk (1963) and the engineering aspects by Wiegel (1964) is available. In addition, a rather comprehensive treatment by Marine Advisers (1965) in a report on the San Onofre area is available. Only the immediately pertinent facts will be brought out in this report.

The predominant sources of tsunamis can be limited to the areas of earthquake and volcanic activity in the circumpacific belt. Distant sources relative to the Diablo Canyon site are probably to be found in the Aleutian area, the Kuril-Kamchatka region, and along the South American coast. By the time such tsunamis reach the California coast, they have dispersed much

of their energy and have assumed the form of a wave train. Too, the path of travel, approximating a great circle route, would cause these waves to approach the California coast at a glancing angle. This decreases the energy available at the impact because of dispersion of energy density by refraction along the shelf. The result is a history of moderate response (within the tidal range) for the California coast.

The "sensitive" areas mentioned earlier are restricted zones encompassing a few miles along the coast which have historically shown an abnormally high response as compared to the coast in general. Two generally mentioned are Crescent City and Avila Beach. Our concern in this report is aimed at Avila Beach, on San Luis Obispo Bay, because of its proximity to the Diablo Canyon site.

Avila Beach has shown extreme high or low water levels, as much as twice the tidal range and often two to three times as great as the rest of the coast. The possibility that this situation might be carried over to the Diablo Canyon site is considered in this report.

The method selected was to obtain records of wave amplitude from which to derive background spectra for Avila Beach and Diablo Canyon. A comparison of the energy peaks can show whether they bear a similarity or dissimilarity of energy distribution in the spectral "valley" (referring to a frequency range normally displaying low energy) in which tsunamis occur. This indicates the nature of the reaction at Diablo Canyon site to tsunamis, i.e., whether it more nearly resembles Avila Beach or the rest of the coast.

This method is rooted in past work by several investigators. Again, a discussion of the technique can be found in Van Dorn (1965) and Munk (1963). A spectral "valley" exists between the low frequency tides and the higher frequency swell and surfbeat. It is in this "valley" of frequencies (approximately 2 to 12 cycles per hour) that tsunamis frequencies occur. While traveling in deep water the tsunamis, as long waves, can be treated sufficiently well by a series of approximations. However, as the wave nears shore, it is modified in a non-linear manner by the local undersea topography, and there results a variation of the wave height and wave period from mile to mile along the coast. It has not been possible to apply offshore spectra measurements to a nearshore situation.

At the same time, the normal spectra (that is, when a tsunami is not in evidence) of nearshore observations have shown some marked characteristics. Namely, that "In general it is found that the spectra of different tsunamis at any one station look alike, whereas one tsunami at different stations has no reproducible features. The inevitable conclusion is that tsunami records are governed most strongly by the bottom topography near the recording station and not by the character of the source", (Munk, 1963).

As an example, Munk compared the spectra from the tsunami at Acapulco of 28 July 1957 to the day-to-day background spectra. The tsunami spectra are two to three orders of magnitude above the background spectra but exhibit a close correlation to their frequency response. (See accompanying Figure 2). It is this relationship that served as the basis of the tsunami study at the Diablo Canyon site.

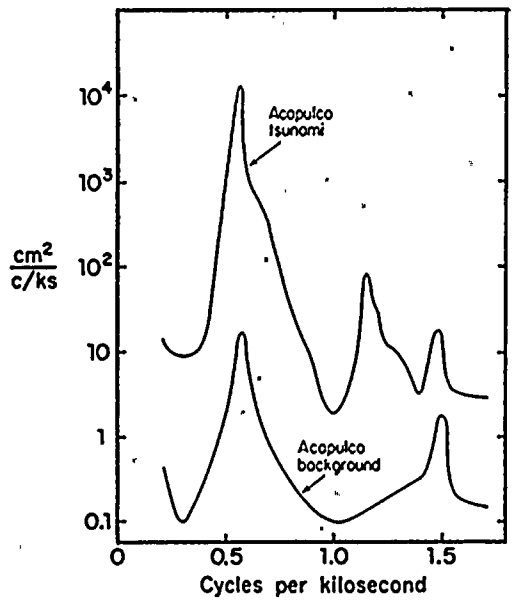

Figure 2. Spectra of background activity and of the tsunami of 28 July 1957 at Acapulco (Munk, 1963).

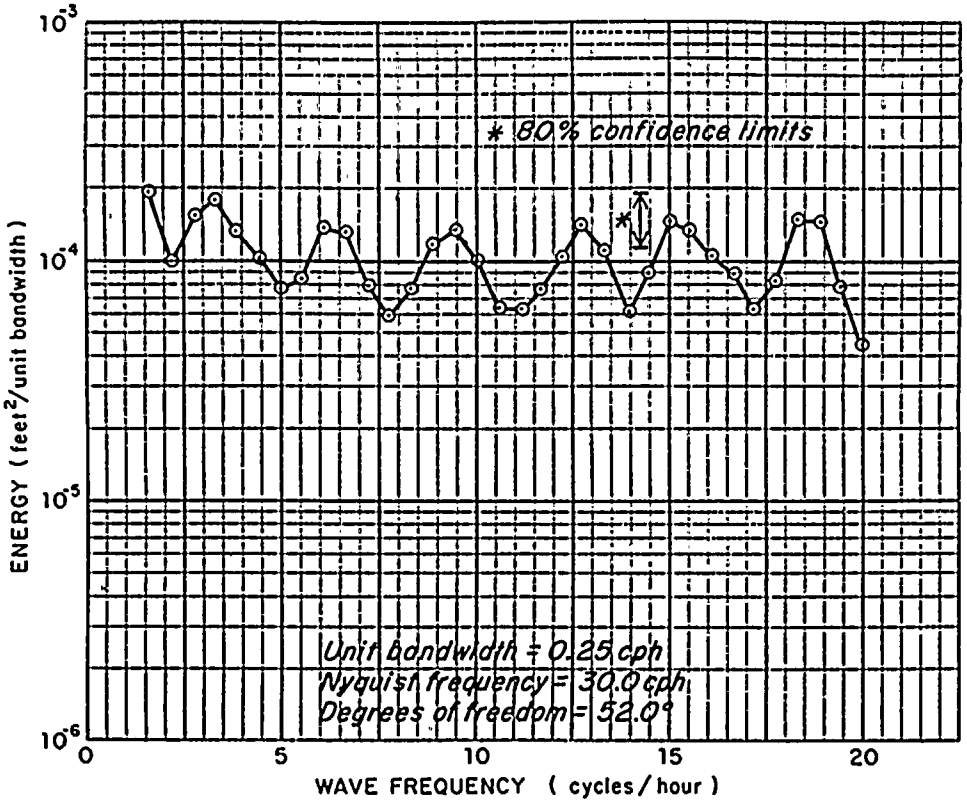

Figure 3. Long-wave energy spectrum at Diablo Canyon.
November 1966

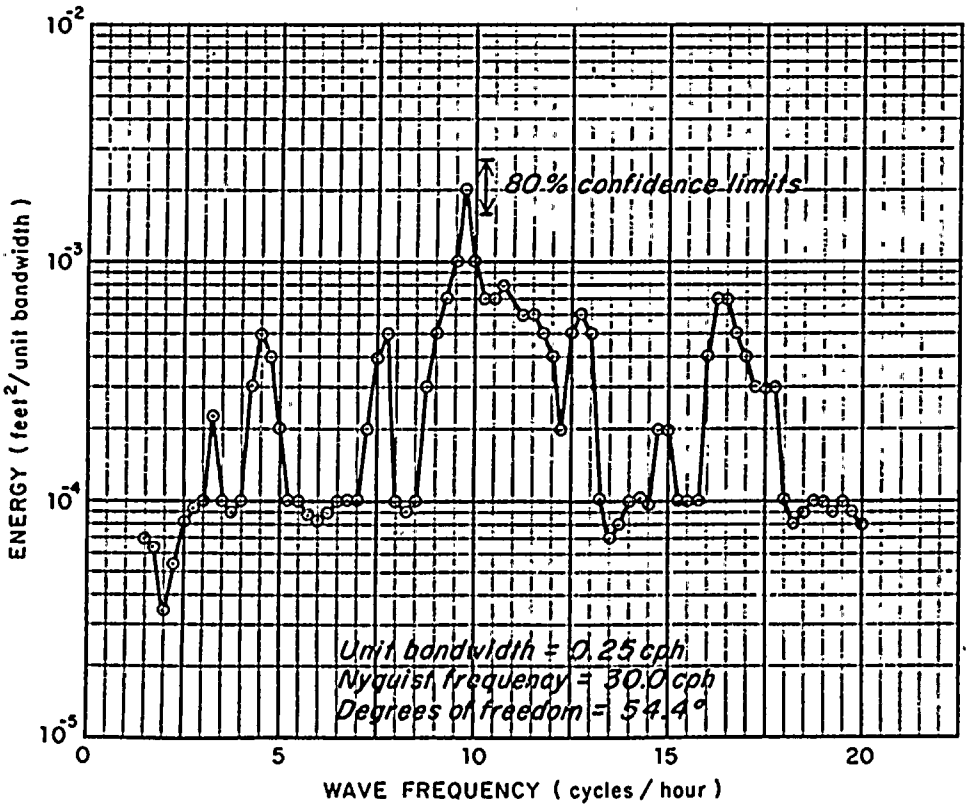

Figure 4. Long-wave energy spectrum at Avila.
November 1966

During November and part of December 1966, wave recordings were made at Avila Beach (from the Union Oil Company pier) and at the Diablo Canyon site. Spectra resulting from the analysis of these records are included (Figures 3 and 4). The critical features of the Avila spectra are the energy peaks at about 4 cycles per hour (cph) and at about 9-10 cph. In direct contrast, the Diablo Canyon spectra display a random peaking. In this case, the significance of the random peaking lies in the fact that the record shows no tendency to resemble the Avila Beach pattern, with none of the peaks standing well above the rest of the curve. The spectra are based on measurements from two different days so that the features may be regarded as reproducible.

Having determined that the two areas do not resemble one another in the manifestation of the response, we would venture to speculate on their individual responses.

Diablo Canyon site is probably subject to the non-amplified attack experienced by most of the coast. The embayments in the vicinity of the site are too small to produce any resonance features in the range of tsunami periods. The result would be a tsunami runup in the tidal range of 5-6 feet above the water level present at the time of incidence.

Runup is a term used to denote the elevation on land reached by the inundating water (BEB Technical Report No. 4). Some of the Japanese work has been directed to correlation between the coastal features and runup height. One pertinent fact derived from these studies, and others, is that a steep slope or a cliff at the shoreline will enhance runup. There is further indication that

the magnitude of enhancement may increase with the incident wave height. Since amplification is not an indicated characteristic of the Diablo Canyon area, the enhancement of runup by the cliffs is not significant for the incident wave heights anticipated.

Avila Beach, on the other hand, is probably influenced by resonant amplification due to the natural periods of oscillation of the bay. An analytical treatment may be developed as follows.

If the shape of a rectangular bay is assumed to be like the configuration diagrammed in Figure 5, and if a node is located at the mouth (the node in this case being described by a line joining all points having no vertical motion) and one antinode forms along the shore (the first harmonic), the period may be computed for an averaged depth from Merian's Formula.

$$T \approx \frac{4L}{\sqrt{g\bar{h}}}$$

L is about 2.0 nautical miles or about 12,100 feet

$g = 32.2$ ft./sec^2

$\bar{h} = 15$ fathoms $= 90$ feet

$$T \approx \frac{48,400}{\sqrt{2,890}} = \frac{48,400}{53.8} = 898 = 15 \text{ min. or } 4 \text{ cph}$$

For the extra wide mouth, a correction would have to be added amounting to as much as five minutes. One should, therefore, expect that a major energy peak for the power spectrum would fall within the range of 20 minutes, or three to four cph. Secondary and tertiary harmonics could be present showing energy peaks within six-ten cph.

There is the further possibility that an oscillation could be set up

between the two walls described by the second, longer area outlined in Figure 5. This would offer longer periods of perhaps 20 to 30 minutes (2-3 cph), a range wherein the tsunamis' periods will most often occur (please see Iida's diagrams in Figure 6). Such an agreement of periods offers the greatest propensity for amplification.

The resonant periods of an embayment may also be excited by other energy inputs. It is entirely possible that a storm or a "ground swell", if its period were appropriate, could excite the seiche of the embayment and thus induce a higher water surface elevation. This concentration of wave activity in a few narrow ranges of frequencies would result in greater incident wave forces.

A further indication that this may be the mode of amplification is the fact that historical records (see table in Section I) show damage accompanying storms from the southeast (December 10, 1907) and a "ground swell" (February 9, 1960).

We suggest, therefore, that Avila Beach is sensitive to tsunamis, and further speculation on the response at Avila Beach is unwarranted since our intent is to simply show the dissimilarity between Avila Beach and the Diablo Canyon site. Such differences do appear to be evident. There appears to be no indication that the Diablo Canyon site shoreline will respond to tsunamis in the same manner as does the Avila Beach area.

III. LOCALLY-GENERATED TSUNAMIS

Locally-generated tsunamis must be reviewed in more detail than those generated at some distance. The nearness of the source reduces both the dispersion of energy density and the loss of energy possible during travel over long distances for long periods of time. This means that a closer inspection of the relationship between generation area and the affected area is required.

Some of the major features to be considered must be:

1.) The offshore seismicity.

   a.) Magnitudes, M, particularly those greater than 7.0 (Richter) which, from Japanese data, begin to show a high correlation with tsunami generation.

   b.) The orientation of such possible seismic generators, because the greater energy is directed normal to their long axis.

   c.) Whether vertical motion is likely to accompany a seismic disturbance since a vertical component is considered necessary for tsunami generation.

2.) The offshore topography.

   a.) A steep slope at the incident area will cause high wave buildup.

   b.) Canyons or ridges may cause channeling.

   c.) Slumping of sediments on steep slopes may cause tsunamis by energy coupling.

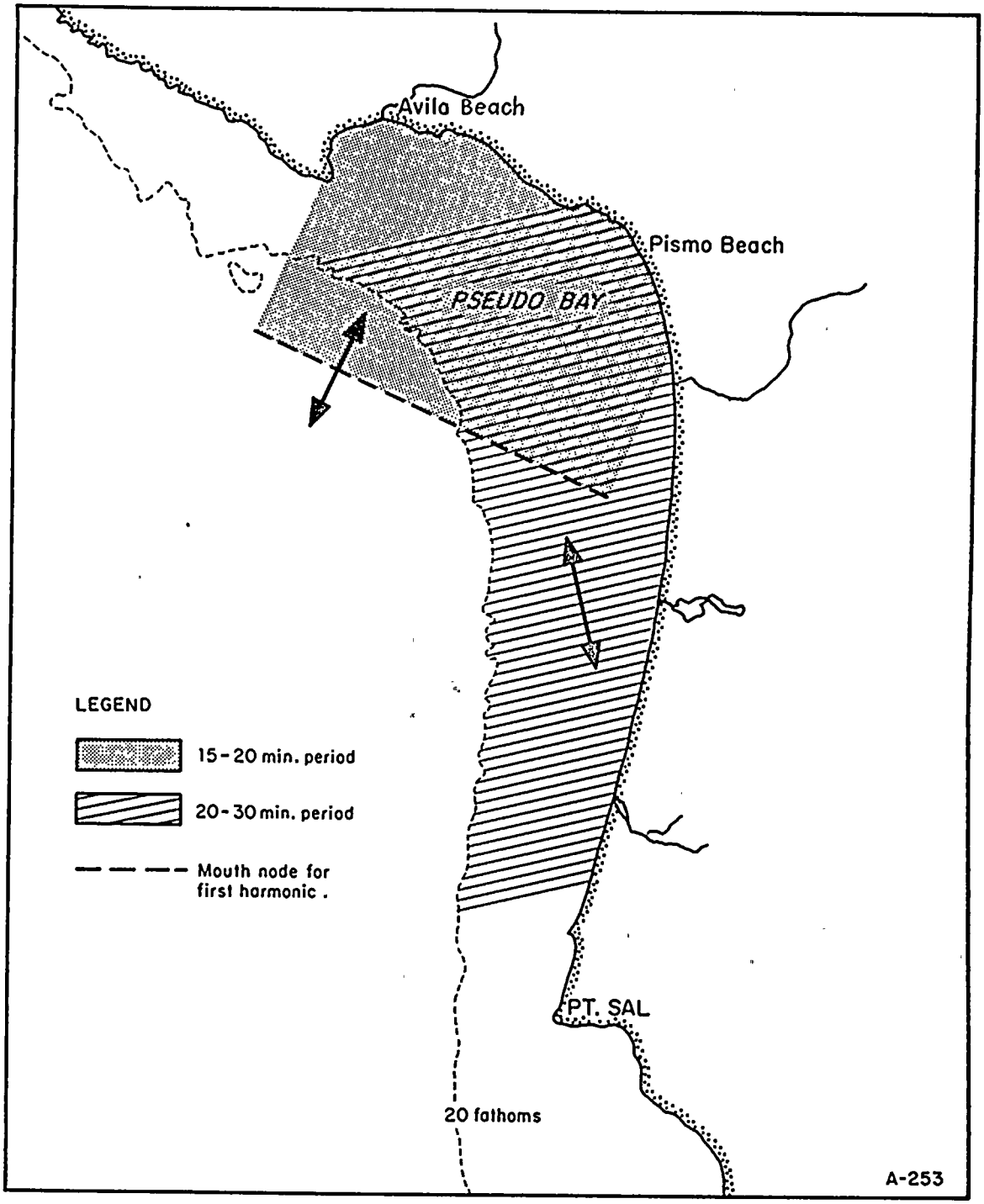

Figure 5.

A suggested bay configuration which may relate to seiching (shaded), and a possible area of reflection. (hatched).

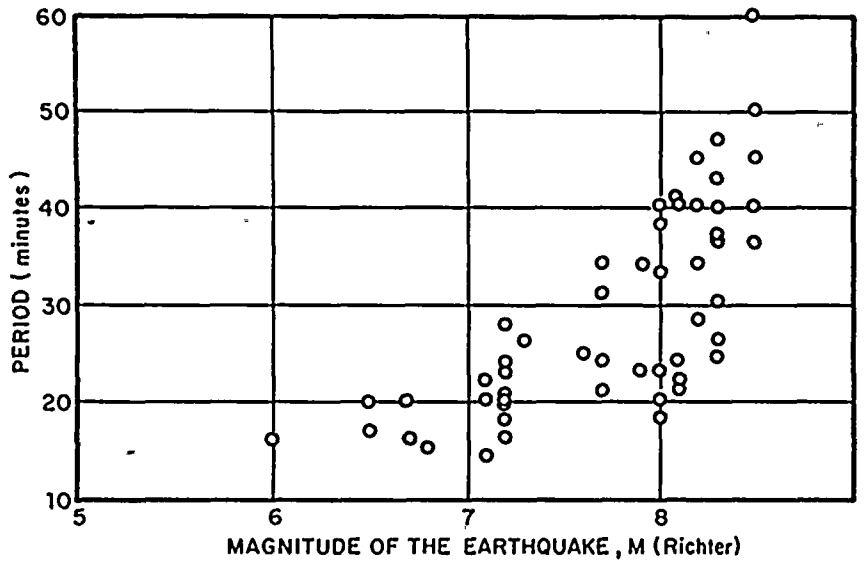

Figure 6a. Relationship between the predominant periods of tsunamis (analyzed from observations at various tide gauge stations) and earthquake magnitudes.

(from Iida, 1963a)

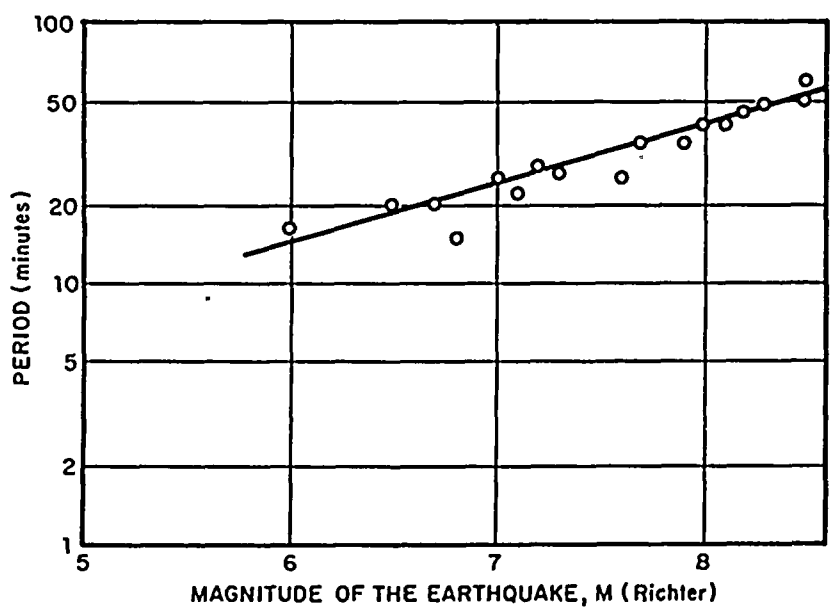

Figure 6b. Relationship between the maximum period of a tsunami and earthquake magnitude.

(from Iida, 1963a)

3.) Coastal configuration.

a.) Coastal canyons or river beds may channel the incident waves.

b.) A steep slope on shore will enhance runup.

Dr. Benioff and Dr. Smith, in a separate report to Pacific Gas and Electric Company (dated December 1966), have outlined the probable areas of seismic activity along the California coast north and south of the Diablo Canyon area. They list the location for three probable offshore earthquakes. We might consider first the possibilities of tsunami generation by each of them, and then go on to consider the other sources and the effects of the intervening region on the waves indicated. Because we will be dealing solely with the California region, we shall draw heavily on the Notes from the Tsunami Conference mentioned earlier. We may turn to the Japanese data for upper limits to wave heights and runup elevations that may be correlated with earthquake magnitude.

It is probably worthwhile to restate the parameters effective in generating a tsunami from an "earthquake-fault" occurrence. The length of the fault and magnitude and direction of the slip are quite critical. Whether or not a vertical component can arise from the slip movement is often considered as the deciding argument in the effectiveness of the fault as a tsunami generator. Strike-slip and dip-slip faulting form the two extremes; the horizontal motion of the strike-slip fault offers the least efficient coupling, and vertical motion of the dip-slip conversely offers the most efficient coupling between sea bottom and water. While the depth of water over the generating

point may not govern the total energy imparted to the water, it does affect the magnitude and period of the tsunami wave(s) produced. Deep water may produce tsunami waves of greater magnitude and shorter period.

The orientation of the long axis of the fault to the shore has several implications: (1) a greater percentage of tsunami energy is directed perpendicular to the major fault axis, (2) a fault axis directed normal to the shore in an offshore area of extreme relief may create a vertical component of motion where only horizontal motion along the slip occurs.

Considering specifically, then, the probable seismic generators listed by Drs. Benioff and Smith: the Santa Ynez Fault Extension is the first mentioned. It is an east-west trending fault which orients approximately perpendicular to the coast. Its movement is estimated to be horizontal, and since the relief is not extreme in the area its vertical component would appear to be small. The length of the fault is 80 miles, and its slip motion of 10 feet in the horizontal offers a poor energy coupling with the overlying water. Water depths in the area of the fault are generally shallow. One can envision a radiation pattern with its maximum directed parallel to shore, but with the beam width rather broad, reducing the capability for directionality. In effect, it would appear that if indeed any tsunami could be produced by the Santa Ynez Extension, it would have to be of very moderate magnitude. The November 4, 1927 earthquake is an historical example having occurred in the same area. It produced a tsunami which reached a runup height of about six feet at Avila Beach and Pismo Beach. There is still some speculation by authorities in the field of tsunami research as to whether the tsunami was generated by the

fault or by an accompanying slump. The 1812 Santa Barbara earthquake may possibly be considered as another example because of its having originated in the same general area. It is difficult, however, to conclude very much of definite value from the records of the accompanying tsunami. Even with the extensive investigation carried out by Marine Advisers, Inc. of historical documents, mission records, private letters, and Dr. Louderback's private papers, the true nature of the tsunami is sketchy. It seems that wave heights might have been approximately of tidal range in the vicinity of the Morro Bay-Avila Beach area. No other significant seismic events are foreseen for the region generally to the south of the Diablo Canyon site. No other tsunamis of significant size have originated from the site southward.

To the north of the site area, the seismic report lists two possible offshore seismic events. That of major magnitude is the San Andreas Fault Extension after it dips below the sea at the mouth of Alder Creek. Although it is some 420 miles from the site, its fault length (100 miles) and magnitude (7.0 Richter) bring it into the category of a possible local source for tsunamis. It appears to offer a minimal possibility for tsunami generation, however, because of the strike-slip nature of its movement. The offshore relief along the trace of the fault line is moderate and does not indicate any vertical component of motion arising from the horizontal slip of 10 feet suggested by the Benioff-Smith report. The very poor coupling offered by the conditions in evidence would transmit a very low percentage of energy to the overlying water. The historical evidence bears this out. The 1906 earthquake near San Francisco created no tsunami, nor did the earlier 1857 earthquake in

the same region.

The last offshore source of earthquake-fault generation indicated by the report is the Gorda Escarpment. Conditions here would appear to offer good possibilities for tsunami generation. The motion is anticipated to be all vertical, approximately 5 feet. This should offer good coupling between the ground motion and the water above.

This should, by the accepted definition of local sources, be classified as a distant source, since it is located more than ten diameters from the area of interest (a long dimension of 40 miles located 420 miles from Diablo Canyon). It will be treated here, however, because it is near the dividing line in classification between local and distant sources. We will be mindful that the distance of travel will allow for some dispersion of the initial wave into a wave train form, and that it will reach the site with some reduction of energy from its initial form.

Concerning the seismic disturbance as a tsunami generator, the orientation of the fault's major axis is east-west, suggesting maximum radiation parallel to the coastline and minimum radiation onshore; however, the relatively short length of the fault is related to the radiation pattern in such a manner that a short generating axis means a fairly broad beam width and thus poor directivity. Water depths in this area may be considered to be deep relative to the other two possible sources. Considering all of these factors and remembering the distance of the source from the site, an upper limit to wave height generation of about 3.5 feet and to runup heights of about 6 feet is reasonable (Iida's data, 1963a, Figure 7, and Tables 1 and 2).

Table 1

Magnitude of Tsunamis
(according to Iida)

Magnitude 0	The first classification includes tsunamis with wave-height of the order of one meter (3.28 feet.); no damage.
Magnitude 1	The second classification includes tsunamis with wave-height of the order of 2 meters (6.56 ft.); house-damage along the coast, ships washed ashore.
Magnitude 2	The third classification includes those tsunamis with wave-height of the order of 4-6 meters (13-20 ft.); some destruction of houses, considerable loss of life.
Magnitude 3	The fourth classification comprises those tsunamis with wave-height of 10-20 meters (33-66 ft.); damaged area along the coast running about 400 kilometers.
Magnitude 4	The fifth classification of tsunami is those of the severest with the maximum wave-height of more than 30 meters (100 ft.); damaged area along the coast running more than 500 kilometers.

Note: Magnitudes given here are in wave heights, measured from wave trough to wave crest. Amplitudes, as a rough estimation, may be considered as one-half the wave height or that portion of the wave above the water level.

Runups, rather than wave heights, are given in Table 2. Runup is the ultimate concern on shore because it is the elevation attained by the water.

mis with wave-height
no damage.

nami with wave-height
use-damage along the

tsunamis with wave-
20 ft.); some
ss of life.

ose tsunamis with
.); damaged area along
s.

ose of the severest
e than 30 meters
t running more than

ured from wave
stimation, may be
rtion of the wave

Table 2. Runup is
levation attained

Table 2

Magnitude, Energy, and Runup Elevation of Tsunamis in Japan
(after Iida, 1963a)

Tsunami Magnitude Classification (m)	Tsunami Energy ergs	Tsunami Energy (ft-lb)	Maximum Runup Elevation (meters)	Maximum Runup Elevation (ft)
5	25.6×10^{23}	18.9×10^{16}	> 32	> 105
4.5	12.8	9.4	24-32	79.0-105
4	6.4	4.7	16-24	52.5-79
3.5	3.2	2.4	12-16	39.2-52.5
3	1.6	1.2	8-12	26.2-39.2
2.5	0.8	0.59	6-8	19.7-26.2
2	0.4	0.29	4-6	13.1-19.7
1.5	0.2	0.15	3-4	9.9-13.1
1	0.1	0.074	2-3	6.6-9.9
0.5	0.05	0.037	1.5-2	4.9-6.6
0	0.025	0.018	1-1.5	3.2-4.9
-0.5	0.0125	0.0092	0.75-1	2.5-3.2
-1	0.006	0.0044	0.50-0.75	1.6-2.5
-1.5	0.003	0.0022	0.30-0.50	1.0-1.6
-2	0.0015	0.0011	< 0.30	< 1.0

In addition to direct seismic generation of tsunamis, a secondary source of generation must be considered. Submarine landslides or slumping may occur along the shelf and slope regions, and if sufficiently large may produce tsunamis. Several tsunamis have been attributed to this source. Some indication of the prospects of future generation can be gained from such considerations as the rate of sediment buildup along the shelf, the historical evidence of slumping in older sediments, and the steep ness and depth of the offshore features. The central California shelf zone is characterized by a relatively low rate of sediment renewal. No major rivers empty at the heads of submarine canyons, which reduces the likelihood of frequent, large-scale slumping down the canyon walls. The offshore shelf and slope are not steep enough to facilitate high speeds in slumping, nor are any trenches present which would offer great depths of water, synonymous with offering great potential energy to the slump material.

Continuous acoustic profiling by Curray (Bull. G.S.A. In Press) in the northern section of the California offshore region (Cape Mendocino to south of Monterey) shows the existence of some relict slide areas, probably of tertiary age. It is the older material that seems to offer the greater prospect for slumping because of the low rate of present day transport and buildup.

Slumping offers a much poorer coupling than does seismic activity. Wiegel has shown from laboratory experiments that probably less than 1% of the energy of the slump is transmitted to the surrounding water. The largest known slide in the area is that located down the slope west of the Farallon Islands off San Francisco. It is possibly 500 meters thick and extends about

15-20 kilometers in its east-west dimension. To gain an understanding of the size of tsunami that might be generated by such a slide we may assume a density of about 2, a north-south dimension of 15 kilometers and an individual drop of 10 meters. With a coupling efficiency of 1%, which may be on the high side, an energy of some 10^{21} ergs would result. Considering the energy values versus magnitude of tsunamis from Iida (Table 2) a tsunami magnitude of 0.5-1.0 may be expected. This transposes to a wave height of approximately 7.0 feet and runup of perhaps 8.0 feet at Diablo Canyon.

In summary then: the seismic sources anticipated by Drs. Benioff and Smith would offer the possibilities of generation of moderate tsunamis, with the best generator the Gorda Escarpment; slumping may be a secondary concern, with the largest slide known to have occurred in the local area capable of having generated a tsunami wave up to about 7.0 feet.

The offshore topography in the vicinity of the site seems to offer no unusual features that may converge or channel the approaching waves. The ridge with 150-foot relief directly off Diablo Canyon, its long axis parallel to the coastline, would appear to slightly disperse the energy density of the tsunamis propagating along the coast. Because of the moderate nature of the prospective tsunamis and the steepness of the shelf offshore from Diablo Canyon, bore formation is not indicated.

It must be stressed that the nature of the area's response to incident tsunamis is one of dominance of the downsurge as the extreme expression. Avila has shown a drawdown maximum of more than 11 feet with a duration of 9-14 minutes during the 1964 Alaskan tsunami. During the same disturbance,

the areas near Morro Bay (still in the Estero Bay region) experienced observed drawdowns of 6-7 feet maximum with an undetermined duration. In view of the indications of Section II that Avila may be governed in great part by the oscillations of San Luis Obispo Bay, the Diablo Canyon area probably would follow the Estero Bay region and show drawdowns on the order of 7 feet.

There is still to be considered the extreme elevation of water level possible. This might be achieved by the superposition of the tsunami and extreme tidal stand during an accompanying storm. The tide range approaches 6 feet and we may assume a storm surge of 1 foot with shorter period storm waves of 3 foot amplitude. This may be considered representative of the Diablo Canyon area. As the hypothetical tsunami runup height we may assume 8 feet as the greatest magnitude, as shown by the preceding considerations. At high tide stand (MHHW) with the storm, a total height of 15 feet above MLLW, with short-period heights up to 18 feet MLLW could be experienced (adding the amplitude of the storm wave). At low tide stand (MLLW) without the storm surge but with the short period storm waves, and assuming the maximum extreme of the tsunami were a downsurge, a drop in water level of as much as -6 feet MLLW with short period drops to -9 feet MLLW may be possible. The duration of the longer period extremes might be reckoned at up to 15 minutes (1/2 of one of the dominant tsunami periods).

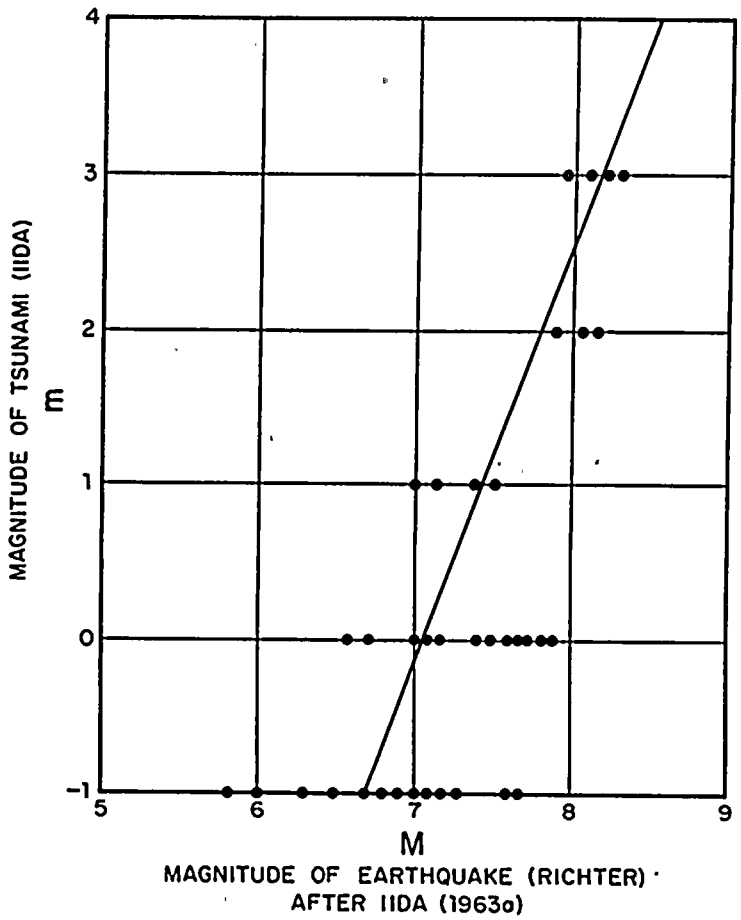

Figure 7. Magnitude of tsunamis correlated with earthquake magnitude.

CONCLUSIONS

The history of response to distantly-generated tsunamis at the Avila Beach area shows a slightly greater response than the California coast in general, but this is shown to be a local feature of the embayment wherein a Coast and Geodetic Survey tide gauge for the Avila Beach area is located. Our investigation indicates that the Diablo Canyon site may be considered to be as responsive as the coast in general, i.e., on the order of the average astronomical tidal range (six feet).

Locally-generated tsunamis are estimated to offer runup heights on the order of 8 feet after considering not only the possible sources of seismic activity postulated by Benioff and Smith, but slumping or submarine landslides as well.

The situation of a tsunami occurring simultaneously with a high or low tide and considering a storm (at high tide only) producing a 1.0 foot surge and 3.0 foot amplitude shorter period waves in the area could produce possible upper and lower water levels of 18.0 feet and -9.0 feet MLLW respectively. The duration of the levels is dependent on the periods of the waves in combination.

REFERENCES

Benioff, H. and S. Smith, 1966, Seismic Evaluation of the Diablo Canyon Site, report to Pacific Gas and Electric.

Beach Erosion Board, 1957, Technical Report No. 4, U.S. Army Corps of Engineers, p. 89.

Carr, John H., 1953, Long-period waves or surges in harbors, Trans. ASCE, 118, paper No. 2556, pp. 588-603.

Curray, J. R., Large gravity slides, continental slopes of central California, Bull. Geol. Soc. Am. (In press)

Green, C. K., 1946, Seismic sea wave of April 1, 1946, as recorded on tide gages, Trans. AGU, v. 27, No. IV, pp. 490-500.

Honda, K., et al., 1908, An investigation on the secondary undulation of oceanic tides, J. College of Sci. Imp. Univ. of Tokyo, 24, 1-113.

Iida, K., 1963a, On the estimation of tsunami energy, Proc. tsunami meetings associated with the Tenth Pacific Science Congress, Monograph No. 24, IUGG, pp. 167-173.

Iida, K., 1963b, Magnitude, energy, and generation of tsunamis, and catalogue of earthquakes associated with tsunamis, Proc. tsunami meetings associated with the Tenth Pacific Science Congress, Monograph No. 24, IUGG, pp. 7-18.

Iida, K., 1958, Magnitude and energy of earthquakes accompanied by tsunami and tsunami energy, J. Earth Sciences (Nagoya Univ.), v. 6, No. 2, pp. 101-112.

Kaplan, Kenneth, 1955, Generalized laboratory study of tsunami runup, U.S. Army Corps of Engineers, Beach Erosion Board, Tech Memo No. 60.

Marine Advisers, Inc., 1965, Examination of tsunami potential at the San Onofre Nuclear Generating Station, Unpubl. report to So. Calif. Edison Co., submitted to Atomic Energy Commission Reactor Licensing Division, 1965.

Miller, Gaylord R., 1964, Dissertation on Ph.D., Tsunamis and Tides, Univ. of Calif., San Diego.

Munk, W. H., 1963, Long Ocean Waves, The Sea, v. I., Interscience Publishers, New York, pp. 659-661.

REFERENCES (Continued)

Munk, W. H., F. Snodgrass, and M. J. Tucker, 1959, Spectra of low frequency ocean waves, Bull. Scripps Inst. of Oceanogr., v. 7, 4, pp. 283-362.

Svyatlovski, A. E., 1957, Tsunamis, Council for Seismology, USSR Acad. of Sciences Publ. House, Moscow, 45 pp.

Thorade, H., 1931, Probleme der Wasserwellen, Probleme d. kosm. Physik, 13/14.

U.S. Coast and Geodetic Survey, 1960, The tsunami of May 22, 1960 as recorded at tide stations, Dept. of Commerce.

U.S. Coast and Geodetic Survey, 1965, Prince William Sound, Alaskan Earthquakes, Dept. of Commerce.

Van Dorn, W. G., 1965, Tsunamis, Advances in Hydroscience, v. 2, pp. 1, 48, Academic Press, New York.

Wastler, T. A., 1963, Application of spectral analysis to stream and estuary field surveys, Part I. Individual power spectra, U.S. Dept. of Health, Education and Welfare, Public Health Service.

Wiegel, R. L., 1964, Oceanographical Engineering, Prentice Hall, Inc., Englewood Cliffs, N.J.

Wiegel, R. L., 1955, Laboratory studies of gravity waves generated by the movement of a submerged body, Trans. Amer. Geophys. Union, v. 36, No. 5, pp. 759-774.

This report is submitted by Marine Advisers, Inc., La Jolla, California, on January 5, 1967.

Approved by:

Paul L. Horrer
President

Noel B. Plutchak
Principal Investigator

DIABLO CANYON SITE

SAN LUIS OBISPO COUNTY

REPORT PREPARED BY THE METEOROLOGY OFFICE

PACIFIC GAS AND ELECTRIC COMPANY

SEPTEMBER 29, 1966

(REVISED DEC. 20, 1966)

APPROVED: Leon M. Hunsaker

Leon M. Hunsaker

Senior Meteorologist

A. Available Data

The meteorological data presented in this report was obtained from stations located near Diablo Canyon. Table 1 lists these stations and the type of information gathered in addition to the approximate period of record.

B. Temperatures

Table 2 summarizes the temperature data from Pismo Beach and Morro Bay. The information shows a winter mean temperature of 54°F, and a summer mean of about 60°F. Considering the extremes at these locations, the highest and lowest temperatures likely at the site would be near 102°F and 26°F respectively. About three days during the year, the temperature would be 90°F or higher, and about five days, 32°F or lower.

C. Precipitation

Annual precipitation along the coast near the site varied from 13.87 inches at Morro Bay to 21.11 inches 12 miles inland at San Luis Obispo. Thus, a reasonable estimate of annual precipitation at Diablo Canyon would be about 15 to 17 inches. Slightly more than 80 percent of this amount would fall during the months November through March. Using the ten-year record of Pismo Beach as a guide, the annual rainfall has varied from a low of 8.96 inches in 1953 to a high of 27.39 inches in 1958. The same figures for San Luis Obispo are 9.94 inches in 1953 to 29.34 inches in 1958. The average monthly rainfall in the "wet" season would range from about 1.7 to about 4.7 inches. Also, during the "wet" season, about 22 days would have 0.1 inch or more rainfall, and an additional 11 days would have 0.5 inch or more. A summary of the available precipitation data is provided in Table 3.

Snowfall at the site would be extremely rare. However, on the nearby higher hilltops, a trace of snow may fall during the coldest winter storms.

D. Storms

Stormy weather would occur mainly during the months November through March, although a few storms either side of this period each year would not be unlikely. Storms during the winter season can be expected to produce about eleven days of precipitation greater than or equal to 0.50 inch in 24 hours. Only two days with precipitation of this magnitude would fall outside this season. Southeasterly winds will usually accompany storm activity and gusts equal to or in excess of 40 miles per hour can be expected at times.

Winds of hurricane force would be extremely rare.

Thunderstorms, although infrequent, can be expected a few times a year including both winter and summer seasons. The average occurrence of lightning is less than three days per year.

Small hail (one quarter inch or less in diameter) may fall a few times during the winter season accompanying the passage of colder, more vigorous storm systems.

E. Winds

Santa Maria and Point Arguello are the only two locations near the site with reliable records of wind measurement. Six wind rose figures are attached showing the following:

For Santa Maria (1938-1941)

Figure 1 - Annual Surface Windrose

Figure 2 - Seasonal Surface Windroses

For Santa Maria and Point Arguello (1959-1962)

Figure 3 - Annual Surface Windrose

Figure 4 - Annual 1000 MB Windrose

Figure 5 - Annual 100 ft. Windrose

Figure 6 - Annual 950 MB Windrose

Santa Maria's annual surface and seasonal wind roses are based on several hourly observations per day taken during the period June 1938 to December 1941. Table 4 summarizes this data on an annual basis.

Records from Santa Maria and Point Arguello were combined to produce Figures 3 through 6 showing annual frequencies during the period January 1959 to July 1962. Data were obtained from observations twice daily, 4 a.m. and 4 p.m., PST. The wind speed data is summarized in Table 5.

The most significant indication from the accumulated information is the high frequency of northwesterly winds. At Santa Maria/Point Arguello, for example, the surface wind blows from the northwest quadrant 48.4% of the time annually. In the winter season, however, southeast winds are almost as frequent as northwest winds.

The annual average surface wind speed at Santa Maria/Point Arguello is about 9 miles per hour; while at about 1800 feet it reaches nearly 15 miles per hour. The average surface elevation of these two stations is about 300 feet above mean sea level.

Topography plays an important role in wind determination at any location. Hills in the vicinity of Diablo Canyon are expected to produce some channeling of the northwesterly flow. At points of land that extend out towards the ocean, higher wind velocities than those at the site can be expected.

F. Stability

Stability at a given point is determined by the change of temperature in the vertical, or what is commonly called the "lapse rate." The subsiding or descending air associated with the Pacific Anticyclone produces a temperature inversion along the California coast. Under the inversion, the atmosphere is relatively unstable; while above, stable.

A seasonal variation in the strength and height of this inversion occurs due to the southward movement of the Pacific Anticyclone in the winter (November to March). Almost coincident with this development, the Pacific storm track moves southward allowing stormy weather to enter the state. When storms occur, the inversion may disappear altogether. On the other hand, the inversion is the strongest and most persistent in summer (May to September) when the Pacific Anticyclone is nearest the West Coast.

Figure 7 shows the variation of the inversion's height at Santa Maria/Point Arguello each month at 0300 PST (Pacific Standard Time) and 1500 PST. In summer, when the inversion is strongest, the average heights are 370 meters at 0300 PST and 499 meters at 1500 PST. In winter, the average heights are 271 meters at 0300 PST and 679 meters at 1500 PST.

G. Annual Diffusion Model

1. Discussion of Basic Modelling Criteria

Diffusion models for continuous sources are essentially mass continuity equations that define the spatial distribution of the effluent as a function of travel distance downwind from the source. As pointed out by Pasquill (1962, pp 184-185), any complete expression of this type must specify the following features:

1) The form of the distribution of concentration along both the crosswind and vertical coordinates of the plume.
2) The crosswind and vertical dimensions of the plume of diffusing material.
3) The continuity or material balance condition in which any losses of material through decomposition, decay, deposition, or other removal processes are specified.

Most practical formulas currently used for estimating ground-level diffusion patterns downwind from continuous elevated point sources are in the form of a Gaussian plume equation given by the expression:

$$\chi\{x,y,0;h\} = \frac{Q}{\pi \bar{u}\, \sigma_y(x)\, \sigma_z(x)} \exp\left[-\frac{1}{2}\left\{\frac{y^2}{\sigma_y^2(x)} + \frac{h^2}{\sigma_z^2(x)}\right\}\right] \tag{1}$$

where h is the effective release height and the other symbols follow conventional usage. It has been shown (Cramer, 1959; Cramer et al., 1965) that the downwind distance dependence of the standard deviations of the crosswind and vertical concentration distributions are conveniently expressed by

$$\sigma_y(x) = \sigma_A'' \, x^q \tag{2}$$

and

$$\sigma_z(x) = \sigma_E'' \, x^p \tag{3}$$

where p and q are constants; Sigma A" and Sigma E" are, respectively, the standard deviations of azimuth and elevation angle expressed in units of radians x meters^{1-q} and radians x meters^{1-p}. If the effects of multiple reflection of the effluent between the base of a temperature inversion and the ground surface (Milly, 1958; Bierly, and Hewson, 1962), and the time averaging of the concentration estimates are included, the general expression for the ground-level concentration becomes

$$\bar{\chi}\{x,y,0;h,\tau,H_m\} = \frac{Q}{\pi \bar{u}\, \sigma_A'(\tau)\, \sigma_E'\, x^{p+q}} \exp\left(-\frac{y^2}{2\sigma_A'^2(\tau)\, x^{2q}}\right)$$
$$\cdot\left\{\exp\left(-\frac{h^2}{2\sigma_E'^2 x^{2p}}\right) + \sum_{n=1}^{\infty}\left[\exp\left(-\frac{(2nH_m-h)^2}{2\sigma_E'^2\, x^{2p}}\right) + \exp\left(-\frac{(2nH_m+h)^2}{2\sigma_E'^2\, x^{2p}}\right)\right]\right\} \tag{4}$$

where H_m is the height of the inversion base above ground level and Tau is the time over which Chi-Bar is measured. In general, the vertical diffusion coefficient Sigma E' is not significantly dependent on Tau due to the limitation on the maximum size of vertical eddies imposed by the proximity of the ground surface. The lateral diffusion coefficient Sigma A' on the other hand, is significantly dependent on Tau due to the

quasi-continuous variation of the lateral component of the wind velocity over a very broad frequency range. It has been found empirically (Cramer, 1959; Cramer et al., 1964; and others) that the dependence of Sigma A' on Tau is given by a one-fifth power law of the form

$$\sigma_A\{\tau\} = \sigma_A\{\tau_o\}\left[\frac{\tau}{\tau_o}\right]^{1/5} \tag{4a}$$

Also, in defining the lateral and vertical plume dimensions, provision is often made for a region of rectilinear expansion close to the source in accord with theoretical expectation. In this case, Equations (2) and (3) above may be expressed as

$$\sigma_y\{X\} = \sigma_A' X_r \left[\frac{X}{X_r}\right]^q \quad ; \qquad X \geq X_r \tag{2a}$$

$$\sigma_z\{X\} = \sigma_E' X_r \left|\frac{X}{X_r}\right|^p \quad ; \qquad X \geq X_r \tag{3a}$$

where X_r is the distance downwind from the source over which rectilinear expansion occurs. In the case of the continuous point source, appropriate values for X_r generally fall within the range of 10 to 100 meters. Appropriate values for q generally are between 0.9 and 0.8 while the corresponding values for p range from about 1.0 to 0.6, depending on the thermal stratification (Cramer, 1959).

If Equations (2) and (3) are inserted in Equation (1) and the resulting expression is maximized, the maximum ground-level concentration Chi_{mg} (Cramer, 1959) is

$$\chi_{mg} = \frac{Q\left[\frac{p+q}{p}\right]^{\frac{p+q}{2p}} \sigma_E'^{\,\frac{p+q}{p}-1}}{\pi\,\bar{u}\,h^{\frac{p+q}{p}}\,\sigma_A'} \exp\left(-\frac{p+q}{p}\right) \tag{5}$$

Similarly, the distance X_{max} from the stack at which Chi_{mg} occurs is given by

$$X_{max} = \left[\frac{h^2 p}{\sigma_E'^2 (p+q)}\right]^{\frac{1}{2p}} \tag{6}$$

When both p and q are unity, the above expressions become

$$\chi_{mg} = \frac{2Q}{\pi \bar{u} e h^2} \cdot \frac{\sigma_E'}{\sigma_A'} \tag{5a}$$

and

$$X_{max} = \frac{h}{\sqrt{2}\ \sigma_E'} \tag{6a}$$

The ratio Sigma E'/Sigma A' is generally within the range from 1.0 to 3.0 for sampling times of the order of 10 minutes to 1 hour. Pasquill (1962, p. 250) cites a large number of smoke puff observations made near Harwell during the daytime from which it was deduced that the average value of the ratio (Sigma A'/Sigma E') for a 15-minute averaging time is 1.5 at 100 ft. above the ground and 1.06 at 500 feet.

2. Long Term Diffusion Models

The long term ground-level diffusion patterns downwind from a continuous elevated point source have previously been investigated by Meade and Pasquill (1958). On the assumption that the instantaneous plume width is narrow, the integral of concentration taken along an arc of radius X downwind from the source is to a sufficient approximation given by the expression (see Pasquill, 1962, p. 245)

$$\int_{-\infty}^{\infty} \chi\{x, y\}\, dy \tag{7}$$

It follows that the long term average concentration Chi-Bar around a circle of radius X is

$$\overline{\chi}_{(circle)} = \frac{1}{2\pi x} \cdot \frac{2Q}{\bar{u}\sqrt{2\pi}\,\sigma_z} \exp\left(-\frac{h^2}{2\sigma_z^2}\right) \tag{8}$$

Also, the long term average concentration over an octant of the circle is

$$\overline{\chi}_{(octant)} = \frac{f(\theta)}{12.5} \cdot \frac{1}{2\pi x} \cdot \frac{2Q}{\bar{u}\sqrt{2\pi}\,\sigma_z} \exp\left(-\frac{h^2}{2\sigma_z^2}\right) \tag{9}$$

where $f(\theta)$ is the percentage frequency of wind directions affecting the octant. Meade and Pasquill then obtained values of $f(\theta)/\bar{u}$ for various octants from routine wind records for six five-month seasons. In the absence of measurements of either the vertical extent of the plume or elevation angle, Meade and Pasquill used measured ground-level concentrations and regression analysis techniques to obtain an empirical solution of Equation (9) at a fixed downwind distance of 1500 yards. The analysis was not extended to other distances since this was not necessary for the purpose of the work. Gifford (1961) has presented a long term concentration model of the same form as that used by Meade and Pasquill.

Following Meade and Pasquill (1958), for purposes of calculating long term diffusion patterns, the equation of the ground-level concentration for emission from a continuous elevated point source may be written in the form:

$$\overline{\chi}\{r, \theta, 0; h\} = \frac{2\,Q\,f_i(\theta)}{\sqrt{2\pi}\,\bar{u}\,\theta_i\,\sigma_E'\,r^{1+p}} \exp\left(-\frac{h^2}{2\sigma_E'^2 r^{2p}}\right) \tag{10}$$

where r is the radial distance downwind from the source (meters); h is the effective stack height (meters); and $f_i(\theta)$ is the fraction of azimuth wind direction assigned to an arbitrary angular sector θ_i.

The form of the crosswind or lateral distribution of concentration in this case is given by the long term azimuth wind distribution.

If Equation (10) is maximized, the radial distance r at which the maximum ground-level concentration occurs is

$$r_{max} = \left[\frac{p h^2}{(1+p)\, \sigma_E'^2} \right]^{\frac{1}{2p}} \tag{11}$$

The expression for the maximum concentration, obtained by substituting Equation (11) in Equation (10) is

$$\overline{\chi} = \frac{2\, Q\, f_i}{\sqrt{2\pi}\, \bar{u}\, \theta_i\, \sigma_E' \left[\frac{p h^2}{(1+p)\, \sigma_E'^2} \right]^{\frac{1+p}{2p}}} \exp\left(- \frac{1+p}{2p} \right) \tag{12}$$

For p = 1, this expression becomes

$$\chi_{max} = \frac{4\, Q\, f_i\, \sigma_E'}{\sqrt{2\pi}\, \bar{u}\, \theta_i\, h^2\, e} \tag{13}$$

The effect of an inversion "lid" at height H_m, where $H_m > h$, may be included by replacing the exponential factor in Equation (10) with the exponential factor of Equation (4) involving vertical expansion:

$$\overline{\chi}(r, \theta, 0; h, H_m) = \frac{2\, Q\, f_i(\theta)}{\sqrt{2\pi}\, \bar{u}\, \theta_i\, r^{1+p}}$$

$$\cdot \left\{ \exp\left(- \frac{h^2}{2\sigma_E'^2 x^{2p}} \right) + \sum_{n=1}^{\infty} \left[\exp\left(- \frac{(2nH_m - h)^2}{2\sigma_E'^2 x^{2p}} \right) + \exp\left(- \frac{(2nH_m + h)^2}{2\sigma_E'^2 x^{2p}} \right) \right] \right\} \tag{14}$$

H. Meteorological Investigations

In order to obtain meteorological data of a pertinent local nature for design and operating considerations, a measurement network will be constructed at the site. Measurements will be oriented toward obtaining the meteorological data needed as input to the analytical model described in Section G. above.

The on-site data collection system will consist of meteorological instruments mounted on a 250 foot tower at the plant site and on a 100 foot tower at the top of a 914 foot hill overlooking the site. Measurements will also be taken at four additional locations. The meteorological data gathering network is shown in Figure 8.

The meteorological equipment which will be used is as follows:

1. Observational network for coastal plain.
   This network consists of:
   a. A 250' tower located at the plant site (Point E on Figure 8).
   b. Two 33' poles located at points near the southern boundary of the site (Points A and B on Figure 8). Measurements from these locations will verify the expected channeling effect under northwesterly wind flow patterns.

2. Observational network for top of hills.
   This network consists of:
   a. A 100' tower located on top of the 914' hill which overlooks the site.

3. Observational network for Diablo Canyon.
   This network consists of:
   a. Two 33' wood poles, one located near the canyon mouth and the other approximately a mile up the canyon.

4. Towers E and F will be instrumented as follows:
   a. At top of both towers:
      1) Wind
         a) Bi-Vane
         b) Cup and Vane
      2) Temperature Sensor (ΔT) - 250' tower only.
   b. At bottom:
      1) Wind
         a) Cup and Vane at 30' level on 250' tower only (Point E, Figure 8).
      2) Temperature
         a) Temperature Sensor (ΔT) - 250' tower only. (Install at 30' level on 250' tower.)

b) Ambient Temperature - both towers. (Install at 30' level on 250' tower and at regular instrument shelter height (5-6' above ground on or near 100' tower).)

c. Cup and vane wind equipment should be installed on top of the 33' wooden poles (Points A, B, C, and D on Figure 8). In addition, an ambient temperature measurement should be made (5-6' above ground), at Point B near the southern boundary of the site.

d. A recording rain gage near the plant site.

REFERENCES

Bierly, E. W. and Hewson, E. Wendell (1962), "Some Restrictive Meteorological Conditions to be Considered in the Design of Stacks," Journal of Applied Meteorology, pp. 383-390.

Cramer, H. E. (1959), "Engineering Estimates of Atmospheric Dispersal Capacity," Industrial Hygiene Journal.

Cramer et al. (1964), "Meteorological Prediction Techniques and Data System," GCA Report Prepared for U.S. Army Chemical Corps Proving Ground, Dugway, Utah, 252.

Gifford, Frank A. (1961), "Atmospheric Dispersion Calculations Using the Generalized Gaussian Plume Model," Vol. 2, No. 4, Nuclear Safety, reprint.

Meade and Pasquill (1958), "A Study of the Average Distribution of Pollution Around Staythorpe," International Journal of Air Pollution, Vol. 1, p. 60.

Milly, George H. (1958), "Atmospheric Diffusion and Generalized Munition Experiments," ORG Study NR 17, U.S. Army Chemical Corps, 290.

Pasquill, F. (1962), Atmospheric Diffusion, D. Van Nostrand Co., New York, 297.

TABLE - 1

STATION INDEX

Station	Elevation (feet)	Observer	Period of Record From	Period of Record To	Type of Observation
Morro Bay	115	Fire Department	Feb., 1959	Jan., 1965	Temperature, Precipitation
Pismo Beach	80	Police Department	Jan., 1951	Jan., 1960	Temperature, Precipitation
Point Arguello	367	Weather Bureau	July, 1959	July, 1962	Wind
San Luis Obispo	300	Cal State Poly College	Jan., 1951	Jan., 1961	Precipitation
Santa Maria Airport	238	Weather Bureau	June, 1938	Dec., 1941	Wind
Santa Maria Airport	238	Weather Bureau	Jan., 1959	July, 1959	Wind

TABLE - 2

TEMPERATURE DATA

Month	Mean Temperature	Mean Maximum	Mean Minimum	Extreme Maximum	Extreme Minimum	Mean No. of Days Above 90°F	Mean No. of Days Below 32°F
November	58.3(56.0)	69.4	47.1	91	29	0	0
December	54.6(53.0)	65.3	43.9	92	28	0	1
January	51.7(52.4	61.3	42.0	80	24	0	2
February	53.7(53.3)	64.0	43.4	82	29	0	1
March	54.8(53.1)	65.5	44.0	88	30	0	1
Wet Season Average	54.6(53.6)	65.1	44.1				
April	56.0(54.8)	66.1	46.1	90	32	0	0
May	57.3(54.1)	67.5	47.1	89	36	0	0
June	59.8(56.8)	69.8	49.7	96	40	1	0
July	60.5(58.2	68.7	52.3	104	38	0	0
August	60.6(59.7)	68.5	52.7	102	43	0	0
September	62.1(59.7)	71.8	52.3	99	41	1	0
Dry Season Average	60.1(57.7)	69.3	50.8				
October	60.6(60.9)	71.3	49.8	95	32	1	0

NOTES: 1. Data from Monthly California Climate Publications and ten year supplement.

2. Numbers in parenthesis are for Morro Bay (7 years of records). All others are from Pismo Beach from 1951 to 1960.

TABLE - 3

PRECIPITATION DATA

Month	Pismo Beach (10 Years of Records)			San Luis Obispo Poly (10 Years of Records)			Morro Bay Fire Station (7 Years of Records)
	Total	Days Above 0.1 inch	Days Above 0.5 inch	Total	Days Above 0.1 inch	Days Above 0.5 inch	Total
November	1.82	2	1	1.72	2	1	2.38
December	2.65	4	3	3.94	4	2	1.80
January	3.79	6	3	4.72	6	3	1.94
February	3.05	6	2	4.12	6	3	3.45
March	2.10	4	1	3.34	4	2	1.74
Wet Season Average	2.68			3.57			2.26
April	1.92	3	2	1.60	4	2	1.42
May	.34	1	0	.51	2	0	.25
June	.04	0	0	.11	0	0	.05
July	.06	0	0	.01	0	0	.00
August	.01	0	0	.02	0	0	.02
September	.20	0	0	.20	1	0	.23
Dry Season Average	.13			.17			.11
October	.46	1	0	.82	1	0	.59
Total	16.44			21.11			13.87

Data obtained from monthly California climate publications (Morro Bay) and ten year supplement 1951-1960 (San Luis Obispo and Pismo Beach).

TABLE - 4

ANNUAL WIND DATA SUMMARY, SANTA MARIA AIRPORT

1939 TO 1941

Wind Speed (mph)	N	NNE	NE	ENE	E	ESE	SE	SSE	S	SSW	SW	WSW	W	WNW	NW	NNW	Total	%
Calm (0-3)																	2213	37
4-15	78	28	83	25	193	200	231	28	67	14	83	77	865	830	494	28	3324	55
16-31	13	22	37	0	2	2	64	34	27	7	8	8	107	118	57	4	510	8
32-47	0	2	0	0	0	0	8	2	0	0	0	0	0	0	1	0	13	-
Over 47	0	0	0	0	0	0	4	0	0	0	0	0	0	0	0	0	4	-
Total	91	52	120	25	195	202	307	64	94	21	91	85	972	948	552	32	6064	
Percent	2	1	2	-	3	3	5	1	2	-	1	1	16	16	9	1	Calm 37	100

TABLE - 5

WIND SPEEDS - POINT ARGUELLO AND SANTA MARIA

JANUARY 1959 TO JULY 1962

Wind Speed (mph)	Frequency of Occurence (Percent) 0'	360'	1000'	1780' *
0-3	17.4	13.9	4.3	6.3
4-7	23.5	24.8	20.9	22.7
8-12	33.2	30.3	21.8	20.2
13-18	17.1	20.3	22.1	24.6
19-24	6.1	6.5	16.0	11.1
25-31	2.5	3.9	9.7	9.3
32-38	0.1	0.1	3.6	3.4
39-46	0.1	0.0	1.5	1.9
47 and greater	0.0	0.0	0.3	0.3
Total	100.0	100.0	100.0	100.0
Total Recordings	2548	2137	2440	2471

*Note: Headings in feet above mean sea level.

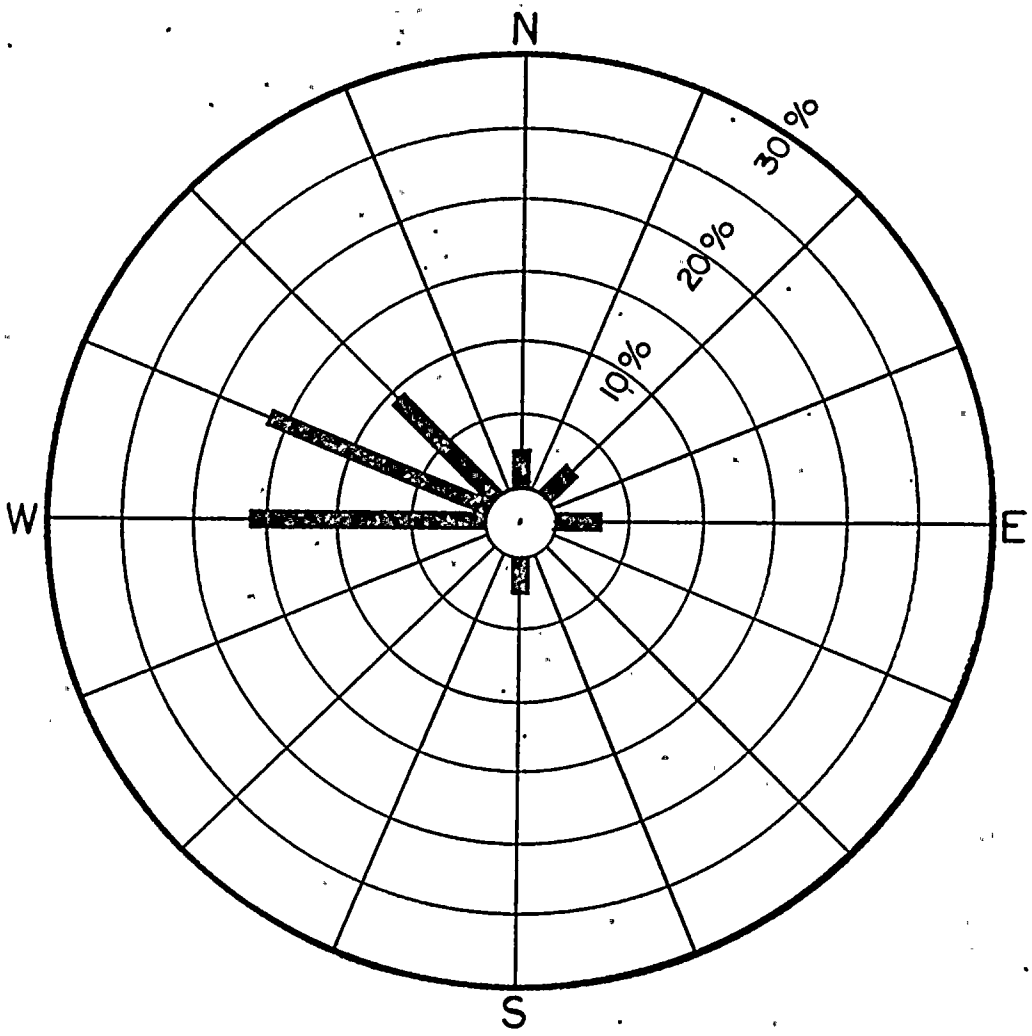

NOTES:

1. CALM CONDITIONS (0-3 mph) RECORDED 37 % OF THIS PERIOD
2. PERIOD OF RECORD JUNE 1938-DEC. 1941.
3. BASED ON SEVERAL OBSERVATIONS PER DAY

Figure 1. ANNUAL SURFACE WINDROSE SANTA MARIA

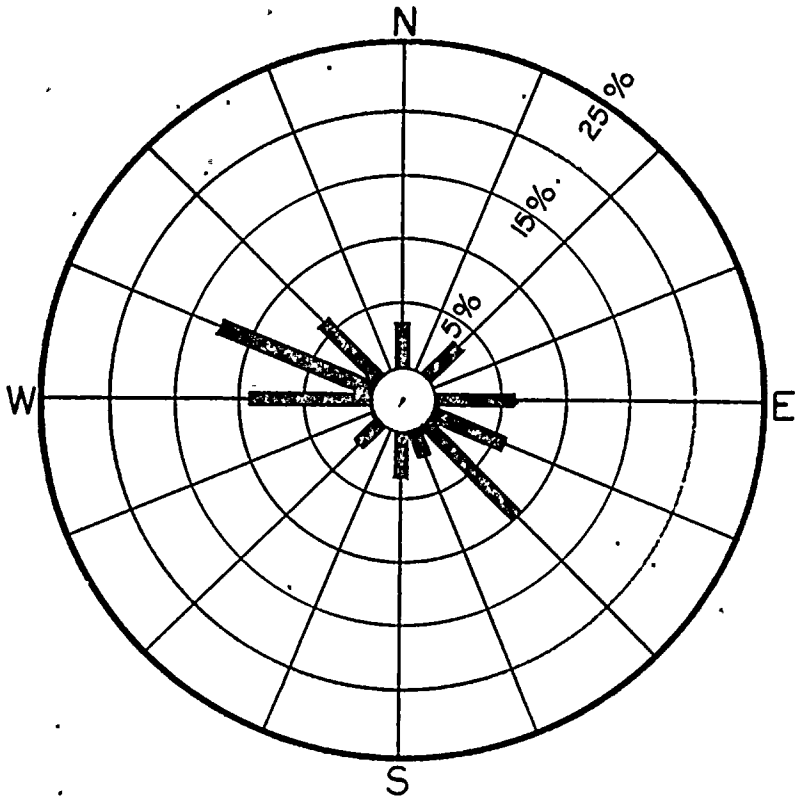

CALM CONDITIONS (0-3 mph) EXISTED 33 % OF THIS PERIOD WET SEASON (NOV.-MAR.) 1938-1941

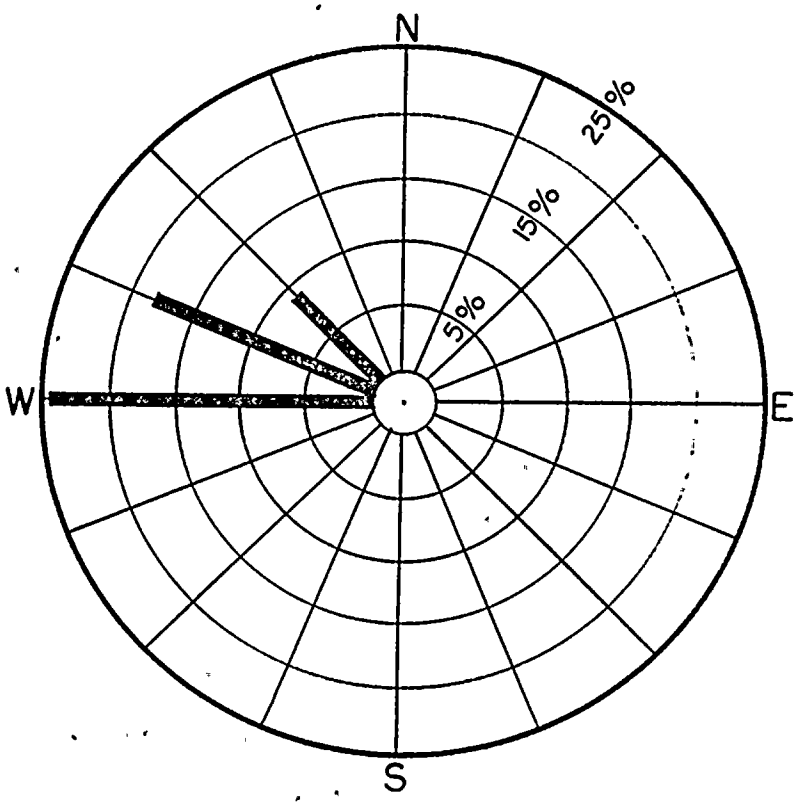

CALM CONDITIONS (0-3 mph) EXISTED 40 % OF THIS PERIOD DRY SEASON (MAY-SEPT.) 1938-1941

Figure 2. SEASONAL SURFACE WINDROSES SANTA MARIA

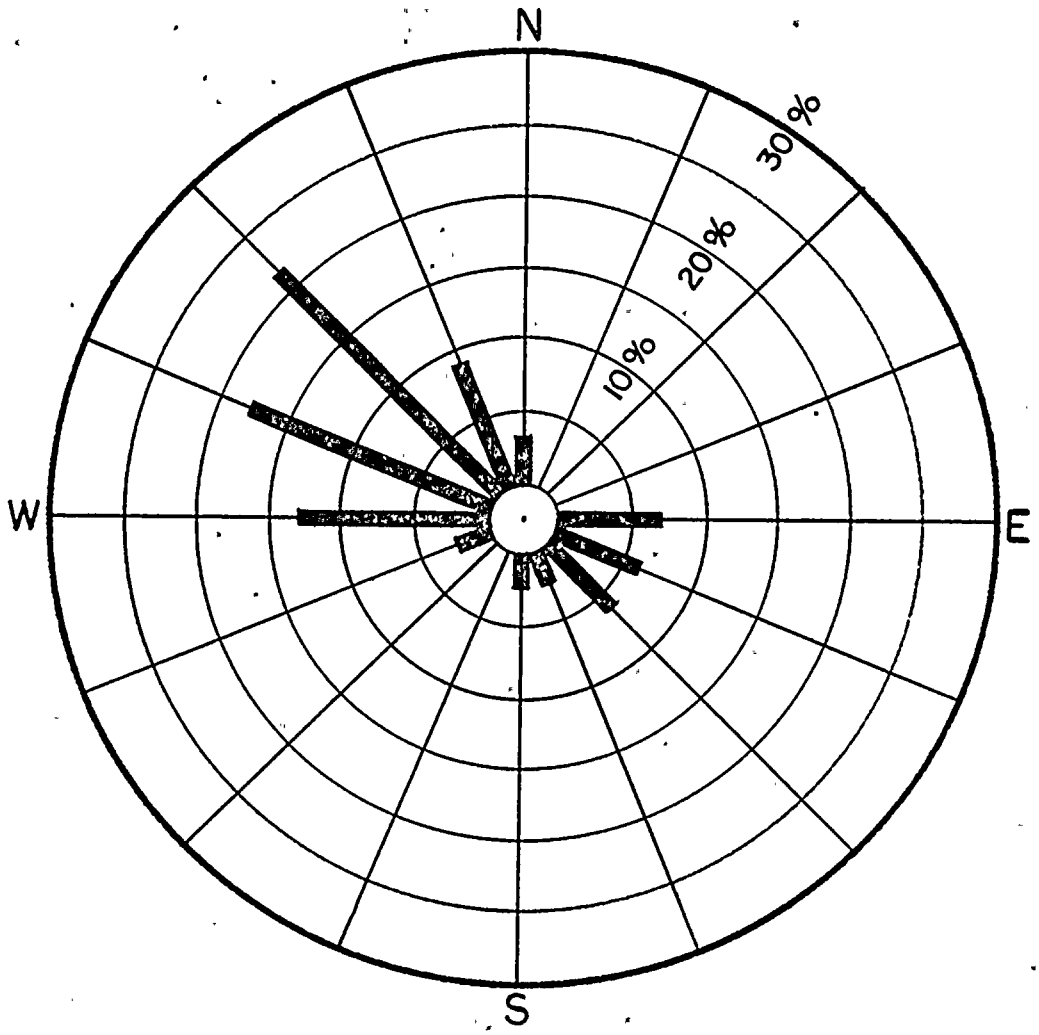

NOTES:

1. CALM CONDITIONS (0.mph) EXISTED 13 % OF THIS PERIOD
2. PERIOD OF RECORD JAN. 1, 1959 JUNE 30, 1962
3. BASED ON TWO OBSERVATIONS PER DAY

Figure 3. ANNUAL SURFACE WINDROSE

POINT ARGUELLO & SANTA MARIA

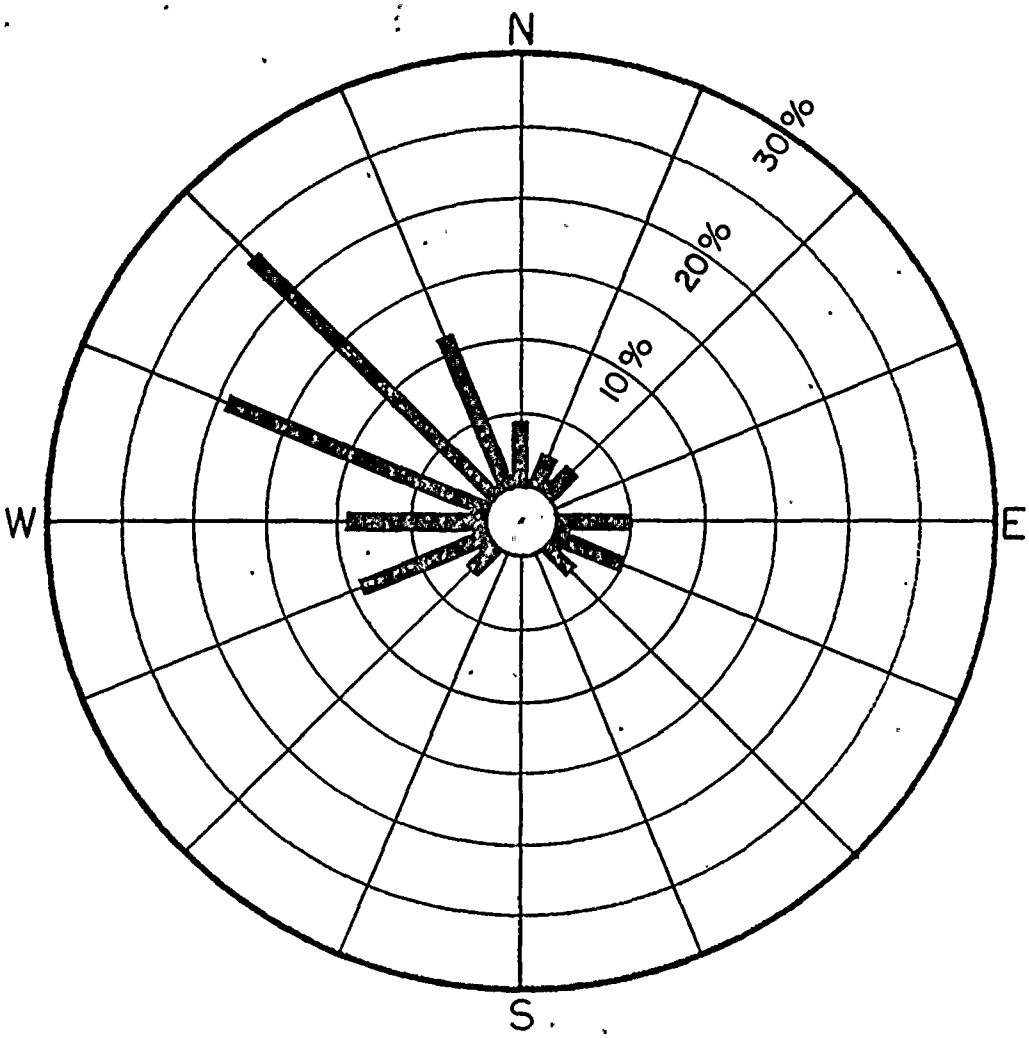

NOTE:

1. CALM CONDITIONS EXISTED 8 % OF THIS PERIOD
2. PERIOD OF RECORD FROM JAN.1.1959 TO JUNE 30 1962
3. TWO OBSERVATIONS PER DAY TAKEN AT 4 AM. AND 4 PM. P.S.T.

Figure 4. ANNUAL 1000 MB (370 ft) WINDROSE

POINT ARGUELLO & SANTA MARIA

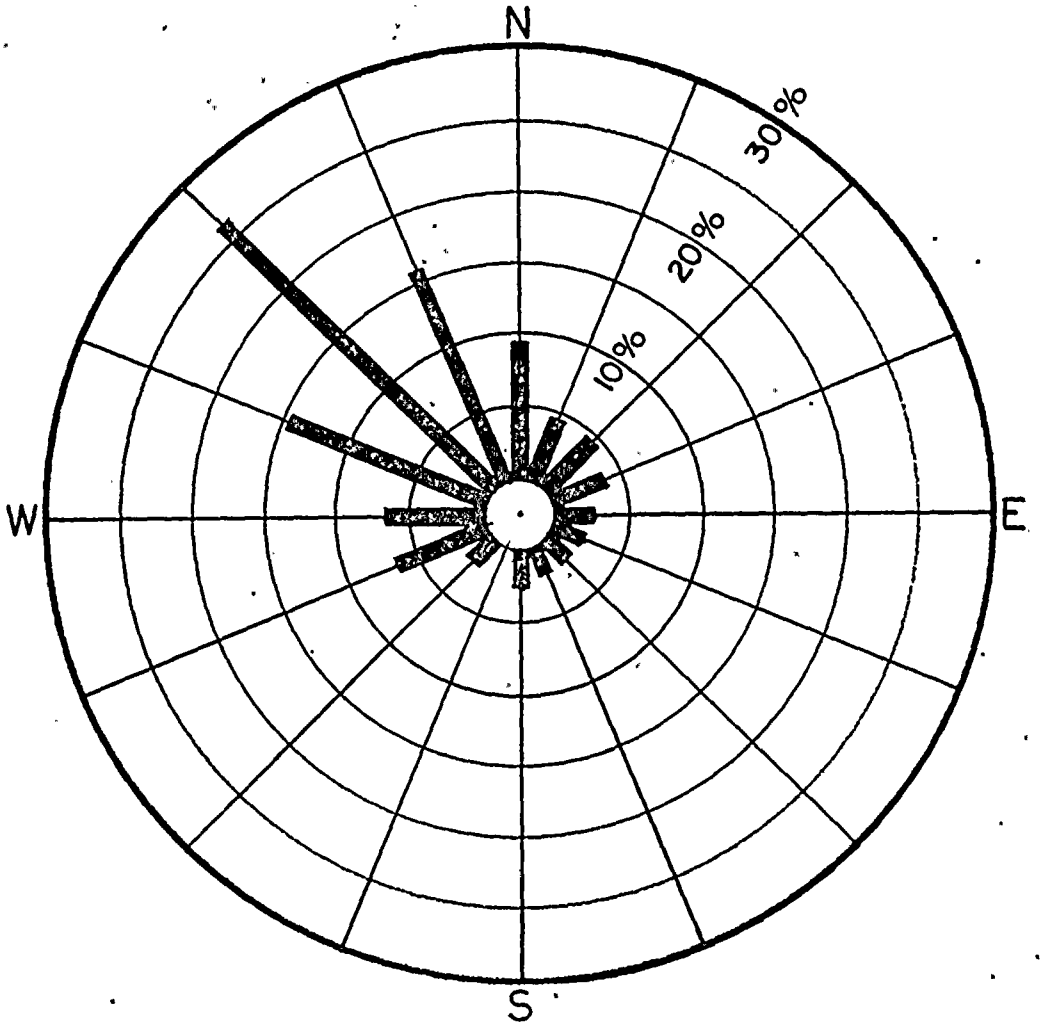

NOTES:

1. CALM CONDITIONS EXISTED 3% DURING THIS PERIOD
2. PERIOD OF RECORDS JAN. 1, 1959 TO JUNE 30, 1962.
3. TWO OBSERVATIONS PER DAY TAKEN AT 4 AM. AND 4 PM. P.S.T.

Figure 5. ANNUAL 1000 ft WINDROSE POINT ARGUELLO & SANTA MARIA

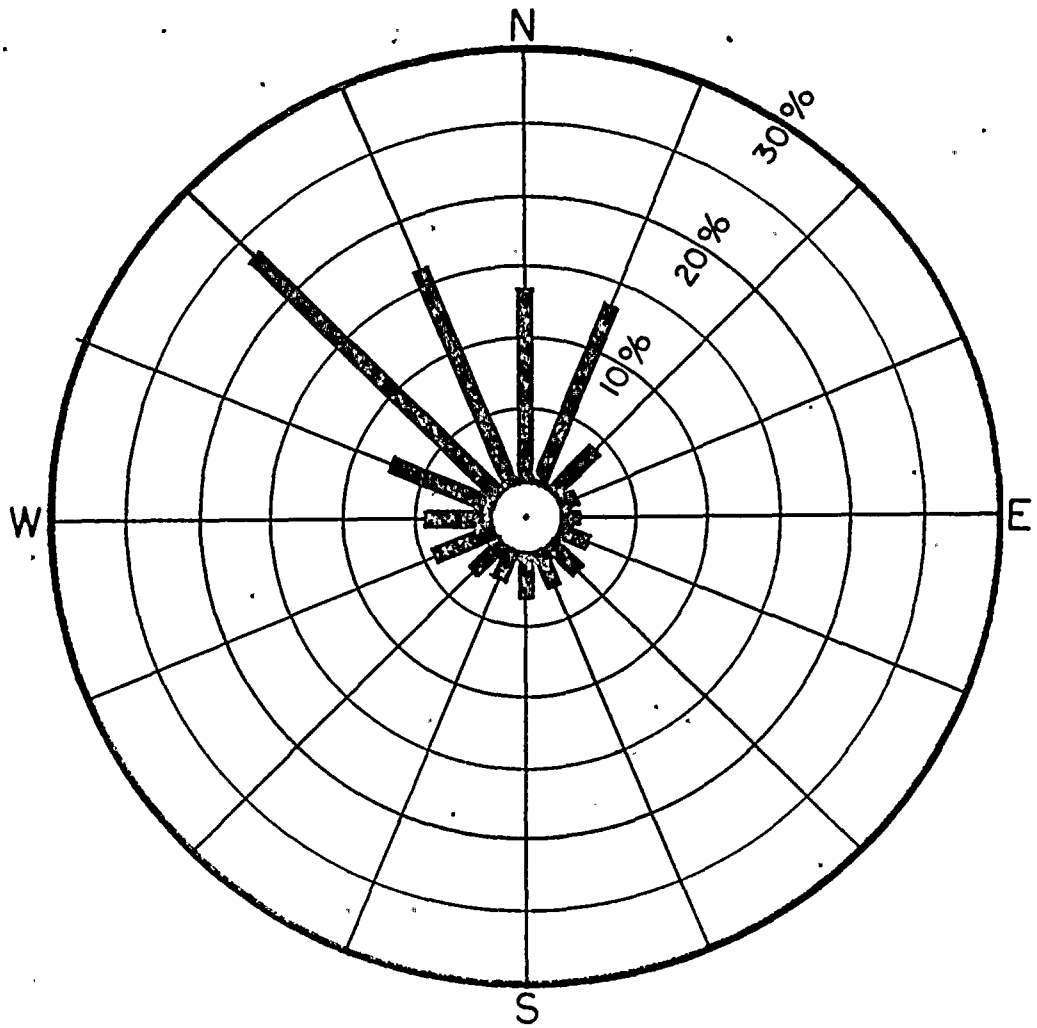

NOTE:

1. CALM CONDITIONS EXISTED 1.4% DURING THIS PERIOD.
2. PERIOD OF RECORDS JAN. 1, 1959 TO JUNE 30, 1962
3. TWO OBSERVATIONS PER DAY TAKEN AT 4 AM. AND 4 PM. P.S.T.

Figure 6. ANNUAL 950 MB (1780 ft) WINDROSE

POINT ARGUELLO & SANTA MARIA

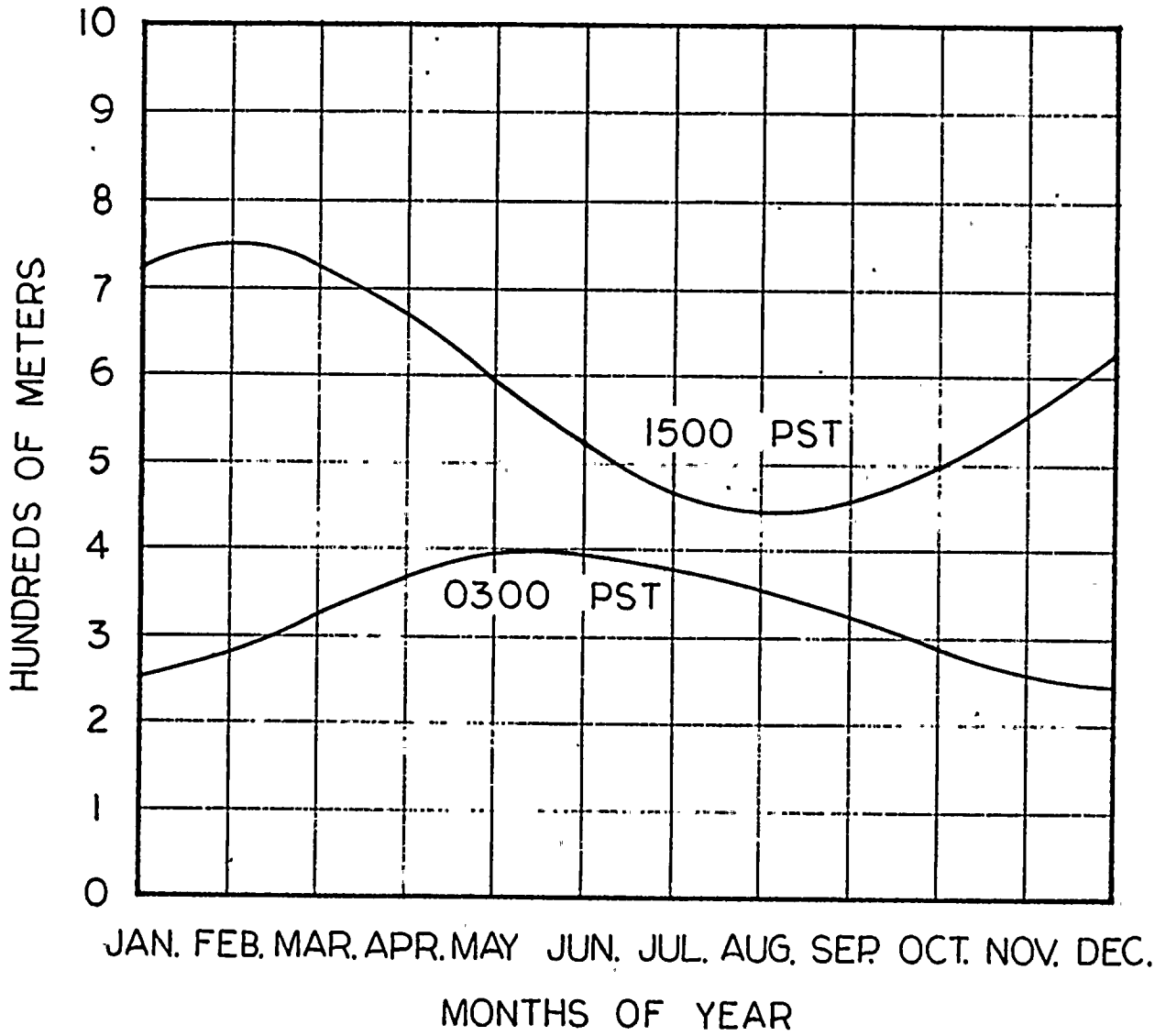

Figure 7. ANNUAL INVERSION BASE HEIGHT (POINT ARGUELLO)

MAP OF TERRAIN AT DIABLO CANYON SITE AND LOCATION OF METEOROLOGICAL DATA GATHERING NETWORK

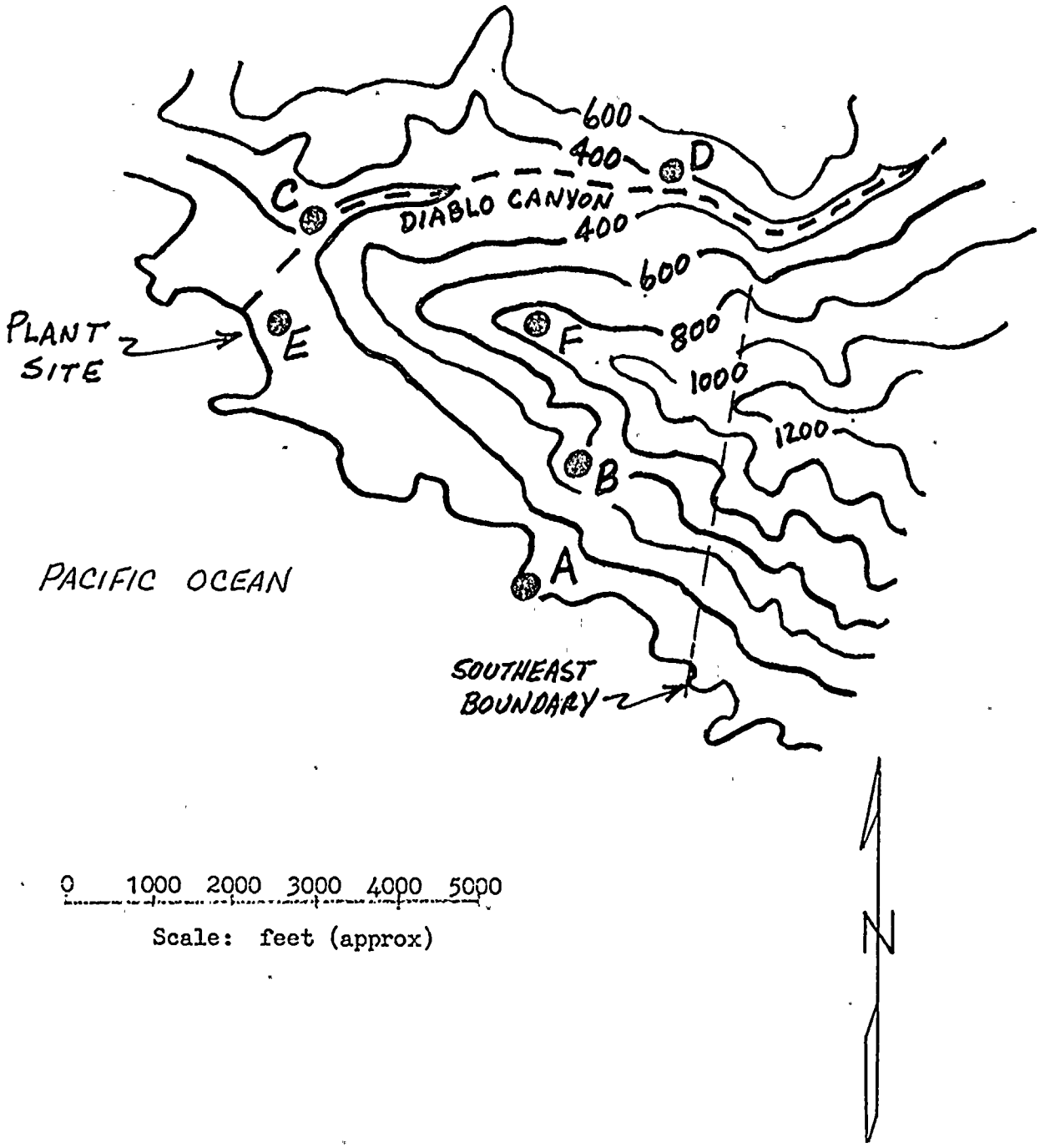

0 1000 2000 3000 4000 5000

Scale: feet (approx)

FIGURE 8